Formulation of Non-Ionic Surfactant Vesicles for Therapeutic Delivery of siRNA in Cancer Treatment

A thesis submitted by

Mohammad Ali Radi Obeid

Strathclyde Institute of Pharmacy and Biomedical Sciences

University of Strathclyde

Glasgow, UK

Presented in fulfilment of the requirements for the degree of Doctor of Philosophy

September 2017

Declaration

This thesis is the result of the author's original research. It has been composed by the author and has not been previously submitted for examination which has led to the award of a degree.

Signed:

Date:

بسم الله الرحمن الرحيم

By the name of Allah

****

Acknowledgments

First and foremost, I would like to express my greatest gratitude to Allah (SWT) for blessing me and giving me the strength that has led me to complete this thesis.

I would like to express my sincere gratitude and appreciation to my supervisors: Dr. Valerie Ferro, Dr. Rothwelle Tate, and Prof. Alexander Mullen for their excellent guidance, invaluable insights, motivation, and constructive criticism during the entire period of this research. Their help and guidance made studying a PhD the best experience I have ever had. They are amazing supervisors with a great sense of humour. It was a great honour to be their student. My sincere thanks also goes to Dr. Ibrahim Khadra for his valuable time, advice and support. I must also thank Dr. Christine Dufes and Dr. Katharine Carter for their help in the animal work.

My acknowledgements also go to the Ministry of Higher Education and Scientific Research and Yarmouk University in Jordan for awarding me the scholarship and providing me with the opportunity to study abroad to undertake my PhD studies in the United Kingdom.

I thank all my friends and colleagues inside and outside Strathclyde University with whom I have shared good times and memories and for the advice and help they have given me.

I would like to express my deepest gratitude to my father Ali, and my mother Feryal, for their prayers and strong encouragement in my academic endeavours over the years. It is their devotion and wisdom that constantly drives me to do my best in every aspect of my life. Without their support and guidance, I would not be the person I am today.

My deepest thanks and appreciation goes to my wife Shatha for standing beside me throughout my PhD journey and helped me every single moment by all means and by all the powers she has, so that I can hold this degree. She has been my inspiration and motivation for continuing to improve my career for a brighter future to our family. I would not have done this without you in my life. I also thank my wonderful daughter Noor who always makes me smile and enlightened my life in spite of all the time it took me away from her.

Thanks to my sisters and brothers (Lubna, Ossama, Leema, Ahmad, Hadeel, Hanadi, Maen, and Safa'a) for supporting me at all times and during all situations. My special thanks also goes to my parents-in-law (Nayef and Samar) who have always stood beside me with their support and encouragements.

Abstract

RNA interference (RNAi) is a post-transcriptional gene regulatory mechanism that involves the degradation of a target messenger RNA (mRNA) through the incorporation of short interfering RNAs (siRNA) which is complementary to the target mRNA. Unmodified, naked siRNA is unstable and cannot freely penetrate the cell membrane. The application of siRNA based therapeutics is limited by the development of an effective delivery system to deliver therapeutic siRNA to the cytoplasm of the target cells. Lipid-based nanoparticles, such as liposomes, are the most commonly investigated systems for siRNA delivery. However, another type of lipid-based system known as non-ionic surfactant vesicles (NISV) which are commonly used for drug delivery of various therapeutic agents, are relatively safe and non-expensive have not been extensively studied for siRNA delivery. Therefore, the aim of this study was to investigate the potential of NISV in siRNA delivery. Different manufacturing methods are used for the preparation of NISV and most of them are limited to bench scale and cannot be used on a larger industrial scale. This project sought to optimise the formulation method of NISV and to investigate their potential to effectively deliver siRNA to tumour cells *in vitro* and *in vivo*. Different methods of NISV manufacturing were compared including: thin-film hydration method (TFH), heating method, and microfluidic mixing. The formation of spherical nanoparticles was confirmed by examining the morphology of the NISV prepared by the three methods with atomic force microscopy (AFM) or scanning electron microscopy (SEM). TFH and heating methods were able to produce small (< 200 nm) and homogeneous NISV only after using a post-manufacturing size reduction step such as extrusion. This was time consuming and it was difficult to control batch to batch variations. Microfluidic mixing was found to produce NISV of the desired size and dispersity required for regulatory

approval, in a single step, without the need of size reduction and homogenisation. Moreover, the preparation time was significantly reduced with controllable parameters, which suggested this method would make production feasible on a larger scale. Therefore, microfluidic mixing was chosen to prepare different NISV formulations and to investigate the optimisation of the factors related to this method, including the mixing time, mixing ratio, and the type of hydration media used. These were found to have significant effects on the physical characteristics of the vesicles such as size, polydispersity index, and charge. Particle size was shown to be decreased significantly ($p<0.05$) by increasing the ratio between the aqueous and lipid phase as well as by increasing the total flow rates in the mixing process. Optimum ratios were found to be 3:1 between the aqueous and lipid phase at a total flow rates of 12 ml/min. Moreover, changing the type of aqueous media used to prepare the particles also resulted in significant effects on the particle size, dispersity, and charge. Smaller particles (desirable for siRNA delivery) were obtained using distilled water (DW), Tris, and (4-(2-hydroxyethyl)-1-piperazineethanesulfonic acid) (HEPES) buffers while the use of phosphate buffered saline (PBS) or normal saline (NS) resulted in the preparation of larger particles. Therefore, for the next experiments that involved siRNA transfections, NISV were prepared with DW. After optimising all these parameters, *in vitro* studies were conducted with the NISV formulations made with either monopalmitin glycerol (MPG) or Tween85 (T85) as a non-ionic surfactant, in addition to cholesterol and dimethyldioctadecylammonium bromide (DDAB) as a charging material, at different molar ratios of these components. Cytotoxicity evaluation of the prepared NISV formulations were carried out on non-small lung cancer cells (A549), human melanoma cancer cells (A375), breast cancer cells (A780), and mouse melanoma cells (B16-F10-LUC). These experiments were carried out with the use of normal human prostate cells

(PNT2) as a control. The used cancer cell lines were selected as they are among the most abundant cancers types worldwide. Cytotoxicity studies indicated that all the NISV formulations were not toxic at or below 40 µg/ml. The prepared NISV formulations had high siRNA encapsulation efficiency (~90%). Fluorescent microscope and flow cytometry studies on A549 cells, using fluorescent labelled negative control siRNA loaded in all the NISV formulations tested, indicated high cellular uptake by the cells. These uptake results were confirmed with B16-F10-LUC mouse melanoma cells, where the prepared NISV were able to successfully deliver siRNA into the cells compared to naked siRNA, which was not taken up by the cells. Following these experiments that proved cellular uptake of siRNA delivered by NISV, siRNA targeting either green fluorescent protein (GFP) in copGFP-A549 cells, or luciferase enzyme in B16-F10-LUC cells were encapsulated in NISV that contained either MPG or T85 as a non-ionic surfactant. Inhibition of GFP expression by anti-GFP siRNA (siGFP) delivered using different NISV formulations was evaluated by fluorescence measurement, flow cytometry, polymerase chain reaction, and Western blotting studies. These results indicated that all the NISV formulations were able to deliver siGFP to the cells and significantly ($p<0.05$) suppress GFP expression. These results were confirmed by transfecting the luciferase producing B16-F10-LUC cells with anti-luciferase siRNA (siLUC) using the same NISV formulations. Measuring the level of luciferase expression after siLUC transfections using a luciferase protein assay system successfully demonstrated the suppression of luciferase expression. Among all the NISV prepared, significant GFP and luciferase gene knockdown results were achieved when using NISV that contained T85 as the non-ionic surfactant. This superior formulation was then used in *in vivo* experiments using nude BALB/c mice inoculated with B16-F10-LUC cells that induce melanoma cancer-expressing luciferase. After

intra-tumoural injection with this formulation, siLUC was delivered to the cells and suppressed luciferase expression at a significantly ($p<0.05$) higher level than mice treated with naked siLUC. These *in vivo* results confirm the ability of NISV to successfully delivery siRNA into the cytoplasm of the target tumour cells and suppress the target protein. In conclusion, NISV prepared by microfluidics have been demonstrated extensively and for the first time to have the potential to be used as a delivery system for siRNA. These results have shown that NISV can be used to overcome the barriers, such as low stability and poor cellular uptake, in siRNA-based therapeutics. NISV are a promising delivery system which can be investigated more extensively to target different over-expressed proteins in the process of developing different effective cancer medications.

Preface

This dissertation consists of six chapters. Chapter 1 is an overview of the various lipid-based nanoparticles that have been developed for use in cancer treatment and in siRNA delivery. This chapter entitled *"Lipid-based nanoparticles for cancer treatment",* is part of a book chapter. This chapter was an invited submission by the editor, Alexandru Mihai Grumezescu – Pharmaceutical Nanotechnology, ELSEVIER.

Chapter 2 investigates the use of different manufacturing methods such as thin-film hydration method, heating method, and microfluidic mixing for the preparation of monodisperse NISV. This chapter entitled *"Comparison of the physical characteristics of monodisperse NISV prepared using different manufacturing methods",* was published in the International Journal of Pharmaceutics (DOI: 10.1016/j.ijpharm.2017.02.007).

Chapter 3 investigates the effects of the aqueous media used for the preparation of NISV by microfluidics on the physical characteristics of the prepared particles. This chapter entitled *"The effects of hydration media on the characteristics of NISV prepared by microfluidics",* was published in the International Journal of Pharmaceutics (DOI: 10.1016/j.ijpharm.2016.11.015).

Chapter 4 evaluates the effectiveness of NISV prepared by microfluidics in transfecting A549 (human lung cancer) cells by anti-GFP siRNA and measuring the level of GFP suppression using different methods such as fluorescence measurements, flow cytometry, polymerase chain reaction, and Western blotting. This chapter entitled *"Formulation of NISV prepared by microfluidics for therapeutic delivery of siRNA into*

cancer cells", was published in Molecular Pharmaceutics (DOI: 10.1021/acs.molpharmaceut.7b00352).

Chapter 5 describes proof of concept studies using NISV as the delivery system for siRNA to confirm the results obtained in chapter 4 to suppress luciferase enzyme expression both *in vitro*, using B16-F10-LUC (mouse melanoma) cells that express luciferase, and *in vivo* using nude mice bearing B16-F10-LUC melanoma tumours treated by intra-tumoural injection of anti-luciferase siRNA formulated in NISV. This chapter, entitled *"Proof of concept studies for siRNA delivery by NISV: In vitro and in vivo evaluation of protein knockdown",* is a research paper currently in preparation for submission to the Journal of Controlled Release.

Chapter 6 deals with the general conclusions for the thesis with some suggestions for the future work in the field of siRNA delivery through NISV.

Publications and presentations

Peer reviewed articles

- **OBEID, M. A**., GEBRIL, A. M., TATE, R. J., MULLEN, A. B. & FERRO, V. A. 2017. Comparison of the physical characteristics of monodisperse non-ionic surfactant vesicles (NISV) prepared using different manufacturing methods. *International Journal of Pharmaceutics,* 521(1): p. 54-60.

- **OBEID, M. A.**, KHADRA, I., MULLEN, A. B., TATE, R. J. & FERRO, V. A. 2017. The effects of hydration media on the characteristics of non-ionic surfactant vesicles (NISV) prepared by microfluidics. *International Journal of Pharmaceutics,* 516**,** 52-60.

- **OBEID, M. A.**, ELBURI, A., YOUNG, L. C., MULLEN, A. B., TATE, R. J., FERRO, V. A. 2017. Formulation of non-ionic surfactant vesicles (NISV) prepared by microfluidics for therapeutic delivery of siRNA into cancer cells. *Molecular Pharmaceutics*.

- AL QARAGHULI, M. M., ALZAHRANI, A. R., NIWASABUTRA, K., **OBEID, M. A.,** FERRO, V. A. 2017. Where traditional drug discovery meets modern technology in the quest for new drugs. *Annals of Pharmacology and Pharmaceutics* 2(11), 1-5.

Poster presentations:

- **OBEID, M. A**., TATE, R. J. & FERRO, V. A. 2015. Microfluidic-controlled manufacture of non-ionic surfactant vesicles for drug delivery. Poster presentation at Fifth APS international PharmSci conference 2015 (Nottingham, UK)

- **OBEID, M. A**., MULLEN, A. B., TATE, R. J., & FERRO, V. A. 2016. Physical Characteristics of Monodisperse Non-Ionic Surfactant Vesicles Prepared Using Different Manufacturing Methods. Poster presentation at the 43rd Controlled Release Society conference, July 2016 (Seattle, USA)

Oral presentations:

- **2015:** Inaugural Microfluidics User Group Meeting: Enhancing Nanoparticle Formulation & Scale Up. Aston University, Birmingham, UK.

  Title: Controlled Monodisperse Niosome Formulations Prepared by Microfluidics

- **2016:** 43rd Controlled Release Society conference. July 2016, Seattle, USA
  Title: Physical Characteristics of Monodisperse Non-Ionic Surfactant Vesicles Prepared Using Different Manufacturing Methods

- **2017:** Nanomedicine Translation Advisory Board (NanomedTAB). April 2017, King's College, London, UK.
  Title: Formulation of Non-Ionic Surfactant Vesicles (NISV) for therapeutic delivery of siRNA in cancer treatment

Table of Contents

Contents

List of Figures

List of Tables

List of Abbreviations

%	Percentage
<	Less than
>	More than
°C	Degrees Celsius
A260/280	Ratio of absorbance at wavelengths 260 nm and 280 nm
AFM	Atomic force microscope
ANOVA	Analysis of variance
ATCC	American Type Culture Collection
B2M	2-microglobulin
Bp	Base pair
BSA	Bovine serum albumin
cDNA	Complementary deoxyribonucleic acid
Chol	Cholesterol
CT	Cycle threshold
DCP	Dicetyl phosphate
DDAB	Dimethyldioctadecylammonium bromide
DMEM	Dulbecco's modified eagle medium
DMSO	Dimethyl sulphoxide
DNA	Deoxyribonucleic acid
dsRNA	Double stranded RNA
DW	Distilled water
EC_{50}	Half maximal effective concentration
ELISA	Enzyme-linked immunosorbent assay
Eq.	Equation
et al.	And others
etc.	Et cetera (Latin); for example, such as
FACS	Fluorescence-activated cell sorting
FCS	Foetal calf serum
FDA	US Food and Drug Administration
FITC	Fluorescein isothiocyanate
FRR	Flow rate ratios
g	Gram
GAPDH	Glyceraldehyde 3-phosphate dehydrogenase
GFP	Green fluorescent protein
h	Hour
HEPES	(4-(2-hydroxyethyl)-1-piperazineethanesulfonic acid)
HPLC	High Performance Liquid Chromatography
i.e.	id est (Latin); that is
i.v	Intravenous
kDa	Kilodalton
L	Litre
LUV	Large unilamellar vesicle
M	Molar
MFI	Median fluorescent intensity
mg	Milligram
MIC	Minimum inhibitory concentration
min	Minute

MIQE	Minimum information for publication of quantitative real-time PCR experiments
miRNA	Micro ribonucleic acid
ml	Millilitre
MLV	Multilamellar vesicle
mm	Millimetre
mM	Millimolar
mmol	Millimole
MPG	Monopalmitin glycerol
mRNA	Messenger ribonucleic acid
MW	Molecular weight
n	Number of replicates
ng	Nanogram
NISV	Non-ionic surfactant vesicles
nm	Nanometre
nM	Nanomolar
nmol	Nanomole
NS	Normal saline
p	Value of significance
PBS	Phosphate buffered saline
PC	Phosphatidylcholine
PCR	Polymerase chain reaction
PDI	Polydispersity index
pDNA	Plasmid of deoxyribonucleic acid
PEG	Polyethylene glycol
pH	Potentia hydrogenii (Latin); power of hydrogen, the negative logarithm of the hydrogen ion concentration
pka	apparent acid dissociation constant
qPCR	Quantitative polymerase chain reaction
qRT-PCR	Quantitative real time polymerase chain reaction
Rf	Retardation factor
RISC	RNA-induced silencing complex
RNA	Ribonucleic acid
RNAi	RNA interference
RNase	Ribonuclease
RPMI	Roswell Park Memorial Institute
RT	Reverse transcriptase
RT-	Minus reverse transcriptase
RT-PCR	Reverse transcriptase polymerase chain reaction
s	Second
SD	Standard deviation
SEM	Scanning electron microscopy
siRNA	Short interfering ribonucleic acid
SUV	Small unilamellar vesicle
TBST	Tris-buffered saline with Tween 20
TFH	Thin-film hydration
TFR	Total flow rates
Tween 85	Polyoxyethylenesorbitan trioleate
UK	United Kingdom
USA	United States of America

v/v	Volume by volume
w/v	Weight by volume
w/w	Weight by weight
ZP	Zeta potential
µg	Microgram
µL	Microlitre
µm	Micrometre
µM	Micromolar

Chapter 1

Introduction and literature review of lipid-based nanoparticles for cancer treatment

Abstract

Lipid-based nanoparticles provide a versatile mode of cancer treatment by delivering drugs to the target site in order to improve the drug pharmacokinetics and/or reduce their toxicities. Several of these nanoparticle-based anticancer therapeutics are currently being investigated in clinical trials with some already approved for clinical practice. In this chapter, the main features of these nanoparticles will be highlighted and their types and classes described. Examination will be made of some of the approved formulations and some of those currently investigated in clinical trials. In addition, the major techniques that are involved in their manufacturing and characterisation along with the major challenges in translating basic research to the clinic will be reviewed. Moreover, the use of lipid-based nanoparticles in the delivery of siRNA will be discussed.

Keywords: cancer treatment, lipid-based nanoparticles, drug delivery, liposomes, niosomes, micelles, formulation method, particle characterisation.

1.1. Introduction

Cancer consists of a group of diseases characterised by abnormal cell growth with the potential to metastasise to other tissues or body organs. It is one of the leading causes of death worldwide, with more than 100 different types of cancer characterised [1].

Treatment options include chemotherapies, radiation therapy, surgery, and gene therapy [2]. Chemotherapies include chemicals that interfere with cell proliferation and division with the result of apoptosis (cell suicide) and death [3]. Frequent challenges encountered by current chemotherapeutic agents include intolerable cytotoxicity, nonspecific action, uncontrollable drug concentration at the tumour site, and the development of drug resistance with prolonged use of these chemotherapies [4]. As these treatments target rapidly dividing cells, they may have effects on normal cells as well as on cancerous cells and this is the origin of unwanted side effects such as hair loss, nausea, fatigue, and vomiting [3]. Thus, there is an urgent need for new therapeutic options. Development of drug delivery technologies is considered one approach to improve current treatment options, by increasing the selectivity and specificity at the tumour site and reducing unwanted exposure to normal cells.

Recently, there have been significant advances in the development and application of nanoparticles especially in the field of drug delivery and there has been a consistent rise in the number of commercially available nanoparticle therapeutics reaching clinical stage, with many currently in the marketplace [3, 5]. In its simplest definition, drug delivery can be attributed to the use of a delivery tool to convey and release a bioactive agent to a particular site in the body at a specific rate [6]. Cancer nanotechnology is a term used to express the application of nanotechnology in the development of cancer therapeutics. The goal of cancer nanotechnology is to develop novel technologies that can provide new treatment options or improve currently used medications [7]. High

percentages of drugs, including anticancer medications, are limited by their high toxicity, poor solubility, nonspecific *in vivo* distribution, rapid elimination, and unwanted side effects [8], but currently, significant developments in the field of drug delivery have been achieved in order to resolve these limitations [6]. Moreover, drug delivery systems can improve the pharmacokinetics of highly degradable and unstable protein and peptide therapeutic molecules by offering an effective tool to protect these drugs and increase their *in vivo* half-lives [9]. In addition, significant milestones have been achieved in the field of gene silencing in humans utilising nanoparticles as delivery agents. The first reported evidence of gene silencing in humans was reported in 2010, achieved by the systemic administration of short interfering RNA (siRNA) therapeutics using targeted nanoparticles [10]. This chapter provides an overview of the use of nanoparticle delivery systems in cancer treatment with the focus on lipid-based nanoparticles, including manufacturing methods, characterisation and the current achievements in this field.

1.2. The use of nanoparticles in cancer drug delivery

Nanoparticles are physical entities with a size range of 1-1000 nm. They are used as an efficient tool to facilitate drug targeting and improving drug bioavailability [5] as well as decreasing the toxicities of many drugs. This results in an improvement in the drug's therapeutic index which is the difference between its therapeutic efficacy and toxicity [11]. Nanoparticles have different classifications, some based on particle size, shape, and origin, while others are based on chemical structure as either organic or non-organic. However, regardless of the classification, nanoparticles possess pertinent features, namely their high surface-to-volume ratio, which is much greater than other particles (such as micron- or larger-sized particles) [5, 11]. This feature provides nano-sized particles with a very limited volume for transportation of cargo, but a large surface

area for interactions with biological membranes [5]. Other characteristics include their quantum properties and ability to encapsulate and carry a variety of compounds [11].

The major challenge in drug delivery is to get the drug to the site of action and avoiding off-target, collateral effects on non-diseased tissues. This is critical in improving chemotherapies where for example tumour metastases may lie deep in different organs. In terms of drug targeting, nanoparticles have different characteristics, such as controllable size, which facilitate accumulation in tumour tissues, enable penetration of different biological barriers and cell membranes, and confer the ability to escape destruction by lysosomes after endocytosis; all these properties make nanoparticles an optimal drug carrier. Furthermore, after delivering their payload, nanoparticles should be eliminated from the body safely and in a reasonable time with minimal side effects. Therefore, the ideal nanoparticle should be non-toxic, biocompatible, biodegradable, non-immunogenic, and be able to escape early hepatic or renal clearance [5, 11, 12].

Nanoparticle drug carriers facilitate the delivery of a range of molecules such as nucleic acids, peptides, proteins and poorly water-soluble drugs that are not membrane permeable. In a nucleic acid delivery context, nanocarriers should protect their cargo until they reach the target site without change in structure or activity [5, 13]. The drug maybe covalently attached to the outer surface of the nanoparticles or may be encapsulated in their core [5] and once the delivery system reaches its target site, the drug usually detaches from the nanoparticles by diffusion, swelling, or degradation [12]. AmBisome (liposomal amphotericin B, used to treat cancer patients with fungal infections) and Doxil (liposomal doxorubicin) were among the first anti-cancer medications on the market using lipid-based nanoparticles [14]. The US Food and Drug Administration **(**FDA**)** have approved several nanoparticle-based drugs for human use (Table 1.1) with many others now in different phases of clinical development (Table

1.2). It is believed that nanotechnology-based drug delivery will have a growing share of the anticancer therapeutics in the coming years [15, 16].

Table 1.1 FDA approved nanoparticle-based drugs

Active drug	Formulation	Route of administration	Trade name	Indication	Company	Ref
Paclitaxel	Albumin-bound	IV	Abraxane	Metastatic breast cancer, non-small cell lung cancer	Abraxis Bioscience	[17]
Daunorubicin	Liposome	IV	DaunoXome	Kaposi's sarcoma	Galen Limited	[18]
Cytarabine	Liposome	IV	DepoCyt	Malignant lymphomatous meningitis	Pacira Pharmaceuticals	[19]
Doxorubicin	Liposome	IV	Doxil/Caelyx	Kaposi's sarcoma, ovarian cancer, breast cancer, multiple myeloma	Orthobiotech, Schering-Plough	[20]
Paclitaxel	Polymeric micelle	IV	Genexol-PM	Breast and non-small cell lung cancer	Samyang Biopharmaceuticals	[21]
Vincistine	Liposome	IV	Marqibo	Acute lymphoblastic leukaemia	Talon Therapeutics	[22]
Mifamurtide	Liposome	IV	Mepact	Non-metastatic osteosarcoma	Takeda pharmaceuticals	[23]
Pegaspargase	PEG conjugate of l-asparaginase	IM/IV	Oncaspar	Acute lymphoblastic leukaemia	Enzon Pharmaceuticals	[24]

Abbreviations: IV, intravascular; IM, intramuscular; PEG, polyethylene glycol

Table 1.2 Lipid-based nanocarriers in clinical trials

Active drug	Formulation	Target	Status	Sponsor
Vincristine Sulfate	Liposome	Acute myeloid leukemia	Phase II	Comprehensive Cancer Center of Wake Forest University
Doxorubicin	Liposome	Ovarian cancer	Phase I	Shanghai Fudan-Zhangjiang Bio-Pharmaceutical
Vincristine Sulfate	Liposome	Acute lymphoblastic leukemia	Phase III	Nanjing Luye Sike Pharmaceutical
Doxorubicin	Pegylated liposome	Recurrent ovarian cancer	Phase I	National Cancer Institute
Cytarabine-Daunorubicin	Liposome	Acute myeloid leukemia	Phase I	Fred Hutchinson Cancer Research Center
188Re-BMEDA	Liposome	Primary solid tumour	Phase I	Institute of Nuclear Energy Research, Taiwan
Doxorubicin	Liposome	Breast cancer	Phase II	M.D. Anderson Cancer Center
Cytarabine:Daunorubicin	Liposome	Acute myeloid leukemia	Phase II	Celator Pharmaceuticals
Doxorubicin	Liposome	Metastasic breast cancer	Phase I	MedSIR
Grb2 Antisense Oligonucleotide	Liposome	Leukemia	Phase Ib/IIa	Bio-Path Holdings, Inc.
Cytarabine	Liposome	Acute lymphoblastic leukemia	Phase II	National Cancer Institute, Naples
Vinorelbine	Liposome	Advanced malignancy	Phase I/IIa	Taiwan Liposome Company
Mitomycin-C	Liposome	Solid tumours.	Phase I	Lipomedix Pharmaceuticals Inc.
FUS1	Lipid nanoparticles	Lung cancer	Phase I/II	Genprex, Inc.
Tetravalent RNA cancer vaccine	Lipoplex	Melanoma	Phase I	BioNTech RNA Pharmaceuticals GmbH
Pbi-shRNA	Lipoplex	Ewing's Sarcoma	Phase I	Strike Bio, Inc.

1.3. Lipid-based nanoparticles in cancer treatment

In this section, the focus is on different types of lipid-based nanoparticles used as drug delivery systems for anticancer therapeutics, along with their characteristics and advantages. These include liposomes, solid lipid-based systems, lipidoid particles, NISV, and micelles as detailed in Figure 1.1.

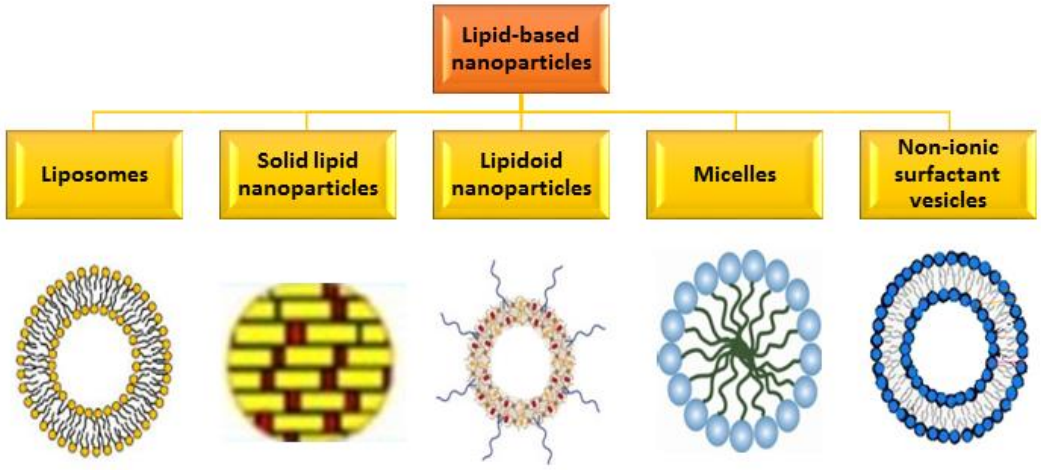

Figure 1.1 Schematic diagram of the most commonly used lipid-based nanoparticles for anticancer drug delivery.

1.3.1. Liposomes

Liposomes, initially known as spherules, are amongst the most advanced drug delivery systems. They are a controlled self-assembly of amphiphilic phospholipids that form spherical lipid bilayers enclosing an aqueous interior moiety for drug encapsulation [13, 25]. Liposomes were one of the first drug delivery systems introduced and considered the first generation of lipid-based nanoparticles [26]. The use of liposomes as a drug delivery system was first explored by Gregoriadis to deliver anticancer and antimicrobial drugs to cells [27, 28].

1.3.1.1. Liposome composition

Liposomes are composed mainly of phospholipids with other constituents such as cholesterol and polymer-conjugated lipids. Phospholipids have a hydrophilic head and hydrophobic tail which upon exposure to water spontaneously form a bilayer with the hydrophobic tails oriented towards each other and the hydrophilic heads facing the aqueous media on both sides.

Due to the lipid bilayer structure of liposomes, these nanocarriers are considered versatile as they can encapsulate both hydrophilic and hydrophobic drugs [26]. Hydrophilic chemotherapeutic drugs (e.g. Cytarabine) can be encapsulated by entrapping these drugs in the aqueous core of the liposomes, while hydrophobic anticancer drugs such as some anthracyclines can be achieved by incorporation of these drugs within the lipid membrane bilayer [29].

Phosphatidylcholine (PC; also known as lecithin) and phosphatidylethanolamine (PE) are examples of natural phospholipids used in liposome preparations. PE is usually used in limited amounts in liposome formulations as it has the ability to form non-bilayer structures under physiological conditions and destabilise the liposome membrane [30]. PC forms the major lipid constituent of the liposome membrane [31]. Other phospholipids that can be used include phosphatidylglycerol (PG), phosphatidylserine (PS), and phosphatidylinositol (PI) [13, 32]. Cholesterol is another major constituent of the liposome membrane and this sterol molecule aids in the stability of these formulations. Cholesterol inserts its sterol ring system into the hydrophobic domain of the phospholipid bilayer with its hydroxyl group orientated towards the aqueous phase. The role of cholesterol in these formulations is to decrease the fluidity of the lipid membrane bilayer, reduce the permeability of hydrophilic molecules through the bilayer membrane, and improve the stability of these vesicles in blood [26]. Other

additives in liposome formulations include polymers containing hydrophilic groups, such as polyethylene glycol (PEG) and sialic acid derivatives [33-35]. Nanoparticles which contain these polymers showed longer blood circulation due to their stealth properties and the steric stabilization as a result of presence of these polymers [36].

The flexibility of the liposome structure facilitates control over different stages of drug delivery. For example, the type of the lipid used can be based on the type of drug to be encapsulated. Cationic lipids are suitable for the delivery of negatively charged drugs. Also different targeting moieties can be easily attached to the surface of liposomes.

Liposomes have several characteristics such as: 1) high safety profile as it is composed of components resembling that of the plasma cell membrane which makes it biocompatible and biodegradable; 2) the ability to deliver a variety of payloads such as deoxyribonucleic acids (DNA), siRNA, chemotherapy drugs, antigens, proteins and many others; 3) they prevent the interaction of the payload with other molecules, thereby increasing the drug's stability; 4) they can be easily accumulated at the target tissue (through either active or passive targeting) with high delivery outcomes; 5) features like particle size, lipid composition, surface charge, surface targeting moieties, drug-to-lipid ratio and manufacturing techniques can be easily optimised; and 6) offer an excellent way to improve the therapeutic efficacy of poorly soluble drugs as well as minimising the side effects of the encapsulated drug [14, 26, 32].

Once the liposomes carrying their payload reach the target site, content release from the liposomes can be controlled in different ways: 1) modification of the liposome lipid content; 2) loading more hydrophilic cargo in the aqueous compartment; and 3) use of remote loading to enhance the cargo accumulation inside the liposomes [32]. An additional way to control the release from the liposomes is to use lipids that are sensitive

to environmental stimuli (pH, oxidative environment, shear stress). Such lipids are of particular interest for siRNA delivery where pH-dependent fusogenic lipids aid endosome escape and siRNA release to the cytosol [37].

1.3.1.2. Types of liposomes

Liposomes can be classed based on different factors such as the number of lipid bilayers within the liposome membrane, the surface charge, method of preparation or particle size. Based on their particle size and the number of the lipid bilayers, liposomes are classified into:

1. Small unilamellar vesicles (SUVs) with a size range of 20–100 nm and consist of a single lipid bilayer [26].
2. Large unilamellar vesicles (LUVs) which are particles > 100 nm and, like SUVs, consist of a single lipid bilayer [26].
3. Giant unilamellar vesicles (GUVs) with a particle size > 1000 nm [26].
4. Multilamilar vesicles (MLVs) usually range in size from 0.5-10μm and consist of multiple lipid bilayers with an onion-like structure. MLVs consist of several unilamellar vesicles formed inside each other and separated by the aqueous phase [26].

Physiochemical properties of nanoparticles such as size and surface charge have significant effects on the behaviour of these nanoparticles *in vivo* which will have impact on their anticancer effects [38]. Based on the surface charge, liposomes can be classified into three types: cationic, anionic, and neutral liposomes. Surface charge of the nanoparticles determine the extent of circulation distribution, and their cellular uptake [39, 40]. Neutral and negative charged nanoparticles have longer circulation half-lives *in vivo* as they adsorb less to serum proteins compared with cationic

nanoparticles, where the serum proteins attach to their surfaces and enhance opsonisation for recognition by the reticuloendothelial system (RES) [41]. However, cationic nanoparticles have been shown to have higher binding, resulting in internalisation by angiogenic endothelial cells in tumours compared with normal cells. Moreover, cationic nanoparticles have been found to be more effective in inhibiting tumour growth than their neutral or anionic counterparts in a variety of tumour models (such as breast, prostate, and pancreatic cancers) [42]. Other types of liposomes include modified vesicles such as transferosomes that, in addition to phospholipids, incorporate a single chain surfactant (known as an edge activator) [43] and ethosomes that are composed of phospholipids, ethanol, and water [44]. Both of these modified formulations are used mainly for transdermal drug delivery.

1.3.1.2.1. Cationic liposomes

Cationic liposomes are produced using lipids that induce a positive charge on the surface of liposomes such as dioleoyl phosphatidylethanolamine (DOPE), 1, 2-dioleoyl-3-trimethylammonium-propane (DOTAP), N-[1-(2, 3-dioleoyloxy) propyl]-N, N, N-trimethyl-ammonium methyl sulphate (DOTMA), oleic acid (OA), and dimethyldioctadecylammonium bromide (DDAB). Cationic liposomes can form stable complexes with negatively-charged therapeutic agents such as siRNA to form lipoplexes with high ability to mediate siRNA delivery and have been utilised extensively as a delivery system in mammalian cells *in vitro* [12, 25, 37]. The common features of these cationic liposomes are their water solubility and their high cationic charge density at physiological pH. Moreover, cationic liposomes can interact with negatively charged cell surfaces which is crucial for delivery into target cells as this interaction can increase cellular binding and uptake [37].

An advancement in the design of ionisable cationic liposomes has been the modulation of their apparent acid dissociation constant (pK_a), whereby values of 7 or lower were demonstrated to be of importance in siRNA encapsulation and *in vivo* activity. When the pH of the preparation medium is below the pka of the lipids, the amino groups are protonated and bear a positive charge that interact with negatively charged siRNA to form stable liposomes. In the physiological environment where the pH is 7.4, the surface of these lipids is almost neutral thus improving their circulation and reducing their toxicity. Finally, in the acidic environment of endosomes, the amino groups are protonated and their positive charge promotes interaction with anionic endosome lipids to induce destabilisation of the endosome membrane and promote the release of siRNA into the cytosol [45-47]. Currently, the most active cationic liposomes being used in clinical trials are those with pka values between 6.2-6.5 [47]. Several research groups have investigated the use of cationic liposomes for the delivery of anticancer agents. EndoTAG-1 is the first cationic liposome formulation carrying paclitaxel in clinical trials. In preclinical programmes, EndoTAG-1 inhibited tumour growth in animal experimental models such as B16 melanoma and Sk-Mel 28 melanoma [48]. Cationic liposomes have been proven to be effective in siRNA transfection. Chae *et al.* (2004) successfully encapsulated siRNA into DOTAP-containing liposomes to target the sphingosine-1-phosphate receptor 1 (S1P receptor 1) gene that has an important role in tumour angiogenesis, resulting in target gene down regulation in a mouse lung cancer model [49]. Moreover, Yano *et al.* (2004) effectively developed cationic liposomes encapsulating siRNA against human oncogene bcl-2 mRNA and found that this liposomal system could effectively reduce bcl-2 levels [50]. Although cationic liposomes offer excellent advantages as delivery systems, especially for siRNA, potential toxicities need to be considered before further clinical application [12]. The

major challenges for the excessive use of cationic liposomes are their dose-dependent toxicity, hepatotoxicity and pulmonary inflammatory response by promoting the release of reactive oxygen species (ROS) and increasing intracellular calcium levels [12, 25, 32]. Moreover, cationic liposomes can interact with negatively-charged cellular constituents such as opsonins and serum protein resulting in haemolysis [51]. In addition, cationic lipids also activate the complement system which causes rapid clearance by macrophages of the RES [12, 32]. These toxicities increase with multivalent cationic liposomes, compared with monovalent cationic liposomes [12, 25].

Several cationic liposome formulations coated with PEG, have been developed for systemic delivery of nucleic acids for gene silencing. Of these formulations, stabilised nucleic acid lipid particles (SNALPs) by Tekmira Pharmaceuticals Corporation are the most noteworthy [52]. SNALPs consist of a lipid bilayer with a mixture of ionisable cationic lipids (such as DLinDMA or more recently DLin-KC2-DMA), a lipid with a high transition temperature such as 1,2-distearoyl-sn-glycero-3-phosphocholine (DSPC), cholesterol, and PEG-modified lipids. This lipid combination allows for excellent cellular uptake and endosome escape of the nanoparticle nucleic acid contents [12, 32]. SNALPs have a mean particle size of 100 nm and have been successfully investigated for systemic siRNA delivery [53]. SNALPs have a PEG coat to shield and stabilise the vesicles and prevent early clearance. Cationically-charged lipids are favoured for siRNA complexation, and the fusogenic lipids facilitate SNALP cellular uptake and siRNA endosome escape [54].

Morrissey *el al.* (2005) were the first to confirm the effectiveness of these nanocarriers in siRNA delivery against viral diseases [55], while, Judge *et al.* (2009) developed a SNALP delivery system for siRNA against the essential cell-cycle protein, polo-like kinase 1 (PLK1) which is involved in cancer cell proliferation. In a mouse model

bearing Hep3B orthotopic liver tumours, intravenous administration of SNALP/anti-PLK1 siRNA twice a week for three weeks resulted in notable and significant tumour growth suppression [56].

1.3.1.2.2. Anionic liposomes

Phospholipids with anionic head groups are the primary components of cell membranes and are essential for membrane stability and intracellular trafficking [46]. Naturally occurring anionic lipids including phosphatidylglycerol, phosphatidylinositol, phosphatidic acid, and phosphatidylserine are found in cell membranes and play an important role in cell signalling, lipid-protein interaction and membrane trafficking [45, 46]. In a study to evaluate the lymphatic uptake of zidovudine-loaded liposomes incorporated into either cationic or anionic liposomes, Kaur *et al*. (2008) reported that anionic liposomes showed improved lymphatic uptake compared with cationic liposomes [57]. Anionic liposomes effectively increased the anti-leukemic activity of doxorubicin while reducing their chronic cardiac toxicity [58]. For the delivery of siRNA, divalent cationic bridging agent such as calcium has been used to form stable anionic lipid-siRNA complexes as a delivery system with minimal cytotoxicity compared to cationic liposomes [32]. Tagalakis *et al.* (2014) developed anionic liposomes for siRNA delivery and assessed this system *in vitro* for their physical properties, biocompatibilities, cytotoxicity, and efficacy. They found that an anionic formulation showed promising results *in vitro*, but there is a need for additional research to optimise the design, content, formulation, and characterisation of the anionic nano-complexes [53]. Moreover, Kapoor *et al.* (2012) developed an anionic liposome based on DOPG:DOPE (40:60 molar ratio) for siRNA delivery using calcium bridges and they achieved almost 99% siRNA encapsulation with this system [59].

1.3.1.2.3. Neutral liposomes

Charged lipids have been initially used for siRNA delivery, based on their success in DNA delivery, but the toxicity concerns of the cationic component and lipids remain the main challenge for such formulations. Neutral liposomes, composed of neutral lipids such as 1, 2-dioleoyl-sn-glycero-3-phosphatidylcholine (DOPC), are shown to overcome toxicities and other problems associated with cationic liposomes with high delivering efficiencies for products such as siRNA [32, 51]. Neutral liposomes show high safety profiles with low toxicities, increased circulation time, less interaction with proteins, no RES uptake, and no inflammatory cytokine induction [12, 32, 51]. This safety profile makes neutral liposomes highly attractive nano-carriers for systemic delivery. Liposomal doxorubicin (Doxil®) is a currently approved FDA anticancer medication formulated by encapsulating doxorubicin into small unilamellar neutral liposomes with PEG attached to the surface of these particles. In addition, liposomal daunorubicin (DaunoXome®) is a liposome formulation, which is formed exclusively of neutral lipids distearoylphosphatidylcholine and cholesterol, and thus also features neutral surface charge. Both formulations exhibit long circulation and high accumulation in tumour tissues [60]. Neutral liposomes have also been examined for nucleic acid delivery. Merritt *et al.* (2008) have successfully developed liposomal formulations using DOPS for the delivery of siRNA targeting oncoprotein EphA2 and proangiogenic cytokine interleukin 8 (IL-8) and proved that this formulation was highly effective *in vivo* in reducing the gene expression in a mouse model with ovarian cancer [61]. Moreover, Ozpolat *et al.* (2010) developed neutral liposomes based on DOPC as a delivery system for siRNA and reported a lack of toxicity for this system against fibroblasts, hematopoietic, and bone marrow cells compared with cationic liposomal systems [62].

1.3.2. Solid lipid nanoparticles

Solid lipid nanoparticles (SLNs), also referred to as lipospheres, form a relatively new drug delivery system. They are particles with a size range from 50 – 1000 nm and are made from lipids that remain in a solid state at room and body temperature [63]. These particles have advantages such as ease of preparation, good stability, versatile chemistry, and controlled drug release. SLNs are synthesised using solid lipids such as mono-, di- or triglycerides (e.g. tristearin, tripalmitin, trilaurin), phospholipids, lipid acids (e.g. stearic acid, palmitic acid), glyceride mixtures or waxes, cholesterol, surfactants such as Tween 80, lecithin, and sodium glycholate, which can be used in SLN engineering to increase their stability [64]. Significant research has been reported for the use of SLNs in anticancer therapeutic delivery of for example paclitaxel [65, 66]. The availability of a wide range of intravascular (IV) compatible solid lipids and surfactant choices makes these lipid nanoparticles a versatile platform for drug delivery with promising future use with different chemotherapeutics. SLNs have the advantages of physical stability over a long period as a result of the solid status of their matrix, protection of labile drugs, controlled release, low cost and ease of preparation [63, 67]. Potential disadvantages of these formulations are low drug loading capacity and drug expulsion during storage [68]. The development of newer versions of SLNs such as polymer-lipid hybrid nanoparticles, lipid-drug conjugate nanoparticles, Nanostructured Lipid Carriers (NLC) further expand the use of these lipid nanoparticles as a delivery system for different hydrophilic and ionic compounds and overcome the problems associated with SLNs [63]. SLNs are able to protect labile anticancer drugs such as camptothecin and doxorubicin and deliver them effectively to the site of action [69, 70].

1.3.3. Lipidoid nanoparticles

Lipidoid (from the Greek which means lipid-like) nanoparticles are a typical class of lipid-based molecules, which utilise cholesterol and PEG-coated lipids. Lipidoid particles are synthesised from linear acrylic alkane esters or epoxide derivatives with amine compounds via additive reactions [71]. Akinc *et al*. (2008) developed a chemical method to allow the rapid synthesis of a large library of lipidoids that can be used for siRNA delivery. These unique structures manifest as a hybrid structure between cationic lipids and first generation dendrimers [72]. The difference between the members of this library and traditional cationic lipids is that the latter are formed from a cationic head group and two hydrophobic tails while lipidoids are cationic due to the presence of reversibly protonable amine groups. Moreover, lipidoids contain upto seven tails emanating from the amine backbone [73]. Lipidoids can be used directly as a carrier for siRNA or they may replace the cationic lipids in the construction of cationic liposomes. Moreover, these formulations have been shown to provide gene silencing at lower doses of siRNA than those required by other nanoparticles, thus reducing possible toxicities [47]. One of the leading lipidoid-based nanocarriers for siRNA delivery, targeting ApoB or FVII factor, showed up to 90% reduction in the expression of these targets in hepatocytes in nonhuman primates and mice with liver cancer [72]. Brock *et al.* (2008) have developed a lipidoid delivery system to deliver siRNA targeting the HoxA1 gene for the treatment of breast cancer. They found that this lipidoid system was able to facilitate interactions with the cell membrane and endosomal escape and effectively suppressed cell proliferation and reduced mammary tumour incidence in mice [74].

1.3.4. Micelles

Micelles are colloidal systems formed spontaneously by amphiphilic molecules. The type of molecules determines the category of the resultant micelles to be either lipid, polymeric or lipid-polymeric hybrid micelles. While liposomes or niosomes have a lipid bilayer structure encapsulating an aqueous moiety, lipid micelles form a monolayer with the lipophilic tails forming the inner core and the hydrophilic heads exposed toward the aqueous environment. Micelles can vary in shape from spherical, rod-like or ellipsoidal structures depending on their composition [64, 75]. The lowest concentration of amphiphilic molecules at which micelles are formed is called the critical micelle concentration (CMC) in which at this concentration these molecules start to form the micellar structure, their assembly being driven by the decrease of free energy. Micelles are usually used as nano-carriers for the delivery of hydrophobic drugs, which are localised in the inner core of the micellar structure [76]. Lipid micellar nano-structures have a relatively low hydrophobic volume, which limits their drug loading capacity. Moreover, lipid micelles tend to dissociate upon dilution to a concentration less than the CMC *in vivo* or *in vitro* [64]. Several applications of the micellar structure in anticancer drug delivery have been carried out. The first polymeric micelles entrapping paclitaxel was Genexol-PM [77]. Hamaguchi *et al*. (2005) developed a micellar system for paclitaxel delivery that was shown to have a 25-fold improved drug accumulation in colon tumours in mice and a corresponding increase in anti-tumour activity compared to the commercial formulation Taxol® [78]. Moreover, Gill *et al.* (2012) developed a micelle-based formulation of paclitaxel and parthenolide (which is a drug that can suppress nuclear factor kappa B that is responsible for paclitaxel resistance) in a modified vitamin E micellar system. Modified vitamin E can be used as a solubiliser and a vehicle for lipid-based drug delivery formulations. This

system was shown to be significantly superior to paclitaxel or parthenolide administered alone *in vitro* [79].

1.3.5. Non-ionic surfactant vesicles

NISV, also known as niosomes, are lipid-based particles that are similar, in terms of structure to liposomes as they are composed of an aqueous moiety encapsulated by lipid bilayers, which make them able to encapsulate drugs and serve as drug carriers. Niosomes were first developed by the cosmetic industry and since then have increased in interest as a drug delivery system [80]. NISV are self-assembly vesicles composed of non-ionic surfactants of an alkyl or dialkyl polyglycerol ether and cholesterol along with other materials such as charge-inducing agents [81]. Among various non-ionic surfactants, sorbitan fatty acid esters (Spans), polyoxyethylene fatty acid esters (Tweens), alkyl ethers, and alkyl glyceryl ethers (Brijs) are commonly used to formulate niosomes [82]. These surfactants are amphiphilic molecules with both a hydrophilic head and hydrophobic tails. These compounds have no charged groups in their hydrophilic heads. Similar to liposomes, the bilayer structure of niosomes enables them to encapsulate hydrophilic substances into their aqueous core and hydrophobic molecules into their lipid bilayer [83]. Cholesterol plays a crucial part in the formation of the NISV because it can affect the cohesion of the vesicles, the mechanical strength, permeability to water and membrane rigidity [84]. Other additives are charged molecules, which enhance the overall stability of the niosomes during storage by preventing vesicle aggregation by electrostatic repulsion. Examples of these molecules include those that produce anionic surface charge such as dicetyl phosphate and phosphatidic acids and cationic surface charge such as stearylamine and cetylpyridinium chloride [81]. Interest in niosomal formulations has recently increased, not only because of their potential to carry and encapsulate a variety of drugs, but also

because of the advantages that these formulations have such as low cost, high stability and ease of storage which make them possible alternatives to liposomes. Niosomes have been investigated as potential drug delivery systems for anticancer drugs [85, 86], gene delivery [87], anti-inflammatory and anti-infective agents [88, 89], peptides [90] and many others [91, 92].

In terms of niosomes developed as anticancer delivery systems, Tavano *et al.* (2013) developed transferrin (TF) conjugate niosomes for the delivery of doxorubicin, which were shown to have greater cellular uptake and a significant reduction in viability in a dose- and time-related manner against MCF-7 and MDA-MB-231 human breast cancer cell lines [93]. Hong *et al.* (2009) successfully developed PEG-niosomes for the delivery of hydroxycaptothecin to solid tumours following IV administration. This system was shown to have strong cytotoxicity and high cellular uptake *in vitro* into three cancer cell lines (KB, K562 and S180 cells) and was proven to have high anti-tumour activity against S180 tumours in mice [94]. 5-fluorouracil (5-FU) loaded niosomes have been developed for topical treatment of different forms of skin cancers and shown improved cytotoxicity against cancer cells and high percutaneous permeation in human *stratum corneum* and epidermis membranes in comparison with the free drug [95].

1.4. Techniques for synthesising lipid-based nanoparticles

The basic principle for the formation of lipid based nanoparticles, regardless of the method of preparation, is the hydrophilic/hydrophobic interaction between lipid-lipid and lipid-water molecules with the input of energy (in the form of heating, sonication, or shaking) to aid in the arrangement of the lipid components into bilayers or micelles [96].

1.4.1. Classical methods of preparation

Four classical methods are involved in lipid-based nanoparticle preparation. The main differences between these methods is the way in which the lipids are separated from the organic solvent and re-dispersed in aqueous media [96]. These techniques involve the use of a large amount of organic solvents that have to be removed from the final formulation as the residues of these solvents could result in toxicity. Moreover, the particles produced by these methods differ in shape and size which require post-manufacturing size control steps [37].

1.4.1.1. Hydration of a thin lipid film

This is a simple and widely used method for lipid based nanoparticle synthesis which was first described in 1965 and usually referred to as the Bangham method [97]. In this method, a mixture of lipids are dispersed in organic solvent; the most common being chloroform, methylene chloride, methanol, ethanol, ether, or a mixture of these. The organic solvent is usually evaporated using a rotary evaporator at reduced pressure to form a dry lipid film on the flask wall which can then be hydrated by the addition of aqueous buffer at a temperature above the phase transition temperature of lipids, followed by agitation until the lipid film has completely dispersed [98]. The desired drug to be encapsulated in the formed vesicles can either be included in the aqueous hydration media for hydrophilic drugs or dissolved with the lipid components for hydrophobic drugs. This method results in the preparation of large multilamilar vesicles with different sizes ranging from 0.05-30 μm [99]. After particle formation, a further particle size reduction step is required to reduce the particle size to the desired range either by sonication or extrusion through polycarbonate filters [99]. Although this method is easy and widely used, it provides a relatively poor drug encapsulation efficiency of about 5-15% for water soluble drugs [26].

1.4.1.2. Reverse-Phase Evaporation (REV) Technique

This method is based on creating inverted micelles and involves two steps: 1) preparation of water-in-oil emulsion of lipids and buffer by mechanical methods or sonication in the presence of excess organic phase followed by 2) the removal of the organic phase under vacuum. The removal of the organic phase from the mixture causes the formation of large unilamellar and oligolamellar vesicles encapsulating aqueous media [31]. The particles formed by this method have a high aqueous volume-to-lipid ratio enabling encapsulation of large hydrophilic molecules [37]. This method has been reported to allow for a drug encapsulation efficiency of up to 65% [100]. Although this method can achieve high drug encapsulation, it involves exposure of the drug to organic solvents and mechanical agitation. Thus, sensitive molecules such as proteins, and nucleic acids may encounter conformational changes, protein denaturation, or nucleic acid strand breakage as a result of these harsh conditions [31].

1.4.1.3. Solvent injection method

This method involves the dispersion of lipids into ethanol or ether and the formed solution to be injected into an excess amount of aqueous media by syringe-type infusion pumps to form the nanoparticles. When ethanol is used as an organic solvent, it dissolves in water and is diluted to a point below a critical concentration which causes the dissolved lipids to self-assemble in the aqueous phase and form small particles (under 100 nm) [101]. However, since ether is immiscible with water, the ether injection method involves the injection of ether-lipid solution into a warmed aqueous phase above the boiling point of ether. Upon injection, the ether vaporises and the dispersed lipids form mainly large unilamellar vesicles with high entrapment for water-soluble drugs [102].

1.4.1.4. Detergent removal method

Lipids are solubilised with detergent to form mixed micelles followed by the removal of the detergent by controlled dialysis, column chromatography, or adsorption using Bio-Beads (Bio-Rad Laboratories, Hercules, CA) to form homogenous large unilamellar vesicles or multilamilar vesicles depending on the type of detergent used and the method of detergent removal [103]. Detergents that are commonly used in this method are those that have a high CMC in the order of 10-20 mM such as sodium cholate, sodium deoxycholate, alkyl glycoside, and Triton X-100 [31].

1.4.2. More recent preparation methods

1.4.2.1. Heating method

This is one of the newer methods that has been reported for the preparation of lipid based nanoparticles without the need to use any organic solvent. In this method, lipid components are hydrated in an aqueous media followed by the heating of these components up to 120°C with mechanical stirring [104]. This process is usually carried out in the presence of 3% (v/v) glycerol, which will increase the stability of the vesicles and does not need to be removed from the final preparation, as it is physiologically acceptable and safe. The particle size can be controlled by the nature and charge of the lipids, along with the stirring speed [96].

1.4.2.2. Spray-Drying

Spray-drying involves the dispersion of lipid components in organic solvent, followed by sonication and then spray drying under controlled conditions. Since the obtained spray-dried product is very amorphous, the dried product can be easily hydrated with aqueous media and the lipid vesicles are spontaneously produced by agitation with high encapsulation efficiencies [105]. In this method, the main factor that controls the

particle size is the volume of aqueous media used for hydrating the spray-dried product [37].

1.4.2.3. Freeze-drying of double emulsions

In this process, a homogenous dispersion of lipid components in *tert*-butyl alcohol/water co-solvent systems in appropriate ratios are used to form a clear isotropic monophasic solution. This solution is then sterilised and freeze-dried under controlled conditions and reduced pressure. Relatively homogenous dispersions of MLVs are formed spontaneously on the addition of aqueous media to the freeze-dried product followed by shaking [106]. The product can be stored in the lyophilised state and rehydrated immediately before use. The limitations of the extensive use of this method are particle size instability during freeze-drying, high cost of freeze-drying, and varying encapsulation efficiency of the produced particles [99].

1.4.2.4. Super Critical Reverse Phase Evaporation (SCRPE)

In this method, pressurised carbon dioxide with ethanol acts as a solvent in which the lipid components are initially dissolved. The vesicles are formed by rapid depressurisation with simultaneous mixing of the precipitating lipids into the aqueous phase [107]. This method yields large unilamellar particles with a size range from 0.1-1.2 μm. The organic solvent is then removed under vacuum and the resulting particles sized by filtration or extrusion. This method allows for one-step production of large unilamellar nanoparticles with high encapsulation efficiencies [99, 108]. This method has gained interest because of the antimicrobial properties of carbon dioxide, which results in sterile formulations which could be beneficial in the production of lipid-based nanoparticles for clinical use [109].

1.4.3. Modified ethanol injection methods

Recent methods based on an ethanol injection technique include the cross flow injection technique, microfluidic mixing, and membrane contractor.

1.4.3.1. The cross flow injection technique

In this method, lipids are dissolved in ethanol and injected into aqueous buffer through a cross-flow injection module (two tubes welded together forming a cross and at the connecting point there is an injection hole). The characteristics of the produced lipid particles can be controlled by different parameters such as the injection hole diameter, the buffer flow rate, the injection pressure and the lipid concentration. This method allows for scalable particle preparation for pharmaceutical applications [37, 110].

1.4.3.2. Microfluidic mixing

Microfluidics is a new approach that has recently been developed to prepare nanoparticles featuring the precise manipulation of fluids on a micrometre scale [111]. Microfluidics involves flow in channels with cross-sectional dimensions in the range of 5-50 μm where these small dimensions of the microchannel allow for fast mixing either by diffusion or convection [112]. In this method, lipids dissolved in an organic phase and aqueous phase are injected into two separate microchannels. Well-defined mixing is generated by interfacial diffusion or convection when multiple flow streams are injected into the microchannel. Upon mixing, the lipid-based nanoparticles will spontaneously self-assemble. The aqueous phase can be injected either from a single inlet to be mixed with the lipid phase or can be injected into two side inlets intersecting with the centre lipid phase inlet. Different micromixers have been designed for the preparation of lipid-based nanoparticles based on different channel layouts including a microfluidic hydrodynamic focusing (MHF) platform [113], T- or Y- shaped mixers [114], droplet based microfluidic systems [115] or a staggered herringbone micromixer

(SHM) which induces chaotic advection mixing that allows stretching and folding of fluid streams over the cross sectional area of the microchannel [116]. Microfluidics results in high encapsulation efficiency and can produce nanoparticles with a size range of 20-100 nm in diameter [111, 116, 117]. Factors that control the particle size include the flow rates of both fluids, the flow ratios of the aqueous to the lipid phase and the type of the aqueous media used [117, 118].

1.4.3.3. Membrane contractor

This method is based on permeation of the lipid phase (dissolved in ethanol) through a membrane with a specific pore size into an aqueous phase. Nitrogen gas at a pressure of less than 5 bar is used to help the organic phase pass through the pores. The aqueous phase flows on the membrane surface at the same time and removes the formed vesicles within the membrane device [119]. Factors that control the prepared particle size include the organic phase pressure, the aqueous phase flow rate and the lipid concentration [120].

1.4.4. Other methods of nanoparticle preparation

Other methods, mainly used for SLN preparation, include high shear homogenisation and ultrasound, high pressure homogenisation, solvent emulsification/evaporation, and dilution of microemulsions [68]. The direct dissolution, the film casting, dialysis, and the oil in water emulsion methods are used mainly for micelle preparation [121].

1.5. Lipid-based nanoparticle characterisation

Nanoparticle characterisation is an important factor in order to assess quality and effectiveness of these nanoparticles as drug delivery agents and to obtain quantitative and qualitative measurements that allow comparison between different batches of the produced nanoparticles. Various characteristics can be measured including the average

particle size, polydispersity index (PDI), zeta (charge) potential (ZP), lamellarity, drug encapsulation efficiencies, shape, and the extent of drug release. Other commonly monitored parameters include lipid analysis, stability, the ratio of lipid-to-drug concentration, and phase transition. These factors will have impact on the physiological behaviours of the nanoparticles and their therapeutic efficacy. A description of the most commonly used methods for nanoparticle characterisation is presented below (Table 1.3):

Table 1.3 The most commonly used methods for nanoparticle characterisation

Nanoparticles parameter	**Applied technique**
Particle size	DLS, SEC, AFM, SEM, TEM, STM, FCS, RS, NSOM, SAXS
Morphology	AFM, SEM, TEM, STM
Surface charge	ZP (Electrophoretic mobility)
Lamellarity determination	Magnetic resonance, electron microscopy, SAXS
Particle stability	DLS, drug release studies
Encapsulation efficiency	Spectrophotometry, fluorescence spectroscopy, HPLC, enzyme based methods, gel electrophoresis
In vitro drug release	Dialysis tube diffusion technique

Abbreviations: DLS, dynamic light scattering; SEC, size exclusion chromatography; AFM, atomic force microscopy; SEM, scanning electron microscopy; TEM, transmission electron microscopy; STM, scanning tunnelling microscopy; FCS, fluorescence correlation spectroscopy; RS, Raman scattering; NSOM, near-field scanning optical microscopy; SAXS, small-angle X-ray scattering; ZP, zeta potential; HPLC, high performance liquid chromatography.

1.5.1. Particle size analysis and morphology

The average particle size and distribution of lipid nanoparticles are crucial parameters to be characterised as they will regulate the circulation, distribution, and elimination of these nanoparticles [122, 123]. Several techniques are available for measuring particle size including dynamic light scattering (DLS), microscopy techniques, size exclusion chromatography (SEC), and many others.

DLS, also known as photon correlation spectroscopy (PCS), is one of the most commonly used methods which can measure the size and PDI of small particles, molecules or polymers at the nanometre scale in solution or suspension depending on the elastic light scattering when a laser light is passed through the sample [124]. This method is fast, inexpensive, non-destructive, accurate, measure the particles size in their natural environment, minimal sample volume is used, and has the ability to measure diluted samples [124, 125]. DLS does not yield any information about the particle shape and morphology. Non-reliable results might be generated in the presence of particle aggregates or dust particles. Moreover, DLS has limited utility for analysing samples with heterogeneous distribution (large PDI) along with non-accurate results for non-spherical particles as this analysis is based on the assumption that the particles are spherical in shape [124, 126].

Electron microscopy using atomic force microscopy (AFM), scanning electron microscopy (SEM), transmission electron microscopy (TEM), and scanning tunnelling microscopy (STM) provide valuable information on the shape and morphology, particle size, stability, lamellarity and the possible aggregation process of these particles during their storage [127-129]. However, these types of microscopes are complicated to use, expensive, time consuming, and require careful sample preparation as they sometimes require the removal of the lipid particles from their native environment [122]. The shape

can have influential effects on nanoparticle degradation, transport, specificity of delivery, and internalisation [130, 131]. Additionally, the shape of the nanoparticles affects biocompatibility and retention, and the disposition and translocation into tissues and organs [122, 132]. Several other techniques are used for particle size measurement including fluorescence correlation spectroscopy (FCS), Raman scattering (RS), near-field scanning optical microscopy (NSOM), nuclear magnetic resonance (NMR), small-angle X-ray scattering (SAXS), field-flow fractionation (FFF), flow cytometry and use of particle size analysers (including Mastersizer, NanoSight, qNano) [122].

1.5.2. Surface charge

The surface charge of a particle is the overall charge that a particle acquires in a particular medium. It is a physical property of the surface of any particle in suspension and it provides an index of the interaction potential between the particles [37]. Surface charge measurement is generally estimated by ZP and used to predict the stability of the particles in the colloidal system. If all the particles have a large ZP then they will tend to repel each other, preventing aggregate formation, while particles with low ZP have no force to prevent particle aggregation and flocculation. Particle suspensions with ZP > +30mV or <-30 mV are considered to be stable. ZP can be calculated using different instruments such as a Zetasizer [122, 133]. Surface charge has potential effects on receptor binding and physiological barrier penetration as positively charged nanoparticles show improved cellular uptake compared to their negatively charged or neutral counterparts thus rendering cationic nanoparticles ideal for tumour and nucleic acid drug delivery [122]. However, positively charged nanoparticles might have higher toxicity than their negatively charged counterparts [134].

1.5.3. Lamellarity determination

The number of lipid bilayers in nanoparticles will have an effect on the encapsulation efficiencies, drug release and their intracellular fate. Particle lamellarity determination can be performed by methods that are based on visible or fluorescence signal changes of lipid markers upon reagent addition [37]. Magnetic resonance is another method used for lamellarity determination which has been used to assess the distribution of lipids within bilayers and to study membrane structure [37, 135]. Other lamellarity determination techniques include imaging methods using electron microscopy and the use of small-angle X-ray scattering (SAXS) [122, 136].

1.5.4. Particle stability

The stability of nanomedicines refers to their ability to retain the same properties after being manufactured for a minimum period of time. Vesicle stability involves chemical, physical and biological stability, which are all inter-related. The evaluation of these parameters is a major determinant of the possible *in vitro* or *in vivo* application of the nanoparticles [81]. Nanoparticle stability may be affected by factors such as temperature, moisture, pH, surface charge, solvents, exposure to physiologic conditions, enzymatic degradation, microbial degradation, or the presence of other excipients in the formulation [137]. Generally, stability is determined by monitoring any changes in particle size, ZP, or drug release over time and under various conditions such as temperature and in the presence of (simulated) biological fluids [138].

1.5.5. Encapsulation efficiency and *in vitro* drug release

Lipid-based nanoparticle preparations contain a fraction of un-encapsulated drug in the same mixture of the encapsulated drug. Encapsulation efficiency (EE) is defined as the total amount of the encapsulated drug found in the particle solution *versus* the initial amount of drug used and can be expressed as:

EE= (amount entrapped/total amount) ×100

where the "total amount" is the drug used in the preparation [81].

One method to determine the EE is by separating the free drug from the encapsulated drug using ultracentrifugation or dialysis [139, 140]. Once the free drug is separated from the drug-loaded lipid nanoparticles, the lipidic structure is disrupted by methanol or Triton X-100 to release the entrapped drug. Then the amount of drug encapsulated is quantified using a method depending on the characteristics of the drug; these include spectrophotometry, fluorescence spectroscopy, high performance liquid chromatography (HPLC), enzyme based methods or gel electrophoresis (for nucleic acids) [37].

In vitro drug release can be evaluated using a dialysis tube diffusion technique [37]. In this method, a specific volume of the lipid particles is placed in a carefully selected dialysis bag and placed in a compartment containing the dissolution medium. The entire system is kept at 37°C under continuous stirring. At specific time points, samples of the dialysate are taken and analysed for the drug content by techniques depending on the drug [141].

1.6. The challenges facing nanoparticle formulation

1.6.1. Challenges related to *in vivo* nanoparticle elimination

Following IV administration, nanocarriers face the first barrier along their way to the target cells, which is removal by the RES (also termed the mononuclear phagocytic system (MPS)), which plays a key role in nanoparticle clearance. Upon entering the blood circulation, nanoparticles are adsorbed with various blood components (such as albumin, apolipoprotein, antibodies and other proteins) in a process called opsonisation which are then recognised by the RES and eliminated through RES organs such as the

liver, spleen, lungs and bone marrow [142]. Moreover, upon entry into these organs, these nanoparticles can bind non-specifically with cell membrane proteins and trigger the secretion of cytokines such as tumour necrosis factor (TNF), interleukins, and interferons leading to inflammation and toxicity that can cause tissue damage. This rapid uptake of the nanocarriers substantially reduces their accumulation at the desired target sites and reduces their half-life [14, 143]. The physicochemical properties of the nanoparticles such as shape, size, surface charge, outer surface chemistry, and hydrophobicity play key roles in mediating the process of opsonisation [143, 144]. Moreover this effect will be seen for larger nanoparticles which will be eliminated more rapidly than smaller ones [51, 145]. Usually the RES is able to trap intravenously injected particles with a size >100 nm in diameter leading to their degradation and elimination while particles with a diameter <4 nm are usually eliminated directly through renal clearance. So the optimal diameter of nanoparticles for both avoiding early clearance along with high tumour delivery should be in the range of 5-100 nm.

To overcome early opsonisation and thus elimination from the blood, nanoparticles can be engineered in terms of size, surface component, charge, and core structure to reduce this early elimination. The most commonly applied strategy to block early elimination is to graft hydrophilic polymers on the surface of the nanoparticles to induce “stealth” properties to the surface of the nanoparticles and block non-specific protein adsorption and phagocyte uptake [144]. PEG is the most commonly used synthetic polymer to prevent early nanoparticle elimination and hence increase their half-life. PEGs are hydrophilic, biocompatible, electrostatically neutral, and are flexible polymers that form an aqueous coat around the nanoparticle surface. This will reduce the degree of opsonisation and subsequent activation, uptake and elimination by the immune system which will result in increasing the residence time of the nanoparticles in the circulation

and consequently increase the accumulation of the nanoparticles within tumour tissues [26]. PEG can act as a linker for which a targeting ligand can be attached for specific targeting of the PEGylated nanoparticles and better interaction with the cell surface receptors expressed on the targeted cells [45]. PEG can take up different conformations depending on the PEG content on the surface of the nanoparticles. PEG forms a mushroom conformation when the PEG content is below 4 mol %, while it forms a transition configuration in the presence of a 4–8 mol % of PEG, whereas PEG forms a low coiled extended brush configuration at a PEG concentration above 8 mol %. The brush conformation is the ideal mode that ensures full coverage of the nanoparticle surface and hence provides full protection from opsonisation. However, it is difficult to prepare stable, PEGylated nanoparticles that have a brush configuration and maintain the integrity of their lipid membranes at the same time [3, 26]. With greater densities of PEG being employed, micelles composed of PEG-lipids may exist and destabilise the nanoparticles. So an optimum level of PEG should be used to increase the nanocarriers in circulation. In general, a PEG density of 8% to 10% is thought to be required to obtain a brush configuration, which cause optimal hindrance from protein binding, hence RES elimination [14, 37, 45, 51]. Doxil®, a liposomal doxorubicin formulation incorporating PEG-2000 (PEG-2000-DSPE) and containing around 5 mol% graft of PEG, is an example of a FDA approved PEGylated liposomal therapeutic [98]. However, stealth nanoparticles are never completely ideal and there is still some opsonisation that occurs with substantial RES uptake [51]. It has been reported that a high percentage of PEG can strictly hinder the uptake of the nanoparticles by target cells and prevent endosomal escape of their therapeutic contents once in the cellular environment due to inhibition of intracellular trafficking, which is referred to as the PEG dilemma [146]. Bearing in mind that a high PEG density will hinder the

nanoparticles from binding with target cells, several reports describe ways to overcome this problem. For example nanocarrier systems with a sheddable PEG coat with short acyl chains that quickly dissociate from the nanoparticles after injection in response to pH or reducing environment allowing them to interact with the target cells have been developed [3]. It has been found that, after repetitive dosing of PEG coated nanoparticles, anti-PEG IgM antibodies are produced as a result of the prolonged contact of the PEG containing nanoparticles with immune cells. These anti-PEG IgM antibodies bind to the surface of PEG allowing for its opsonisation and elimination, an effect called the accelerated blood clearance (ABC) phenomena. Dams *et al.* (2000) were the first to report that after IV administration of PEGylated empty liposomes, significant changes in the pharmacokinetic profile of the subsequent injected liposomes was noticed up to four weeks after the first injection [147]. ABC will result in a significant decrease in the half-life of the subsequently injected doses [148, 149]. The design of PEGylated nanocarriers with a sheddable PEG coat, such as rapidly diffusible PEG [150] or serum esterase sensitive PEG [151], have been used to avoid the production of anti-PEG antibodies and subsequent ABC. Although there are reports suggesting that the ABC phenomenon might not be PEG-specific and is dose-dependent, the anti-PEG mechanism is still of concern [3]. Regarding the effect of the PEG acyl chain, as the acyl chain length increases, the residence time of the PEG on the nanoparticle surface increases, thus preventing nanoparticle interaction with cells and subsequently with the endosomal membrane [47]. The rate of anti-PEG IgM antibody production, and as well as the ABC rate, are proportional to the length of the PEG alkyl chain. In the work of Judge *et al.* (2006) the replacement of 18C alkyl chain PEG by the 14C moiety resulted in a 10-fold reduction in the production of anti-PEG IgM which was explained by the increase of the diffusion rate of the PEG out of the

lipid bilayer [152]. Tagami *et al*. (2009) showed that the systemic administration of PEG-coated lipoplexes containing siRNA caused anti-PEG IgM antibody production which further enhanced ABC of subsequent doses [153]. This production of anti-PEG IgM antibody was also observed with immunostimulatory plasmid deoxyribonucleic acid (pDNA) associated liposomes, coated with PEG and administered systemically [154]. This suggests that the use of immunostimulatory nucleic acids will further increase IgM production [52]. So in order to diminish the ABC phenomena on a nanocarrier, it is important to use non-immunogenic therapeutics in order to minimise the production of anti-PEG antibodies [51].

Other than PEG, hydrophilic polysaccharides, HPMA (poly [N-(2-hydroxypropyl) methacrylamide]), PVP (poly (vinylpyrrolidone)), PMOX (poly (2-methyl-2-oxazoline)), PAcM (poly (nacryloylmorpholine)), PAA (poly (acrylamide)), PG (poly(glycerol)), PVA (poly(vinylalcohol)), pNIPAM (poly(n-isopropylacrylamide)), pAAs(poly(amino acids)), and PEG-containing copolymers such as poloxamers, poloxamines and polysorbates are examples that can provide a hydrophilic stearic coat and increase the half-life of nanoparticles in the circulation [155, 156]. However, the lack of consistent experimental data makes it difficult to directly compare them with PEG. In particular, these polymers are thought to avoid the ABC effect and have a lower viscosity than PEG which would make them an alternative to PEG, but more experimental and characterising studies are required before implementation of their wide application [156]. Finally, the ABC phenomenon depends on particle size, since small (9.7–31.5 nm) polymeric micelles with a PEG coat do not show ABC [157]. Therefore, the ideal stealth structure is one that contains sufficient PEG to allow prolonged circulation and efficient accumulation at the target site, but at the same time

it needs to be rapidly eliminated after delivery to avoid systemic overexposure and an ABC effect [37, 51].

1.6.2. Challenges related to the manufacturing process

The first challenge of manufacturing is related to physico-chemical characterisation of nanoparticles. Structure, composition, size, charge, dispersity, porosity, aggregation behaviour, drug loading and release profiles are among the main physico-chemical features of nanoparticles [158]. Variability within these features makes it difficult to predict the behaviour of the formulation before and after administration. Moreover, nanoparticles may interact with different biological fluids (e.g. blood) and various molecules (e.g. proteins and antibodies) after administration. This interaction might lead to aggregation which might alter the effect of the nanoparticles in biological systems. Other issues include stability and storage which might affect the overall physico-chemical properties of the nanoparticles which might have an impact on the behaviour of these formulations *in* vivo [159]. The second challenge in manufacturing is related to nanoparticle safety. Addressing safety and toxicity is an important part in the development of nanoparticles based medicines. Several studies have reported toxicity concerns of nanoparticle-based therapeutics [142]. This has led to the emergence of nanotoxicology as an independent field of research [160]. Features such as particle size, charge, hydrophobicity and many others affect the interaction of the nanoparticles in a biological environment and their subsequent toxicological effects [159]. Acute toxicity of nanomedicines usually involve RES activation, inflammation, haemolysis, oxidative stress, or impaired mitochondrial function [161, 162].

The third challenge is related to the large scale production of nanoparticles. The development of new nanomedicines usually starts at laboratory scale, which involves the production of small amounts of these formulations. However, due to the various

physico-chemical features of the nanoparticles, batch-to-batch variations may occur in large-scale production [163]. Therefore, industrial scale production of nanoparticle-based anticancer medicines requires strict control of all the physico-chemical properties on a batch to batch basis.

The fourth challenge is the cost. The relatively high cost of the raw materials used to prepare the different types of lipid based nanoparticles, multi-step production processes, and many post-manufacturing characterisations makes the production of nanomedicines expensive. The production of Doxil®, which is a FDA-approved liposomal doxorubicin, is much more expensive than the production of the free drug.

The fifth challenge involves regulatory issues in nanoparticle formulation. Although there is a significant increase in nanomedicine research and an increasing number of clinical studies implementing these therapeutics, regulatory agencies such as the FDA and European Medicines Agency (EMA) to date have not issued specific guidelines for controlling these nanomedicines. This makes any regulatory decisions on nanoparticle-based drugs reliant on an individual case by case assessment of the applied drug [142]. In 2014, the FDA issued guidance for industry that defined nanomaterials entitled "Considering Whether an FDA-Regulated Product Involves the Application of Nanotechnology" [164]. However, it is now crucial for the regulatory authorities to refine and standardise specific requirements and prerequisites for the approval of nanoparticle-based medications.

1.7. Targeting lipid-based nanoparticles into tumour cells

The ability to target nanoparticle drug delivery systems, including lipid-based nanoparticles, is an interesting feature in the field of drug delivery in order to increase the selectivity and accumulation of the anticancer drugs into tumour cells while

reducing unwanted toxicities on normal cells. The major advantages of using nanoparticles that are targeted into tumour cells include improving the pharmacokinetics and pharmacodynamics of the encapsulated drug, development of controlled release formulations, increasing the specificity into cancer cells and reducing the toxicity along with enhancing the cellular uptake and intracellular delivery of the anticancer drugs [165]. Two types of targeting strategies are possible: passive and active targeting.

1.7.1. Passive targeting

Passive targeting is achieved by utilising the unique pathophysiology of tumour cells and the physiochemical properties of the nanoparticles. Usually particles with a mean size of 100-200 nm are attractive for tumour targeting as particles with this size range tend to accumulate passively in tissues with leaky blood vessels with abnormal architecture (i.e., tumour and inflamed tissues) after IV administration due to large inter-endothelial junctions, increased numbers of fenestrations and abnormal basement membranes of these tissues [98]. Healthy tissues such as muscles that have normal vascular endothelial have limited permeability to particles with this size range, which reduce the unwanted side effects of the encapsulated drugs in these tissues [45]. Moreover, the lack of the lymphatic drainage system in the tumour tissues also enhances the retention of nanoparticles that penetrate the extracellular matrix from the systemic circulation. Consequently, nanoparticles loaded with anticancer drugs entering tumours will not be efficiently removed by the lymphatic system which will enhance nanoparticle accumulation in the tumour [26]. These two factors form the enhanced permeability and retention (EPR) effect phenomenon. This passive phenomenon plays a major role in the passive targeting of nanoparticles [26]. Only nanoparticles with a long half-life will have the chance to accumulate at the leaky tumour vasculature, thus

producing stealth nanoparticles with reduced RES uptake as an important prerequisite for enhanced tumour targeting [47].

1.7.2. Active targeting

Active targeting with nanoparticles can be achieved through surface modification of the nanoparticles with tumour cell specific ligands that can recognise and bind to complementary molecules or receptors that are over expressed on the surface of the targeted cells. This approach can enhance the selectivity of the targeted nanoparticles towards cancer cells. Antibodies and antibody fragments such as monoclonal antibodies, fragment antibodies, and single chain fragment variable antibodies, peptides and proteins such as transferrin, small molecules such as folic acid, and aptamers are the most extensively studied ligands [54]. The most commonly studied receptors with nanoparticles for active cancer cell targeting include, TF receptors, folate receptors, epidermal growth factor receptors (EGFR), cell surface glycoproteins, and single-stranded DNA (ssDNA) and RNA aptamers [26]. Kobayashi *et al*. (2007) developed liposomal doxorubicin conjugated to TF to target multidrug resistant human small cell lung cancer and compared it with free drug and non-targeted liposomes. In their model, the TF conjugated liposomal doxorubicin showed significantly higher accumulation of doxorubicin in cancer cells with higher cytotoxic effects compared to the free and non-targeted formulation [166]. Furthermore, Yang *et al.* (2014) examined a murine *in vivo* model with human epidermoid carcinoma (KB) treated with stealth liposomes containing ursolic acid and modified with folate conjugates to target folate receptors. Their work showed that the targeted liposomes were reported to have the longest lifespan compared to the non-targeted formulations and free drug [167]. Sato *et al.* (2007) developed a targeted cationic delivery system, galactosylated cationic liposomes (GCLs), for targeted siRNA delivery to downregulate the endogenous hepatic gene

Ubc-13 in hepatic carcinoma cells. *In vivo* results showed the targeted siRNA-GCLs were able to inhibit Ubc-13 gene expression by 80%, compared to non-targeted liposomes and naked siRNA, which did not induce any effects on Ubc-13 gene expression [168]. A novel targeted cationic liposomal system for siRNA delivery based on DOTAP and DOPE, targeted against HER-2, was developed by Pirollo *et al.* (2006). In this system an anti-TF receptor single chain antibody fragment (TfRscFv) was used as a targeting ligand to target the over expressed TF receptors in cancer cells and *in vivo* experiments confirmed the ability of this system to deliver siRNA to different tumours in mice [169].

1.8. Nanoparticles in RNAi therapeutics

There is a growing need for new effective and safe treatment options for cancer to treat the increasing number of cancer cases with minimal side effects. One promising field is gene therapy with nucleic acids such siRNA.

One of the most significant advances in biology was the discovery of RNA interference (RNAi) by Fire *et al.* (1998) who discovered that double-stranded RNA (dsRNA) caused potent and specific interference of gene expression in the nematode *Caenorhabditis elegans* [170]. Following this discovery, Elbashir *et al.* (2001) were among the first to investigate the application of RNAi for the treatment of human disease in which they demonstrated that synthetic siRNA can specifically interfere with gene expression in several human cell lines [171]. The *in vivo* effects of RNAi and its therapeutic potential was then demonstrated in adult mice by effective targeting of a sequence from the Hepatitis C virus [172]. Since then, there has been a significant increase in research in this field to investigate the possible clinical application of this technology to treat different diseases [173]. RNAi is an endogenous post-

transcriptional gene regulatory mechanism where non-coding, dsRNA molecules interfere with the expression of certain genes in order to silence them [173]. siRNA, an example of molecules that follow this regulatory pathway, are small RNA molecules with an ability to regulate the expression of genes and have great potential for treatment of various drug resistant diseases. siRNA are dsRNA composed of 21-23 base pairs (bp) in length with a characteristic and highly specific sense and antisense strand structure [174]. In mammalian cells, siRNA can be generated by the activity of RNase III endonuclease dicer on long dsRNAs or short hairpin RNAs (shRNAs). Once in the cytoplasm, siRNA is incorporated into an RNA-induced silencing complex (RISC) followed by its cleavage into sense and anti-sense strands. While the sense strand is expulsed from the complex, the anti-sense strand remains bound to the RISC. The activated RISC shuts down messenger RNAs (mRNAs) which is perfect or near perfect complementary to the siRNA anti-sense strand and triggers the cleavage of this mRNA by an RNA endonuclease (Argonaut 2) [175]. This cleavage occurs between base 10 and 11 relative to the 5′ end of the antisense siRNA strand and causes silencing of the gene encoded (Figure 1.2). After releasing the degraded fragments of mRNA, the RISC will regenerate for a new round of mRNA cleavage by siRNA [12, 176].

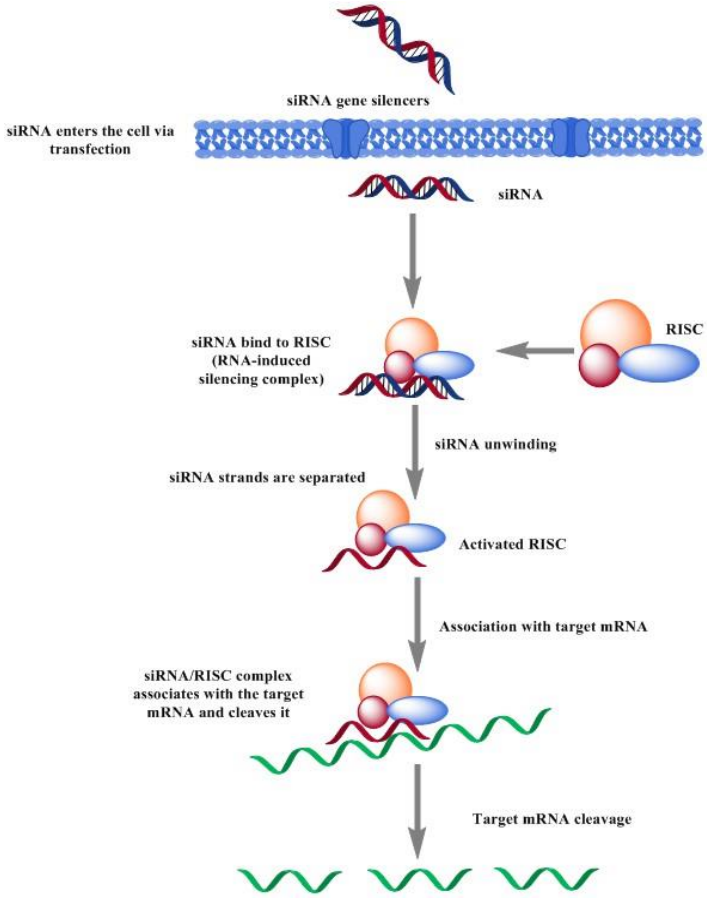

Figure 1.2 Schematic diagram of the mRNA degradation through siRNA

siRNA has shown promising results as a therapeutic agent for cancer, infection, human immunodeficiency virus (HIV), and diabetes [177]. For therapeutic applications, synthetic siRNA is designed to target overexpressed or mutated oncogenes and genes that are involved in cancer cell proliferation, survival, invasion, angiogenesis, metastasis, oncogenesis, cell cycle regulation, apoptosis, cell senescence, tumour host interaction and resistance to chemotherapy or radiotherapy [5, 12]. siRNA is a promising therapeutic molecule that has different advantages compared to conventional therapies. siRNA interfere with the function of endogenous gene expression in the cytoplasm with high specificity and low toxicity whereas traditional drugs act either by blocking or activating their targets. Also in comparison to traditional drugs, the

discovery and identification of gene specific siRNA is less time consuming, less expensive and provides more potent and specific medications [47, 54]. Moreover, siRNA have a lower possibility of causing non-specific side effects and thus have a high safety profile [178].

1.8.1. Therapeutic applications of siRNA

Use of siRNA acts as a loss-of-function strategy that can be used to inhibit the expression of any target protein of known sequence [179]. Each patient has a unique spectrum of gene mutations and the unique target specificity of siRNA makes personalised treatment for each patient possible based on individual overexpressed genes [32]. siRNA has been successfully tested as a therapeutic agent *in vitro* in a number of studies. For example, β-secretase 1 (BACE1) enzyme, which is an integral membrane glycoprotein that is involved in Alzheimer's disease, has been successfully suppressed by siRNA targeting its expression in different cell systems [180]. The RNAi mechanism could potentially be used for the treatment of a long list of human diseases including viral infections, genetic disorders, autoimmunity, and cancer [173]. The potential efficacy of siRNA-based treatments has been demonstrated in melanoma [181], lung cancer [182], bladder cancer [183], prostate cancer [184], and ovarian cancer [185]. However, the development of siRNA-based therapeutics has been hampered by some limitations such as the determination of the target gene that is involved in cancer progression and the development of a proper delivery system to carry siRNA specifically to its target cells [179]. Unmodified (naked) siRNA are rapidly degraded and cleared by nucleases which results in a short half-life. The half-life reported for unmodified siRNA in serum ranges from several minutes to around an hour [186-189]. Moreover, naked siRNA has a large molecular weight (approx. 13kDa) with a high negative charge on the siRNA phosphodiester backbone (approx. 40 negative

phosphate charges) which makes it difficult to freely cross cellular membranes as a result of electrostatic repulsion with the negatively-charged cell membrane [190]. Finally, siRNA has possible side effects such as immunogenicity, off-target effects, saturation of RNAi machinery and competition within the miRNA pathway [13, 32, 52]. That is why earlier studies using siRNA-based therapies entered clinical trials that were limited to local application of siRNA, including intravitreal and intranasal routes [37].

Many anatomical and physiological barriers in the human body hamper the systemic delivery of siRNA. The first barrier includes renal clearance and removal by the RES in the liver, spleen, lung and bone marrow. The second barrier is the endothelial lining and extracellular matrix that prevents the therapeutic molecules from reaching their target tissue. The third barrier is endosome escape and subsequent biodistribution. After siRNA is successfully delivered to the cells, how it can escape the endosome is a major challenge. If siRNA remains in the endosome for a long time, it will be degraded and eliminated [46, 53]. Therefore, wide and effective application of siRNA therapeutics depends on the development of effective and safe delivery systems that can protect the siRNA from nucleases and facilitate its access to intracellular sites of action with high specificity and minimal toxicity as in the case of oligonucleotide delivery [178, 190].

When designing a carrier system for siRNA, multiple parameters have to be taken into consideration to increase the siRNA half-life and avoid any extra and intracellular barriers before the siRNA can reach its target mRNA [52]. At tumour level, nanoparticles containing siRNA must diffuse through the extracellular matrix, spread all over the tumour mass and upon accumulation the targeting moiety at the surface of the nanoparticles should recognise the overexpressed receptors on the tumour cells' surfaces. The delivery system encapsulating siRNA must then be internalised by the

target cells, usually by receptor mediated endocytosis, then it must be released from the endosomal compartment into the cytosol where the RNAi process and the complementary mRNA is located while avoiding lysosomal enzyme degradation [52]. Pore formation and membrane disruption on the endosome membrane are common strategies for siRNA molecules for endosome escape. Fusogenic lipids, cell penetrating peptides, chemical agents and pH buffering polymers are frequently used materials in siRNA-nanoparticles to help in endosome escape [47, 54]. siRNA-nanoparticles can be modified by short cationic amphiphilic peptides (AMPs), which will bind to the endosome lipid bilayer leading to internal membrane tension which will finally create pores in the endosome membrane and improve siRNA endosome escape [54]. pH sensitive and polycationic lipidic carriers in the endosome with high proton buffering capacity induce extensive ion and water inflow into the endosome with subsequent endosome membrane rupture and siRNA release [52, 54]. Other major challenges for siRNA-based therapies include minimising off-target effects (including saturation of the indigenous RNAi machinery), increasing resistance to nucleases, controlling the specificity of the siRNA, and avoiding immune responses such as α/β interferons and toll-like immunity that can lead to systemic inflammation *in vivo* through inducing the production of type I interferons and inflammatory cytokines [25, 46].

Many different types of nanocariers have been investigated as a possible delivery system for siRNA to provide solutions to expand their clinical application. Currently lipid-based nanoparticles are the most promising for systemic application which can be easily engineered to avoid early clearance from the body. In this regard, major advances have been achieved by the development of PEGylated liposomes and SNALPs which have been the most extensively tested systems for the delivery of siRNA [47]. High yields have been observed with cationic particles such as cationic liposomes as they

will form stable siRNA-lipid complexes with high delivering efficiencies [191, 192]. Biodistribution studies in mice of cationic lipid nanoparticles carrying siRNAs have shown that they have a maximal value at five minutes post-injection followed by a rapid decline to 72 hours post-injection and then a slower decline for 65 days post-injection [193]. Moreover, siRNA is an anionic molecule which can be easily encapsulated inside the aqueous core of the lipid nanoparticles such as liposomes and niosomes [51]. The encapsulation of siRNA into lipid nanoparticles protects them from enzymatic degradation, facilitates their uptake by tumour cells and promotes their escape from the endosomal compartment after delivery, resulting in efficient cytoplasmic delivery [32, 51].

1.8.2. siRNA in clinical trials

Significant progress has been made for the development of an effective siRNA-based medication since the discovery of the RNAi mechanism, with several potential siRNA medications evaluated in clinical trials. The first siRNA-based drug in clinical trial was for the treatment of macular degeneration, targeting the vascular endothelial growth factor (VEGF) pathway, and used naked siRNA [46]. Since then many siRNA-based therapeutics have entered clinical trials for local or systemic disease treatment (Table 1.4). With the development of siRNA delivery systems, there has been an increasing number of siRNA-based therapies that have entered systemic clinical testing, although the use of naked siRNA continues to be explored [194]. Currently, more than twenty siRNA-based therapeutics have undergone clinical trials and several of these are in Phase III trials with most trials using lipid-based nanoparticles [195]. Several clinical trials targeting a variety of cancer types with siRNA using different types of nanocarriers are currently underway. These include APN401, TKM-PLK1, siG12D LODER, and many others (Table 1.4). APN401 is an ongoing Phase I clinical trial to

determine the side effects and best dose of siRNA in treating patients with different types of cancers (NCT02166255) [196]. TKM-PLK1 is siRNA based anticancer treatment using lipid based nanoparticles against polo-like kinase (PLK) currently in Phase II clinical trials after promising results from Phase I trials to treat patients with hepatocellular carcinoma (HCC), Gastrointestinal Neuroendocrine Tumors (GI-NET), and adrenocortical carcinoma (ACC) (NCT01437007, NCT01262235, NCT02191878) [197]. Silenseed Ltd, has developed a drug called siG12D LODER, composed of polylactic glycolic acid (PLGA) for siRNA delivery targeting KRASG12D which is a mutant version of the KRAS (Kirsten rat sarcoma) gene overexpressed in the majority of pancreatic ductal adenocarcinomas and they have completed a Phase I/II clinical trial (NCT01188785) and are beginning a Phase II trial (NCT01676259). Moreover, the M.D Anderson Cancer Centre is undertaking a Phase I clinical trial targeting EphA2, which is a cell surface receptor tyrosine kinase involved in neuronal cell migration and overexpressed in solid tumours using siRNA encapsulated in neutral liposomes (siRNA-EphA2-DOPC) (NCT01591356) [198]. Dicerna has developed a liposome-based delivery system for a RNAi therapeutic to target MYC oncogene, which is a gene associated with oncogenesis and its expression is upregulated in many types of cancer, and has initiated clinical trials in patients with advanced hepatocellular carcinoma [199]. Alnylam Pharmaceuticals has two products in their pipeline for siRNA delivery using lipid nanoparticles for cancer treatment which target transthyretin (TTR) in patients with transthyretin mediated amyloidosis (ATTR) (NCT01960348) and VEGF and kinesin spindle protein (KSP) in patients with advanced solid tumours with liver involvement (NCT00882180). Moreover, some trials are currently on the way with different combinations between siRNA-based therapies with other treatment modalities such as chemotherapy and radiotherapy [200].

These clinical trials and many others for the treatment of different types of cancer provide hope for developing new treatments for cancer and avoiding conventional chemotherapeutics. Continued success in the field of siRNA therapy depends on the improvement of the delivery systems and increasing their ability to carry siRNA to the targeted cells with improved pharmacokinetics and minimum toxicity.

Table 1.4 Selected clinical trials of siRNA

Drug name	Disease	Target	Delivery system	Manufacturer	Status	ClinicalTrials.gov Identifier
APN401	Metastatic tumors not removable by surgery	Cancer Vaccine	-	Apeiron	Phase 1	NCT02166255
TKM-PLK1	HCC, ACC, GI-NET	PLK	SNALP	Arbutus	Completed Phase I/II	NCT01262235 NCT02191878 NCT01437007
siG12D LODER	Pancreatic cancer	KRAS-G12D	LODER polymer	Silenseed Ltd	Phase II	NCT01676259
siRNA-EphA2-DOPC	Solid tumour	EphA2	Neutral liposomes	M.D Anderson	Phase I	NCT01591356
ALN-TTR02	ATTR	TTR	Lipid nanoparticles	Alnylam Pharmaceuticals	Phase III	NCT01960348
ALN-VSP02	Advanced solid tumours with liver involvement	VEGF, KSP	Lipid nanoparticles	Alnylam Pharmaceuticals	Completed Phase 1	NCT00882180
Atu027	Advanced solid tumours	PKN3	Lipid nanoparticles	Silence Therapeutics	Completed Phase 1, completed Phase Ib/IIa	NCT00938574 NCT01808638
ALN-RSV01	RSV	RSV nucleocapsid	Naked siRNA	Alnylam Pharmaceuticals	Completed Phase II	NCT01065935
TKM-100201	Ebola Virus Infection	EBOV polymerase L, VP24, and VP35 regions	SNALP	Tekmira Pharmaceuticals	Terminated Phase 1	NCT01518881
Bevasiranib	Wet AMD, Diabetic AMD	VEGF	Naked siRNA	OPKO Health, Inc.	Terminated Phase III, completed Phase II	NCT00499590, NCT00306904
SYL040012 (bamosiran)	Open Angle Glaucoma, Ocular Hypertension	ADRB2	Naked siRNA Eye drop	Sylentis	Completer Phase II	NCT02250612
CALAA-01	Solid Tumor	RRM2	Cyclodextrin nanoparticles	Calando Pharmaceuticals	Terminated Phase 1	NCT00689065

DCR-MYC	Solid Tumours with liver metastasis Multiple myeloma Non-Hodgkin's lymphoma, Hepatocellular Carcinoma,	MYC	Lipid nanoparticles	Dicerna Pharmaceuticals	Phase I, Phase Ib/II	NCT02110563, NCT02314052

Abbreviations: PLK, polo-like kinase; HCC, Hepatocellular Carcinoma; GI-NET, Gastrointestinal Neuroendocrine Tumors; ACC, Adrenocortical Carcinoma; TTR, transthyretin; ATTR, transthyretin mediated amyloidosis; VEGF, vascular endothelial growth factor; KSP, kinesin spindle protein; PKN3, protein kinase n3; RSV, respiratory syncytial virus; VP24, virus protein 24; VP35, virus protein 35; ADRB2, adrenergic receptor B2; RRM2, ribonucleotide reductase subunit M2; SNALP, stable nucleic acids lipid particles.

1.9. Project aim

Nanoparticles are an established technology and as their research has matured, this has led to the clinical introduction of a number of lipid-based drug delivery systems. These have enhanced the therapeutic profile of new and existing drugs and allowed better clinical outcomes to be realised. Various types of these nanoparticles have opened up many promising options towards cancer treatment through the applications of new therapeutic options such as gene therapy with siRNA. The translation of these products from bench to bedside has proved to be challenging to the regulatory authorities, since often their diverse and unique composition and structures to deliver stratified or personalised medicine has prevented a generic regulatory framework to be applied. However, as additional experience of nanotechnology-based products entering the clinic is derived from robust pharmacovigilance, regulatory frameworks will evolve, and the relative merits of particular delivery systems and associated manufacturing methods will become better understood to further drive innovation in an area that holds tremendous promise to revolutionise advances in biotechnology.

Pre-clinical data and clinical trials with different siRNA therapeutics have now confirmed the effectiveness and safety of siRNA-based therapies as a potential treatment of different diseases such as cancer. siRNA therapeutics have a promising future and they are considered a revolutionary class of drug molecules. However, many challenges and barriers such as siRNA stability, immunogenicity, and systemic delivery still need to be resolved for the full application of these therapeutics. The effective application of siRNA based medications rely on the development of delivery systems that can carry siRNA and protect them from degradation, increase their circulation time, specifically deliver their load to target tissues, and induce a rapid endosome escape.

Different nanoparticle systems have been used for this purpose each with various advantages and disadvantages based on their composition, structure, physical, and chemical characteristics. Among these, lipid-based nanoparticles have several advantages as a drug delivery system including ease of formulation, long circulation time, and the feasibility to include ligand binding polymers for targeting.

The major aim of this project was to formulate optimised NISV for siRNA delivery in order to increase the circulation time of their siRNA load with successful delivery to the target site. NISV for siRNA delivery is a new area that has not been extensively investigated. NISV provide a good alternative to liposomes, with lower production costs and higher stability. NISV in their structure resemble liposomes as well as naturally occurring cell membranes, which facilitate their uptake by target tissues. The optimised NISV should have high stability and minimal toxic effects. Figure 1.3 represents a diagram showing how NISV could be used to encapsulate siRNA, allow them to interact with cells, and then deliver siRNA to the cytoplasm where the RNAi mechanism occurs.

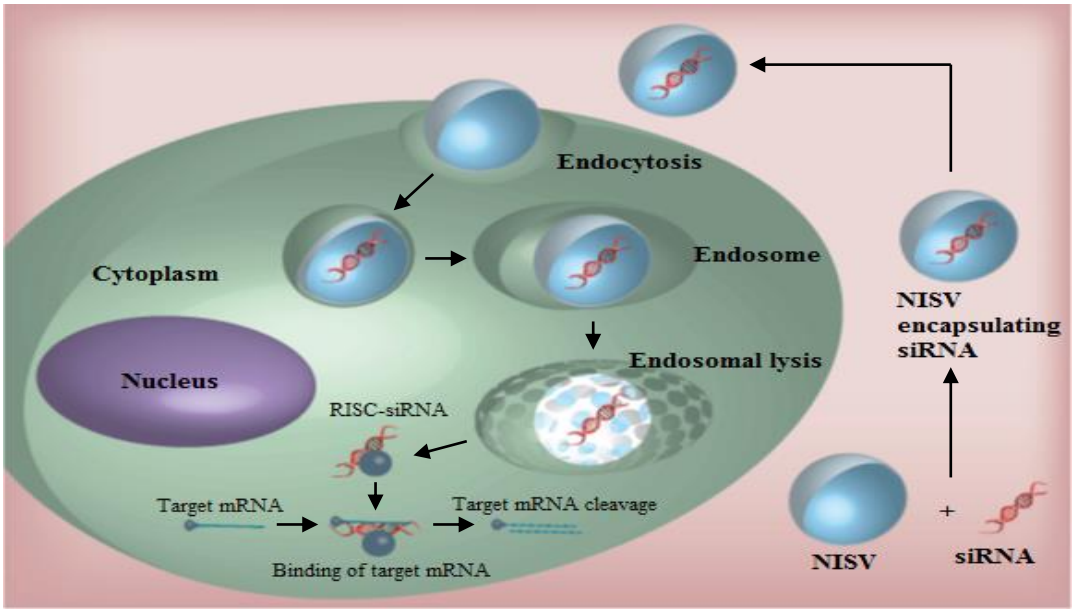

Figure 1.3 Schematic diagram representing the encapsulation of siRNA into NISV followed by the internalisation by the cell and siRNA release into the cytoplasm. siRNA then associate with the RISC and degrade the target mRNA that is complementary to the antisense strand of siRNA. (Adapted from Paecharoenchai *et al*., 2013).

For the formulation of NISV, different manufacturing methods such as the conventional film-hydration method, heating method, and microfluidic mixing were explored (Chapter 2). NISV resulting from each method was evaluated based on their size, charge, and morphology and then the best manufacturing method to proceed with was used in further experimentation. For vesicle physiochemical characterisation, AFM, SEM, dynamic light scattering, fluorescence microscopy were used. Then the effect of the type of aqueous media used in NISV formulations by microfluidics was evaluated in Chapter 3 to further optimise the formulations. After optimising the method of formulation and related factors, different NISV formulations were prepared and the most favourable formulations were tested *in vitro* on different cell lines (Chapter 4). This included evaluating their cytotoxicity on A375, PNT2, and A549 cells. The selected NISV formulations were then evaluated for their abilities to encapsulate siRNA and deliver them to the target cells (which were A549 and B16-F10-LUC cells). These cell lines

were chosen as cancer models as they are among the most common cancer types worldwide. The EE of negative control siRNA in different NISV formulations was evaluated using the Quant-iT™ microRNA Assay Kit. The percentage cellular uptake of siRNA was evaluated using fluorescence activated cell sorting (FACS). After evaluating the cellular uptake, the most efficient formulations were loaded with siRNA targeting green fluorescent protein (GFP) in A549 cells or luciferase enzyme in B16-F10-LUC cells. In Chapter 4, GFP expressed by A549 cells was knocked-down by siRNA. The effectiveness of the used siRNA in protein knockdown was evaluated through fluorescence measurements, FACS, PCR, and Western blotting. In Chapter 5, the effectiveness of NISV in siRNA transfection was evaluated in B16-F10-LUC cells, targeting luciferase enzyme to confirm the results obtained in Chapter 4. The efficacy of luciferase suppression was evaluated using a luciferase assay system to quantify the luciferase levels for cells treated with siRNA encapsulated in NISV and compared with cells treated with naked siRNA. Following these *in vitro* experiments, the most effective formulation was then used to evaluate its efficacy in luciferase enzyme knock-down by siRNA *in vivo* in nude mice through intra-tumoural injection.

Chapter 2

Comparison of the physical characteristics of monodisperse NISV prepared using different manufacturing methods

Abstract

NISV are synthetic membrane vesicles formed by self-assembly of a non-ionic surfactant, often in a mixture with cholesterol and a charged chemical species. Different methods can be used to manufacture NISV, with the majority of these requiring bulk mixing of two phases. This mixing process is time-consuming and leads to the preparation of large and highly dispersed vesicles, which affects the consistency of the final product and could hinder subsequent regulatory approval. In this study, the physical characteristics of NISV prepared using two conventional methods (thin-film hydration method and heating method) have been compared with a recently introduced microfluidic method. The resulting particles from these methods were assessed for their physical characteristics and *in vitro* cytotoxicity. Using microfluidics, nano-sized NISV were prepared in seconds, through rapid and controlled mixing of two miscible phases (lipids dissolved in alcohol and an aqueous medium) in a microchannel, without the need of a size reduction step, as required for the conventional methods. Stability studies over two months showed the particles were stable regardless of the method of preparation and there were no differences in terms of EC_{50} on two human cancer cell lines: A375 (human melanoma cancer cells) and A2780 (breast cancer cells). However, this work demonstrates the flexibility and ease of applying lab-on-chip microfluidics for the preparation of NISV that could be used to significantly improve formulation research and development, by enabling the rapid manufacture of a consistent end-product, under controlled conditions.

Key words: Non-ionic surfactant vesicles, microfluidics, thin-film hydration, heating method, drug delivery, cytotoxicity.

2.1. Introduction

NISV or "niosomes", are synthetic bilayer vesicles typically formed by the self-assembly of non-ionic surfactants [81], cholesterol and the addition of a charged species. The self-assembly of non-ionic surfactants into bilayer vesicles, first reported in the 1980s by a group of cosmetic researchers from L'Oréal industries [201], have since been applied extensively as drug delivery systems. NISV exhibit more advantages over liposomes, in terms of cost and stability, and constituent surfactants have a wider range of chemistries that can be selected to provide greater potential for innovation related to vesicle composition [81, 83].

NISV have been used to deliver hydrophilic drugs that are encapsulated in the interior aqueous compartment or adsorbed on the bilayer surface, and hydrophobic drugs that are localised within the lipid bilayer of the NISV [84]. NISV have also been used to improve solubility and subsequent bioavailability of poorly soluble drugs, as exemplified by aciclovir and griseofulvin [202, 203]. Moreover, these particles can also improve the stability of peptide drugs, e.g. they have been shown to protect encapsulated insulin in the gastrointestinal tract from degradation by proteolytic enzymes and exhibit good stability in the presence of bile acid salts such as sodium deoxycholate [90]. In recent years, NISV have also been used as carriers for contrast agents for clinical imaging applications in medical diagnostic tools [92].

Various conventional bulk methods have been used in the preparation of NISV (e.g. thin-film hydration, reversed phase evaporation, and heating methods), which utilise mixing of two liquid phases on a bench scale at elevated temperature, in order to facilitate spontaneous self-assembly of the lipid components into bilayer vesicles [81, 204, 205]. The hydration of a thin lipid film is a simple and widely used process, in which a mixture of lipids are dispersed in an organic solvent (such as chloroform) followed by evaporation of the solvent using a rotary evaporator to form a dry lipid film on the flask wall. NISV are then self-assembled by hydrating the lipid film with an aqueous buffer at a temperature above the phase transition temperature

of lipids [97]. Another method reported by Mozafari *et al*. is the heating method [206], in which NISV can be prepared without the use of organic solvents, where the various components are hydrated in aqueous media at room temperature followed by heating at 120°C with mechanical stirring [207]. However, the methods described above, result in the production of large particles, with high polydispersity, as a result of inadequate control of chemical and mechanical environments. These methods necessitate the use of post-production size-altering steps, such as extrusion or sonication, in order to obtain smaller and more homogeneous vesicle dispersions [81, 205].

The ability to control vesicle size and polydispersity is a crucial factor in the success of any manufacturing method as the particle size of the delivery system influences *in vivo* performance [208]. Microfluidic mixing is a recently developed method used to prepare liposomes, which results in the production of small vesicles with efficient encapsulation of a therapeutic agent [209]. In microfluidics, lipids are dissolved in an organic phase and the aqueous phase is introduced from different inlets into a precisely defined microchannel that allows for fast mixing between the two phases at high flow rates and at a temperature above the phase transition of the lipids. By controlling flow rate ratios (FRR) between the aqueous and organic phase and total flow rates (TFR) of both phases, homogeneous small vesicles can be prepared in a single step [208, 210].

2.1.1 Chapter aims

The main objective of this work was to compare the characteristics of NISV prepared by these different manufacturing methods. Previously reported work has successfully investigated the development of NISV for vaccine delivery composed of monopalmitin glycerol (MPG), cholesterol (Chol) and dicetyl phosphate (DCP) at a molar ratio of 5:4:1 of MPG:Chol:DCP [211] so this was used to prepare the NISV by the three methods. The prepared particles were then compared for their physical characteristics, stability over time and *in vitro* cytotoxicity.

2.2. Materials and methods

2.2.1. Materials

MPG was purchased from Larodan Fine Chemicals AB (Sweden). Chol, DCP, PBS tablets, resazurin powder, serum-free and antibiotic-free Roswell Park Memorial Institute medium (RPMI 1640), L-glutamine, penicillin–streptomycin, and foetal bovine serum (FBS) were purchased from Sigma–Aldrich (UK) (all at cell culture grade). Sodium pyruvate (100mM) and minimum essential medium non-essential amino acids (MEM NEAA) were purchased from Life Technologies (UK). The human cell lines skin malignant melanoma (A375) and ovarian carcinoma (A2780) were purchased from the American Type Culture Collection (ATCC®).

2.2.2. Preparation of NISV by the thin-film hydration (TFH) method

NISV were prepared using the thin-film hydration (TFH) method as described elsewhere [212]. Briefly, MPG, Chol and DCP were mixed at a molar ratio of 5:4:1 with a total weight of 22.5 mg (MPG: 9.96mg, Chol: 9.27mg, DCP: 3.27mg). The mixture was placed in a round bottomed flask and dissolved in 9 ml chloroform. Chloroform was then evaporated using a rotary evaporator (Rotavapor R-3, BTECH, Switzerland) operated at 50rpm under vacuum at 50°C until complete solvent evaporation and a thin lipid film formed on the flask wall. The thin-film was hydrated with 9 ml of PBS (pH 7.4) at 50°C by rotating the flask at 50 rpm for 1 h until the lipid film was completely hydrated and a milky suspension was formed with a final concentration of 2.5 mg/ml.

2.2.3. Preparation of NISV by the heating method

NISV were prepared by the heating method as described elsewhere with modifications [207]. Briefly, MPG, Chol and DCP at a molar ratio of 5:4:1 were hydrated at room temperature with PBS (10 mM, pH 7.4). The mixture was then heated to 140°C with continuous stirring for two min to form the NISV with a final concentration of 2.5 mg/ml.

2.2.4. NISV particle size reduction

NISV suspensions prepared by the TFH and heating methods were manually extruded 21 times using an Avanti miniextruder containing a 100 nm pore diameter polycarbonate (PC) membrane (Avanti polar lipids, Alabaster, AL, USA) at 50°C to reduce the particle size and distribution (Figure 2.1). An odd number of passages was used in order to collect the unilamellar NISV in the syringe opposite to the one that the extrusion process started with in order to avoid the presence of any large particles that did not cross through the PC membrane.

Figure 2.1 Avanti miniextruder containing a 100 nm pore diameter polycarbonate (PC) membrane used for particle size reduction.

2.2.5. Preparation of NISV by microfluidics

NISV were prepared by microfluidic mixing using a NanoAssemblr™ (Benchtop, Precision NanoSystems Inc., Vancouver, Canada) as described by Obeid *et al*. [118]. NanoAssemblr™ is a microfluidic micromixer that enables a controlled nanoprecipitation process by controlled laminar flow mixing using a herringbone mixer through a two-inlet channel microfluidic system. The NanoAssemblr™ contains a microfluidic cartridge (52 mm thick and 36 mm height with moulded channels of 300 µm in width and 130 µm in height with staggered herringbone structures). The lipids dissolved in ethanol, and the aqueous buffer were pumped separately using disposable syringes into the two inlets of the microfluidic micromixer (Figure 2.2). After the connection point between the aqueous and the lipid phase, the two phases passed through a series of herringbone structures that forced them into a rotational flow to cause the fluids to wrap around each other and force the orientation to be changed between half cycles. This resulted in a chaotic flow profile which is characterised by an exponentially shrinking characteristic diffusion length and rapid adjective mixing between the two streams, which allowed the formation of controlled sized NISV [116]. The NanoAssemblr™ micromixer allowed the control of the TFR (0.5 – 20 ml/min) and the FRR (1:1 to 5:1 of the aqueous to lipid phase) between the two inlet streams through computerised controlled syringe pumps. To prepare NISV at a final concentration of 2.5 mg/ml, MPG, Chol and DCP were dissolved in ethanol to prepare a stock solution of 20 mg/ml for each of the components. Specific volumes from each stock solution were mixed together to prepare the lipid phase of MPG, Chol and DCP in a molar ratio of 5:4:1. The lipid phase was injected into the first inlet and the aqueous phase into the second inlet of the microfluidic micromixer, with the mixing temperature set at 50°C. The FRR of aqueous phase to lipid phase was set at 3:1 and the TFR was set at 12 ml/min (9 mL/minute for the aqueous phase and 3 mL/minute for the lipid phase). Dispersions were

collected from the outlet stream and immediately diluted with aqueous in order to reduce the final ethanol content in the preparation to 6.25% (v/v).

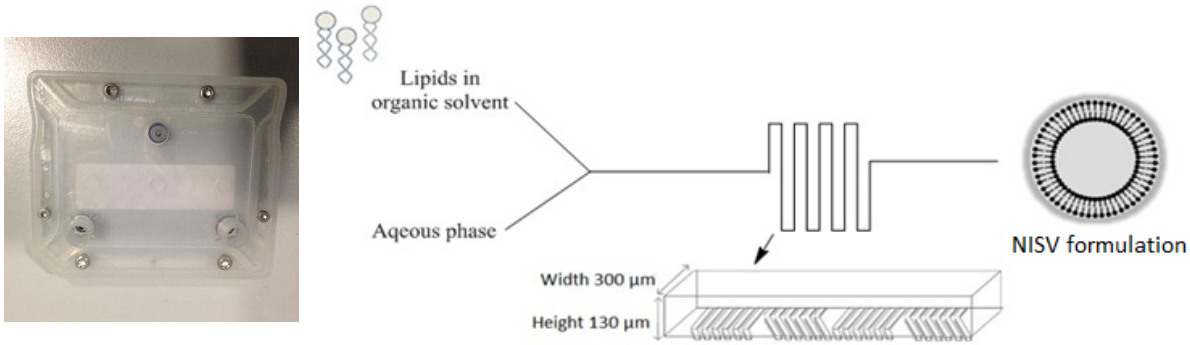

Figure 2.2 The NanoAssemblr™ microfluidic cartridge and a schematic diagram showing the preparation of NISV through microfluidic mixing.

2.2.6 Particle size, polydispersity, and charge of NISV

Particle size, PDI and ZP were measured with a Zetasizer Nano-ZS (Malvern Instruments, UK). The measurements were performed for NISV prepared by each method at 25°C at a 1 in 20 dilution in PBS. All samples were prepared in triplicate and the Z-average, PDI, and ZP reported.

2.2.7 Stability studies of NISV prepared by different methods

NISV prepared by all methods were tested for their stability over a two month period at either 4, 25, 37, or 50°C storage in controlled temperature rooms. Size, PDI, and ZP were measured at 0, 10, 20, 30, 40, 50, and 60 days.

2.2.8 Morphological analysis of NISV using atomic force microscopy (AFM)

Morphological examination of the NISV was performed by atomic force microscopy (AFM). Five µL of each formulation was deposited onto freshly cleaved mica surfaces (G250-2 Mica

sheets 1" x 1" x 0.006"; Agar Scientific Ltd., Essex, UK), and air dried for ~1 h before AFM imaging. The images were obtained by scanning the mica surface in air under ambient conditions using a Dimension FastScan BioAFM (Bruker, CA, USA) operated on Peak Force QNM mode. The AFM measurements were obtained using ScanAsyst-air probes; the spring constant was calibrated by thermal tune (0.52 N m^{-1}; Nominal 0.4 N m^{-1}) and the deflection sensitivity calibrated using a silica wafer. AFM images were collected by random spot surface sampling (at least three areas). The analyses were performed using the Nanoscope Analysis v1.4 (Bruker, USA).

2.2.9. *In vitro* cytotoxicity studies

NISV were assessed for cytotoxicity on two different cell lines (A375 and A2780). Each cell line was seeded in a 96-well plate at a density of 1×10^4 per well in RPMI 1640 medium supplemented with 10% (v/v) FBS, 1% (v/v) L-glutamine and 1% (v/v) penicillin-streptomycin, 1% (v/v) sodium pyruvate, and 1% (v/v) MEM NEAA and incubated at 37 °C, 5% CO_2 and 100% humidity for 24 h. The cells were treated with a range of concentrations of NISV (9.77-1250 µg/ml) prepared by each method. Dimethyl sulphoxide (DMSO) was used as a positive kill control and one column per plate contained untreated cells and medium. PBS alone without the particles was also included to ensure that the media itself used to prepare the particles was not toxic. The plates were then incubated for 24h and then treated with 20 µL of resazurin (0.1 mg/ml) to each well and incubated for a further 24 h. Resazurin is bio-reduced by viable cells from blue into a pink resorufin product, which indicates the presence of metabolically active cells and results in both a colorimetric and fluorometric change. After 24 h, the quantity of resorufin was measured on a SpectraMax M5 plate reader (Molecular Devices, Sunnyvale, CA, USA) at 560 nm - 590 nm. The absorbance reading at this wavelength is directly proportional to the number of metabolising cells in the medium. In this study, cell

viability was calculated and expressed as a percentage of the positive control (i.e., untreated cells):

$$\% \text{ Cell viability} = \left(\frac{\text{Absorbance of cells treated with NISV at } \lambda ex = 560 \text{ nm}, \lambda em = 590 \text{ nm}}{\text{Absorbance of untreated cells } \lambda ex = 560 \text{ nm}, \lambda em = 590 \text{ nm}}\right) \text{ x } 100$$

2.2.10. The effects of TFR and FRR on NISV prepared by microfluidics

The effects of the TFR and FRR on the characteristics of the NISV prepared by microfluidics were also investigated. The TFR of aqueous buffer and lipid phase was varied from 0.5 ml/min to 12 ml/min and the FRR of the aqueous to lipid phases was varied from 1:1 to 5:1 and the particle size, charge and PDI measured.

2.2.11. Statistical analysis

All experiments were performed in triplicate and one way analysis of variance (ANOVA) was used to assess statistical significance. Tukey's multiple comparisons test and a t-test were performed for paired comparisons. The statistical analysis was performed using Minitab software version 17. A value of $p < 0.05$ was considered to be statistically significant. Graphs were produced using OriginPro 2015.

2.3. Results

2.3.1. The effect of the manufacturing method on the particles size, PDI and ZP

Table 2.1 shows the characteristics of NISV, prepared by the TFH and heating methods (before and after extrusion) and those prepared by microfluidics.

DLS revealed that the particle size of the extruded NISV prepared by the TFH method and heating method were small and monodisperse (124.7 ± 0.72 nm and 152.34 ± 1.76 nm, respectively) while the non-extruded particles were large and polydisperse (Table 2.1). However, particles prepared by microfluidic mixing were small with a narrow particle distribution (165.90 ± 0.92 nm). Microfluidics can prepare small and monodisperse particles in minutes. However, the preparation of these particles with the other methods took hours to get the same results as those obtained with microfluidics. The PDI values of the extruded NISV prepared by the TFH and heating methods were low (0.12 ± 0.01 and 0.10 ± 0.02 respectively) and comparable to the PDI value of the particles prepared by microfluidics (0.08 ± 0.02) with no significant difference ($p>0.05$). Moreover, since all the particles prepared by the three methods used the same lipid compositions, the ZP values for the extruded particles prepared by the TFH and the heating methods and by microfluidics were the same with no significant difference ($p>0.05$) (Table 2.1).

Table 2.1 Comparison of particle characteristics prepared by the TFH method, heating method, and microfluidic mixing in terms of size, PDI and ZP. n=3 ± SD

Method of preparation	Size (nm)	PDI	ZP (mV)
TFH (before extrusion)	1027.17 ± 75.79	0.83 ± 0.03	-12.30 ± 3.22
TFH (after extrusion)	124.70 ± 0.72	0.12 ± 0.01	-28.70 ± 1.39
Heating method (before extrusion)	3938.00 ± 95.25	0.85 ± 0.04	-14.50 ± 1.25
Heating method (after extrusion)	152.34 ± 1.76	0.10 ± 0.02	-36.67 ± 3.14
Microfluidic mixing	165.90 ± 0.92	0.08 ± 0.02	-31.38 ± 1.80

2.3.2. The effects of the manufacturing method on overall NISV stability

Figure 2.3 shows the stability in terms of particle size, PDI, and ZP of the NISV prepared by the three methods when stored at four different temperatures over two months. Samples were characterised immediately after preparation and again at each time point. The method of preparation was shown to have no effects on particle stability as the particles prepared by the three methods exhibited nearly identical particles size and size distribution as the original samples at all the tested temperatures.

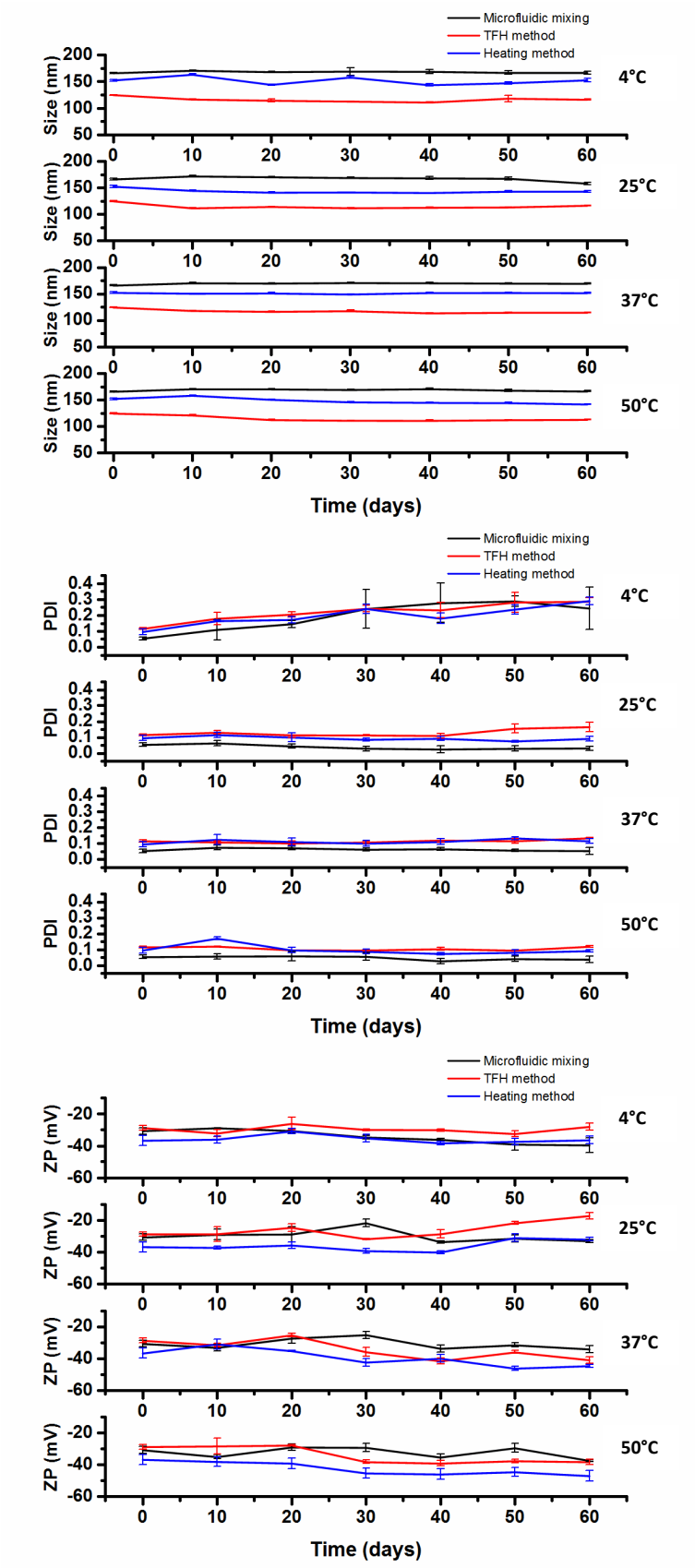

Figure 2.3 Size, PDI, and ZP of NISV prepared by the TFH method, heating method, and microfluidic mixing and stored over 60 days at 4°C, 25°C, 37°C and 50°C. The data represents the mean ± SD (n=3).

2.3.3. Morphological analysis of NISV prepared by different methods

Figure 2.4 shows the morphology of NISV prepared by the TFH and heating methods after extrusion, and by microfluidics. All the particles were spherical in shape regardless of the method of preparation. Some images showed large particle aggregates, which are due to the high concentration of these particles in the tested samples, which formed upon drying the sample on the mica surface.

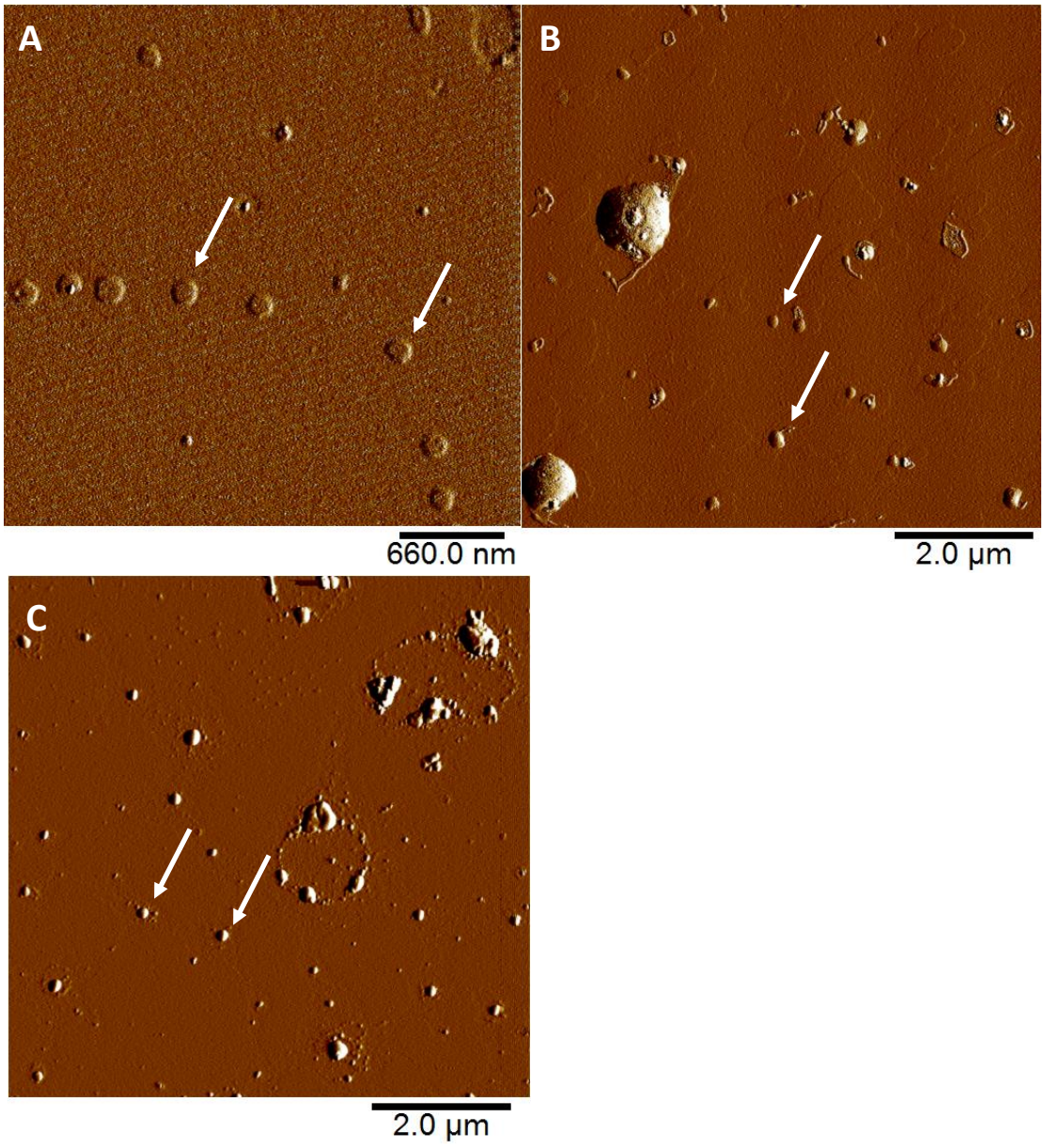

Figure 2.4 AFM images for the NISV prepared by the (A) TFH method post extrusion, (B) heating method post extrusion, and (C) microfluidic mixing.

2.3.4. Cytotoxicity study of NISV prepared by different methods

Figure 2.5 shows the cytotoxicity of the NISV prepared by the three methods on A375 and A2780 cell lines and Table 2.2 shows the calculated EC_{50}. All three formulations show the same cytotoxicity profile, as the difference in the EC_{50} between the particles on both cell lines was not significant ($p>0.05$). NISV with a concentration ≤ 150 µg/ml were found to be non-toxic where 100% cell viability was observed for both cell lines regardless of the method of manufacturing. The buffer alone used in the vesicle preparation was not toxic and the cells were 100% viable.

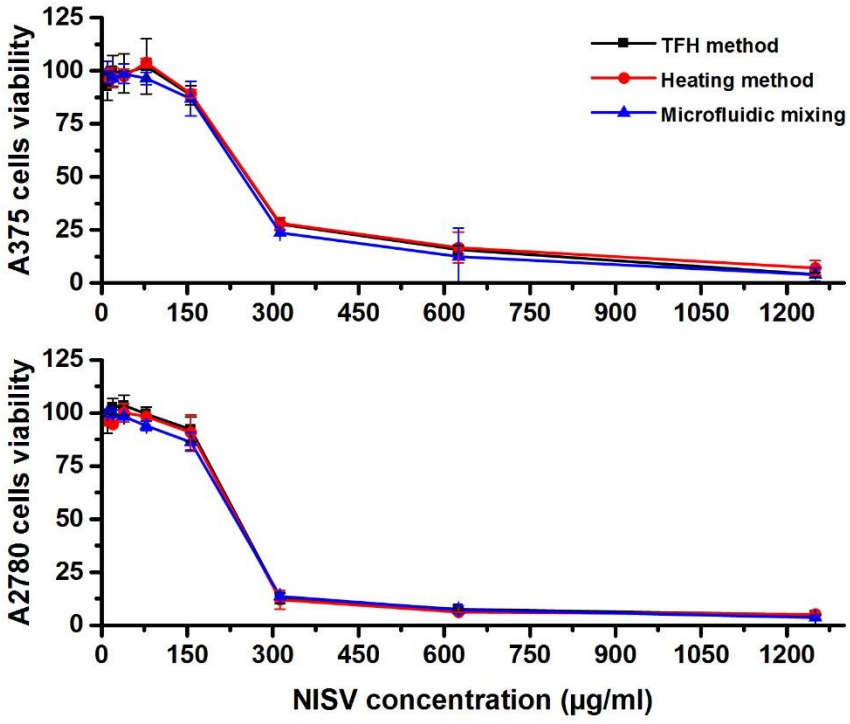

Figure 2.5 Cytotoxicity of the NISV prepared by three methods on A375 and A2780 cell lines. The data represents the mean ± SD (n=3).

Table 2.2 EC_{50} values in (µg/ml) of NISV, prepared using three different manufacturing methods, on A375 and A2780 cells. The data represents the mean ± SD (n=3).

Method of preparation	EC_{50} (µg/ml)	
	A375 cell line	A2780 cell line
TFH method	254.7 ± 11.5	229.9 ± 14.43
Heating method	258.9 ± 19.53	224.6 ± 28.32
Microfluidic mixing	240.1 ± 13.81	228.9 ± 5.651

2.3.5. The effects of TFR and FRR on NISV prepared by microfluidics

Figure 2.6 shows the changes of the particles size by changing the FRR from 1:1 to 5:1 (aqueous: lipid phases) and the TFR from 0.5-12 ml/min. As can be seen in same figure, as the aqueous/ethanol FRR increased from 1:1 to 5:1, significant ($p<0.05$) reduction in NISV size was observed and found to be TFR dependant. At a TFR < 3 ml/min, the difference between the particles prepared at FRR of 3:1 and 5:1 was not significant ($p>0.05$). However, at higher TFR (> 3 ml/min), the difference between these two FRRs was significant ($p<0.05$). For example, at a TFR of 0.5 ml/min, the particle size prepared at FRR of 1:1, 3:1 and 5:1 were 219.71 ± 15.69 nm, 181.14 ± 6.65 nm, and 183.32 ± 4.88 nm, respectively while at a TFR of 12 ml/min, the particle size for NISV was 177.73 ± 5.26 nm at FRR 1:1, 165.90 ± 0.92 at FRR 3:1 and particles prepared at FRR 5:1 was 145.25 ± 4.64 nm. The TFR was shown to have a significant ($p<0.05$) effect on particle size where the increase in the TFR from 0.5 ml/min to 9 ml/min resulted in an overall reduction in particle size at all the FRR. However, further increase in the TFR above 9 ml/min was not associated with a significant decrease in particle size at all the FRR (Figure 2.6).

Regarding the effects of the FRR on the total particle charge, the increase in the solvent concentration at lower FRR (1:1) resulted in a higher percentage of the charged material (i.e.

DCP) in the particles. Therefore, as the FRR increased from 1:1 to 5:1 there was a decrease in the absolute value of the ZP from about -30 mV at 1:1 to about – 20mV at 5:1 regardless of the TFR. This means that the FRR factor also has an effect on the ZP in addition to its effect on particle size. However, this effect on the ZP was not significant ($p>0.05$).

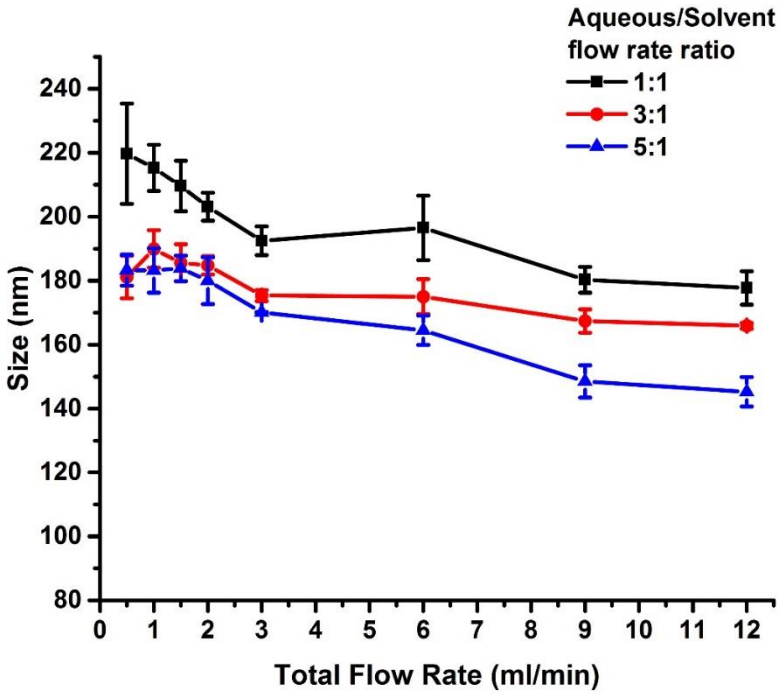

Figure 2.6 Size changes of NISV prepared at different TFR and FRR of the aqueous and lipid phase. The data represents the mean ± SD (n=3).

2.4. Discussion

The objective of this work was to assess the physicochemical properties of the NISV produced by three different methods. The TFH and heating methods have previously been reported to produce large multilamilar vesicles that require a post-manufacturing size reduction step [213], as confirmed by this study. Microfluidic mixing on the other hand was shown to produce small sized nanoparticles with a low distribution in a single production step [209].

Traditionally, the production of small and monodisperse particles using the TFH and heating methods were limited by the use of a post-manufacturing size reduction step to produce particles of the required size and to reduce the PDI. This has limited the use of these methods to bench scale since there is a much longer industrial scale process required to produce a consistently sized end-product. However, microfluidic mixing allows the production of controlled particle size with homogenous distribution in a single step without the need for post-manufacturing size reduction (Table 2.1). This offers the potential to facilitate the production of NISV at larger scale. Moreover, the production of these small particles by microfluidics can save time as the total preparation time took minutes while the production of small particles by the other methods required several hours. Recently, a large scale production instrument has been developed through parallelisation of several microchannels together to allow for industrial scale production of lipid nanoparticles by microfluidics [214].

Next, the stability of the vesicles over two months was evaluated, at different storage temperatures following extended incubation by monitoring any changes in the particles size, PDI, and ZP. As can be seen in Figure 2.3, TFH and heating methods (post-extrusion) and microfluidic mixing produced stable particles with respect to size with no significant change at all storage temperatures. Also, there was no significant change in the particles' PDI and ZP at all the tested temperatures regardless of the method of preparation (Figure 2.3). Temperature can have an energy input to the system and can sometimes lead to changes in the crystalline

structure of the lipids or might cause changes in the ZP and these changes might affect the stability of the particles [215]. Several researchers have reported the instability of the particles when stored at high temperatures. In two different studies, Feritas *et al.* (1998 and 1999) reported the instability of their SLN with the introduction of energy to the system. This instability was reported in terms of size increase and reduction of ZP when the particles were stored at 50ºC [216, 217]. At 4ºC, this was generally the most favourable storage condition although some reports indicate the instability of the formed particles when stored at low temperatures [215]. In this study, all three methods exhibited excellent stability at four different temperatures with no significant increase in the average particle size, PDI, and ZP ($p>0.05$) when stored for two months even at the higher storage temperatures. These data indicate that microfluidics not only enables rapid, robust, and scalable production of NISV, but also supports the stable formation of these vesicles which is necessary for applications requiring prolonged shelf life such as in pharmaceutical drug delivery. Although there was some residual ethanol in the formulations prepared by microfluidics, this good vesicles stability suggests that the amount of ethanol sequestered in the NISV bilayer is not significant as high ethanol content will promote rapid disruption of the bilayer structure, which is not the case in these formulations. However, this residual ethanol can be removed, if necessary, via conventional batch purification techniques such as evaporation, extraction, or dialysis [218].

Morphological observations of AFM images confirmed the formation of spherical particles of NISV prepared by the TFH and heating methods after extrusion and by microfluidics (Figure 2.4). These results confirmed that the particles prepared by microfluidics in a single step are similar to the extruded particles prepared by more traditional TFH and heating methods.

Regarding the effects of the manufacturing methods on particle cytotoxicity, the viability of A375 and A2780 cells were measured after treatment with a range of NISV concentrations (9.76 -1250 µg/ml) prepared by all three methods. Cell metabolic activity measurements by

conversion of resazurin showed no difference in cytotoxicity of the NISV prepared by the three methods as assessed by their EC_{50} values (Table 2.2). NISV with lipid concentrations below 150 µg/ml were non-toxic with 100% cell viability retained. Any difference in the physical characteristics of the particles such as size or charge would affect their cellular uptake, which would then affect cell viability [118, 145]. Here, since the particles prepared by the three methods have comparable characteristics in terms of size and charge, there was no difference in cell viability regardless of the method of preparation. This reflects the potential to have significant impact on various drug delivery applications by improving the manufacturing process of currently available NISV-based drugs. This would be achieved by replacing conventional methods of preparation with microfluidics to obtain the same outcomes, while gaining advantages in terms of rapid production of reproducible particles.

For the formation of lipid-based particles through microfluidic mixing, the rate of mixing as well as the ratio of aqueous-to-solvent streams were anticipated to be crucial factors in particle preparation as these factors will affect the ratio of each phase in the mixing process as well as the mixing time between both phases [210, 219]. Therefore, NISV composed of MPG:Chol:DCP (5:4:1 molar ratio) were prepared by microfluidic mixing at different TFR and FRR. The FRR strongly affected the final solvent concentration. At lower FRR (1:1), the final solvent concentration increased, thus boosting the production of larger particles due to particle fusion and lipid exchange while at higher FRR (5:1), the chance of producing large particles was reduced as a result of reduced solvent concentration. Previous work using hydrodynamic flow-focusing techniques for the preparation of NISV using different types of sorbitan esters surfactant have also been reported to increase NISV size with the decrease in FRR, which is in agreement with results in this study [208].

The effect of the TFR on particle size is still debatable. While some researchers have reported that TFR does not have a significant effect [220], others have reported the contrary [221]. In

this study, TFR was shown to have an impact on particle size especially at values < 9 ml/min. This means that these two factors (FRR and TFR) should be optimised when NISV are formulated by microfluidic mixing.

2.5. Conclusions

In this work, the characteristics of NISV prepared by microfluidics were compared with those prepared by the conventional TFH and heating methods. Microfluidic mixing enabled preparation of small, monodisperse particles in a single step, without the need of a size reduction step as in the case of the other methods. The method of preparation did not have significant effects on particle stability and toxicity. Using microfluidic mixing, a homogenous NISV suspension was prepared with high reproducibility. FRR and TFR between the two phases of the microfluidic mixing are the factors that have significant effects on particle characteristics, which can be optimised in order to produce NISV with a defined size which is important in developing an effective drug delivery system. This work suggests that the use of microfluidic mixing in NISV preparation may facilitate the development and optimisation of these dispersions for nanomedicine applications at both bench and industrial scale.

Chapter 3

The effects of hydration media on the characteristics of NISV prepared by microfluidics

Abstract

One of the methods that is used for NISV preparation is microfluidics that allows the production of NISV in a single step by controlling the mixing parameters. In this chapter, the effect of using different types of aqueous media on the characteristics of the NISV prepared by microfluidics was examined. Five aqueous media were tested: phosphate buffered saline, (4-(2-hydroxyethyl)-1-piperazineethanesulfonic acid) (HEPES) buffer, Tris buffer, normal saline and distilled water. The resulting particles were tested for their physical characteristics and cytotoxicity. The aqueous media were found to have significant effects on the physical characteristics of the particles, as well as their overall stability under different conditions and their cytotoxicity to different human cell lines. Careful consideration should be taken when choosing the aqueous media for preparing NISV through microfluidics. This is an important factor that will also have implications with respect to the entrapped material, but which in addition may help to design vesicles for different uses based on changing the preparation medium.

Key Words

Non-ionic surfactant vesicles, Microfluidics, Hydration media, Drug delivery

3.1. Introduction

NISV are synthetic vesicles constructed through the self-assembly of hydrated non-ionic surfactants with cholesterol and other additives, into a bilayer structure enclosing an aqueous core. Non-ionic surfactants are the basic components of NISV. These surfactants are amphiphilic molecules with both a hydrophilic (water soluble) head and hydrophobic (organic soluble) tail with no charged groups in their hydrophilic heads [83].

All of the reported methods of NISV formulation involve the hydration of the surfactant and lipid mixtures with an aqueous phase at elevated temperature, followed by an optional size reduction with some preparation methods [80]. PBS is a common buffer used for NISV preparation. It is an ionic buffer composed of sodium chloride, sodium phosphate, and (in some formulations) potassium chloride and potassium phosphate and has a pH range from 5.8-8.0 at 25°C [222]. PBS is the preferred buffer for particle formation because the osmolarity and ion concentrations match those of human body fluids such as blood [223]. Other buffers such as (4-(2-hydroxyethyl)-1-piperazineethanesulfonic acid) (HEPES), Tris, citrate and carbonate can also be used [224, 225]. NISV can also be prepared using distilled water (DW) as an aqueous media. However, it is imperative to select an optimal buffer system for drug encapsulation in NISV. For example, phosphate and citrate buffers are not recommended for components that contain calcium ions, as phosphate forms an insoluble calcium phosphate precipitate, while citric acid chelates calcium [226]. Tris buffer is used for the storage of nucleic acids and is suitable for formulating NISV where nucleic acids are being encapsulated. However, Tris can interfere *in vivo* and *in vitro* with copper by chelation and can act as a competitive inhibitor to some enzymes [226, 227].

3.1.1. Chapter aims

In this chapter, the effect of five different aqueous media on the characteristics of empty NISV prepared by microfluidics were investigated. NISV composed of MPG:Chol:DCP at a molar ratio of 50:40:10 was used as a model to examine the various physicochemical aspects of vesicles composed with these lipid components, but prepared using five different aqueous media and using a microfluidic mixing method of preparation. *In vitro* cytotoxicity experiments were subsequently performed to evaluate the effect of the different formulations resulting from the use of the different hydrating media on A375, A2780, and PNT2 (normal prostate epithelium) cells.

3.2. Materials and methods

3.2.1 Materials

PBS tablets, HEPES buffer solution, Tris buffer solution, sodium hydrochloride (NaCl) were purchased from Sigma-Aldrich (UK). The normal human prostate cells PNT2 were purchased from American Type Culture Collection (ATCC®) and kindly provided by Mrs Louise Young, (University of Strathclyde). Other material suppliers have already been described in section 2.2.1.

3.2.2 NISV preparation by microfluidics with different hydration media

NISV were prepared by employing a microfluidic micromixer as described in section 2.2.5. The hydration media used to prepare the vesicles were PBS (10 mM, pH 7.4), HEPES buffer (10 mM, pH 7.4), Tris buffer (10 mM, pH 7.4), 0.9% (w/v) normal saline (NS) and DW.

For the preparation of empty vesicles, a specific volume of each of the tested hydration media was mixed with the lipid phase in ethanol at a volumetric flow rate of 3:1 (aqueous: lipid) in the microfluidic micromixer at a total flow rate of 12 mL/minute at 50ºC. The mixed materials, upon leaving the micromixer outlet, was diluted into an equal volume of the aqueous media used in the preparation in order to reduce the ethanol content in the final preparation to 12.5%. The NISV mixture was then dialysed overnight against 1000 volumes of aqueous media used in the vesicle preparation using SnakeSkin™ Dialysis Tubing (10,000 Da molecular weight cut off; Thermofisher Scientific, UK) at 25°C.

3.2.3 Particle size, polydispersity and charge of NISV prepared with different hydration media

Particle size, PDI and ZP were measured by DLS as described in section 2.2.6. The measurements were carried out for NISV prepared in each hydration media at 25°C at a 1/20 dilution.

3.2.4 Stability of NISV at different temperatures

Stability of the NISV was evaluated as described in section 2.2.7. Size, PDI and ZP were measured at different time points (0, 1, 2, 3, 4, 6 and 8 weeks).

3.2.5 Morphological analysis of NISV using scanning electron microscopy (SEM)

Morphological analysis of the NISV was carried out using a FEI Quanta 250 field emission variable pressure SEM (FEI, Oregon, USA) equipped with an Everhart–Thornley type detector and running FEI software. Each sample of NISV was diluted 1:50 with the media used in the formulation and 2µl of each diluted sample was dried on a silicon substrate and placed under vacuum. An accelerating voltage of 5 kV was applied to each sample in high vacuum mode and secondary electron images were collected.

3.2.6 High Performance Liquid Chromatography (HPLC) analysis of cholesterol content of NISV

In order to assess the concentration of the NISV produced and to determine the yield and preparation efficacy, NISV were analysed using HPLC to measure the quantity of cholesterol present post-preparation. HPLC was performed using an Agilent Technologies 1260 Series Liquid Chromatography system controlled by Clarity Chromatography software. The conditions of the run were as follows: mobile phase acetonitrile:methanol:2-propanol; (7:3:1, v/v/v), flow rate 1 mL/min, total run time 10 min; column YMCbasic C18, 250 X 3.0 mm, column temperature 60ºC, injection volume 20 µL, detection 205 nm, retention time 1.55 min. A standard curve of Chol (31.25 – 1000 µg/ml) was constructed by measuring the area under the curve (AUC). NISV prepared were lysed with isopropyl alcohol (50%, v/v) and then analysed by HPLC as previously described [228]. The Chol concentration was determined by measuring the AUC and calculating the concentration using the equation generated from the standard curve.

3.2.7 Turbidity assay

To understand NISV behaviour under physiological conditions, the aggregation tendency of the NISV was studied using a turbidity assay [229]. FBS was added to each NISV formulation to a final concentration of 10% (v/v) in each hydration medium. This concentration of FBS was chosen as it is generally used for *in vitro* studies. Turbidity was determined by measuring the absorbance at 298 nm using a HELIOS ALPHA ThermoSpectronic spectrophotometer using serum alone as a background [229]. NISV (625 µg/ml) were incubated at 37 °C and analysed over a 2 h time period and then after 24 h. Relative turbidity was calculated by dividing sample absorbance at a specific time by the time zero value incubated in the corresponding hydration buffer used for NISV preparation.

3.2.8 Cytotoxicity of NISV evaluated using a number of human cell lines

Cytotoxicity studies for NISV were carried out as described in section 2.2.9 using three different cell lines (A375, A2780, and PNT2). Each of the hydration buffers without the particles was also included to ensure that the media themselves are not toxic.

3.2.9 Statistical analysis

All experiments were performed in triplicate and ANOVA was used to assess statistical significance. Tukey's multiple comparison test and t-test was performed for paired comparisons. The statistical analysis was performed using Minitab software version 17. A value of $p < 0.05$ was considered to be statistically significant. Graphs were produced using OriginPro 2015.

3.3. Results

3.3.1 Effect of hydration buffer on the particles size and PDI

Changing the hydration media altered the size of the NISV significantly (Figure 3.1). The smallest particles were formed using Tris, followed by DW and HEPES with particle sizes of 60.96 ±0.36 nm ($p < 0.05$), 71.83 ± 0.44 nm ($p < 0.05$), and 74.10 ± 0.51 nm ($p < 0.05$), respectively. The largest particle size was obtained with NS (168.40 ± 2.26 nm, $p < 0.05$) followed by PBS (166.10 ± 1.23 nm, $p < 0.05$). The PDI of these particles showed that all the formulations, had a narrow size distribution with values of 0.027 ± 0.003 (NS), 0.054 ± 0.010 (PBS), 0.060 ± 0.030 (Tris), 0.091 ± 0.010 (HEPES) and 0.180 ± 0.010 for DW with the value of PDI for particles prepared with DW that was significantly different than the others ($p < 0.05$).

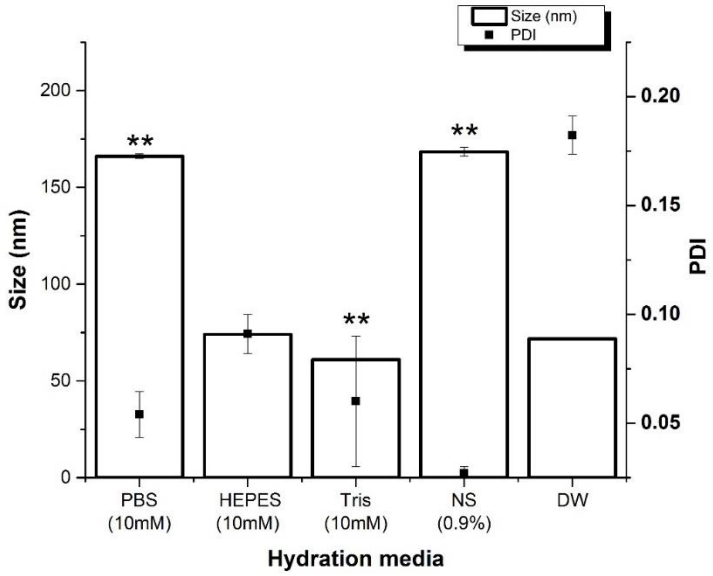

Figure 3.1 Size and PDI of NISV prepared using microfluidics with five different hydration media. The data represents the mean ± SD (n=3) as measured by DLS. *p <0.05 indicates significant difference in size compared with the DW formulation.

3.3.2. The effect of the hydration media on the charge of the resultant NISV

Particles prepared with DW had the highest absolute value of ZP (-76.83 ± 0.81 mV) followed by the particles prepared with Tris (-57.4 ± 3.33 mV), HEPES (-51.87 ± 1.18 mV), NS (-33.2 ± 2.46 mV) and PBS (-30.63 ± 2.06 mV) as shown in Figure 3.2.

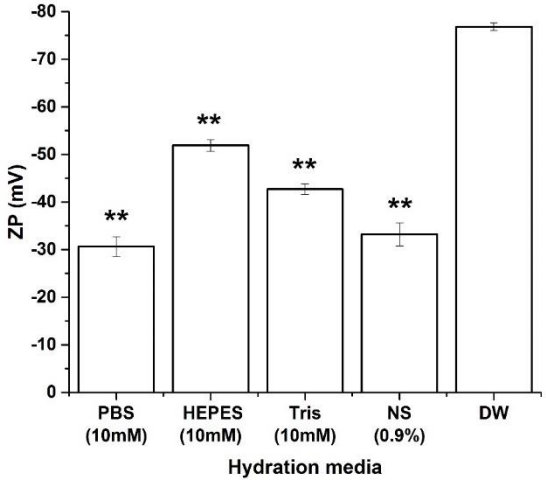

Figure 3.2 ZP for NISV prepared with microfluidics using five different aqueous media. The data represents the mean ± SD (n=3) measured by DLS. $^{**}p < 0.05$ indicates significant difference in size compared with the DW formulation.

3.3.3 Stability of NISV at different storage temperatures

Vesicle stability was assessed by monitoring changes in size (Figure 3.3) and PDI (Figure 3.4) of the particles over time, to predict their swelling, aggregation or precipitation characteristics. For NISV prepared with DW, the particle size showed a slight decrease in the first two weeks and then remained stable throughout the study when stored at 4, 25, and 37°C with no significant change in the particle size ($p > 0.05$). However, for the particles stored at 50°C, there was a significant ($p < 0.05$) increase in the particle size during the study, which increased from 71.8 ± 0.4 nm at time zero to 101.1 ± 0.4 nm at the end of the study. NISV prepared with HEPES buffer was stable at the four different temperatures with no significant ($p > 0.05$) increase in particle size during the study. NISV prepared with NS were stable in terms of size and PDI when stored at 4°C with no significant ($p > 0.05$) change. When these particles were stored at 25 and 37°C, they showed an increase in size during the first week and then remained stable for the rest of the storage duration. However, NISV prepared with NS and stored at 50°C increased significantly ($p < 0.05$) in size from 168.4 ± 2.26 to 208.77 ± 1.89 nm at the end of the study with no significant ($p > 0.05$) increase in the PDI. Particles prepared with PBS remained stable with no significant ($p > 0.05$) change in the particle size regardless of the storage temperature. For NISV prepared using Tris buffer, the particles remained stable at 4 and 25°C with no significant ($p > 0.05$) change in particles size. When these particles were stored at 37°C, the size increased significantly ($p < 0.05$) in the first week from 60.69 ±0.36 nm to 66.84 ± 0.14 nm and then remained stable for the rest of the storage duration. For particles prepared with Tris and stored at 50°C, there was a significant ($p < 0.05$) increase in particle size from 60.96 ±0.36 to 76.18 ± 0.39 nm at the end of the storage.

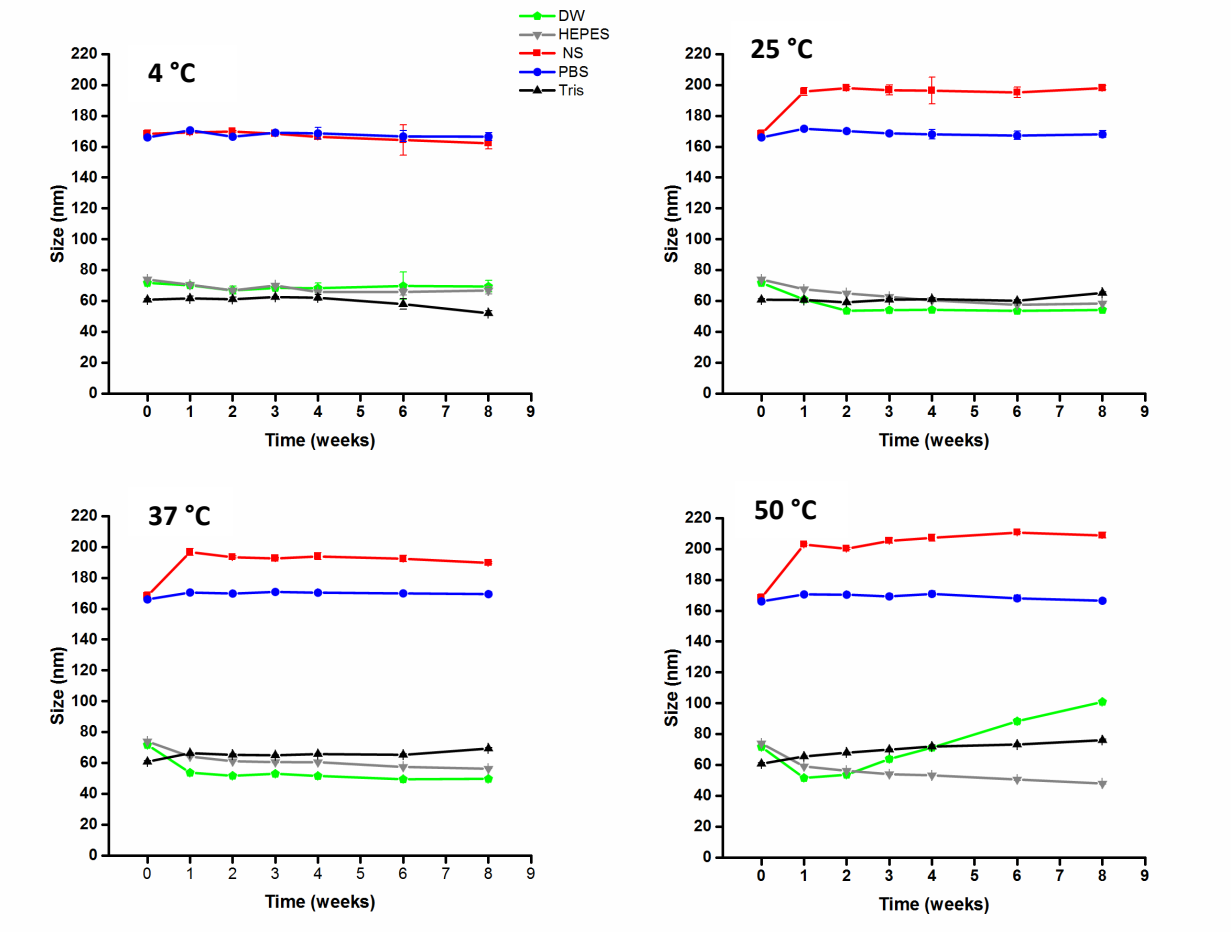

Figure 3.3 Particle size of NISV prepared with microfluidics using five different hydration media, stored at 4, 25, 37 and 50°C. The data represents the mean ± SD (n=3) measured by DLS.

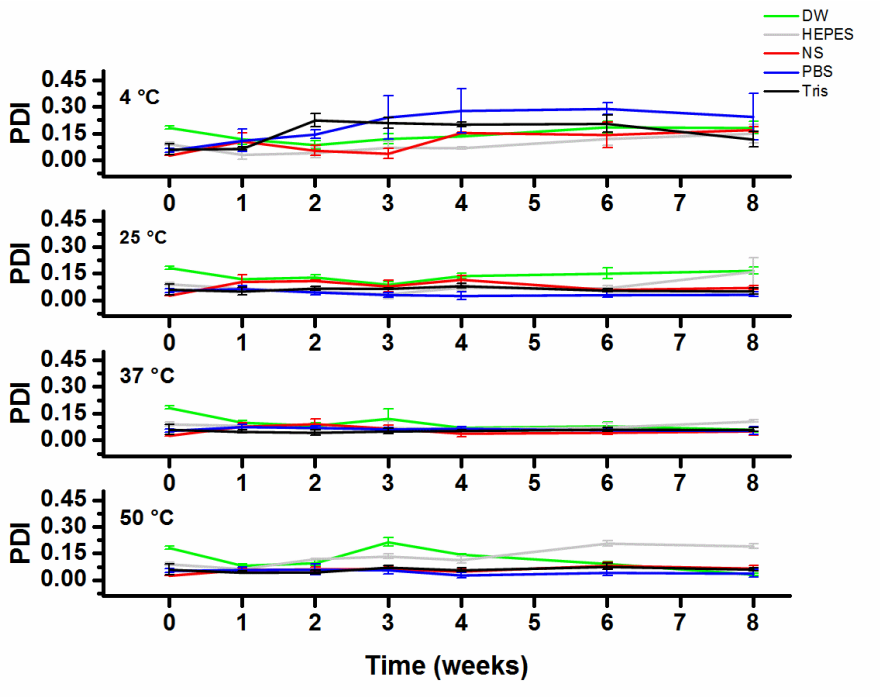

Figure 3.4 PDI of NISV prepared with microfluidics using five different hydration media, stored at 4, 25, 37 and 50°C. The data represents the mean ± SD (n=3) measured by DLS.

3.3.4 SEM imaging of NISV

The morphology of the NISV was analysed by scanning electron microscopy (Figure 3.5). NISV were shown to have an almost spherical shape as seen in some of the images and apparent smooth surfaces regardless of the media used in their preparation.

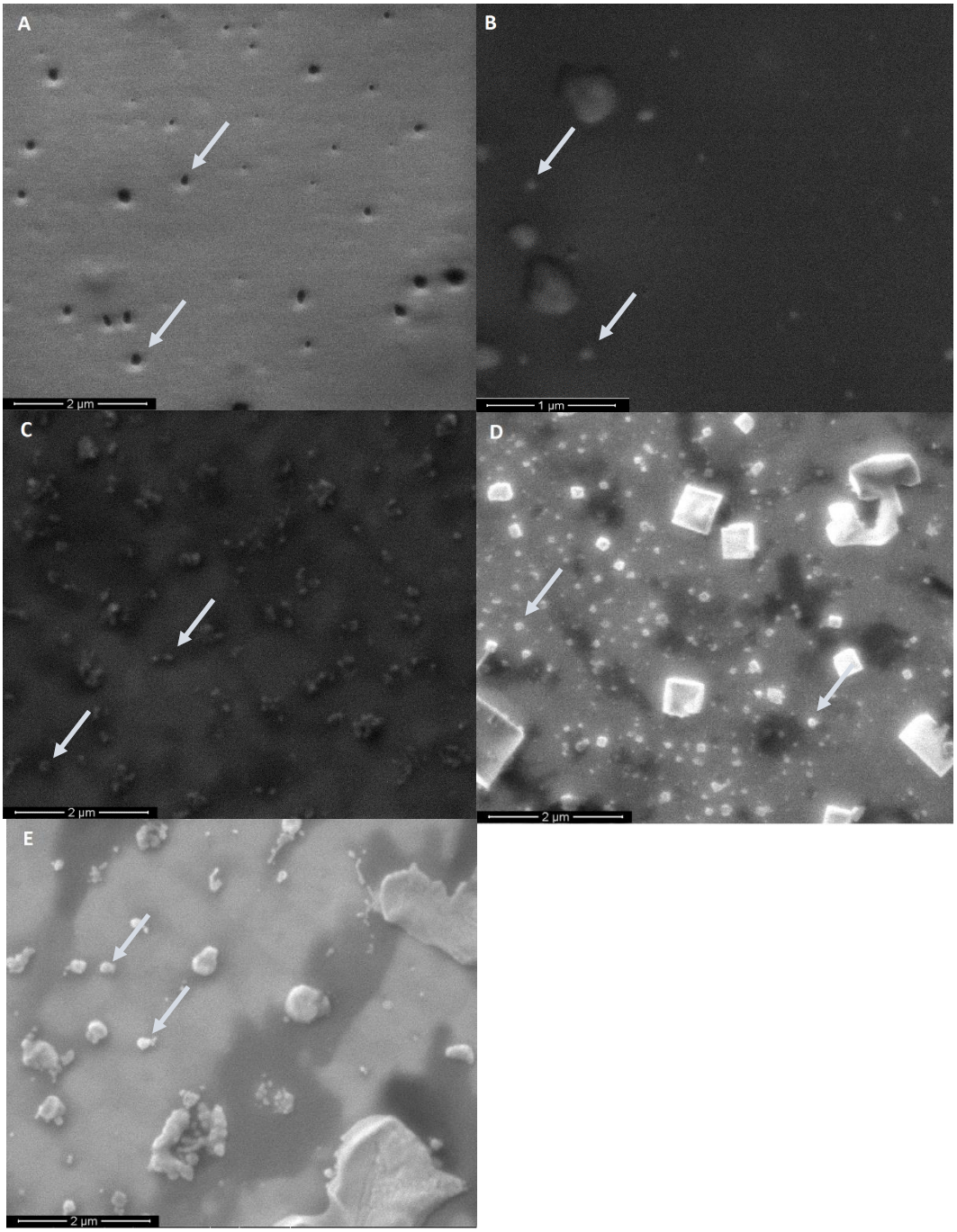

Figure 3.5. Representative scanning electron micrographs of NISV prepared with (A) HEPES, (B) Tris, (C) DW, (D) NS and (E) PBS (Magnification ×40,000). Salt crystals were observed in the NS micrograph as cuboid structures in Figure 3.5 (D). Figure 3.5 (E) showed some large non-spherical aggregates as a result of the high concentration of the particles examined.

3.3.5 HPLC analysis of NISVS prepared with different hydration media

The total Chol content in the NISV formulations was measured using HPLC. Figure 3.6 shows a typical standard curve and the total Chol concentration calculated from it for each formulation shown in Figure 3.7.

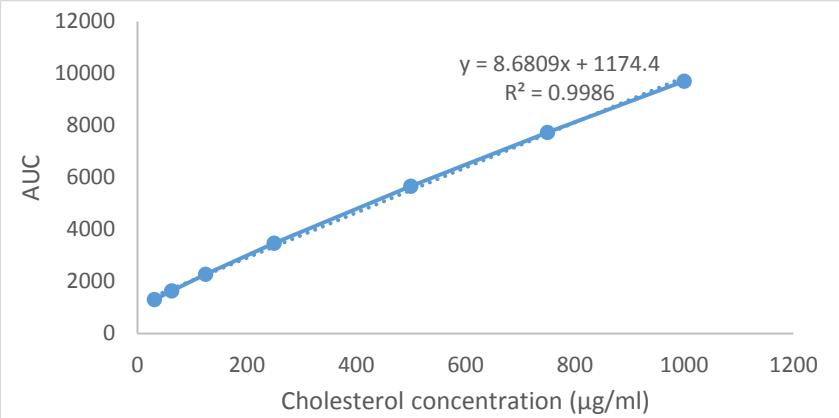

Figure 3.6. A typical cholesterol standard curve prepared by measuring the AUC of various cholesterol concentrations as measured by HPLC.

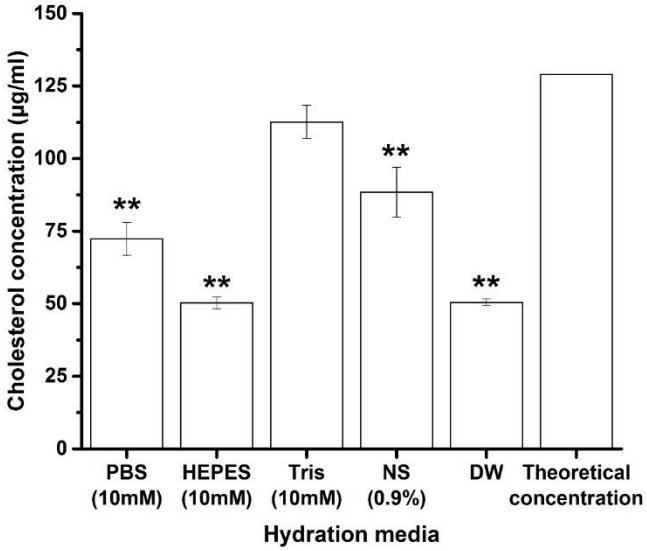

Figure 3.7. Calculated cholesterol concentrations after preparing NISV with microfluidics using different hydration media compared to the theoretical concentration. The data represents the mean ± SD (n=3) measured by HPLC. $^{**}p < 0.05$ significant decrease in Chol concentration compared with the theoretical concentration.

3.3.6 Turbidity assay

The relative turbidity (RT) of the vesicles showed that they were stable at 37°C for 2h (Figure 3.8). For NISV prepared with HEPES and DW, the RT increased slightly within the first five minutes after incubation, but remained stable thereafter. Moreover, RT measurements after 24 h showed that the particles were stable with no increase in the RT values for all formulations.

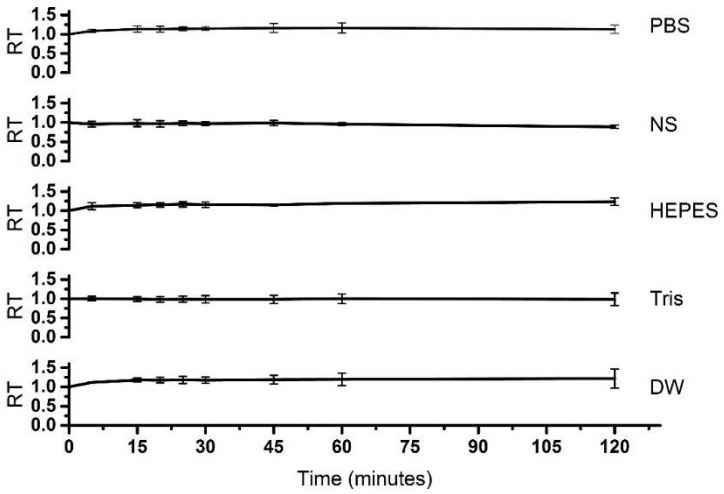

Figure 3.8. Relative turbidity (RT) of the NISV prepared with PBS, NS, HEPES, Tris and DW and incubated at 37°C with 10% v/v FBS. The data represents the mean ± SD (n=3).

3.3.7 Cytotoxicity studies

Table 3.1 shows the calculated EC_{50} and Figure 3.9 shows the cytotoxicity of the formulations on the cells. Cell viability measurements showed that regardless of the media used to prepare the NISV, all the cell lines were 100% viable at a total lipid concentration of 78.1 µg/ml and below.

Table 3.1 The EC_{50} values in (µg/ml) for NISV, prepared by microfluidic mixing using five different hydration media, on A375, A2780 and PNT2 cells. The data represents the mean ± SD (n=3).

Aqueous media used to prepare NISV	**EC_{50} (µg/ml)**		
	A375 cell line	**A2780 cell line**	**PNT2 cell line**
HEPES	403.90 ± 49.57	149.50 ± 9.69	241.10 ± 7.22
Tris	413.70 ± 73.71	142.20 ± 10.38	233.30 ± 6.30
PBS	323.60 ± 0.01	165.10 ± 4.23	257.70 ± 4.40
NS	322.10 ± 75.09	147.20 ± 3.56	248.20 ± 4.79
DW	257.80 ± 24.68	130.00 ± 5.34	217.40 ± 5.31

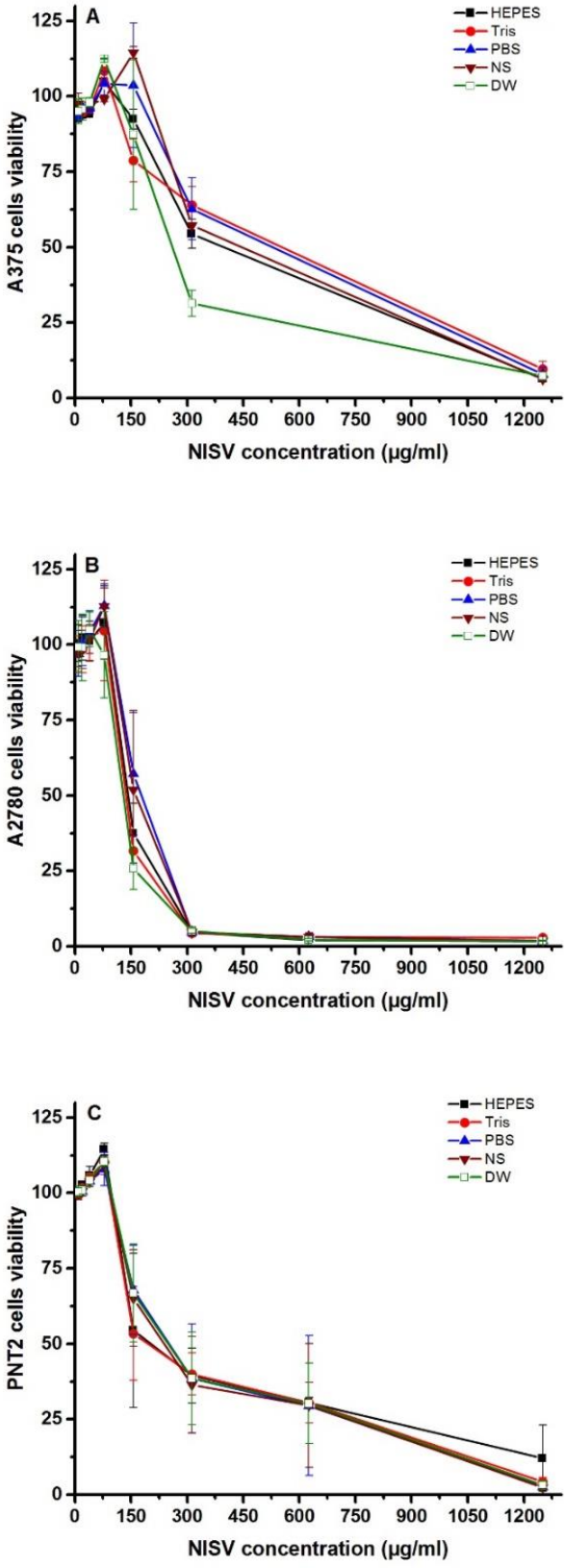

Figure 3.9. Cytotoxicity of the NISV prepared with PBS, NS, HEPES, Tris and DW on (A) A375, (B) A2780 and (C) PNT2 cell lines. The data represents the mean ± SD (n=3).

3.4. Discussion

NISV composed of MPG:Chol:DCP at a molar ratio of 50:40:10 were prepared using microfluidic mixing by changing the aqueous media used in formulating the particles. The production of NISV through microfluidic mixing is based on rapid and controlled mixing of two miscible fluids (aqueous and solvent) in a microchannel [208]. The objective of this work was to assess the effects of the aqueous media on the physicochemical properties of the resultant particles. Five different hydration media were studied.

There was a significant ($p < 0.05$) difference on the size of the different particles, which ranged from 60.96 ± 0.36 nm to 168.40 ± 0.51 nm. The smallest particle size was achieved using Tris followed by DW and HEPES while the largest particle size was obtained using NS followed by particles prepared with PBS. This difference in the particle sizes could be attributed to the ion components of each media. NS and PBS showed similar sizes, while DW, HEPES and Tris were grouped together. The similarity between PBS and NS could be attributed to the NaCl ions, which are the major component in both buffers [230]. HEPES and Tris buffers and DW resulted in smaller particles, but within the same range, so the effects of the ionic components of the HEPES and Tris might have no significant effects as the sizes from both buffers were close to the particles prepared with DW. In drug delivery, small particle sizes (<200 nm) are preferred for drug permeability and tumour targeting as nanoparticles in this size range tend to accumulate passively in tissues with leaky or abnormal architecture blood vessels (i.e. tumour and inflamed tissues) after IV administration in a phenomenon known as enhanced permeability and retention (EPR) [156]. Moreover, it has been reported that larger particles are more rapidly removed from the circulation than smaller particles due to the lower uptake by the RES of smaller particles [231]. He *et al*. reported that *in vitro* macrophage uptake of larger particles was higher compared with smaller counterparts [145]. These factors directly affect the biodistribution and circulation time of NISV [232]. Therefore, the size of the NISV has

significant implications on their efficacy when used as a drug delivery system. Here, although the aqueous buffers resulted in different sizes, the formulations were all below 200 nm, which makes them suitable for tumour-targeted drug delivery. From SEM observations, all the NISV were almost spherical in shape with an apparent smooth surface regardless of the media used in their preparation. The SEM images confirmed the differences in the sizes between the particles (Figure 3.5). Figure 3.5E showed some non-spherical large aggregates as a result of the high concentration of the particles being examined.

The effect of the hydration media on the total charge of the resultant particles could also be attributed to the ions present in the buffers. The surface charge of NISV gives rise to electrostatic repulsion among the nanoparticles, improving the stability of the dispersion system [233]. ZP is an important factor that confers stability on the nanoparticles and higher values ensure that the particles will repel each other and resist aggregation [234]. Particles with ZP values that are < −30 mV or >+30 mV would both be stable dispersions as these values are considered high enough to prevent particle aggregation [233]. Although each of the media examined resulted in particles with different charge, all of them had a ZP < −30 mV, which means that they would be stable regardless of the type of the aqueous media used in their preparation.

Regarding the stability of the formed particles, these results showed that the type of the hydration media used to prepare the NISV might have an effect on particle stability. This effect has been shown to be more obvious at elevated temperatures. All the formulations were stable at 4, 25, and 37°C with no change in particle size and PDI. At 50°C storage conditions, the particles prepared with DW, NS, and Tris increased significantly in terms of size. At elevated temperatures, lipid vesicles undergo a phase transition which affects their permeability and increase the fluidity of the lipid bilayers [224]. Different studies have reported the effects of the temperature and the dispersion media on nanoparticle stability. Some consider the increase

in the temperature as an energy input, attributing this effect to the change in the crystalline structure on the particles' components or ZP which might affect the particle size during storage [215, 235].

Next, the Chol concentration in the different vesicles was examined. The theoretical Chol concentration was 129.05 µg/ml and it was expected that the concentration post-preparation to be close to this. However, after preparation using different media, the calculated concentrations were significantly ($p < 0.05$) lower than the theoretical one for particles prepared with HEPES, PBS, NS and DW. Only particles prepared with Tris buffer had a Chol concentration that was not significantly ($p > 0.05$) different from the theoretical one. For particles prepared with PBS and NS, the Chol concentrations were close to each other with no significant ($p > 0.05$) difference in the calculated concentration. Moreover, the concentration for NISV prepared with HEPES and DW was almost the same for both formulations with no significant ($p > 0.05$) difference and this is the same for the particle size for these two formulations. This indicates that the type of hydration media had a significant effect on the apparent Chol concentration recovered. It is worth noting that the Chol concentration was calculated based on the AUC at the retention time of 1.55 min, but there were some peaks just before and after this time (data not shown) and this might explain the difference between the theoretical and actual concentration after preparation as some interaction were expected to be occurred between Chol and the ions in the buffers that resulted in different separation times.

The interaction of the different NISV with FBS was then examined in an attempt to predict the stability of these particles when exposed to physiological conditions by calculating the RT of each formulation when incubated with 10% (v/v) FBS. The turbidity assay measures the degree of light scattering through a sample with suspended particles. Turbidity depends mainly on the concentration of the suspended particles, the size distribution of the particles in the liquid phase and the difference in the refractive index between the particles and the suspending medium

[236, 237]. Microbiological instability or increase in the particle size of the suspended particles as a result of aggregation will result in an increase in the RT of the liquid [215]. All the NISV showed good stability in terms of RT over two hours at 37°C. This can be seen with the minimal increase of the RT for all formulations with time, bearing in mind that this increase was not significant ($p > 0.05$). This result suggests that all the aqueous media used to prepare the NISV were effective in preventing particle aggregation when incubated with 10% (v/v) FBS.

Finally, the effects of the prepared formulations on the viability of two cancer cell lines (A375, A2780) and a normal PNT2 cell line were studied. Media-dependent toxicity on the A375 cell line was observed. The type of the media used to prepare the particles had a significant ($p < 0.05$) effect on the viability of these cells as there was a significant difference between the EC_{50} of each formula. When the media alone was tested on these cells, they were not toxic and the cells were 100% viable. The media-dependent toxicity on the A375 cells was probably due to the difference in the particle size or surface charge in each formulation which would affect its cellular uptake and the subsequent impact on viability [145]. Moreover, it has been reported that the particle size, shape, and surface chemistry all have effects on cellular internalisation and intracellular trafficking [238]. Since each formulation resulted in different particle characteristics in term of size and charge, this might be the reason for the difference in the cell viability for the A375 cells. Different cell types have different sensitivities and nanomaterial interactions with cells depend on the colloidal forces and the dynamic biophysicochemical interactions between the cells and the particles [239]. These effects of the type of the hydration media used for particles preparation on the cellular viability needs to be investigated more extensively and consideration given to this phenomenon by researchers. For the other cell lines (A2780 and PNT2), although there were differences between the EC_{50} for each formulation, they were not significant and the EC_{50} for each formulation was close to the others, taking into consideration that the media alone were not toxic to any of these cell lines.

3.5. Conclusion

In this chapter, the aqueous media used to prepare NISV by microfluidics were reported, for the first time, to have a significant effect on the physiochemical characteristics of the resultant particles. These findings provide strong evidence that the type of the media used to prepare NISV by microfluidics has significant effects on particle size, distribution and surface charge. The type of the media used should be taken into consideration in order to modulate these characteristics of the formed particles. This is an important factor that will also have implications with respect to the entrapped material as the media can be chosen based on the compatibility with the intended drug to be encapsulated which in addition may help to design vesicles for different uses based on changing the preparation medium. The aim of this thesis is to investigate the use of NISV in siRNA delivery to cancer cells. Therefore, establishing cytotoxicity of the drug delivery system alone and effect of the preparation media on the NISV cytotoxicity, while the media were not cytotoxic on their own, was also an important finding to optimise the NISV formulations.

Chapter 4

Formulation of NISV prepared by microfluidics for therapeutic delivery of siRNA into cancer cells

Abstract

siRNA have a broad potential as therapeutic agents to reversibly silence any target gene of interest through the RNAi mechanism. The clinical application of siRNA requires the use of safe and effective delivery systems which can carry, protect siRNA, and deliver them to the site of action in target cells. In this chapter, the use of NISV for the delivery of siRNA into cancer cells was investigated. Different types of NISV formulations were synthesised by microfluidic mixing and then evaluated for their physiochemical properties such as size, ZP, stability, and morphology. Next, the cytotoxic effects and the siRNA encapsulation efficiencies of NISV were investigated. The ability of NISV to carry and transfect siRNA targeting green fluorescent protein (GFP) into human non-small cell lung cancer A549 cells that stably express GFP (copGFP-A549) and knockdown the GFP expression was studied by fluorescence measurement, flow cytometry, reverse transcription quantitative real-time polymerase chain reaction (RT-qPCR), and Western blotting. This study demonstrated that NISV were able to deliver siRNA to the target cells and induce significant knockdown of GFP expression to varying degrees, depending on the NISV composition. Therefore, NISV were demonstrated to represent a promising and effective platform for therapeutic delivery of siRNA.

Key Words

Non-ionic surfactant vesicles, Microfluidics, RNA interference, Drug delivery

4.1. Introduction

The RNAi mechanism is an endogenous post-transcriptional gene regulatory mechanism that involves the degradation of messenger RNA (mRNA) in a highly sequence-specific manner [170]. The RNAi mechanism involves the incorporation of the anti-sense strand of the siRNA into the RISC in the cytoplasm, followed by cleavage of the target mRNA that is complementary to the anti-sense strand of the siRNA to cause silencing of the gene encoded by that mRNA [175]. Following the discovery of this mechanism, a significant body of research has been carried out to investigate the application of RNAi for the treatment of human diseases [171, 172]. For therapeutic applications, synthetic siRNA can be designed to target genes overexpressed in human diseases such as cancer [173]. However, the successful application of siRNA-based therapeutics is dependent on the efficient delivery of siRNA to target cells [179]. Due to the poor stability of siRNA in physiological fluids and their inefficient cellular uptake, effective delivery of therapeutic siRNA into the cytoplasm of target cells is one of the main challenges in the development of siRNA-based treatments. An ideal siRNA delivery system, for clinical application, should protect the siRNA from rapid digestion, efficiently deliver the therapeutic siRNA into the target cells, and promote the subsequent release of siRNA from endosome vesicles into the cytoplasm, where they can be loaded into the silencing complex for gene silencing. Moreover, the delivery system should be biodegradable with low toxicity.

Non-viral delivery systems such as liposomes, dendrimers, cell-penetration peptides, and many others have been investigated for the delivery of siRNA to expand their clinical application [240]. Lipid-based nanoparticles such as liposomes are by far the most studied drug-delivery system for this purpose. However, due to the limitations of liposomes, such as cost and stability, the delivery of siRNA by NISV as an alternative were investigated in this chapter. NISV are generally superior to liposomes in terms of stability and production costs [81]. However, the application of NISV in the field of gene delivery has not been investigated extensively. Most

of the research in the literature use these vesicles for DNA delivery [241, 242], and there is only a limited number of publications describing their use for siRNA delivery [243], with some of them using particles formed using a combination of surfactants and phospholipids [244].

4.1.1 Chapter aims

In previous chapters, stable NISV through microfluidic mixing were formulated. In this chapter, cationic NISV (CN) were synthesised using microfluidics with different surfactants and their potential application for siRNA transfection were investigated. The aim of choosing a cationic design was to enhance the transfection efficiency and improve intracellular transfer such as endosome escape. Moreover, this positive charge will enhance the stability of these formulations by inducing electrostatic repulsion between particles. The cationic charge on the formulated NISV was achieved using the cationic lipid didodecyldimethylammonium bromide (DDAB), which not only helps with building the NISV bilayer structure, but also offers positive charge to both bind siRNA drugs and mediate cellular uptake via electrostatic adhesion to cellular surfaces that carry a slight negative charge. The prepared CN were evaluated for their physical characteristics, cytotoxicity, siRNA loading efficiency, and transfection efficiency. Results were compared against a commercially available transfection reagent, HiPerFect.

4.2. Materials and Methods

4.2.1. Materials

Polyoxyethylenesorbitan trioleate (Tween 85); DDAB; Tris base; sodium pyrophosphate ($Na_4P_2O_7$); sodium dodecyl sulphate (SDS); bromophenol blue; glycerol; glycine; sodium chloride (NaCl); bovine serum albumin (BSA); ethylenediamine tetra-acetic acid (EDTA); Tween 20; and Dulbecco's Modified Eagles medium (DMEM) were purchased from Sigma-Aldrich (UK). N-(carbonyl-methoxypolyethylenglycol-2000)-1,2-distearoyl-sn-glycero-3-phosphoethanolamine, sodium salt (MPEG-2000-DSPE) was obtained from Lipoid AG (Switzerland). Skimmed milk powder was purchased from Premier Foods Ltd (UK). The human non-small cell lung cancer (A549) cells were purchased from the ATCC®. Human non-small cell lung cancer A549 cells that stably express GFP (copGFP-A549) were purchased from Cell Biolabs, Inc., (UK). Sterile, RNase-free phosphate buffered saline 1M and sterile RNase-free water were purchased from LONZA (UK). A Quant-iT MicroRNA assay kit and Enhanced chemiluminescence (ECL) kit were purchased from Fisher Scientific (UK). AllStars Negative Control siRNA, AllStars AF488-labelled Negative Control siRNA, HiPerFect transfection reagent, and RNeasy Plus Micro and Mini Kits were purchased from Qiagen (UK). TURBO DNA-free DNase Treatment and Removal Reagents kit and PowerUp SYBR Green Master Mix (2X) were purchased from Life Technologies (UK). The anti-GFP DsiRNA (siGFP) duplex sequence**,** and the non-targeting scrambled DsiRNA (Table 4.1) were synthesised by Integrated DNA Technologies (Belgium). A Tetro cDNA synthesis kit was purchased from Bioline Reagents Ltd (UK). 10% Mini-PROTEAN® TGX™ precast gels were purchased from Bio-Rad Laboratories Ltd (UK). A rabbit polyclonal antibody against copGFP was purchased from Evrogen JSC (Russia) and a rabbit polyclonal antibody against glyceraldehyde 3-phosphate dehydrogenase (GAPDH) was purchased from Santa Cruz

Biotechnology (UK). 0.45 µm pore size nitrocellulose membrane was purchased from GE Healthcare Life Sciences (UK). Other material suppliers were described in section 2.2.1.

Table 4.1 Sequences of siGFP and non-targeting scrambled DsiRNA.

siRNA sequence (5'-3')		
siGFP	Sense	rCrGrCrArUrGrArCrCrArArCrArArGrArUrGrArArGrArGCA
	Antisense	rUrGrCrUrCrUrUrCrArUrCrUrUrGrUrUrGrGrUrCrArUrGrCrGrGrC
Scrambled	Sense	rCrGrUrUrArArUrCrGrCrGrUrArUrArArUrArCrGrCrGrUAT
	Antisense	rArUrArCrGrCrGrUrArUrUrArUrArCrGrCrGrArUrUrArArCrGrArC

4.2.2. Formulation of cationic NISV (CN)

CN were prepared by microfluidics as described in Section 2.2.5 using a NanoAssemblr™ (Benchtop, Precision NanoSystems Inc., Canada). To prepare the CN, the required lipid components at the desired ratios were dissolved in ethanol at a final lipid concentration of 10 mg/ml. The lipid phase was then injected into the first inlet and the aqueous buffer (sterile RNase-free water) into the second inlet of the microfluidic microchannel using disposable syringes through syringe pumps. CN were formulated at a TFR of 12 ml/min (9 ml/minute for the aqueous phase and 3 ml/minute for the lipid phase) and a volumetric FRR of 3:1 between the aqueous and lipid phase at 50ºC. The resulting CN dispersions collected from the outlet stream were immediately diluted in an equal volume of sterile RNase-free water in order to reduce the final ethanol content in the preparation to 6.25% (v/v). Different lipid combinations were used to prepare the CN (Table 4.2) and the most stable formulations were used in the subsequent siRNA transfection studies.

Table 4.2 Composition of CN formulations prepared by microfluidic mixing.

Formulation	Lipid components	Molar ratio
A	MPG:Chol:DDAB	40:40:20
B	MPG:Chol:DDAB	30:50:20
C	T85:Chol:DDAB	40:40:20
D	MPG:T85:Chol:DDAB	20:20:40:20
E	MPG:T85:Chol:DDAB:PEG	20:20:37:20:3
F	MPG:Chol:DDAB:PEG	38:38:19:5
G	MPG:Chol:DDAB:PEG	28:48:19:5
H	T85:Chol:DDAB:PEG	38:38:19:5

4.2.3. CN characterisation

Particle size, PDI, and ZP of the formulations were measured by DLS as described in Section 2.2.6.

4.2.4. Stability studies of CN

All formulations of CN were tested for their stability over a two month period at 25°C storage in a controlled temperature room. Z-average, PDI, and ZP were measured every week.

4.2.5. Morphological analysis of CN using atomic force microscope (AFM)

Morphological analysis for the most stable formulations was performed by AFM as described in Section 2.2.8.

4.2.6. Cytotoxicity of CN on a number of human cell lines

A375 and PNT2 cells were grown and maintained in RPMI 1640 medium and A549 were grown and maintained in DMEM medium, both supplemented with 10% (v/v) FBS, 1% (v/v) L-glutamine and 1% (v/v) penicillin-streptomycin. The toxicities of the CN formulations on these cell lines were evaluated as described in Section 2.2.9.

4.2.7. Preparation of CN/siRNA nioplexes

CN/siRNA complexes (termed nioplexes) were prepared as follows: an appropriate volume of siRNA (from 10 μM stock) was mixed with the desired CN formulation (from a 625 μg/ml stock) with pipetting up and down to ensure optimal mixing. The nioplex samples were incubated at 25 °C for 30 min to allow the formation of transfection complexes. For experiments that involved determination of physical characteristics (Z-average, PDI, and ZP, EE) of the formed complexes, AllStars Negative Control siRNA was used. For cellular uptake experiments including flow cytometry and fluorescent microscopy, AllStars AF488-labelled Negative Control siRNA was used. For experiments that involved the GFP knockdown in copGFP-A549 cells, siGFP was used.

4.2.8. Encapsulation efficiency (EE)

The siRNA EE of the most stable formulations was determined using a Quant-iT MicroRNA kit following the manufacturer's protocol. This kit contains a reagent that is fluorescent when it binds to free and non-encapsulated siRNA. The fluorescence was measured using a SpectraMax M5 plate reader (excitation/emission maxima are 500/525 nm). Free and initial siRNA concentrations were determined using a standard curve. For this experiment, negative control siRNA was used at concentrations from 10 - 250 nM, which were tested for EE with 78.125, 156.25, and 312.5 μg/ml from each formulation. The siRNA EE was calculated using the equation:

$$\text{EE} = 100 - \left(\frac{\text{free siRNA concentration}}{\text{initial siRNA concentration}}\right) \text{x } 100$$

4.2.9. Characterisation of CN/siRNA nioplexes

In order to assess changes in CN characteristics after complexing with siRNA, Z-average and ZP were measured for these formulations after complexing with various concentrations of AllStars Negative Control siRNA.

4.2.10. *In vitro* cellular uptake

To study the cellular uptake of nioplexes, A549 cells were seeded in 12-well plates at a density of 1 x 10^5 cells per well in 1100 µL of DMEM medium supplemented with 10% (v/v) FBS, 1% (v/v) L-glutamine and 1% (v/v) MEM NEAA (without antibiotics) for 24 h at 37ºC, 5% CO_2 and 100% humidity. The following day, 100 µl of each of the AF488-labelled Negative Control siRNA-cationic nioplexes (as described in Section 4.2.7) were added drop-wise to the cells, with gentle plate swirling to ensure uniform distribution of the nioplexes. Transfected cells were incubated at 37°C, 5% CO_2 and 100% humidity for 48 h. The quantitative cellular uptake was measured using a fluorescence-activated cell sorter (FACS). For this purpose, the media was removed and the cells were washed with PBS, pH7.4. The cells were trypsinised with 300 µl trypsin and then diluted to 1 ml with PBS. The cell suspension was transferred to FACS tubes (BD Biosciences; UK), centrifuged for 5 min at 1500 rpm and the supernatant aspirated. The cell pellet was then re-suspended in 1 ml FACS buffer (10% v/v FBS in PBS) and analysed on a FACS Canto flow cytometer (BD Biosciences; Oxford, UK). Upon acquisition, the cells were gated using forward scatter versus side scatter (FCS vs SSC) to eliminate dead cells and debris. Cells (10,000) were collected for each sample and the data analysed with DB FACS Diva software. Cellular uptake and median florescence intensity were reported. The results were compared to the positive control HiPerFect transfecting reagent. siRNA alone, CN alone,

and untreated cells were used as controls. The final siRNA concentration after transfection was 10 nM. The results were presented as the mean and standard deviation of triplicate samples. For qualitative uptake measurements, cells were prepared as described above and the cellular uptake of CN/AF488 nioplexes were viewed using a Carl Zeiss Axio-Imager Z1 microscope (Zeiss, Germany) under a 20X water immersion lens with a numeric aperture of 0.80. Fluorescence was excited using a mercury lamp and emission recorded using a fluorescein isothiocyanate (FITC) filter block (485/515-530nm). Analysis of images was carried out with AxioVision 4.8 software.

4.2.11. Silencing efficiency studies

4.2.11.1. Evaluating GFP silencing by fluorescence readings

A549 cells expressing GFP (copGFP-A549) were used in studies assessing the ability of siRNA-nioplexes to downregulate gene expression (the sequence of the copGFP in the copGFP-A549 cells can be found in Appendix 1). To evaluate the transfection efficiency of the selected CN formulations, copGFP-A549 cells were seeded at a density of $2x10^4$ cells per well in 96-well plates in 150µl DMEM medium supplemented with 10% (v/v) FBS, 1% (v/v) L-glutamine, 1% (v/v) MEM NEAA (without antibiotics) 24 h before transfection. The cells were then treated with 50 µl of different ratios (w/w) of CN/siRNA nioplexes (3.69 – 471.8 w/w) prepared as described in Section 4.2.7 using siGFP. Transfected cells were incubated at 37°C at 5% CO_2 and 100% humidity for 24, 48, and 72 h. Experiments with HiPerFect transfection reagent (positive control) were prepared following the manufacturer's protocol. At each time point, the intensity of GFP was determined by measuring the fluorescence at 485-535 nm using a SpectraMax M5 plate reader. The percentage of GFP knockdown (silencing efficiency) was calculated using the formula:

$$\text{Percentage of GFP knockdown} = 100 - \left(\frac{\text{Fluorescence of the transfected cells}}{\text{Fluorescence of the untreated cells}}\right) \text{x } 100$$

4.2.11.2. Evaluating GFP silencing by FACS

To confirm the transfection efficiency of the selected CN formulations, copGFP-A549 cells were seeded in 12-well plates at $1x10^5$ cells/ml in 1100 μL DMEM supplemented with 10% (v/v) FBS, 1% (v/v) L-glutamine, 1% (v/v) MEM NEAA (without antibiotics) 24 h before transfection. Cells were treated with the desired CN formulation encapsulating various concentrations of siGFP (10-100 nM final concentration). Control samples containing cells treated with particles alone (mock transfection), siGFP alone, untreated cells, and untreated A549 cells (not producing GFP) were used as controls. The activity of the CN formulations, in terms of siRNA transfection, were compared to that of the HiPerFect transfection reagent. After transfection, the cells were incubated for 72 h at 37°C, 5 % CO_2 and 100 % humidity, then trypsinised, centrifuged and re-suspended in FACS buffer. A FACS Canto flow cytometer was used to quantify the percentage of GFP expression, the median fluorescence intensity (MFI), and to assess the efficacy of GFP silencing by siGFP delivered by the CN formulations. A control sample (untreated cells) was displayed on a FCS vs SSC dot plot to establish a collection gate and exclude cell debris. MFI data of the GFP in each sample was compared to the MFI of the GFP expressing untreated cells. For each sample, 10,000 events were collected. The data obtained were analysed using FACS Diva software. The MFI of GFP was used to calculate the percentage gene silencing using the formula:

$$\text{Percentage of GFP expression} = \left(\frac{\text{MFI of the transfected cells}}{\text{MFI of the untreated control cells}}\right) \text{x } 100$$

The experiment was carried out in triplicate and reported as the mean ± SD.

4.2.11.3. Polymeric chain reaction (PCR)

4.2.11.3.1. Minimum Information for Publication of Quantitative Real-Time PCR Experiments (MIQE)

The Minimum Information for Publication of Quantitative Real-Time PCR (qPCR) Experiments (MIQE) is a set of guidelines that describe the minimum information required for evaluating and publishing qPCR experiments results [245, 246]. The aim of the MIQE guidelines is to provide the reader with all the information required to either repeat the experiment or be able to judge whether the data is reliable. These guidelines cover all the steps of a qPCR assay including sample acquisition, handling, preparation, quantification of nucleic acids, reverse transcription, qPCR, and data analysis. Figure 4.1 presents an overview of some of the suggested information to be included in publications, which are related to the sample, assay optimisation, PCR method, and data analysis. The MIQE guidelines were followed where possible in the current study.

Normalisation is an essential component of a reliable qPCR assay as it ensures the control of variations in extraction yield, reverse-transcription yield, and efficiency of amplification. This enables comparison of mRNA concentrations in different samples [245]. The most common method of normalisation for internally controlling errors in RT-qPCR is by using a reference (housekeeping) gene [246]; the most commonly used include β-actin, glyceraldehyde-3-phosphate dehydrogenase (GAPDH), 2-microglobulin (B2M), hypoxanthine-guanine phosphoribosyl transferase (HPRT), and 18S ribosomal RNA [247-249]. It is important that the expression of the reference gene is unaffected by the treatment the cells undergo [246]. Based on previous work with NISV within the research group, B2M was an appropriate gene to use (R Tate personal communication).

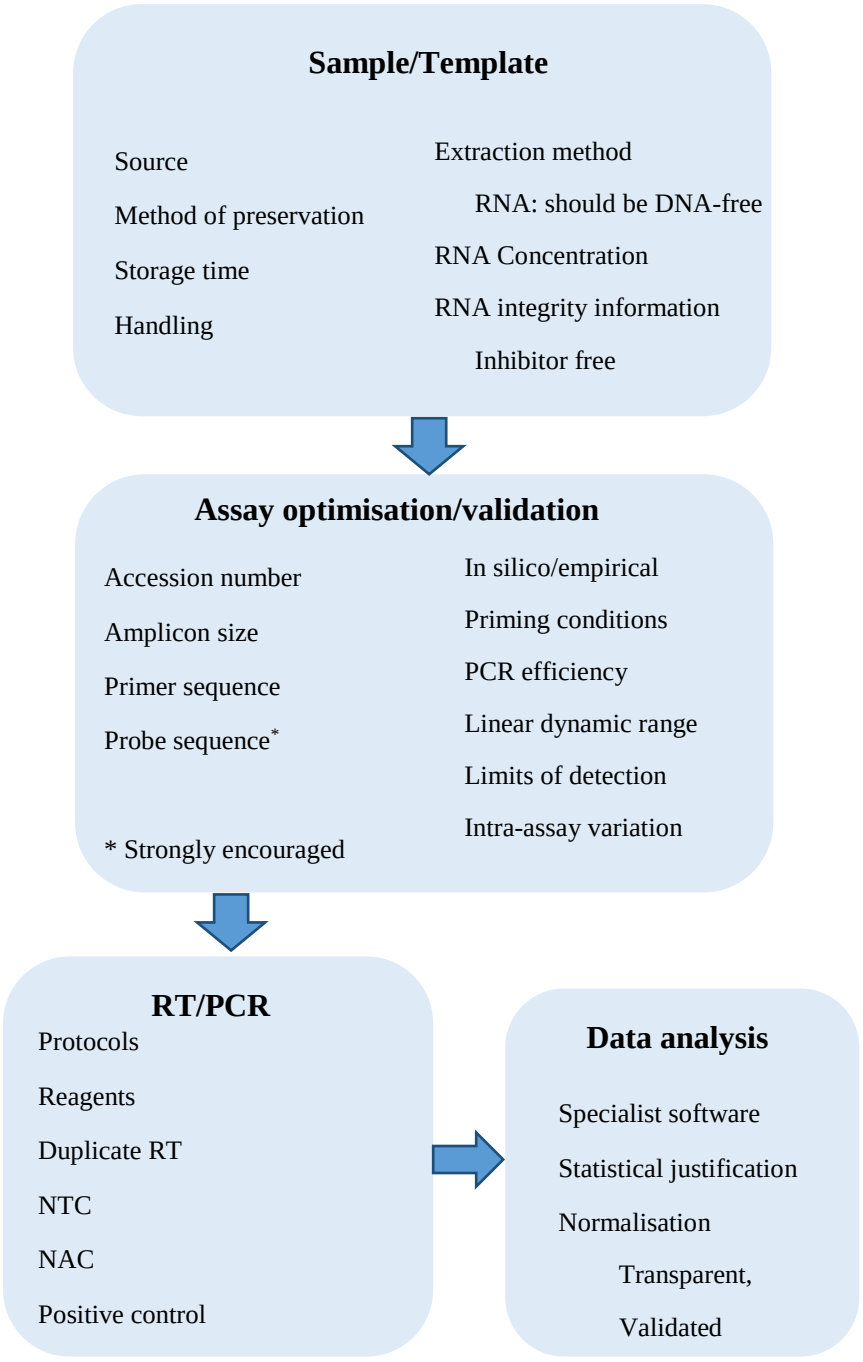

Figure 4.1. Key criteria delineating essential technical information required for the assessment of a RT-qPCR experiment. Accession number: unique identifier of a nucleotide sequence. *In silico*: BLAST specificity analysis. NTC: no-template controls (H_2O). NAC: no amplification controls (RT negative controls) (adapted from Bustin *et al*., 2010).

To verify the silencing efficiency of the selected CN formulations using siGFP, RT-qPCR was carried out to analyse the effect of the treatments on the expression level of GFP and to measure the inhibition level. Cells (copGFP-A549) were seeded in 12-well plates at $1x10^5$ cells/ml in 1100 µl DMEM supplemented with 10% (v/v) FBS, 1% (v/v) L-glutamine, 1% (v/v) MEM NEAA (without antibiotics) 24 h before transfection. Twenty-four hours later, cells were treated with various concentrations (10-100 nM) of siGFP encapsulated in each of the selected CN formulations prepared as described in Section 4.2.7. HiPerFect was used as a positive control transfection reagent. After 72 h, the media was removed and 350 µl of RNeasy lysis buffer added to lyse the cells. RNA was extracted from the cell lysate using RNeasy Plus Micro and Mini Kits according to the manufacturer's instructions. To remove any carryover contaminating genomic DNA, which could interfere with the downstream reverse transcribed-PCR-based gene expression analysis, RNA extracts were treated with TURBO DNA-free DNase Treatment and Removal Reagents kit following the manufacturer's protocol. The RNA concentration was determined using a NanoDrop 2000c spectrophotometer (Thermofisher scientific, UK) by measuring the absorbance at 260 nm (A260) using 2 µl samples. RNA purity, as expressed by the ratio of the absorbance at 260 nm and 280 nm (A260/A280), was also determined by the NanoDrop 2000c spectrophotometer.

4.2.11.3.2. cDNA synthesis

A Tetro cDNA synthesis kit was used to generate cDNA templates from each sample of the RNA extracted from the copGFP-A549 cells for use in RT-qPCR following the manufacturer's protocol. Briefly, 1µl of oligo $(dT)_{18}$ primer mix, 1µl of 10mM dNTP mix, 4µl of 5x RT buffer, 1µl of RiboSafe RNase inhibitor, 300 ng of the RNA extracts, 1µl of Tetro reverse transcriptase (200u/µl), and sterile RNase-free water to make the total volume up to 20 µl were added to a nuclease-free microcentrifuge tube. The mixture of each sample was mixed gently by pipetting and then incubated at 45°C for 30 min. The reverse transcriptase reaction was then terminated

by incubating the samples at 85°C for 5 min then the samples were chilled on ice. Negative control samples were prepared in parallel for each RNA sample as described above using nuclease-free water instead of Tetro reverse transcriptase. Such reactions were designated as the sample "RT-" control as it would be an indicator for any persisting contaminating genomic DNA. A PCR carried out using an aliquot of these negative controls as the template should not generate any products. Prepared cDNA samples were then stored at -20°C until their use in PCR experiments.

4.2.11.3.3. PCR Primers design

Forward and reverse oligonucleotide primers for GFP and for the reference gene, B2M, were designed using GeneRunner version 3.01 (http://www.generunner.net/) and synthesised by Integrated DNA Technologies (Belgium). The parameters for designing the GFP and B2M primers were set so the primers had a length between 18 and 24 nucleotides, a melting temperature (Tm) ≥ 59°C but ≤ 61°C with primer Tm difference set to 0.2, a percentage of guanine-cytosine (GC) between 45 - 65%, and an amplicon between 120 and 150bp long. Specificity of each set of primers was verified with the Primer-BLAST tool [250] (http://www.ncbi.nlm.nih.gov/tools/primer-blast) to make sure that the primers were specific and would not amplify unwanted products. Primer sequences, Tm, and amplicon size are summarised in Table 4.3.

Table 4.3 PCR primer sequences, melting temperatures (Tm) as determined by GeneRunner.

Gene	Primer sequences (5'- 3')		Tm (°C)	Amplicon size (bp)
copGFP (Cell Biolabs Inc.)	Forward	GCGTGCTGCACGTGAGCTTC	65.10	125
	Reverse	GTTGCTGCGGATGATCTTGTCG	62.42	
B2M (NM_004048.2)	Forward	CTCTCTTTCTGGCCTGGAGGCTATC	64.22	126
	Reverse	ATGTCGGATGGATGAAACCCAGAC	62.74	

4.2.11.3.4. SYBR Green quantitative real-time PCR

GFP gene expression assays were carried out using SYBR Green-based RT-qPCR. SYBR Green is a fluorescent dye that binds to double-stranded DNA (dsDNA) in a sequence-independent manner. After binding with dsDNA, fluorescence increases over 1000-fold [251]. Briefly, for each reaction, 10µl of PowerUp SYBR Green Master Mix (2X), 0.6µl of forward primer (10pmol/µl), 0.6µl of reverse primer (10pmol/µl), 1µl cDNA and 7.8µl of nuclease-free water were added to the wells of a nuclease-free PCR 96-well plate. Negative controls with nuclease-free water and "RT-" cDNA reaction mixture for each sample were also set up. The plate was sealed with an optical adhesive film cover, and loaded into a StepOnePlus RT PCR system (Applied Biosystems, UK). Thermal cycling conditions were set for a fast cycling mode as shown in Table 4.4, which was followed by melting curve analysis to assess reaction specificity and to check for non-specific amplification that can result from primer-dimer artefacts or other non-specific product binding SYBR Green. Since SYBR green fluoresces intensely when bound to dsDNA, the product denaturation can be observed as a sudden loss of green fluorescence near the melting (denaturing) temperature by monitoring the fluorescence throughout a specific temperature cycle [252]. A melting curve of the PCR reaction is produced

by gradually increasing the temperature and monitoring the green fluorescence decrease as the duplex DNA target gradually denatures and the SYBR green detaches from it with the highest rate of fluorescence decrease occurring at the Tm of the target gene amplicon [253]. The threshold cycle number (Ct) was calculated for GFP and B2M using StepOnePlus software (v2.1). The expression of GFP and B2M mRNA was analysed by the $2^{-\Delta\Delta Ct}$ relative-quantitative method as described by Livak *et al.* (2001) [254] and Haimes *et al.* (2010) [255].

Table 4.4 PCR thermal cycling conditions.

Fast Cycling Mode (primer Tm ≥ 60°C			
Step	**Temperature**	**Duration**	**Cycles**
UDG Activation	50°C	2 min	Hold
AmpliTaq Fast DNA Polymerase activation	95°C	2 min	Hold
Denature	95°C	3 sec	40
Anneal/Extend	60°C	30 sec	

4.2.11.4. Western blotting analysis of GFP silencing

To further assess the downregulation of GFP expression in copGFP-A549 cells by siGFP transfected through the selected CN formulations, copGFP-A549 cells were seeded in a 12 well plate at $1x10^5$ cells/ml in 1100 µl DMEM supplemented with 10% (v/v) FBS, 1% (v/v) L-glutamine, 1% (v/v) MEM NEAA (without antibiotics) 24 h before experiments at 37ºC, 5% (v/v) CO_2 and 100% humidity. Twenty four hours later, the cells were treated with various concentrations of siGFP (10-100 nM) transfected using each of the selected CN formulations. HiPerFect was used as a positive control transfection reagent. Scrambled negative control siRNA was used at a concentration of 100 nM to prove that transfection of small, non-targeting RNA molecule will not elicit an effect on the cells. Untreated cells, cells treated with naked

siGFP, mock transfection (particles alone without siRNA), and cells that did not express GFP were used as controls. The cells were incubated for 72 h, then the media was removed and the cells were lysed with 250 µl lysis buffer (method of preparation of lysis buffer is detailed in Appendix 2). The GFP levels of samples after transfection were determined by Western blot, normalised with GAPDH levels as a loading control (methods of preparation of all buffers used in Western blotting are detailed in Appendix 2). Twenty-five µl of cell lysate was loaded and separated using 10% Mini-PROTEAN® TGX™ precast gels, subjected to electrophoresis and then transferred electrophoretically at 400 mA for 1 h to a nitrocellulose membrane with a 0.45 µm pore size. The membrane was blocked with 3% (w/v) skimmed milk powder in Tris-buffered saline with Tween 20 (TBST) at 25 °C for one hour. The membrane was incubated with a rabbit polyclonal antibody against copGFP (1:1000 diluted in 1% BSA in TBST at 4°C overnight. The membranes were then washed three times with TBST for 7 min on a shaking platform and then incubated with a secondary antibody anti-rabbit IgG monoclonal antibody (1:0000 diluted in TBST) in 3% (w/v) skimmed milk powder in TBST for one hour at room temperature. Membranes where then washed with TBST thoroughly at room temperature before visualising by a standard enhanced chemiluminescence (ECL) kit according to the manufacturer's protocol. Semi-quantification of the bands was performed by densitometry using ImageJ public domain software from the National Institutes of Health (http://rsb.info.nih.gov/ij/).

4.2.12. Statistical analysis

All experiments were performed in triplicate and ANOVA was used to assess statistical significance. Tukey's multiple comparison test and t-test was performed for paired comparisons. The statistical analysis was performed using Minitab software version 17. A value of $p<0.05$ was considered to be statistically significant.

4.3. Results

4.3.1. Physiochemical characterisation of CN

CN prepared by microfluidics were assessed for their size, PDI, and ZP (Table 4.5). All the prepared formulations were small in size with the largest particles reported for formulation H (120.60 ± 1.13 nm) and smallest particles for formulation E (42.02 ± 0.26 nm). All the prepared formulations had low particle size distribution as indicated by their PDI values (<0.3) except for formulations F and G where the PDI values were > 0.4. As a result of using the cationic lipid DDAB, all the prepared formulations carried an overall positive ZP value. Formulations E-H carried a slightly lower positive charge compared to the other formulations as a result of the presence of PEG in their formulations, which is thought to partially mask the surface charge of the particles [256].

Table 4.5 Comparison of particle characteristics of CN formulations prepared by microfluidic mixing in terms of size, PDI and ZP. n=3 ± SD (For the composition of each formulation please refer to table 4.2)

Formulation	Size (nm)	PDI	ZP (mV)
A	46.30 ± 0.18	0.10 ± 0.02	49.72 ± 2.80
B	49.39 ± 0.56	0.17 ± 0.04	51.48 ± 2.99
C	59.16 ± 1.88	0.19 ± 0.09	47.45 ± 2.43
D	69.04 ± 0.72	0.03 ± 0.01	57.47 ± 0.32
E	42.02 ± 0.26	0.29 ± 0.002	49.13 ± 4.73
F	74.32 ± 4.12	0.42 ± 0.05	45.73 ± 5.21
G	65.53 ± 4.39	0.49 ± 0.04	45.57 ± 7.01
H	120.60 ± 1.13	0.25 ± 0.01	34.20± 3.70

4.3.2. The effects of the lipid composition on overall stability of CN

The stability of the prepared formulations was monitored over two months in terms of changes to Z-average and PDI over time. Only formulations A, B, and C were stable with no significant ($p>0.05$) change in size or PDI (Figure 4.2). However, the other formulations (D-H) showed significant ($p<0.05$) increase in size and PDI over time (data not shown) indicating poor stability for these formulations. Based on these results, formulations A-C were chosen for subsequent experiments and the other formulations were discarded.

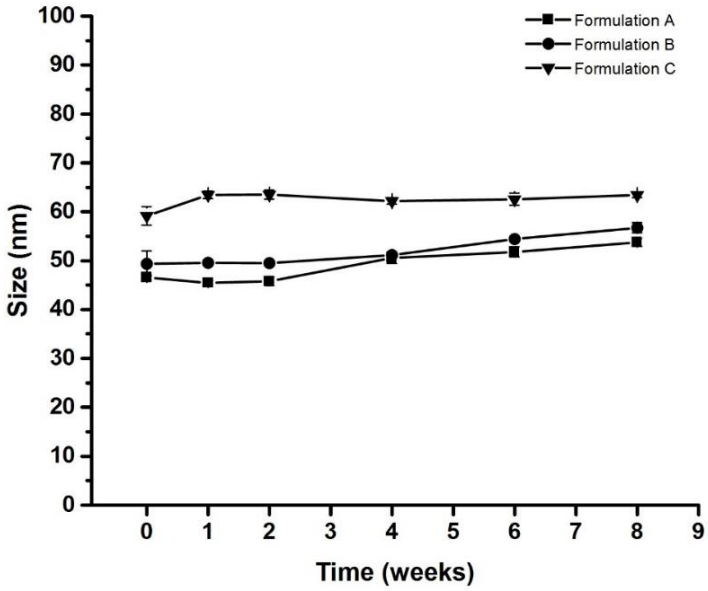

Figure 4.2. Stability of CN formulations A-C over two months at 25 °C. The data represents the mean ± SD (n=3). (For the composition of each formulation please refer to table 4.2**).**

4.3.3. CN morphology

The morphology of the most stable formulations A-C was analysed by AFM (Figure 4.3). All the particles were spherical in shape with a small particle size, which are consistent with the DLS measurements (Table 4.5).

4.3.4. Cytotoxicity of CN on a number of human cell lines

To develop an efficient drug delivery system, it is important to consider the possible toxic effects of these formulations upon the target cells. Therefore, toxicity of the selected formulations was assessed on two cancer cell lines (A375 and A549) and a normal PNT2 human cell line to quantify cell viability. Figure 4.4 shows the cytotoxicity of the CN on the cells and the calculated EC_{50} values. As shown in Figure 4.4, the cytotoxicity increased as a function of CN concentration. For all formulations, concentrations equal or below 78.13 µg/ml were well tolerated by cells, with 100% cells viability for all cell lines. When the CN concentration was increased to above 625 µg/ml, significant ($p<0.05$) cytotoxicity was observed. As a result, all the transfection experiments of siRNA using these formulations were carried out at CN concentrations less or equal to 78.13 µg/ml as a final concentration after transfection to avoid confounding vehicle related cytotoxicity on the gene silencing activity of siRNA.

Formulation A

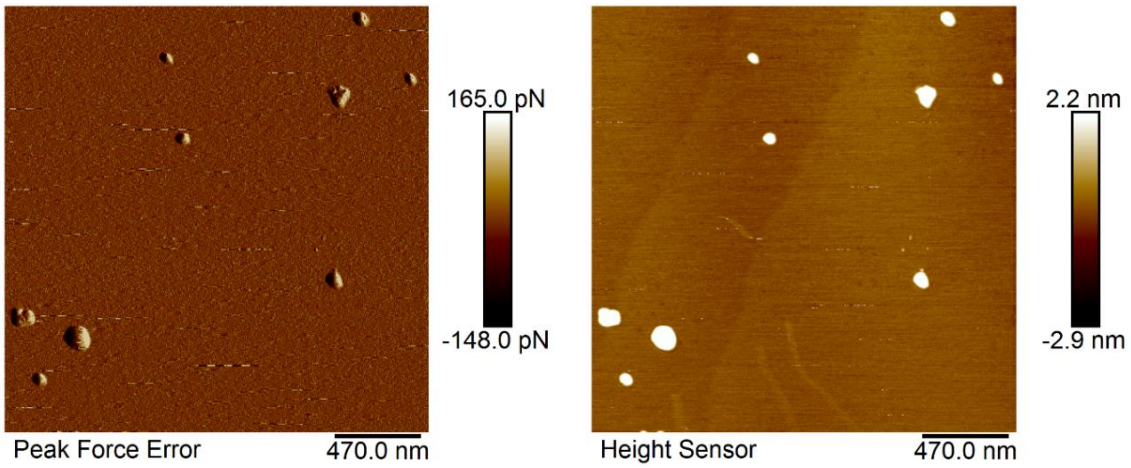

Formulation B

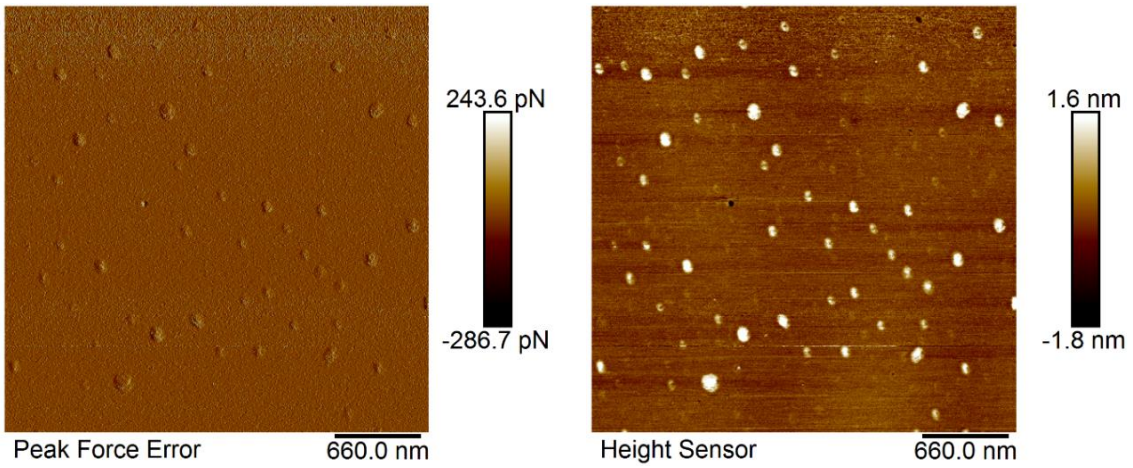

Formulation C

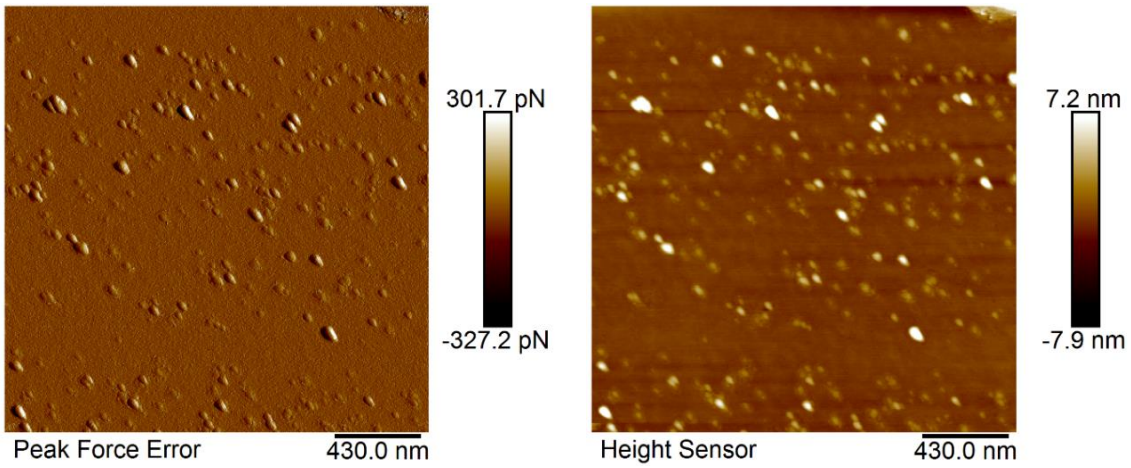

Figure 4.3. AFM images for the formulations A-C of the CN. (For the composition of each formulation please refer to table 4.2**).**

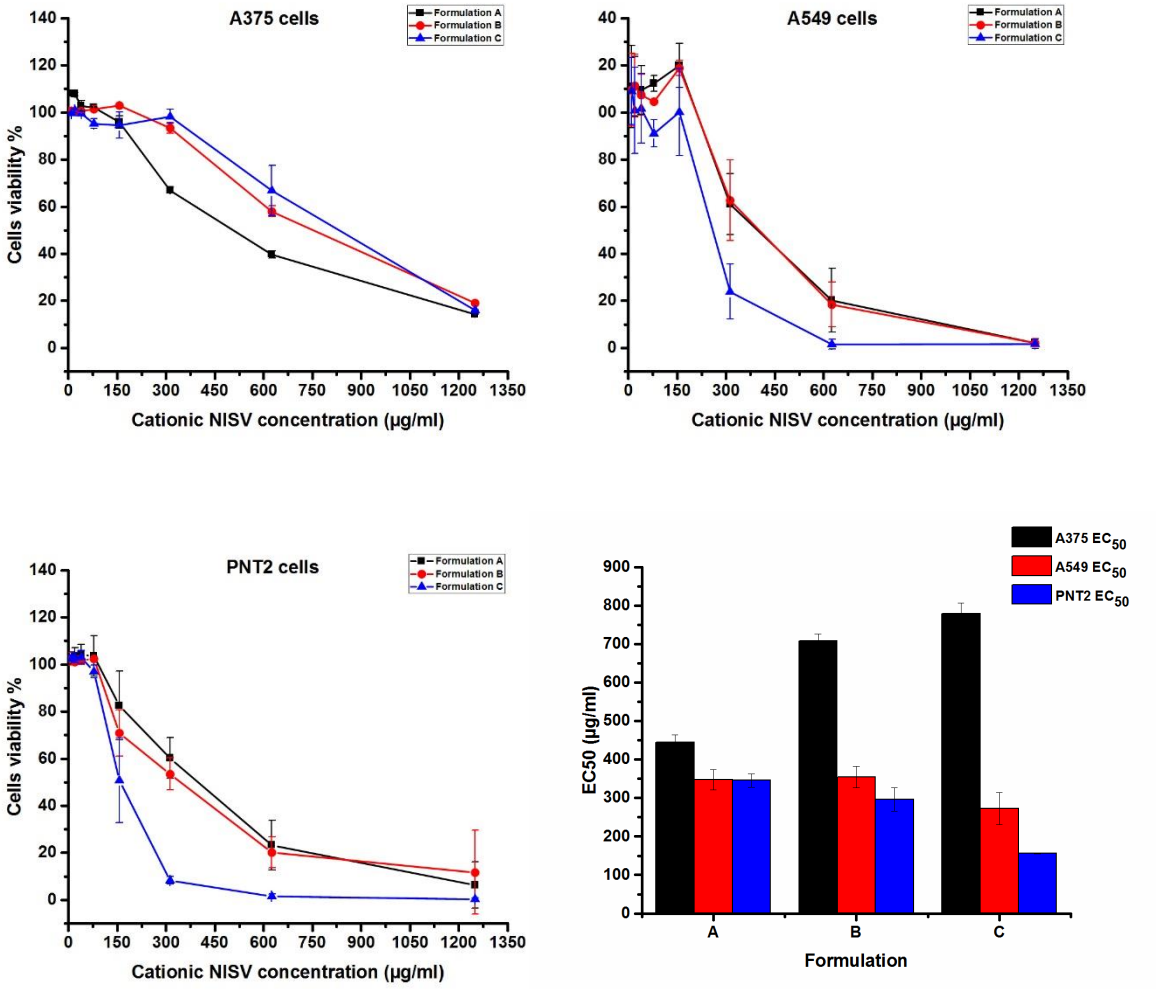

Figure 4.4. Cytotoxicity of the CN (formulations A- C) on A375, A549 and PNT2 cells and the calculated EC_{50} values. The data represents the mean ± SD (n=3). (For the composition of each formulation please refer to table 4.2**).**

4.3.5. Encapsulation efficiency (EE)

The initial and free siRNA concentrations were determined after constructing a standard curve with microRNA standards following the manufacturer's protocol. The EE was determined for formulations A-C using the generated equation ($y = 146569x$, $R^2 = 0.9916$). The siRNA EE was found to be generally high across the formulations (Figure 4.5), with the EE increasing with concentration of CN formulation from 78.125 to 312.5 µg/ml for all the formulations. Consequently, 312.5 µg/ml was chosen as the starting concentration (before transfection, which was diluted 10x in the assay so was non-toxic) in the subsequent experiments for siRNA transfection.

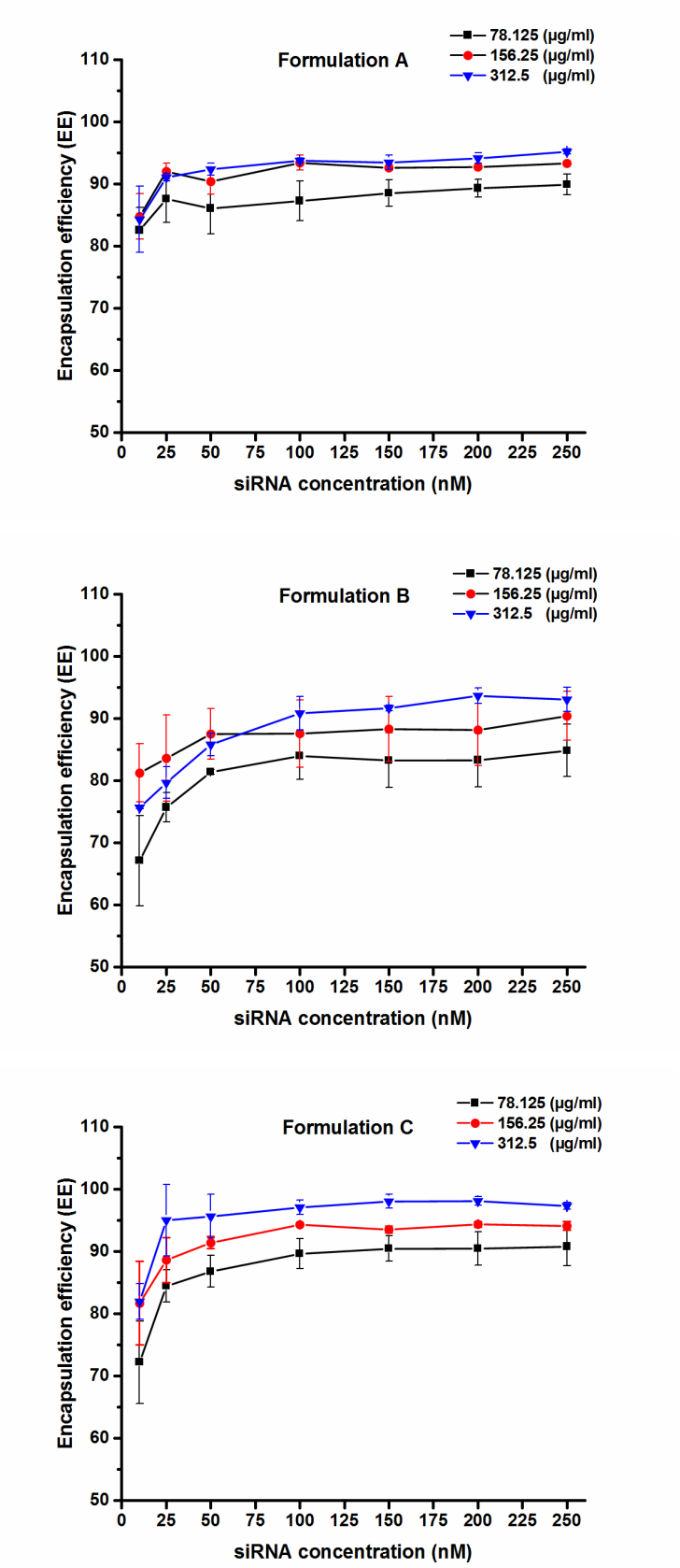

Figure 4.5. Encapsulation efficiency of siRNA with formulations A-C at different concentrations. Each point represents the mean ± SD (n=3). (For the composition of each formulation please refer to table 4.2**).**

4.3.6. Characterisation of CN/siRNA nioplexes

Combining Z-average, PDI, and ZP measurements is a common experimental strategy used to characterise the formation of vector/siRNA complexes. Therefore, the change of these parameters for the three cationic formulations A-C when encapsulating various concentrations of AllStars Negative Control siRNA were investigated and the results were reported for each CN/siRNA (w/w) ratio (Figure 4.6). The CN/siRNA ratio decreased by increasing the weight of the siRNA, whilst using a fixed weight of the CN. As can be seen in Figure 4.6, all three formulations remain at the same size for the empty particles, with no significant increase in the particle size regardless of the quantity of siRNA used except for formulation B with 250 nM siRNA, which had a significantly ($p<0.05$) higher particle size. Encapsulating the negative siRNA into CN was expected to have effects on the total particle ZP. A decrease in the CN/siRNA ratio from 1887 to 75 resulted in a decrease in the ZP from 49.72 ± 2.80 to 47.65 ± 0.07 mV for formulation A, from 51.48 ± 2.99 to 43.7 ± 2.52 mV for formulation B, and from 47.45 ± 2.43 to 45.05 ± 0.49 mV for formulation C.

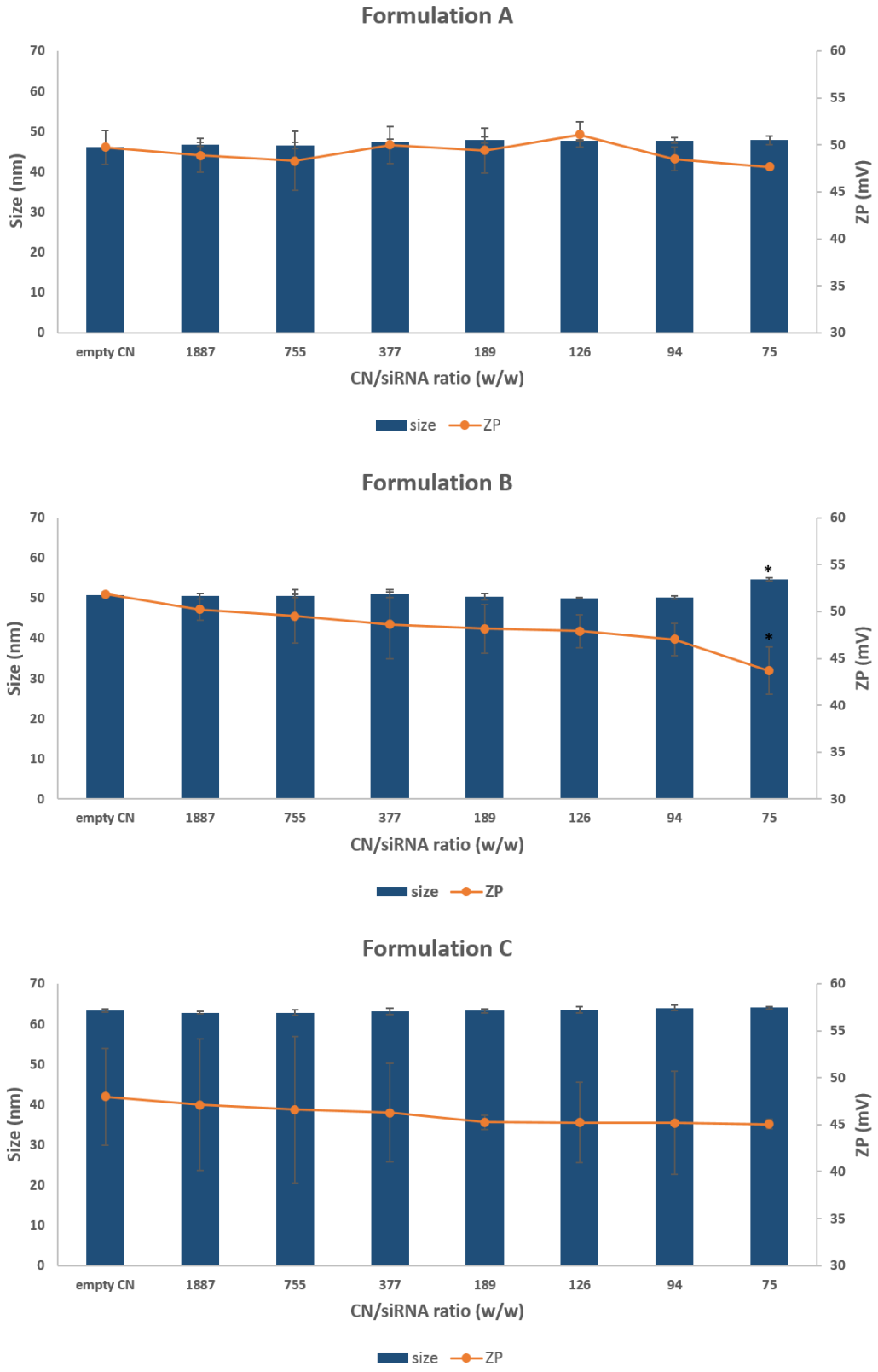

Figure 4.6. Changes of the particles size and ZP when varying the CN/siRNA (w/w) ratios by increasing the siRNA amount at a fixed CN amount. The data represents the mean ± SD (n=3) *p<0.05 compared to empty CN. (For the composition of each formulation please refer to table 4.2**).**

4.3.7. Uptake of siRNA nioplexes by A549 cells: FACS and fluorescence microscopy studies

To study the cellular uptake of siRNA encapsulated in the selected CN formulations, A549 cells were treated with the various nioplexes prepared with AF488- labelled Negative Control siRNA. The treated cells were analysed by fluorescence microscopy for qualitative analysis and by FACS for quantitative cellular uptake (Figure 4.7).

As can be seen in Figure 4.7-A, A549 cells did not present any intracellular siRNA signals after incubation with naked siRNA as evidenced by the lack of any green fluorescence associated with the cells. Cells treated with AF488-labelled Negative Control siRNA encapsulated in the three formulations showed a strong green fluorescence signal indicating siRNA uptake by the cells. The positive control transfection reagent, HiPerFect, also displayed an uptake of the AF488-labelled Negative Control siRNA. The CN formulations alone, without AF488-labelled Negative control siRNA, showed no fluorescence (images not shown). These results were confirmed by FACS studies, where the fluorescence histogram of the cells incubated with AF488-labelled Negative Control siRNA alone was similar to that of the untreated cells. The histograms for the cells treated with AF488-labelled Negative Control siRNA encapsulated in formulations A-C and with the HiPerFect transfection reagent showed a shift in the FITC values compared to the untreated cells (Figure 4.7-B) confirming cellular uptake. However, the histogram images indicate a variation in the degree of the curve shift of the three formulations. To further analyse this variation, the percentage cellular uptake and the MFI for each formulation was measured (Figures 4.8-A and B) and found to be 93.18 ± 2.10 % and 93.15 ± 0.74 % for formulations A and B, respectively with no significant ($p>0.05$) difference between them. These percentages were significantly ($p<0.05$) higher than the uptake achieved using HiPerFect (80.08 ± 1.42 %). The percentage cellular uptake achieved with formulation C was 73.71 ± 0.14 %, which was significantly ($p<0.05$) lower than formulations A, B, and HiPerFect.

However, the uptake achieved with all three formulations and HiPerFect were significantly ($p<0.05$) higher than the siRNA uptake when the cells were treated with siRNA alone without any transfection agent (Figure 4.8-A). To further confirm these results, Figure 4.8-B shows the MFI of the cells when treated with the nioplexes prepared with the three formulations and when treated with the vesicles alone without AF488-labelled Negative control siRNA (mock control). The MFI of the cells treated with AF488-labelled Negative control siRNA using formulation B was the highest followed by the MFI values of the cells treated with formulations A and HiPerFect. Formulation C showed the least MFI compared to the other formulations. However, the MFI values of the three formulations were significantly higher than the MFI of the untreated cells, the cells treated with siRNA alone or cells treated with the particles alone (Figure 4.8-B).

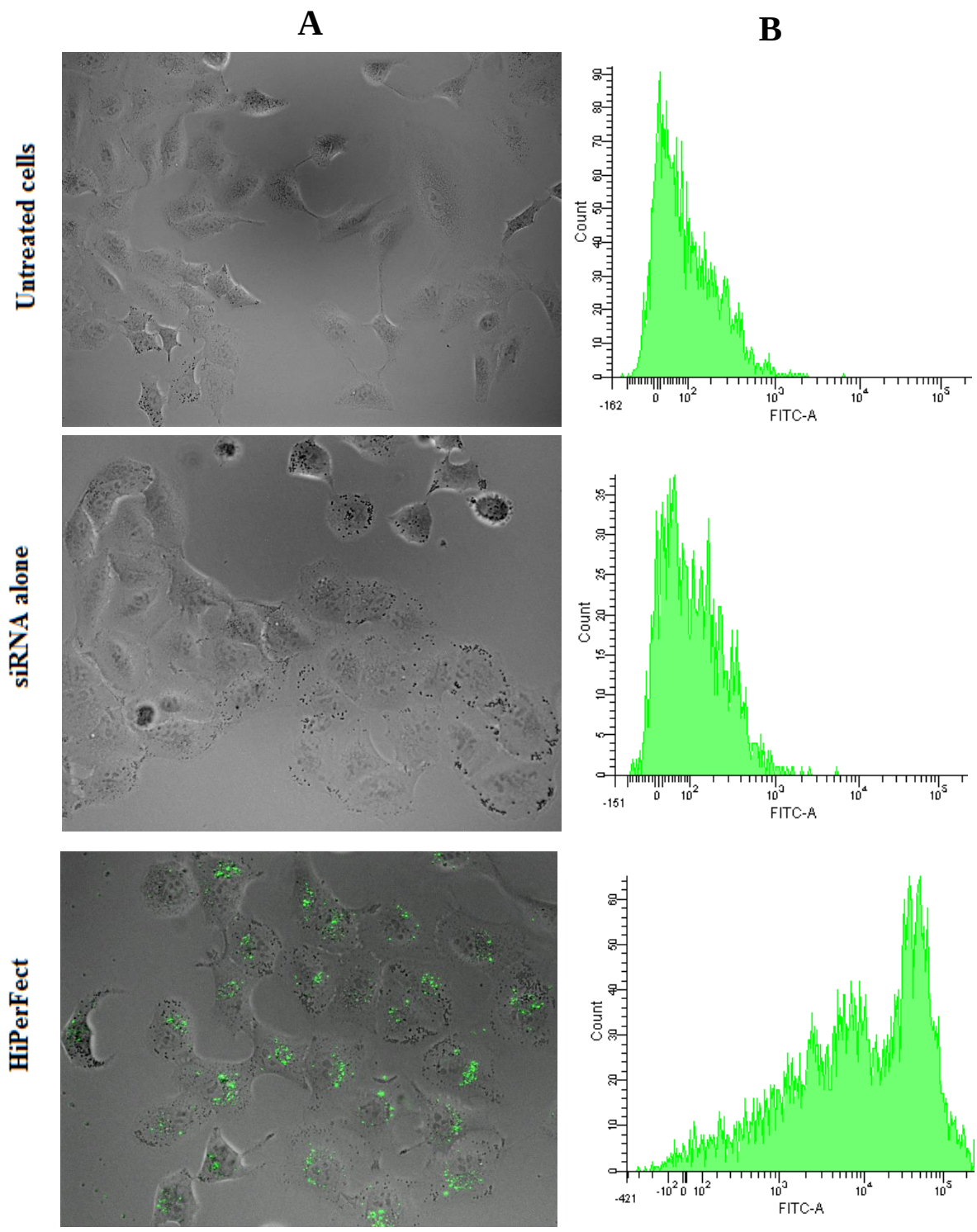
A
B
Untreated cells
siRNA alone
HiPerFect
Count
FITC-A
-162
-151
-421

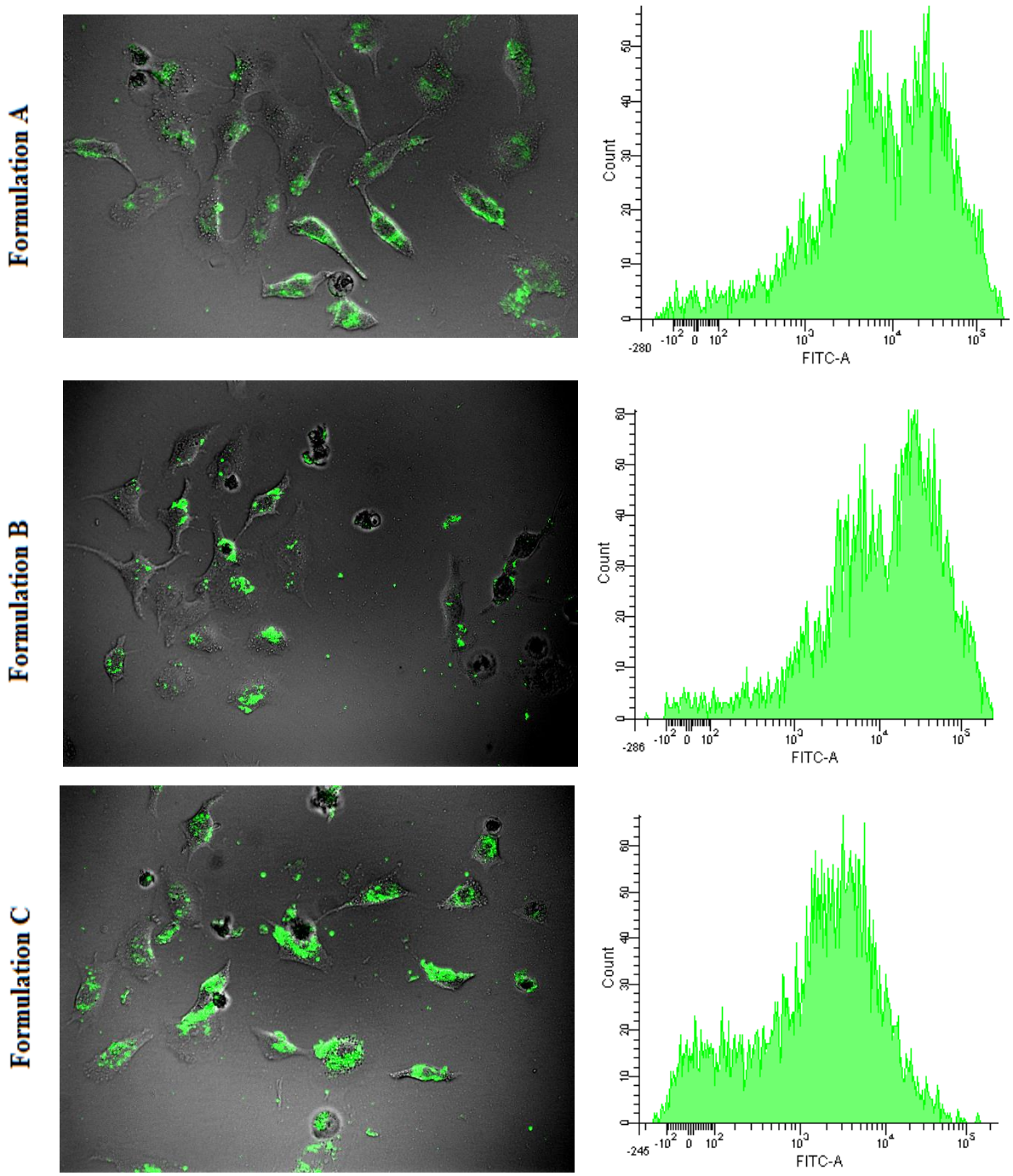

Figure 4.7. (A) Fluorescent microscopic images (objective lens 20X) and (B) flow cytometry histograms of A549 cell uptake when treated with nioplexes made with AF488-labelled siRNA. Images are representative of three independent images from each sample. The data present means ± standard deviation (*n* = 3). (For the composition of each formulation please refer to table 4.2**).**

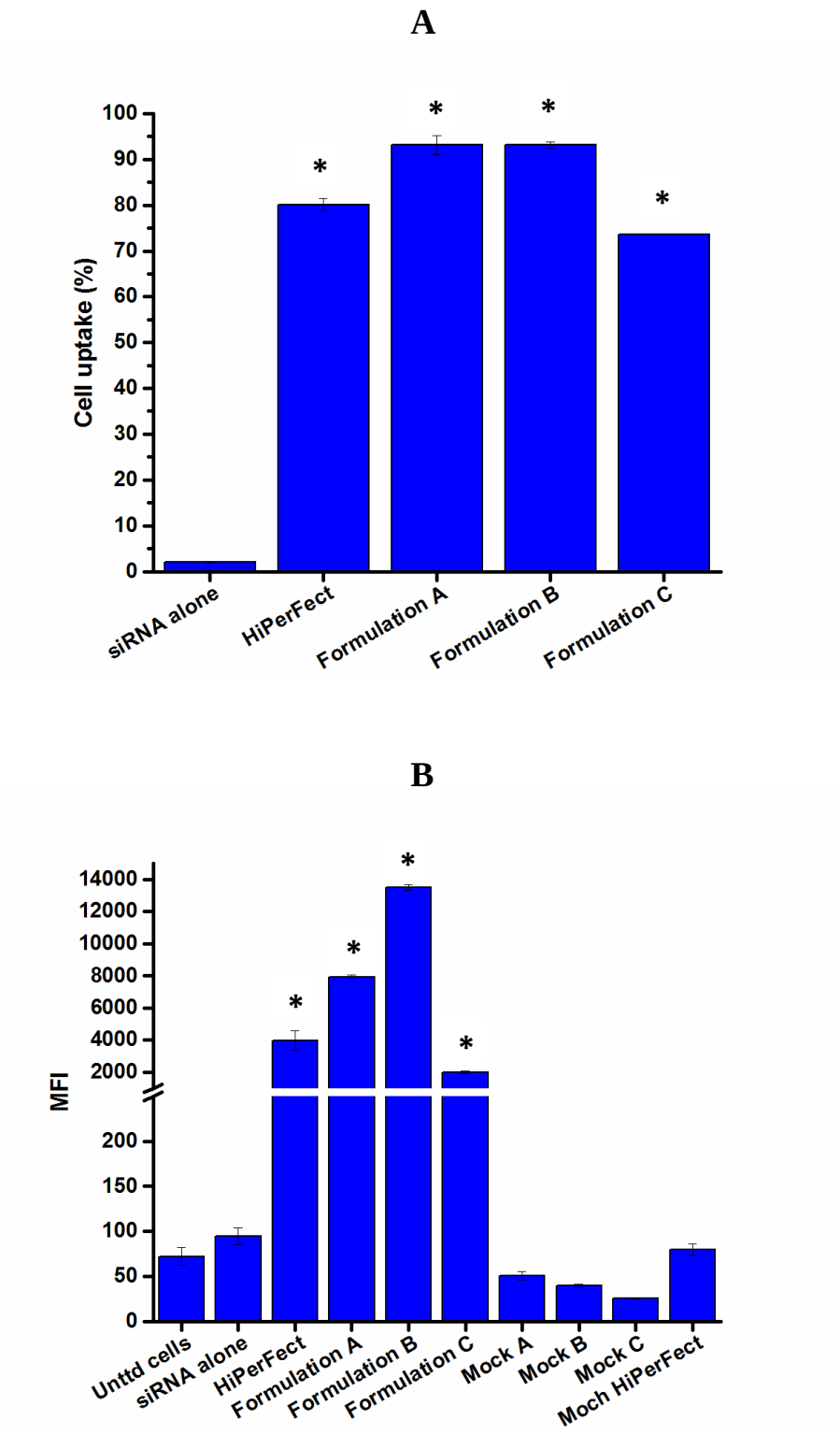

Figure 4.8. FACS results for (A) the percentage cellular uptake of siRNA (*significant ($p<0.05$) difference from cells treated with siRNA alone) and (B) MFI (*significant ($p<0.05$) difference from untreated cells) of A549 cells when treated with nioplexes encapsulating AF488-labelled siRNA. The data represents means ± SD (n = 3). (For the composition of each formulation please refer to table 4.2**).**

4.3.8. Silencing efficiency studies

4.3.8.1. GFP silencing measured by fluorescence readings

A gene silencing study was performed on copGFP-A549 cells using various CN/siRNA ratios to assess the ability of the different formulations to effectively deliver siRNA and silence GFP. GFP silencing activity was determined by measuring the changes in the fluorescence intensity at 24, 48, and 72 h. As can be seen in Figure 4.9, the percentage of GFP knockdown increased progressively with the increase in the CN/siRNA ratio for all formulations until the CN/siRNA ratio of 235.9, where saturation was reached with no further significant increase in the silencing efficiency. Moreover, the effect of the incubation time on the percentage of GFP knockdown for each formulation was studied and increasing the incubation from 24 h to 72 h caused the silencing efficiency to increase significantly ($p < 0.05$) (Figure 4.9) using all the formulations. Formulation C was the most effective and achieved GFP silencing of 74.1 ± 4.72% and 84.5 ± 2.37% after 48 h and 72 h, respectively at a CN/siRNA ratio of 235.9. At the same ratio, formulations A and B were almost the same in their GFP silencing efficiency and the percentages of GFP knockdown were 39.24% ± 6.62 and 45.79% ± 8.73 after 48 h and 44.38% ± 5.3 and 48.07% ± 15.5 after 72 h for formulations A and B, respectively with no significant difference between the two formulations at each time point (Figure 4.9). This indicates that formulation C resulted in significantly ($p < 0.05$) higher GFP knockdown than formulations A and B at each time point. Next, the efficacies of each formulation at CN/siRNA ratio of 235.9 were compared with the efficacy of HiPerFect using the same siRNA quantity. The HiPerFect results cannot be reported as a ratio to siRNA as HiPerFect is a commercial product and the molecular weight has not been disclosed. After 24 h, formulations A-C achieved a GFP silencing of 17.38 ± 10.79%, 32.78 ± 15.04% and 41.33 ± 3.56% which was not significantly ($p>0.05$) different from the GFP silencing achieved with HiPerFect (43.02 ± 8.32%) for all formulations (Figure 4.10). After 48 h incubation, the uptake of the particles increased and the

GFP knockdown for formulation A, B and HiPerFect were 39.24 ± 6.62%, 45.79 ± 8.73%, and 61.63 ± 9.43%, respectively with no significant difference ($p>0.05$; Figure 4.10). Formulation C resulted in a GFP knockdown of 74.10 ± 4.72% which was a significantly higher ($p<0.05$) level of GFP suppression compared to formulations A and B. After 72 h of incubation, the GFP suppression level achieved by HiPerFect was 69.10 ± 10.6% which was significantly ($p<0.05$) different than the GFP suppression achieved by formulations A and B (44.38 ± 5.29% and 48.08 ± 15.52% respectively; Figure 4.10). Formulation C resulted in the highest silencing efficiency after 72 h (84.53 ± 2.4%) which was significantly ($p<0.05$) higher than that achieved by formulations A and B (Figure 4.10).

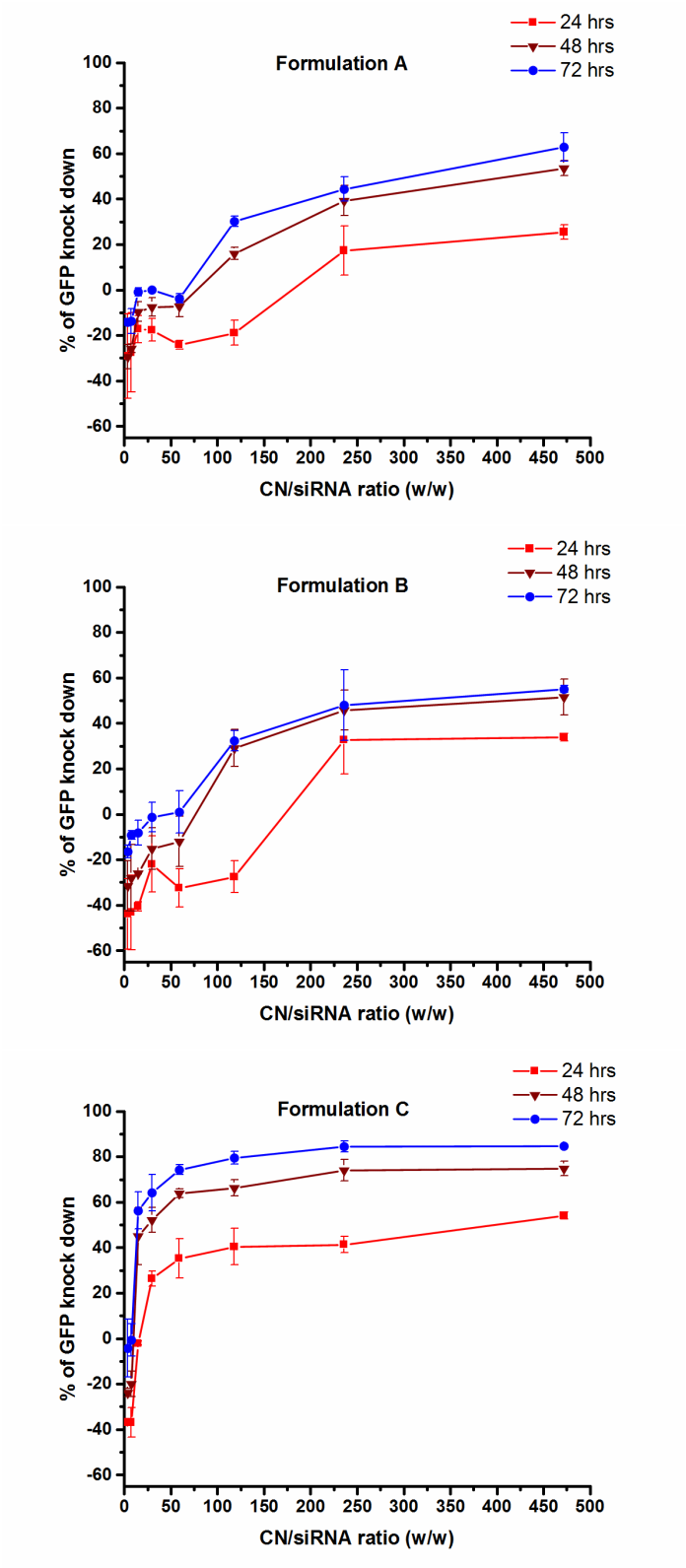

Figure 4.9. Percentage of GFP knock down achieved at various CN/siRNA ratios using formulations A-C at 24, 48, and 72 h. Results represent mean ± SD. n=3. (For the composition of each formulation please refer to table 4.2**).**

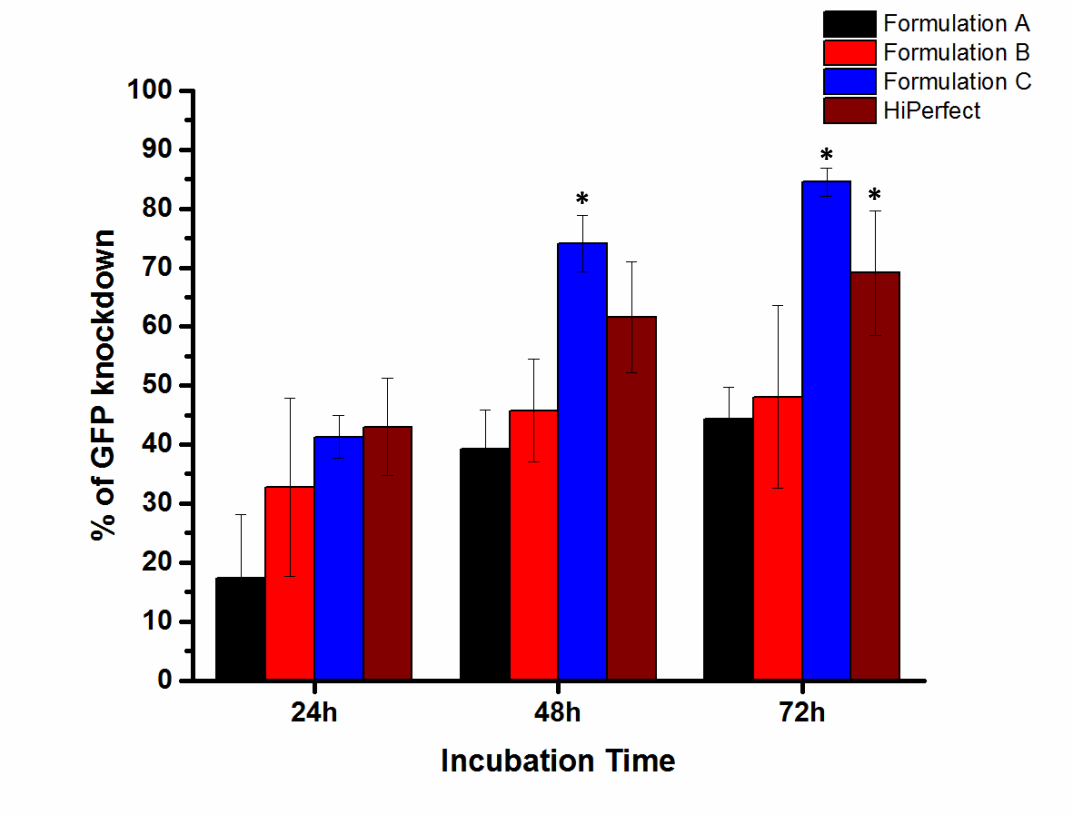

Figure 4.10. Percentage of GFP knockdown achieved at CN/siRNA ratio of 235.9 using formulations A-C and HiPerFect at 24, 48, and 72 h. *Significant ($p<0.05$) difference from other formulations. Results represent mean ± SD. n=3. (For the composition of each formulation please refer to table 4.2**).**

4.3.8.2. GFP silencing by FACS

To confirm the GFP knockdown observed by fluorescence readings, copGFP-A549 cells were transfected with various concentrations (10-100 nM) of siGFP using formulations A-C to investigate the effect of siRNA dose on transfection activity. The results were confirmed using HiPerFect transfecting reagent. siGFP concentrations greater than 100 nM were not evaluated in order to avoid possible off-target effects. Cells were incubated for 72 h after transfection and then collected for FACS analysis. The percentage of GFP expression was calculated compared against untreated cells as 100%. As can be seen in Figure 4.11, all formulations were able to bring down the GFP expression with different percentages similar to what was observed with the fluorescence results. Formulation A was the least effective in silencing GFP with a minimum value of GFP expression of 65.79 ± 9.16%, achieved using 50 nM siGFP. For formulation B, GFP silencing activity increased progressively with siGFP concentration. At 10 and 25 nM, the percentages of GFP expression were 78.53 ± 11.22 and 82.82 ± 13.12% respectively, which was not significantly ($p>0.05$) different from formulation A at the same concentration. However, when the siGFP concentration increased to 50 and 100 nM, the GFP expression was brought down to 40.19 ± 11.68 and 49.97 ± 15.05%, respectively, which was significantly ($p<0.05$) higher than formulation A at the same concentrations. A significant down-regulation of GFP expression was determined using formulation C in which the GFP expression was brought to about 30% compared to untreated cells at all siGFP concentrations used. This knockdown efficiency using formulation C was significantly ($p<0.05$) higher than the knockdown achieved using formulations A and B. For example, at 100 nM siGFP concentrations, the percentage of GFP expression achieved by formulations A-C were 74.58 ± 1.53, 49.97 ± 15.04, and 27.78 ± 16.51%, respectively, indicating a 3- and 2-fold higher siRNA transfection efficiency of formulation C compared with formulations A and B, respectively. These results for formulation C were almost the same as that for HiPerFect, where the

percentage of GFP expression was around 35% at all siGFP concentrations used (Figure 4.11). In contrast, naked siGFP and mock transfection using all formulations showed minimal GFP down-regulation.

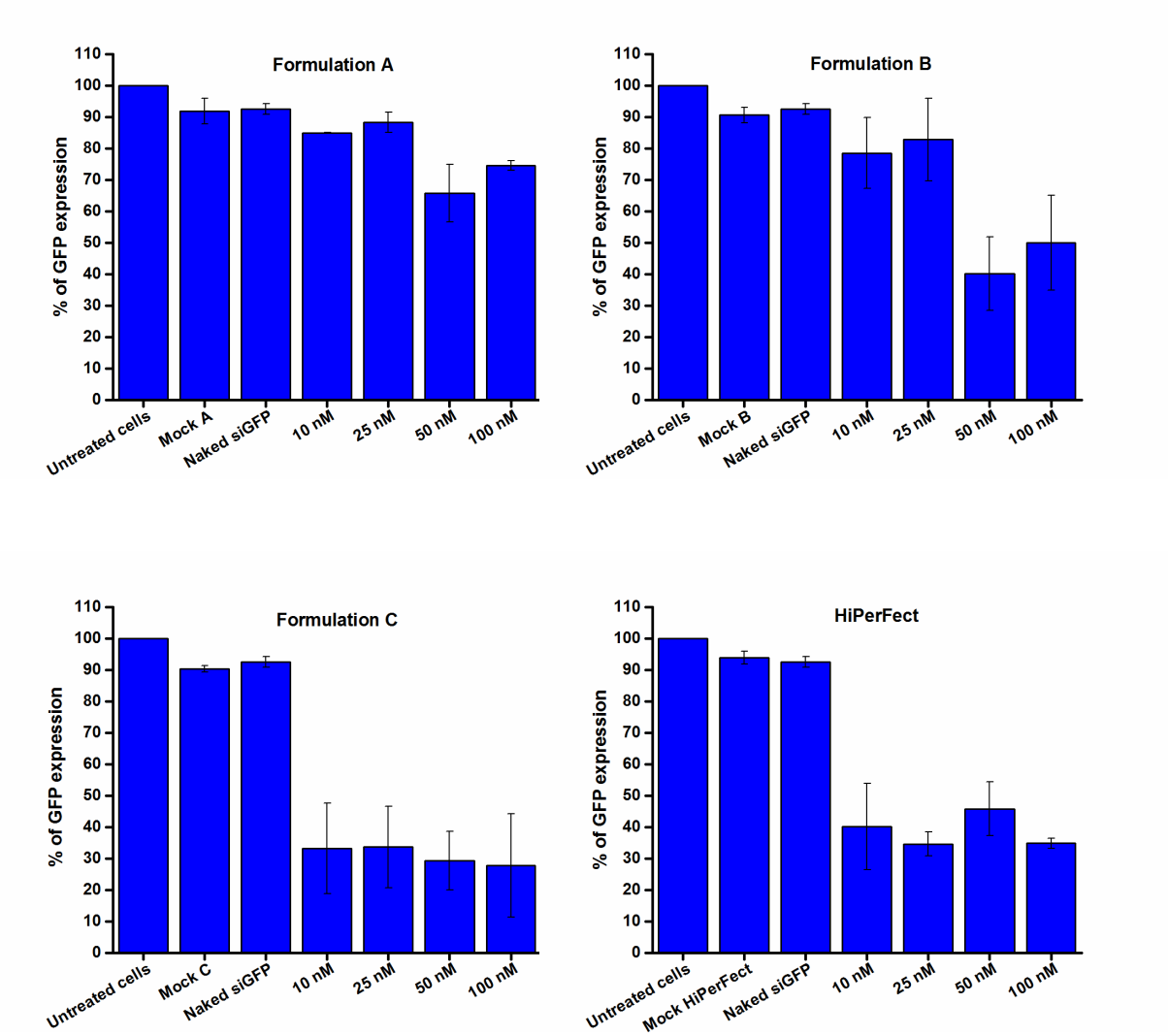

Figure 4.11. Gene down-regulation analysis in copGFP-A549 cells after transfection with different anti-GFP siRNA (siGFP) concentrations (10-100 nM) transfected with formulations A-C and HiPerFect. GFP expression was quantified by flow cytometry analysis. Values represent the mean ± SD (n=3). (For the composition of each formulation please refer to table 4.2**).**

4.3.8.3. GFP silencing measured by RT-qPCR

To further prove the efficacy of formulations A-C in siRNA transfection and to confirm the results obtained by fluorescence measurement and FACS, GFP knockdown efficacy was evaluated by RT-qPCR to determine the level of GFP suppression. The study design was the same as that for FACS analysis in which various concentrations of siGFP were transfected into copGFP-A549 cells using the three formulations, compared with HiPerFect. Cells were incubated for 72 h after transfection and then the mRNA level of the GFP gene was quantified by RT-qPCR. Results were consistent with the results generated by fluorescence measurement and FACS in which all three formulations were able to transfect copGFP-A549 cells with siGFP and induce GFP knockdown (Figure 4.12). When transfecting copGFP-A549 cells with siGFP loaded in formulation A, the GFP expression was brought down to 43.21 ± 1.16%. siGFP concentrations greater than 10 nM did not result in higher significant reduction in GFP expression. When formulation B was used for transfection, the GFP expression was 50.07 ± 1.27%, 42.37 ± 0.02%, and 46.44 ± 2.20% at siGFP concentration of 10, 25, and 50 nM respectively. The highest GFP reduction using formulation B was at siGFP concentration of 100 nM where the GFP expression was brought down to 35.06 ± 0.71% (Figure 4.12). Formulation C was superior to formulations A and B in which the GFP expression was knocked down to 16.71 ± 0.84% using 10 nM siGFP. When the cells were transfected with 25 nM siRNA using formulation C, the GFP expression was 13.99 ±0.81% and higher siGFP concentrations did not result in a higher significant reduction in GFP expression (Figure 4.12). These knockdown efficiency results achieved using formulation C were close to the results achieved using HiPerFect, where the GFP expression was 14.45 ± 0.71% and 13.47 ± 0.18% using 10 and 25 nM, respectively, with no higher significant reduction of GFP expression at higher siGFP concentrations. PCR results also demonstrated that each formulation alone without siGFP (mock), naked siGFP, and scrambled negative control siRNA transfected with each

formulation showed no significant impact of the CN formulations or siRNA treatment, respectively, on expression of GFP compared to untreated cells (Figure 4.12).

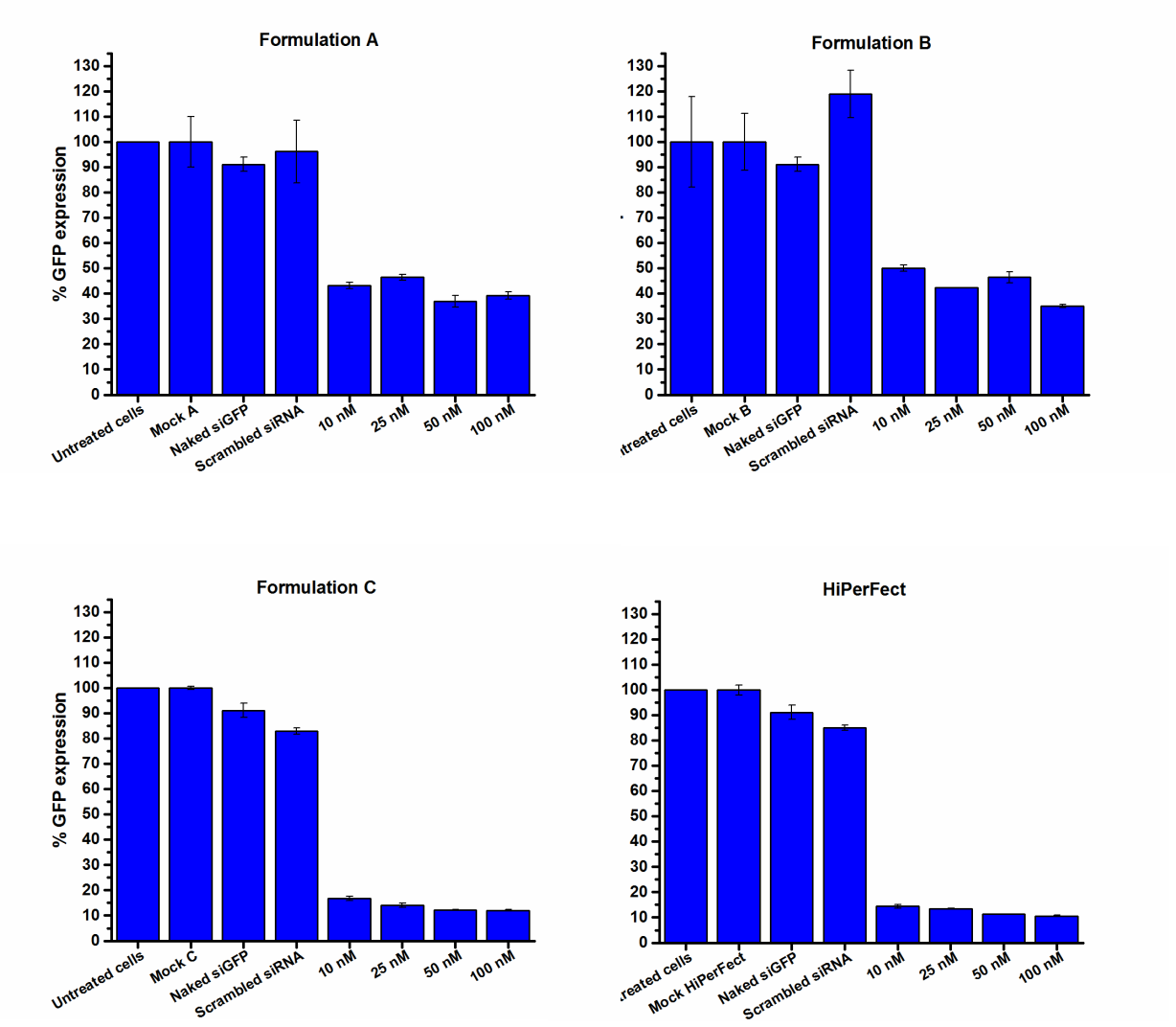

Figure 4.12. RT-qPCR analysis for GFP knockdown after transfecting copGFP-A549 cells with various concentrations (10 – 100 nM) of anti-GFP siRNA (siGFP) using formulations A-C and HiPerFect. Mock referred to cells treated with particles only without siRNA; naked siGFP is cells treated with 100 nM anti-GFP siRNA alone without transfection formulation; and scrambled siRNA is cells treated with negative control siRNA delivered by the desired formulation at 100 nM concentration. Results represent the mean ± SD of three experiments. (For the composition of each formulation please refer to table 4.2**).**

4.3.8.4. GFP silencing measured by Western blot analysis

To further confirm the knockdown results obtained, the relative GFP levels of treated cells with different siGFP concentrations (10-100 nM) transfected with the three formulations (A-C) was evaluated *in vitro* in the copGFP-A549 cells by Western blotting. GFP protein levels were examined by Western blot analysis 72 h after transfection, using GAPDH protein as a reference. These results matched those obtained by measuring the GFP silencing by FACS and RT-qPCR in which all three formulations were able to transfect the copGFP-A549 cells and down-regulate the GFP expression and production by siRNA. As can be seen in Figure 4.13-A, formulation C was able to induce the highest GFP knockdown at all the concentrations used compared with formulations A and B. Moreover, mock transfection, naked siGFP, and scrambled negative control siRNA transfected via all formulations did not induce any GFP suppression, which indicates the effectiveness of the CN formulations and the specificity of the siGFP used. These results also imply that the knockdown of GFP expression is a result of the RNAi mechanism that regulated the expression of the target protein through siRNA. These results were confirmed by the use of HiPerFect (Figure 4.13-A). Semi-quantification of the bands was performed by densitometry using ImageJ and showed that the GFP expression was 18.79 ± 5.54% of the GFP expression in the untreated cells when the cells were transfected with 10 nM siGFP loaded in formulation C, while cells transfected with higher siGFP concentrations (25-100 nM) with formulation C had the same GFP expression (~ 10%). These results achieved by formulation C was comparable with the GFP inhibition achieved using HiPerFect where the GFP expression was about 10% at all concentrations used (10-100 nM) (Figure 4.13-B). The percentage GFP expression in cells treated with 10 nM siGFP using formulation B was 64.83 ± 5.08%, while the GFP expression when the cells were transfected with higher concentrations (25-100 nM) was stable (~55%). Formulation A results were comparable to formulation B where the GFP expression was 68.80 ± 6.18% using 10 nM

siRNA, while cells transfected with 25 nM resulted in GFP expression of 55.19 ± 7.58%. However, higher concentrations of siGFP transfected with formulation A did not achieve higher inhibition of GFP expression (Figure 4.13-B).

A

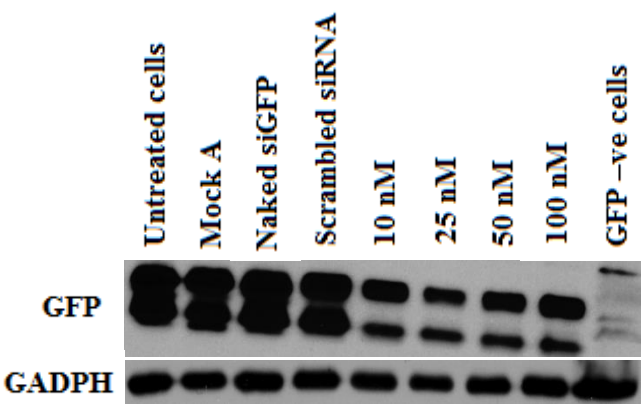

B

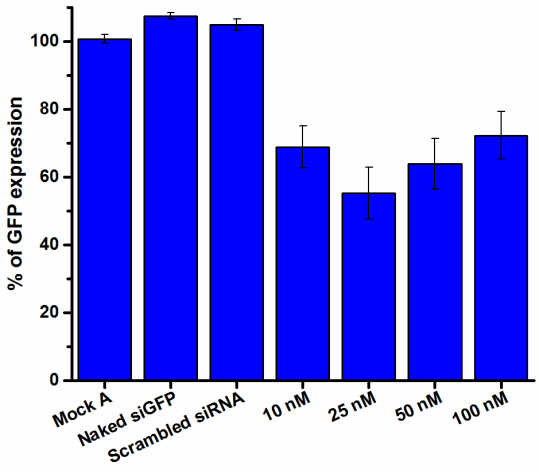

Formulation A

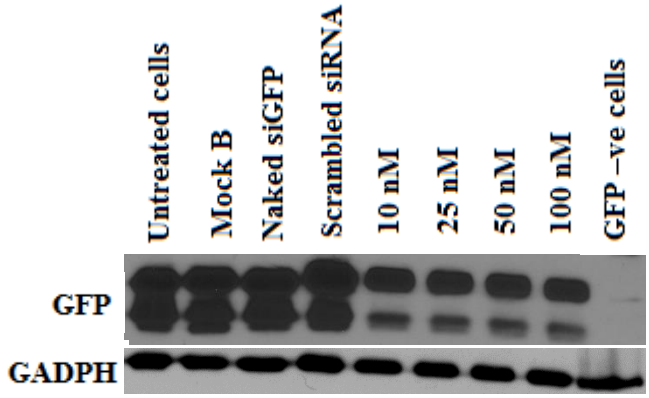

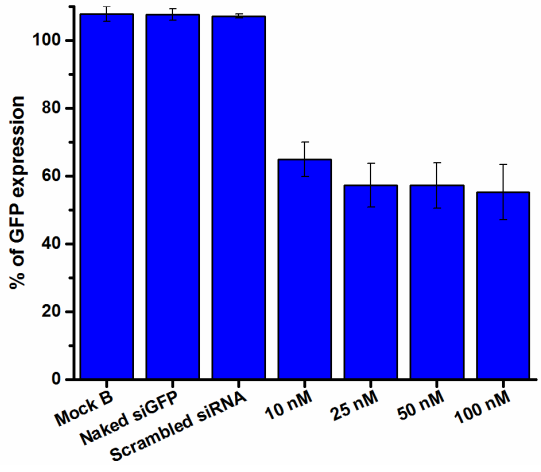

Formulation B

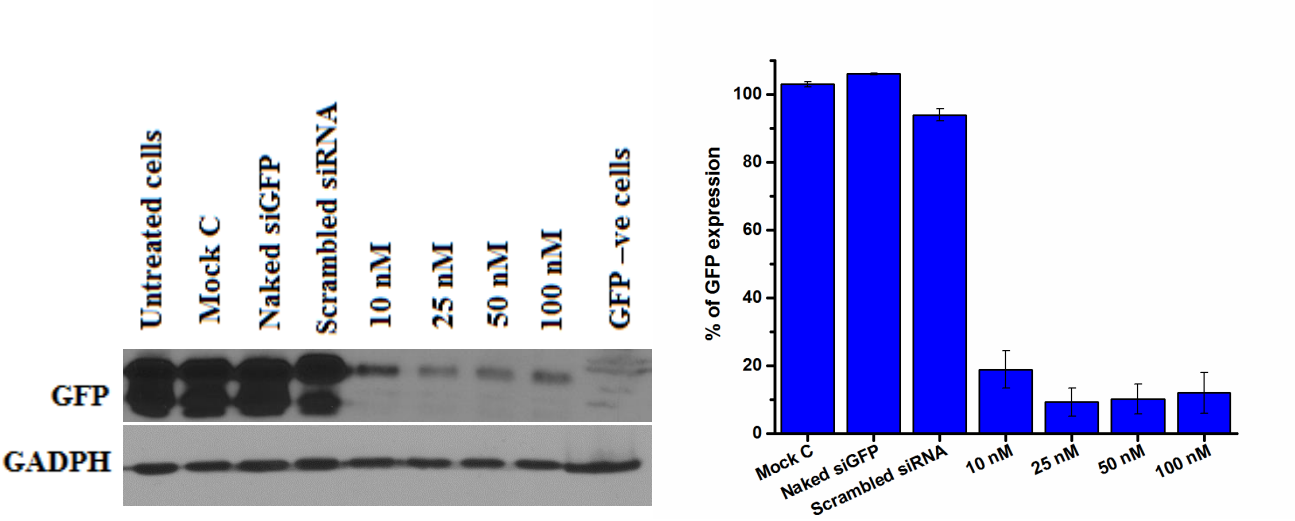

Formulation C

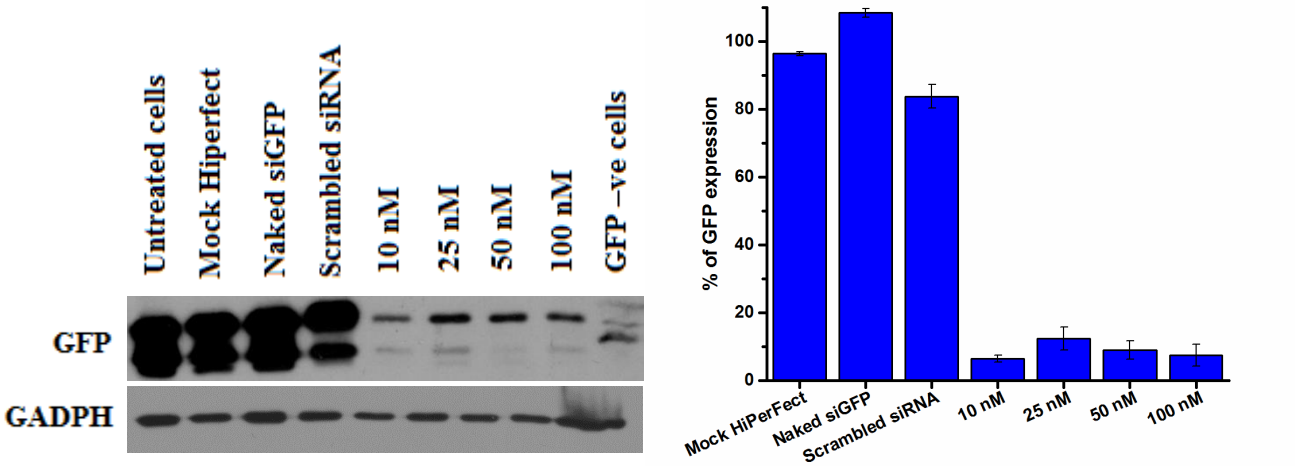

Hiperfect

Figure 4.13. GFP expression after transfecting copGFP-A549 cells with various concentrations (10 – 100 nM) of anti-GFP siRNA (siGFP) using formulations A-C and HiPerFect. (A) GFP expression determined by Western blot**.** Mock (cells treated with particles only without siRNA), naked siGFP (cells treated with 100 nM siGFP alone without transfection formulation), scrambled siRNA (cells treated with negative control siRNA delivered by the desired formulation at 100 nM concentration), and GFP –ve cells (A549 cells that are not producing GFP). (B) Densitometric analysis of the Western blot shown in (A) determined by ImageJ Software. Results represent the mean ± SD of three experiments. (For the composition of each formulation please refer to table 4.2**).**

4.4. Discussion

NISV are gaining more interest as a drug delivery system for various therapeutic agents [118]. Previous work using formulations that combine non-ionic surfactants with phospholipids were used for the delivery of oligonucleotides [257], and for siRNA [244]. However, these formulations were a combination between liposomes and NISV.

The present work explored the potential of NISV as a delivery system for siRNA. Different formulations were prepared by microfluidics and they were found to be monodisperse and small (<200 nm) which is a desirable characteristic for drug delivery systems to enhance the accumulation at the tumour site through the enhanced permeability and retention effect [26]. From the prepared formulations, formulations A-C were shown to have good colloidal stability over two months at 25^{o}C and these were chosen for the siRNA transfection experiments. When particles composed of MPG:Chol:DDAB were prepared at a molar ratio of 50:40:10, there was an aggregation of these formed particles. AFM images of the three stable formulations showed that these particles were small and spherical in shape with no major differences in morphology between the three formulations or the NISV formulations reported previously [258].

Next, the cytotoxicity of the chosen formulations on two cancer cell lines (A375 and A549) and on a normal human PNT2 cell line was measured to make sure any gene knockdown is a result from the siRNA used rather than from the toxic effect of the delivery system. At concentrations less than 78.13 µg/ml, all the formulations were non-toxic to any of the cell lines and this was consistent with what was reported previously for NISV using other formulations [118]. All the following experiments that include siRNA transfection were carried out at a final concentration at or below this concentration.

The selected CN formulations A-C were shown to have high siRNA EE which was similar to other reported cationic liposome formulations [259]. Moreover, the size of these three

formulations did not change remarkably when encapsulating increasing amounts of siRNA. This indicates that these particles are able to retain their characteristics even with high siRNA concentrations, which is adequate for cellular uptake and internalisation processes [238, 260, 261]. The addition of the negatively charged siRNA to the CN formulations resulted in a slight reduction of the total charge of these particles. This reduction on the superficial charge could be explained by the partial neutralisation of the cationic charge carried by the CN due to the negatively charged siRNA molecules. In any case, all three formulations were found to be positively charged at all CN/siRNA ratios regardless of the siRNA concentrations used, which suggests that at all the tested ratios from all formulations, free siRNA is not present and all the siRNA is bound to the CN formulation used. Moreover, this positive charge on the surface of these particles after complexation with siRNA enhances not only the stability of these formulations due to the electrostatic repulsion between the cationic particles [262], but also the interaction with the negatively charged cell surfaces and the subsequent cellular uptake [263].

The transfection efficiency of the selected formulations was evaluated as a measure of cellular uptake of siRNA. Cellular uptake analysis is a primary assay that helps to understand part of the transfection process and shows the efficiency of the formulations to be internalised when they are in contact with the target cells. Gene knockdown by siRNA is an indication that the siRNA has been properly delivered by the vector. However, the transfection process sometimes involves a low number of cells which might be inadequate for gene therapy. Therefore, one of the main objectives of this work was to achieve high percentages of target cell transfection with minimal toxic effects.

To test the effectiveness of formulations A-C in delivering siRNA into the cells and to quantify the cellular uptake, AF488-labelled siRNA was encapsulated into each of the three formulations and transfected into A549 cells. Fluorescent microscopy and flow cytometry were used to assess the cellular uptake. The results were compared with HiPerFect. All three formulations

were able to deliver the siRNA to the cells as indicated by the strong green fluorescent areas on the microscopy images and by the shift in the fluorescence histograms in the FACS results, compared to the untreated cells. Cellular uptake is influenced by different factors such as particle size, shape, surface charge, and chemistry of the nanoparticles [264]. Regarding the effect of particles size on nanoparticles cellular uptake, several studies reported that a 40-50 nm diameter is optimal to maximise the cellular uptake in certain mammalian cells [265, 266]. A lower degree of cellular uptake was noticed for particle sizes above and below this range [38]. Particle shape also influences the uptake into cells. In studies with nanoparticles below 100nm, spherical-shaped nanoparticles showed the highest cellular uptake compared to other shapes [38]. In addition, cationic nanoparticles are usually taken up by the cells at a higher rate than anionic particles as a result of interaction of the positive charge with the negatively charged domains on the cell membrane [267]. By analysing the characteristics of formulations A-C, all three formulations were spherical in shape, carried positive charge, and were within the desired size range. These favourable characteristics resulted in high cellular uptake for all three formulations as observed with the FACS and fluorescent microscope results. The percentage of cellular uptake was similar between formulations A and B and lower for formulation C. Formulations A and B are similar in their composition as both formulations contain the same lipid components in different ratios, while formulation C is composed of Tween 85 as a non-ionic surfactant instead of MPG used in formulations A and B. Taking into consideration that all three formulations are spherical and carry almost the same positive charge, this difference in the cellular uptake between the three formulations is a result of the difference in chemical composition of formulation C compared to formulations A and B. Another explanation for this difference can be attributed to the fact that formulation C is slightly larger in size (~ 60 nm) than formulations A and B (both formulations are ~ 50 nm). This takes formulation C out of the 40-50 nm range, which is optimal for cellular uptake. This

may suggest the reason why the cellular uptake of formulation C, although it was high, remained lower than the uptake of formulations A and B.

Following cellular uptake, an effective delivery system must promote endosomal release of siRNA into the cytoplasm for gene silencing [268]. To further examine the efficacy of the CN formulations in delivering siRNA into cells for the purpose of gene silencing, a series of gene silencing studies on copGFP-A549 cells to target GFP expression by siGFP were carried out. GFP is a protein that exhibits a bright florescence when exposed to light in the blue to ultraviolet range and is used as a marker of gene expression and protein targeting in intact cells and organisms [269]. CopGFP-A549 is a commercially available A549 cell line that is modified by the supplier to ensure they endogenously express copGFP. A decrease in GFP fluorescence in these cells after transfection indicates endosome release of the siGFP into their cytoplasm where the RNAi knockdown mechanism occurs. By monitoring any changes in fluorescence intensity of the GFP-producing cells after transfection with anti-GFP siRNA, the efficacy of the delivery system can be judged. After proving cellular uptake, the endosome release after cellular uptake and the subsequent inhibition of the target protein expression need to be demonstrated.

Therefore, different CN/siRNA ratios using formulations A-C were prepared. The cells were then transfected and the changes in GFP intensity were measured using a fluorescence platereader. For all three formulations, the maximum GFP knockdown was seen after 72 h of transfection. This time point was used in subsequent experiments. From the three formulations studied, formulation C was shown to have the highest gene silencing ability compared to formulations A and B at all time points.

To further confirm these results, copGFP-A549 cells were analysed by FACS after transfection with various concentrations (10-100 nM) of siGFP using formulations A-C. FACS is a

powerful technology that allows the measurement of the fluorescence of individual cells as they pass through a light source [270]. By comparing the fluorescence of the transfected cells with untreated cells, an estimation of the transfection efficiency of the three formulations could be made. FACS analysis showed that all three formulations were able to downregulate GFP expression to varying degrees. Formulation C was able to suppress GFP expression using siGFP by more than 70% compared to the untreated cells at all the siRNA concentrations, which was comparable with the GFP knockdown achieved using HiPerFect. The GFP knockdown using formulation C was superior to the GFP knockdown achieved by formulations A and B. These results were consistent with the results obtained by fluorescence readings. These GFP knockdown results using the CN formulations were higher than the GFP knockdown achieved with other delivery systems. For example, Zhu *et al.* designed multifunctional polymeric micelles for siRNA delivery and targeting GFP production in copGFP-A549 cells. With their system, the maximum GFP knockdown they achieved was about 55% compared to untreated cells after one transfection as shown by FACS [271]. Zhou *et al.* were able to achieve a maximum of 65% of GFP silencing in human breast cancer cells (MDA-MB-231) using 100 nM siGFP transfected through their SPANosomes vesicles [244]. In the work of Conti *et al.*, a maximum GFP knockdown of 37% in A549 cells was achieved using dendrimer nanocarriers regardless of the siGFP concentration used [272].

To further understand the transfection efficiency of the CN formulations, the transfected cells were analysed using RT-qPCR and Western blotting for more quantitative measurements of the GFP expression. Both RT-qPCR and Western blot GFP expression results were consistent with the results obtained by measuring the fluorescence intensity via platereader and FACS. All the prepared formulations were able to suppress the GFP expression with formulation C being superior to formulations A and B. These results demonstrated that the reduction of GFP expression by the CN/siRNA complexes, demonstrated by mRNA by RT-qPCR and the protein

quantification by Western blot, support an RNAi-mediated mechanism of gene silencing after endosome release of siGFP into the cytoplasm where the RNAi mechanism occurs.

Together with the cytotoxicity data, these results also suggests that downregulated gene expression due to non-specific toxic effects of the formulations used can be excluded, since no effect on GFP expression was obvious when the formulations alone were used as controls which confirms that the observed GFP suppression was due to siGFP transfection instead of vehicle-related cytotoxicity.

It is worth noting that at 50 and 100 nM siGFP concentrations transfected via formulations A and B, there was a difference between the GFP expression measured by FACS and RT-qPCR where the later showed higher GFP knockdown. This might be explained by the fact that FACS measures the intensity of the protein itself while RT-qPCR measures the mRNA levels which is a step before the protein expression.

It has been reported in the literature that the transfection efficiency by lipid-based nanoparticles strongly depends on the chemical composition of the lipids used [273, 274]. The data above confirms an efficient delivery of bioactive siRNA into the cytosol after cellular uptake and successful release of nanoparticles or siRNA from endosomes or lysosomes can be concluded as a result of the GFP knockdown. Since it was notable that formulation C induced higher gene downregulation than formulations A and B using the same siRNA concentrations, the variations in the transfection efficiency between the formulations could be explained, in part, by the different endosomal escape ability of the lipids used [275]. Although formulation C showed the least cellular uptake compared to the other formulations, this superiority in GFP knockdown compared to formulations A and B suggests that the presence of Tween 85 enhances the endosome escape for formulation C at a higher rate than the MPG in formulations A and B.

From all the non-ionic surfactant types, Tween surfactants are one of the most commonly used in the pharmaceutical industry. They include Tween 20, Tween 60, Tween 80, and Tween 85 depending on the hydrophobic tail present. An attractive property in the structure of all the Tween surfactants is the presence of the hydrophilic polyoxyethylene chain which has been demonstrated to possess a functional interaction with nucleic acids and is used as a gene transfer helper [276]. Endosome escape is one of the major barriers for efficient gene delivery. Tween surfactants are believed to have a fusogenic property similar to DOPE, which is one of the most commonly used helper lipids in liposome formulations to facilitate endosome escape of liposomes and its nucleic acids cargo into the cytosol by promoting a lamellar-to-inverted hexagonal phase transition of liposome-nucleic acid complexes [277, 278]. From all the Tween surfactant types, Tween 85 is shown to have the highest efficacy when used with NISV for DNA delivery in which the particles formed were proven to have the highest cellular uptake and endosome escape compared to NISV prepared with other Tween surfactants [276]. For all these reasons, the presence of Tween 85 in formulation C was believed to enhance endosome release of the siGFP into the cytosol, where the RNAi mechanism occurs, at a higher rate than formulations A and B, which contribute to the enhanced silencing efficiency of the GFP expression.

This represents the first report on the use of NISV prepared by microfluidics for the delivery of siRNA. The surfactant vesicles therefore could prove a superior technology platform for therapeutic siRNA delivery. The present work demonstrates that CN can be used to deliver siRNA *in vitro*. Future work for these CN formulations should prove their activity *in vivo* to establish their activity in an animal model, which can then be translated into clinical applications. Moreover, future work should be carried out using siRNA to target vital proteins for cancer cells and to monitor the suppression of cancer growth.

4.5. Conclusions

Here, the development of CN prepared by microfluidics as a siRNA delivery vector was reported. The formulations prepared possessed favourable physical characteristics and mediated efficient cytosolic delivery of siRNA. From the chosen formulations, formulation C, composed of Tween 85 as a non-ionic surfactant, showed superiority over the other two formulations composed with MPG as the surfactant. The transfection efficiency of formulation C was shown to be comparable with the cationic transfection reagent, HiPerFect. In conclusion, these novel vectors constitute promising agents for delivery of siRNA and deserve further investigation *in vivo*.

Chapter 5

Proof of concept studies for siRNA delivery by NISV: *In vitro* and *in vivo* evaluation of protein knockdown

Abstract

RNA interference (RNAi) is an effective and naturally occurring post-transcriptional gene regulatory mechanism. This mechanism involves the degradation of a target messenger RNA (mRNA) through the incorporation of siRNA that is complementary to the target mRNA. The application of siRNA based therapeutics is limited by the development of effective delivery system as the naked siRNA is unstable and cannot penetrate the cell membrane. In this study, the use of cationic non-ionic surfactant vesicles (CN) prepared by microfluidic mixing for siRNA delivery have been investigated. In an *in vitro* model, these vesicles were able to deliver anti-luciferase siRNA and effectively suppress the luciferase expression in B16-F10-LUC mouse melanoma cells. More importantly, in an *in vivo* mouse model, intra-tumour administration of CN carrying anti-luciferase siRNA lead to significant suppression of luciferase expression compared with naked siRNA. Hence, a novel and effective system for the delivery of siRNA both *in vitro* and *in vivo* were established which can represent a powerful system for future therapeutic application of gene therapy treatment.

Key Words

Non-ionic surfactant vesicles, Microfluidics, RNA interference, Drug delivery, Luciferase expression.

5.1. Introduction

SiRNA has gained substantial interest as a promising therapeutic agent because of the concept of being able to silence specific upregulated genes through a RNAi mechanism and therefore hindering corresponding protein expression. However, the efficacy of siRNA therapy is significantly hampered by poor cellular membrane penetration, rapid degradation by RNase enzymes, non-specific tissue distribution, and short circulating time [279, 280]. Therefore, therapeutic application of siRNA requires the use of an efficient delivery vehicle that can carry, protect, and efficiently deliver siRNA into target cells [179]. In this regard, lipid-based nanoparticles have been widely investigated as a possible siRNA carrier because of their advantages such as high loading efficiency and biocompatibility [281]. Through their lipid membrane bilayer structure, lipid nanoparticles can protect the siRNA by being embedded in the aqueous core or adsorbed on the surface of the nanoparticles [282]. One type of lipid-based nanoparticles are NISV, which have a membrane bilayer structure similar to liposomes [118]. NISV consist of non-ionic surfactants, in addition to cholesterol and charging species instead of the use of phospholipids in liposomes [81]. The use of non-ionic surfactant in NISV improves the stability of these particles and decreases the production cost compared to liposomes. Nevertheless, there are limited reports about the use of NISV as a delivery vehicle for siRNA [243]. The use of NISV for siRNA delivery has significant research potential that still needs to be investigated and developed in order to mediate high gene silencing for therapeutic applications.

In the previous chapter, a number of CN formulations were developed and shown to be small in size, monodisperse, and stable. These CN were composed of (A) MPG:Chol:DDAB at 40:40:20, (B) MPG:Chol:DDAB at 30:50:20, and (C) T85:Chol:DDAB at 40:40:20. Moreover, the successful delivery of siRNA by these three formulations were investigated. The efficacy

of these CN formulations in delivering anti-GFP siRNA and suppressing the GFP expression in copGFP-A549 cells were demonstrated with superior results obtained with formulation C.

5.1.1. Chapter aims

In this chapter, to confirm the gene silencing results observed in copGFP-A549 cells and to further explore the *in vivo* efficacy of the CN, the biological activity of the three CN formulations was tested on a different cell model using another protein reporter which is B16-F10-LUC mouse melanoma cells stably expressing luciferase enzyme. This model can be used to test the efficacy of CN in delivering anti-luciferase siRNA (siLUC) and inhibit the luciferase expression *in vitro.* Furthermore, this choice also enabled translation to an *in vivo* model by inoculating the animals with these cells to induce a cancer model that expresses luciferase and then to test the *in vivo* efficacy of CN in siLUC delivery. The three formulations were loaded with either AllStars AF488-labelled Negative Control siRNA to confirm cellular uptake of siRNA or with siLUC to confirm the effectiveness of these formulations in delivering siRNA and suppressing luciferase enzyme expression. The most effective formulation *in vitro* was then selected for the *in vivo* experiment to assess the luciferase suppression in the animal model.

5.2. Materials and methods

5.2.1. Materials

Mouse melanoma B16-F10-LUC luciferase expressing cells were obtained from Caliper life Science, Inc. (USA) (the sequence of luciferase enzyme transfected in the B16 cells can be found in Appendix 3). The anti-luciferase siRNA (siLUC) duplex sequence and the non-targeting scrambled DsiRNA (Table 5.1) were synthesised by Integrated DNA Technologies (Belgium). ONE-Glo™ luciferase assay system was purchased from Promega Corporation (UK). D-luciferin was purchased from Caliper Life Sciences (USA). Other materials have been described in Sections 2.2.1 and 4.2.1.

Table 5.1 Sequence of siLUC and non-targeting scrambled DsiRNA used.

siRNA sequence (5'-3')		
siLUC	Sense	rGrArGrGrCrUrArArGrGrUrGrGrUrGrGrArCrUrUrGrGrACA
	Antisense	rUrGrUrCrCrArArGrUrCrCrArCrCrArCrCrUrUrArGrCrCrUrCrGrA
Scrambled	Sense	rCrGrUrUrArArUrCrGrCrGrUrArUrArArUrArCrGrCrGrUAT
	Antisense	rArUrArCrGrCrGrUrArUrUrArUrArCrGrCrGrArUrUrArArCrGrArC

5.2.2. Formulation of CN

CN composed of MPG:Chol:DDAB (40:40:20 or 30:50:20 mole % for formulation A or B respectively) or T85:Chol:DDAB (40:40:20 mole % for formulation C) were prepared by microfluidic mixing as described previously in Section 2.2.5 using RNase free water as the aqueous media.

5.2.3. Cell viability assay

To evaluate the cytotoxicity of the CN, B16-F10-LUC were grown and maintained in RPMI 1640 medium supplemented with 10% (v/v) FBS, 1% (v/v) L-glutamine and 1% (v/v) penicillin-streptomycin. The toxicities of the CN formulations A-C on this cell line were evaluated as described in section 2.2.9.

5.2.4. *In vitro* cellular uptake

Cellular uptake of CN by B16-F10-LUC cells was quantified by FACS as described in Section 4.2.10.

5.2.5. *In vitro* luciferase gene silencing assay

B16-F10-LUC cells were plated in a 96-well plate (7500 cells/well) in 75 μl of RPMI medium containing 10% (v/v) FBS, 1% (v/v) L-glutamine and 1% (v/v) MEM NEAA (without

antibiotics) at 37ºC, 5% (v/v) CO_2 24 h prior to transfection. Cells were then treated with all CN formulations or the positive control HiPerFect, containing siLUC at final concentrations of 0, 10, 25, 50, 100, and 200 nM per well. SiRNA alone (naked siRNA) and particles alone were used as controls. The expressed luciferase level in the cells was measured after 24, 48, and 72 h of transfection using a ONE-Glo™ luciferase assay system following the manufacturer's protocol. Briefly, at each time point, 100 µl of ONE-Glo reagent from the assay kit was added to the cells in each well and incubated at 25 °C for 3 min. The bioluminescence (Relative Luminescence Units, RLU) was measured using an *in vivo* imaging system (IVIS) (IVIS Spectrum®, PerkinElmer, UK). Luciferase activity of a sample was expressed as the percentage luminescence intensity compared to untreated cells. The percentage of luciferase expression was expressed by the equation:

$$\% \text{ expression} = (RLUluc/RLUctl)*100$$

Where RLUluc is the mean of RLU for luc in treated cells and RLUctl is the mean of RLU for untreated cells. The results were reported as the mean and SD of four different experiments.

5.2.6. *In vivo* silencing study

An *in vivo* gene silencing study was carried out using formulation C only, as it was the most effective formulation *in vitro* among the other CN formulations.

5.2.6.1. Formulation C preparation for animal work

Formulation C, composed of T85:Chol:DDAB (40:40:20 mole %) was prepared by microfluidic mixing as described previously in Section 2.2.5 but using sterile RNase free glucose 5 % (w/v) as the aqueous media.

5.2.6.2. Formulation C characterisation

Formulation C prepared using sterile RNase free glucose 5 % (w/v) were characterised for their particle size, PDI, and ZP by DLS as described in Section 2.2.6.

5.2.6.3. Animals

Female BALB/c nude mice, 42-49 days old (average weight of 20 g), were purchased from Charles River Laboratories (UK). Mice were housed in groups of three at 19°C to 23°C with a 12-h light-dark cycle. They were fed a conventional diet (Rat and Mouse Standard Expanded, B&K Universal, UK) with mains water provided *ad libitum*. The *in vivo* experiments described below were performed in accordance with the UK Home Office regulations. The animal work was carried out by Dr. Christine Dufes (University of Strathclyde).

5.2.6.4. Determination of the most tolerable dose of CN/siLUC

Two mice were injected intraperitoneally (i.p) every day with increased concentrations of empty nanoparticles (0.2 ml, starting from 39 µg/ml nanoparticles) and siLUC nanoparticles (0.2 ml, from 625 nM siLUC) in order to determine the maximum tolerable dose of formulations. The mice were monitored daily for any changes in body weight as a surrogate marker of toxicity.

5.2.6.3. *In vivo* luciferase gene silencing study

Twelve mice were injected subcutaneously with $1x10^6$ B16-F10-LUC cells. Seven days later, when the tumours became vascularized and palpable, three mice were intratumorally injected with a single dose of siLUC (625 nM) loaded into CN (39 µg/ml, 0.2 ml). Naked siLUC, particles alone, and untreated mice were used as controls. Three mice were used in each group. The light emitted as a result of luciferase gene expression was visualised in mice using quantitative whole-body imaging [283]. To this end, mice received an i.p. injection of luciferase substrate D-luciferin (150 mg/kg body weight) after 4, 12, 24 and 48 h of treatment and anesthetised by isoflurane inhalation. Ten min post injection, bioluminescence was measured for 2 min using the IVIS Spectrum®. Data were analysed using Living Image® software (PerkinElmer, UK). The resulting pseudo-colour images represent the luciferase expression within the animal. Identical illumination settings were used for acquiring all images.

Luciferase expression in the treated mice was expressed as a percentage of luminescence intensity compared to the untreated mice.

5.2.7. Statistical analysis

Results were expressed as means ± SD of three experiments. Statistical significance was assessed by ANOVA and Tukey multiple comparison test and t-test was performed for paired comparisons using Minitab® software, State College, PE. Differences were considered statistically significant for p values < 0.05.

5.3. Results

5.3.1. Cell viability assay

Toxicity of the three CN formulations was assessed in B16-F10-LUC cells using various concentrations (9.77-1250 μg/ml) to quantify cell viability and determine the EC_{50}. Figure 5.1 shows the dose response curves for the cells treated with the three formulations and the calculated EC_{50} for each formulation. For all formulations, the cell viability decreased significantly with increasing the CN concentration especially at concentrations of 312.5 μg/ml and above where the cells showed minimal viability. The EC_{50} values for all formulations were 136.10 ±9.06, 112.50 ± 6.14, and 84.03 ± 7.39 μg/ml for formulation A, B, and C, respectively. However, all three formulations were not toxic at or below 40 μg/ml in which the cells were 100% viable. Therefore, all subsequent experiments that included siRNA transfection were carried out so the final NISV concentration was below 40 μg/ml for all three formulations.

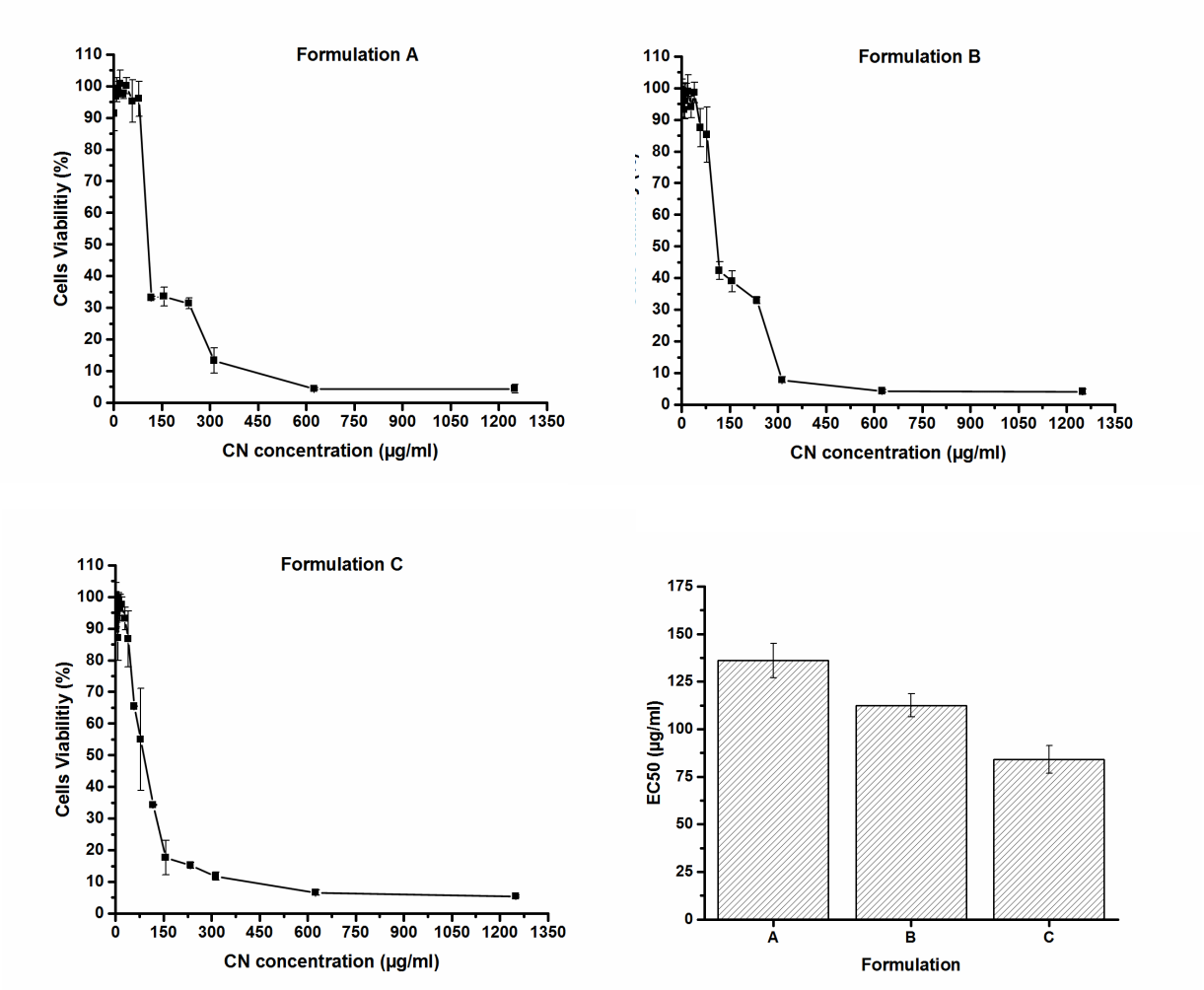

Figure 5.1 Cytotoxicity of the CN formulation (A-C) on B16-F10 cells, showing dose response curves of the three formulations and the calculated EC_{50} values. The data represents the mean ± SD (n=3). (For the composition of each formulation please refer to table 4.2**).**

5.3.2. B16 cellular uptake

To evaluate the cellular uptake of the three CN formulations, B16-F10-LUC mouse melanoma cells were treated with all three formulations loaded with AF488-labelled siRNA. The treated cells were analysed by FACS for quantitative cellular uptake (Figure 5.2). As can be seen in Figure 5.2-A, B16-F10-LUC cells did not show any siRNA uptake after being treated with siRNA alone which can be confirmed by the very low MFI (Figure 5.2-B) and the histogram curve (Figure 5.2-C) compared to untreated cells. All three formulations showed high cellular uptake when the cells were treated with AF488-labelled siRNA encapsulated in the formulations: 94.74 ± 0.58%, 94.30 ± 0.92%, and 88.28 ± 2.29% for formulations A, B, and C, respectively (Figure 5.2-A). This cellular uptake was significantly ($p < 0.05$) higher than the cellular uptake achieved by HiPerFect (70.77 ± 4.35%). Formulation C showed less cellular uptake than formulations A and B and this can be confirmed by the difference in the MFI values resulting from all formulations (Figure 5.2-B), where the MFI was significantly higher for formulations A and B compared to formulation C or HiPerFect. This difference can also be noticed by the alteration in the degree of the curve shift compared to untreated cells (Figure 5.2-C). When the formulation alone without AF488-labelled siRNA was used, the MFI values were low for all the formulations (Figure 5.2-B) and the histogram curves had slightly shifted compared to the untreated cells (Figure 5.2-C).

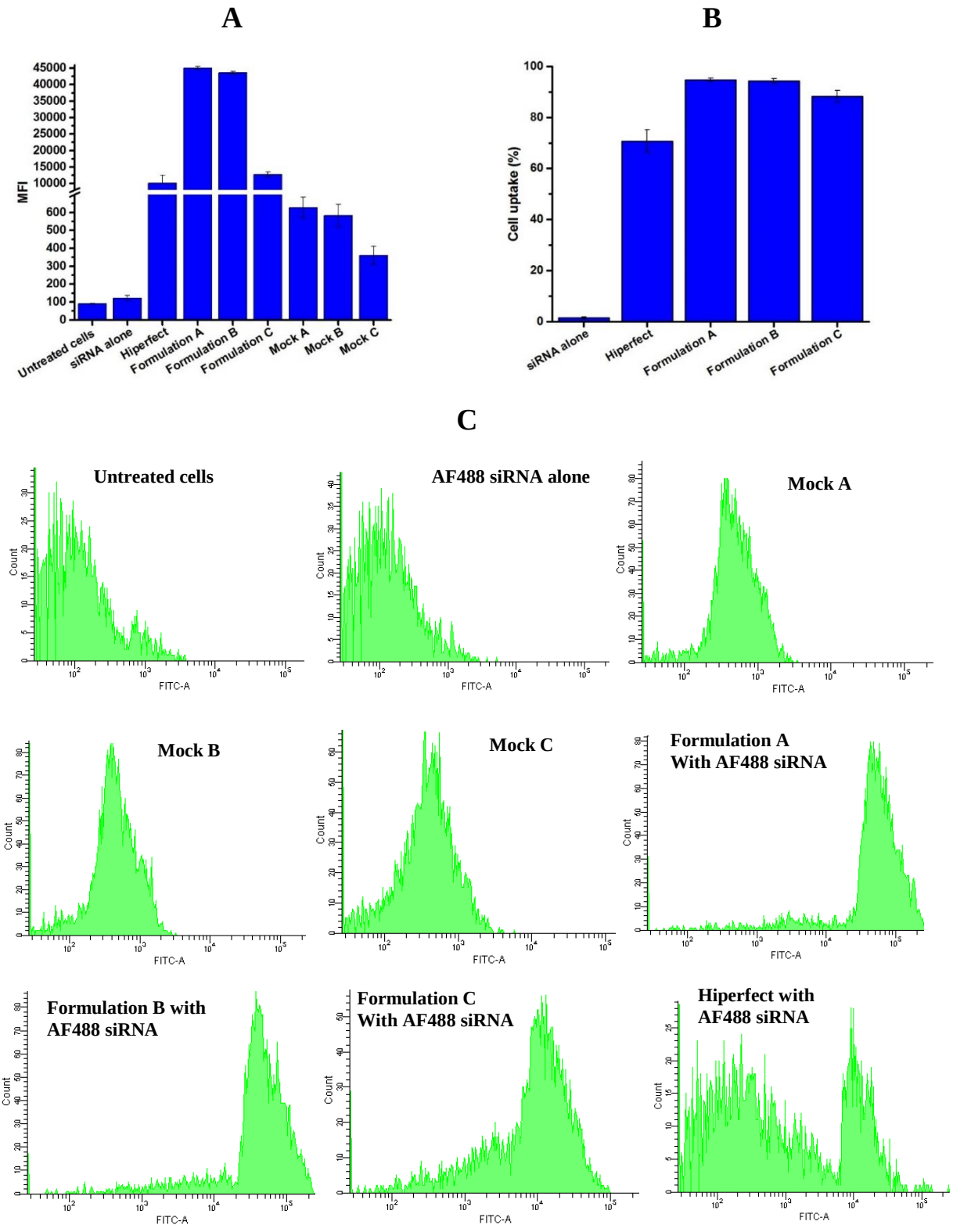

Figure 5.2 FACS results showing (A) MFI, (B) percentages of cellular uptake, and (C) flow cytometry histograms of B16-F10 cellular uptake when treated with formulations A-C or Hiperfect with AF488 labelled negative control siRNA. Images are representative of three independent images from each sample. The data represents means ± SD (*n* = 3). (For the composition of each formulation please refer to table 4.2**).**

5.3.3. *In vitro* Luciferase gene silencing study

The extent of gene silencing by siLUC loaded in the three formulations was examined. To evaluate the gene knockdown efficiencies of the CN formulations, B16-F10-LUC cells stably expressing luciferase were incubated with all three formulations, loaded with various concentrations of luc siRNA, for 24, 48, and 72 h. The specificity of the siLUC was confirmed using scrambled negative control siRNA. Luciferase expression was evaluated by measuring the luciferase luminescence intensity at each time point for the cells treated by each formulation loaded with various concentrations of siLUC (Figure 5.3). The luciferase enzyme knockdown was compared to the untreated cells. Formulation A demonstrated poor transfection after 24 h regardless of the siLUC concentration. After 48 and 72 h incubation, transfection increased as can be seen by the decrease in luciferase expression (around 80%) at both time points for all the concentrations used. Formulation B showed a decrease in the luciferase expression after 24 h with a maximum expression of 79.57 ± 6.07% using 200 nM siRNA. Increasing the incubation time to 48 h resulted in lower luciferase expression (70.00 ± 6.31%) using 200 nM siRNA. Longer incubation for 72 h did not result in improved inhibition of luciferase expression, suggesting the optimal time of incubation to be 48 h (Figure 5.3). Formulation C demonstrated the most significant ($p < 0.05$) transfection efficiency, which was concentration and time-dependent. After 24 h incubation, the percentage of luciferase expression decreased significantly ($p < 0.05$) from 77.01 ± 2.22% to 54.42 ± 2.06% by increasing the siLUC concentration from 10 – 200 nM. After 48 h incubation, all the siLUC concentrations induced the same level of luciferase expression inhibition where the luciferase expression was around 30% regardless of the siLUC concentration (Figure 5.3). Similar to formulations A and B, longer incubation with formulation C did not result in higher luciferase inhibition. This significant luciferase inhibition achieved by formulation C was much higher than the inhibition demonstrated by HiPerFect. With HiPerFect, the luciferase inhibition was dose-dependent at

all time points with the highest knockdown achieved after 48 and 72 h with no significant difference between both time points. When the cells transfected with 200 nM siLUC using HiPerFect, the luciferase expression was 75.54 ± 0.56% after 24 h. This was significantly ($p < 0.05$) higher than the luciferase expression when the cells were treated with formulation C using the same siLUC concentration (luciferase expression 54.42 ± 2.06%). Longer incubation time for cells transfected with HiPerFect, resulted in higher luciferase inhibition, where the maximum effect seen after 48 h using 200 nM, resulted in luciferase expression of 48.35 ± 4.48% with no further effect at longer incubation times (Figure 5.3). No effect was noticed for all formulations at 0 nM siLUC (mock transfection) at all time points. Similarly, no effect was seen when using siLUC alone at all time points (data not shown). This indicates that the decrease in luciferase expression using siLUC was indeed caused by the sequence-specific gene silencing of siLUC.

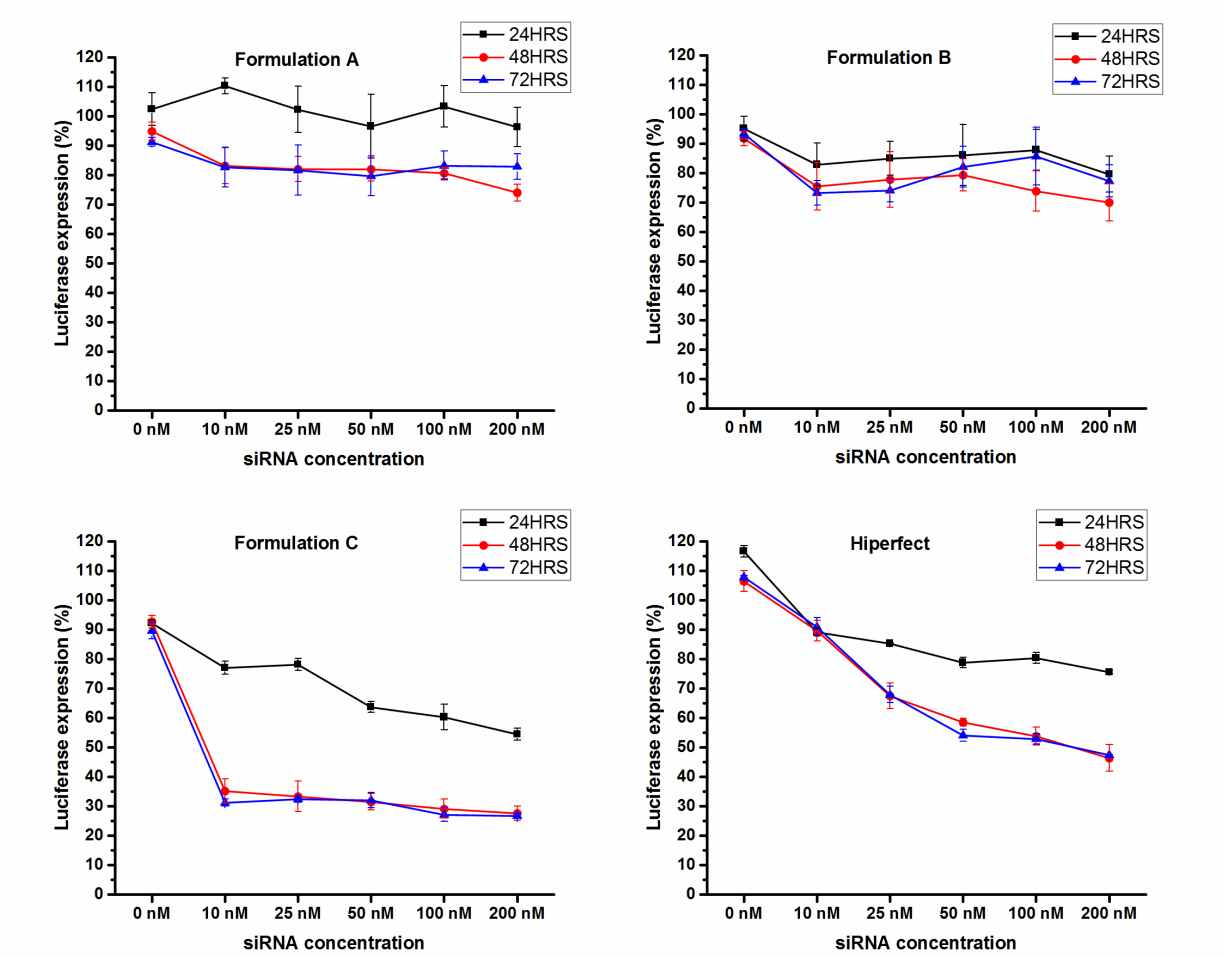

Figure 5.3 Percentage of luciferase expression in B16-F10 cells after being transfected by various siLUC concentrations using formulations A-C and HiPerFect. Luminescence was measured after 24, 48, and 72 h of incubation**.** Data represents mean ± SD (n=3). (For the composition of each formulation please refer to table 4.2**).**

5.3.4. *In vivo* silencing study

5.3.4.1. Formulation C characterisation

Formulation C, prepared using sterile RNase free glucose 5 % (w/v), to be used for *in vivo* work was characterised by DLS to make sure that changing the media from sterile RNase free water (used for *in vitro* studies) to sterile RNase free glucose 5 % (w/v) did not have any effect on particle characteristics. Table 5.2 shows the DLS results in term of particle size, PDI, and ZP for the particles prepared with RNase free glucose 5 % (w/v) and with RNase free water.

Table 5.2. Physical characteristics of formulation C prepared by microfluidics with sterile RNase free glucose 5 % (w/v) and RNase free water. Results represents the mean ± SD (n=3).

Media	Particle size (nM)	PDI	ZP (mV)
RNase free glucose 5 % (w/v)	61.37 ± 0.16	0.18 ± 0.01	55.80 ± 6.55
RNase free water	59.16 ± 1.88	0.19 ± 0.09	49.45 ± 2.43

5.3.4.2. Determination of the most tolerable dose of CN/siLUC

For empty particles, a concentration of 39 µg/ml was found to have no effect on the weight of the animal, which started to decrease when injecting higher concentrations (Table 5.3). This concentration of empty particles was therefore selected and used to encapsulate various concentrations of siLUC. A siLUC concentration at 625 nM was found to be well tolerated by the mouse while higher concentrations caused weight loss (Table 5.4). Therefore, in the subsequent *in vivo* experiments, CN/siLUC nioplexes were prepared using 39 µg/ml of CN encapsulating 625 nM of siLUC.

Table 5.3. Change of the mouse weight when given increasing concentrations of empty particles of formulation C. Particles were prepared with sterile RNase-free 5 % (w/v) glucose.

Empty particles					
Days	1	2	3	4	5
Particle concentration (µg/ml)	39	156	315.5	-	-
siRNA concentration (nM)	0	0	0	-	-
Animal weight (g)	19.2	19.3	18.7	18.6	18.4

Table 5.4. Change of the mouse weight when given increasing doses of siLUC encapsulated in formulation C. Particles were prepared with sterile RNase free glucose 5 % (w/v) at concentration of 39 µg/ml.

Particles + siLUC					
Days	1	2	3	4	5
Particle concentration (µg/ml)	39	39	39	-	-
siRNA concentration (nM)	625	1250	2500	-	-
Animal weight (g)	19	19.3	18.8	18.6	18.8

5.3.4.3. *In vivo* luciferase gene silencing study

To investigate whether CN could release its encapsulated siRNA and inhibit gene expression in the tumours, CN loaded with siLUC (39 µg/ml of CN encapsulating 625 nM of siLUC) were injected intratumorally in nude mice bearing B16-F10-LUC melanoma. Luciferase expression in the tumour was evaluated qualitatively and quantitatively in anaesthetised animals. Mice injected with siLUC alone, CN alone, or left untreated were used as controls. Figure 5.4 shows the average bioluminescence measured for each group. A representative mouse whose emitted light was closest to the average for that group (3 mice per group) is shown (Figure 5.5).

Luciferase expression in mice injected with siLUC encapsulated in CN was significantly decreased 4 h after injection, by about 50% (Figure 5.4). The maximum luciferase expression knockdown (by 70%) was obtained 12 h after injection. This inhibition was reversible and the luciferase expression returned to normal after 24 h. In contrast, the bioluminescence signals in the mice treated with naked siLUC increased over time, suggesting no inhibition of luciferase expression at any time point. Luciferase expression did not appear to be affected by the CN formulation, as the bioluminescence signal increased over time following treatment with empty CN. These results suggest that the inhibition of luciferase expression resulted from siLUC delivery by the CN into the cytoplasm of the cells and the subsequent RNAi mechanism. This demonstrates that siRNA can be released from the CN to cancer cells and can inhibit the target gene expression *in vivo.*

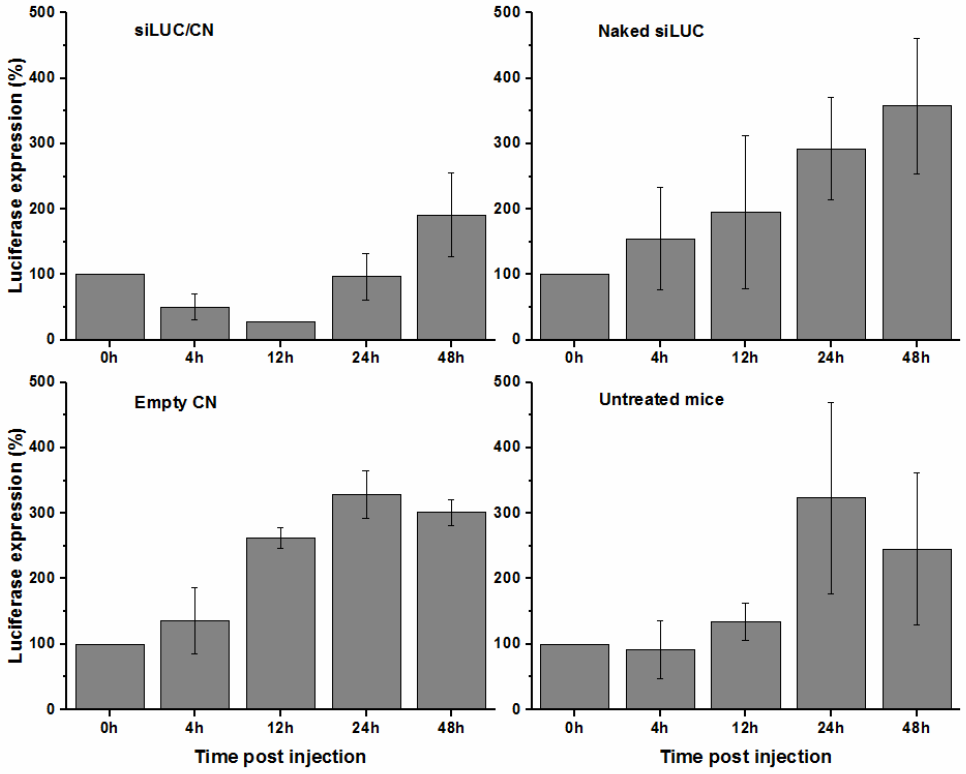

Figure 5.4 Bioluminescence of mice injected with siLUC/CN nioplexes, naked siLUC, empty CN, or left untreated. Readings were taken at t = 0h, 4h, 12h, 24h, and 48h post intra-tumour injection. Results represent the average of readings taken from three mice in each group ± SD.

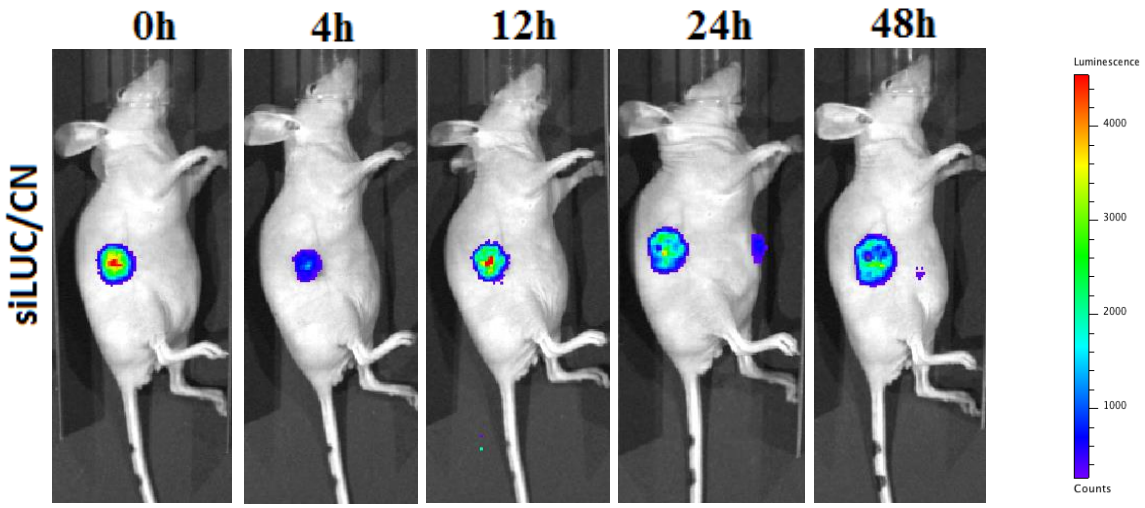
0h
4h
12h
24h
48h
siLUC/CN
Luminescence
4000
3000
2000
1000
Counts

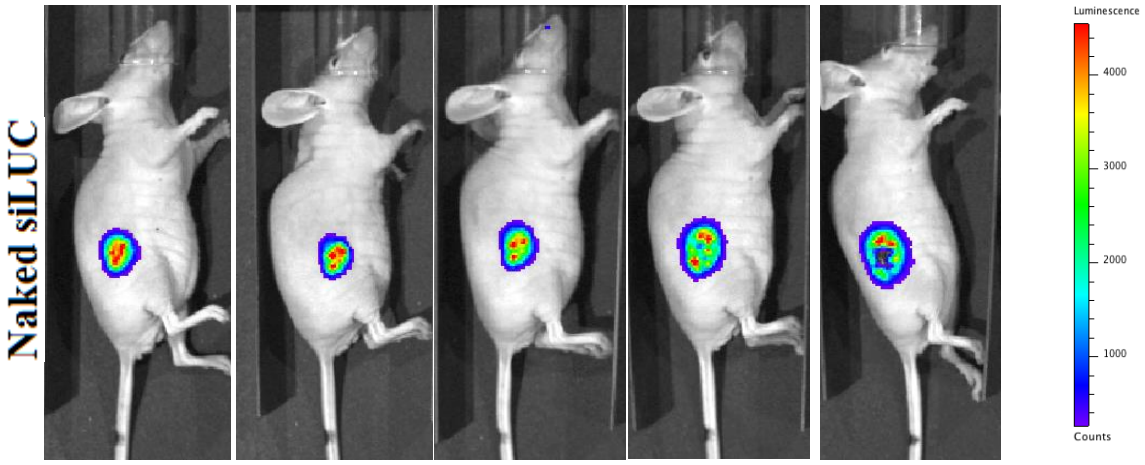
Naked siLUC
Luminescence
4000
3000
2000
1000
Counts

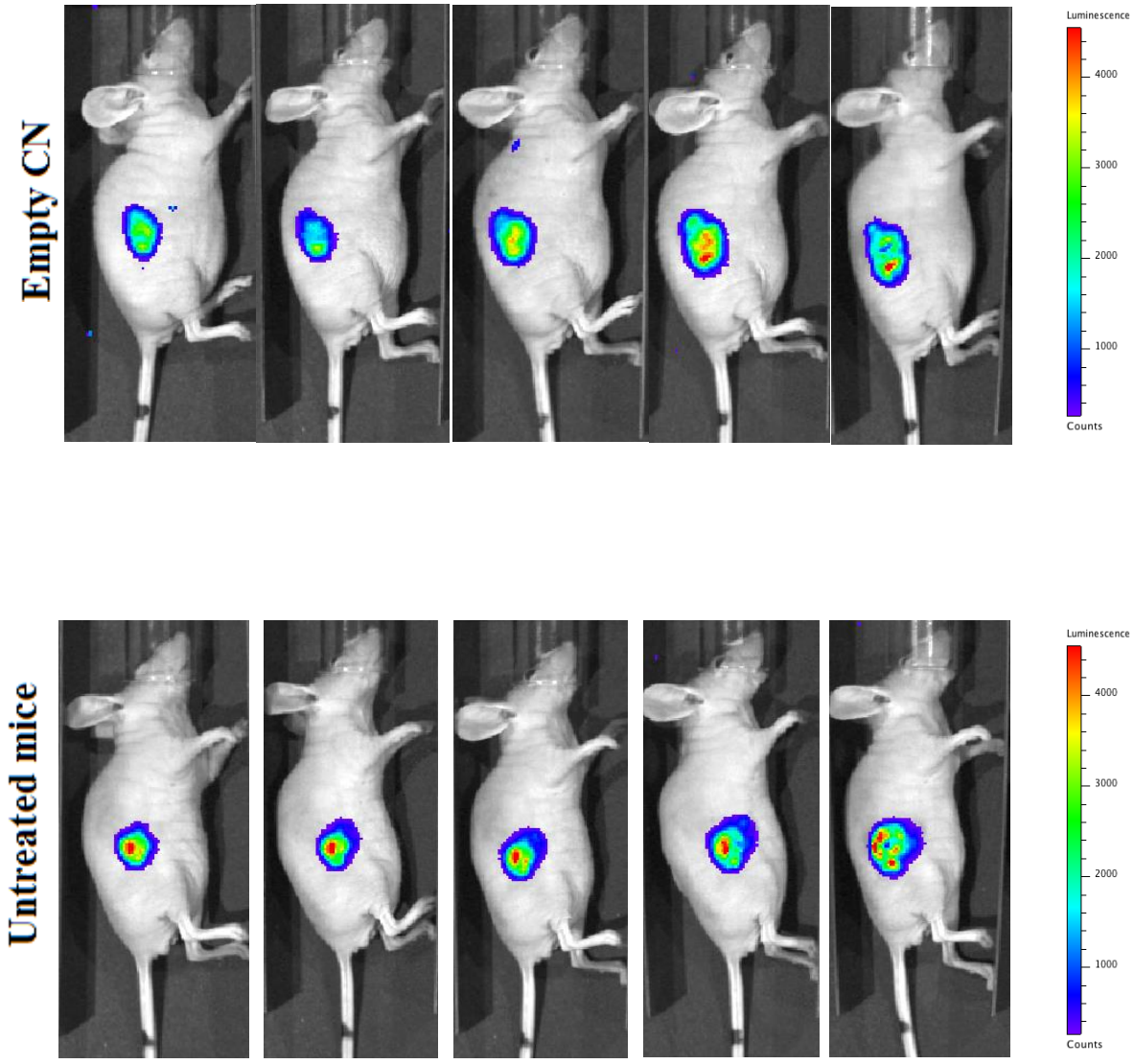

Figure 5.5 IVIS images of mice receiving siLUC/CN, naked siLUC, empty CN, and no treatment at zero time and 4, 12, 24, and 48 hours post intra-tumour injection. A representative mouse whose emitted light was closest to the average for that group (3 mice per group) is shown.

5.4. Discussion

In the previous chapter, three effective CN formulations were prepared and their efficacy in siRNA transfection proven *in vitro*. To confirm the gene silencing observed in copGFP-A549 cells, the biological activity of the selected formulations was then tested on a different cell model, the B16-F10-LUC cells, which could then be used in an *in vivo* tumour model. The cytotoxicity of these formulations was re-evaluated on B16-F10-LUC cells to make sure that any observed luciferase knock-down was a result of the siRNA used rather than vesicle related toxicity. Cytotoxicity results revealed that these formulations were not toxic at or below 40 μg/ml. However, there were differences in the EC_{50} values of the three formulations where the EC_{50} value of formulation C was significantly ($p<0.05$) lower than the EC_{50} values for formulations A and B. This suggests that the presence of T85 in formulation C resulted in higher toxicity of the formulation compared to MPG in formulations A and B. This is in agreement with what was reported in Chapter 4 where the EC_{50} of formulation C was lower than the other formulations when tested on A549 and PNT2 cells.

Next, the transfection efficiency of formulations A-C was examined by analysing the B16-F10-LUC cellular uptake using FACS analysis after treating these cells with each of the formulations encapsulating AllStars AF488-labelled Negative Control siRNA. All three formulations were able to deliver siRNA at high percentages. This high cellular uptake can be attributed to the positive charge on the surface of each formulation, which enhanced the interaction with the negatively charged cellular membrane. As seen before when these formulations were used with copGFP-A549 cells, the cellular uptake was similar between formulations A and B and higher than the uptake by formulation C. As mentioned before for the cellular uptake using copGFP-A549 cells, this similarity of cellular uptake between formulations A and B can be attributed to the similarity in their lipid composition. Moreover,

similar to the results obtained using copGFP-A549 cells, formulation C resulted in less cellular uptake than the other formulations when tested on B16-F10-LUC cells. As explained earlier, this is due to T85 in formulation C instead of MPG in formulations A and B. Cells treated with the empty formulations or with naked siRNA, showed no fluorescence signal indicating that the above mentioned cellular uptake was a result of the siRNA delivery by each of the CN formulations.

After evaluating the cellular uptake, the luciferase gene silencing mediated by siLUC loaded in the three CN formulations was evaluated. Luciferase is a bioluminescence producing enzyme widely used for monitoring siRNA delivering efficacy by monitoring bioluminescence changes after anti-luciferase siRNA treatment [284, 285]. After evaluating cellular uptake mediated by the three CN formulations, the subsequent inhibition of the target luciferase enzyme by siLUC needed to be proven. To examine both the extent of gene silencing and the optimal incubation time, B16-F10-LUC cells were transfected with various siLUC concentrations (10-200 nM) using each of the three formulations and the changes in bioluminescence intensity was monitored at various time points. Results indicated that the time of incubation and the siRNA concentrations had effects on the degree of gene knockdown. For all formulations, efficacy increased with the length of the incubation time until 48 h where further incubation did not result in higher efficacy for all siRNA concentrations. Increasing the incubation time meant higher exposure of the cells to the particles, which would increase the cellular uptake. This suggests that the noticed downregulation effect as a result of siLUC delivery by CN was stable for at least 72 h. Moreover, these experiments were carried out in the presence of serum, which indicates that the CN were able to protect the siLUC from degradation in the presence of serum proteins. Moreover, naked siLUC showed negligible gene silencing effects. These results demonstrate that by using CN formulations, siLUC is protected against degradation,

internalised by the cells, and escaped the endosomes to the cytoplasm where it displayed its bioactivity.

Among the three formulations, formulation C produced the highest luciferase inhibition compared to formulations A and B at all time points. Formulation C was able to induce the highest luciferase suppression among all three formulations where it induced luciferase enzyme expression by about 68% after 48 h incubation using 10 nM siLUC concentration. Higher siLUC concentrations delivered via formulation C did not result in a more significant reduction in luciferase expression. This could be due to the saturation of the gene silencing effect inside the cells. Formulation B was slightly more effective than formulation A in luciferase suppression despite having the same lipid composition. This is in agreement with the results reported in Chapter 4 for the GFP knockdown in the copGFP-A459 cells, where the maximum GFP expression knockdown was achieved with formulation C followed by formulation B then formulation A. Formulation C was more effective at gene knock-down than Hiperfect, by > 50%, which shows a dose-dependent effect. These results for luciferase suppression were consistent with the results reported in the previous chapter on inhibition of GFP expression in A549 cells by siGFP delivered by the three CN formulations. Although formulations A and B resulted in higher cellular uptake compared to formulation C as seen by FACS, formulation C was able to induce a higher gene knockdown effect. This was the same trend when these formulations were examined in copGFP-A549 cells and targeted the GFP expression where the uptake using formulations A and B was significantly higher than formulation C, but the GFP gene knockdown was higher with formulation C. This can be explained by the difference in endosomal escape ability after uptake to the cytoplasm where the RNAi mechanism occurs [275]. Although the uptake of formulations A and B was higher, these formulations seem to get trapped in the endosomes with minimal release, which was reflected by the low luciferase inhibition. This can be concluded because initially these formulations showed the highest

cellular uptake for the AF488-labelled negative control siRNA, but when active siRNA was used, there was no effect which suggests that the siLUC encapsulated in formulations A and B either degraded or the nioplexes were trapped in the endosomes. Formulation C was able to escape the endosome at a higher rate than the other formulations in order to release the siLUC into the cytoplasm and effectively inhibit the luciferase expression. This can be concluded from the highest luciferase suppression activity induced when using formulation C. This could be related to the presence of Tween 85 in formulation C which enhances endosome escape compared to the MPG in formulation A and B. Moreover, downregulation of gene expression due to toxic effects of the formulations can be excluded as non-toxic concentrations of each formulation was used. In addition, no downregulation was seen when the cells were transfected with empty particles of each formulation (0nM siLUC).

High siRNA concentrations can result in off-target effects which is one of the side effects associated with siRNA therapeutics [286]. Previous reports of siRNA delivery targeting luciferase were able to achieve high luciferase suppression only at high siRNA concentrations, which increases the possibility of siRNA off-target effects. For example, Takemoto *et al.* were able to achieve 80% luciferase silencing at only 100 nM siRNA concentration using a siRNA-grafted polymer delivery system [287]. With chitosan nanoparticles, Ragelle *et al.* were able to achieve 71% luciferase suppression using 200 nM of anti-luciferase siRNA [288]. While Li *et al.* were able to induce around 70% luciferase gene silencing using targeted cationic liposomes. However, they were able to achieve this suppression using 250 nM anti-luciferase siRNA [289]. Suma *et al.*, were able to achieve ~75% luciferase reduction using 100 nM anti-luciferase siRNA delivered via a polyaspartamide-derivatives delivery system [290]. In this study, with formulation C, high luciferase silencing was achieved with the minimal siRNA concentration (10 nM) which indicates the efficacy of this CN formulation. Based on the above results, formulation C was selected for the subsequent *in vivo* efficacy evaluation.

Before moving to the *in vivo* experiments, formulation C was formulated with sterile RNAase-free glucose 5% (w/v) instead of water as glucose 5% is more compatible for animal injections. Formulation C prepared with glucose 5% was characterised by DLS in terms of particle size, PDI, and ZP to make sure that this change in the preparation media did not affect the particles' characteristics. By comparing the particles' characteristics when prepared by sterile RNase free water as reported in Table 4.5, there was no significant difference as a result of using sterile RNase-free glucose 5% instead of water. Following that, empty particles and particles with siLUC were used to determine the maximum dose that could be used for *in vivo* experiments to make sure the used doses in the experiment were non-toxic to the animals.

After determining the maximum dose that could be used for the *in vivo* experiments, the mice were intratumorally injected with siLUC encapsulated in formulation C. The intra-tumour injection route was chosen as a first step to offer a localised application of the formulation and to increase the possibilities of cellular uptake. After 4h of treatment, the luciferase expression decreased by about 50.77 ± 20.35 %, indicating that the nioplexes were taken up by the cells, the siLUC was released into the cytoplasm and incorporated in the RISC followed by luciferase expression knockdown. Twelve hours after the treatment, luciferase expression was significantly ($p<0.05$) decreased by more than 70%, indicating that the formulation was taken up by the tumour cells, and luciferase expression was effectively suppressed. This luciferase suppression was reversible and, 24h after injection, the luciferase expression was fully recovered. This reversible effect could be due to the fact that the RNAi mechanism is a reversible mechanism and protein expression would be restored after the inhibition [291, 292]. Another possible explanation for this reversible effect could be due to the growth of the tumour with time which results in higher luciferase expression. It could also be due to the low siLUC dose used and an indication that a higher dose is needed. Moreover, the CN/siLUC complexes could be degraded after the cellular uptake, which would result in diminishing of the RNAi

effect. These results could provide an idea about the possible required dosing intervals to maintain the target gene suppression by siRNA. Although the *in vitro* experiments showed that the maximum effects of luciferase suppression were observed after 48h and lasted for 72h after transfection, here, the *in vivo* experiments suggest that maximum inhibition occurred 12h post-injection and did not last for 24h suggesting additional doses would be required to maintain this effect. In mice injected with naked siLUC, there was no luciferase suppression and the luciferase expression increased with time as the tumour size increased, suggesting that the tumour cells did not take up naked siLUC as a result of its hydrophilic properties. Moreover, mice injected with particles alone showed an increase in luciferase expression over time, as expected, suggesting that the empty particles had no effects on luciferase expression. In the work of Minakuchi *et al.*, significant luciferase suppression was achieved via an atelocollagen delivery system using a single injection via the same route of administration and the same tumour type as used in this study [293]. However, despite the larger dose that they used, based on the tumour size (2.5 μg siRNA/50 μl/50 mm^3 tumor), the luciferase expression was also reversible after 2-3 days [293]. Filleur *et al.*, investigated the use of naked siRNA to suppress luciferase expression by intra-tumoural injection and ended up with negative results, which was similar to the results reported here in which naked siLUC did not induce any gene suppression [294].

These *in vivo* results demonstrate the efficacy of formulation C in delivering and releasing siRNA into tumour cells. Although further experiments are required such as i.v treatment and biodistribution studies, CN mediated siRNA delivery possesses the potential for *in vivo* delivery of siRNA. These results provide proof of concept of the ability of CN to effectively deliver siRNA into mouse melanoma cells. However, these CN formulations can be explored with different types of cancer cells. Moreover, these intra-tumoural injection results could be used as a model for localised treatment of siRNA therapeutics delivered by CN and these

formulations could be explored further for topical applications in treatment of different diseases.

5.5. Conclusions

CN nanoparticles as an effective siRNA delivery system were successfully formulated. These CN were able to deliver siRNA and suppress luciferase expression both *in vitro* and *in vivo*. With these CN formulations, the suppression of over expressed genes in different cancer types can be investigated through siRNA delivery. More than 70% of luciferase knockdown was achieved through CN both *in vitro* and *in vivo*, which will be a promising addition to the field of nucleic acid delivery. In conclusion, CN have been developed to efficiently and safely deliver siRNA to tumour cells both *in vitro* and *in vivo* and demonstrated specific inhibition of luciferase gene expression. These results present the first evidence that combine *in vitro* and *in vivo* gene silencing data of siRNA delivery by NISV. This suggests that NISV might be investigated further for a therapeutic application of siRNA in cancer treatment.

Chapter 6

General conclusions and future directions

The aim of the present research was to formulate an effective delivery system to deliver siRNA to cancer cells. NISV were selected for this purpose with modification of the method of manufacturing and composition. The use of NISV as the delivery system for siRNA presents promising potential to help improve current formulations and offers alternative treatment options for different diseases. This work has shown that NISV can act as a delivery system of siRNA into cancer cells. By demonstrating their efficacy in cancer cells, their application could be extrapolated to consider their use as a therapeutic delivery agent for other diseases such as infections. Different methods of manufacturing have been investigated such as thin film hydration method, heating method, and microfluidic mixing. The parameters that control the production of small, monodisperse, and stable vesicles using these methods were evaluated. From these methods, microfluidic mixing was shown to produce the desired particles in one step without the need of a size reduction step, which is critical in the other methods. In addition, the type of aqueous media used to prepare the particles, mixing rate, and the ratios between the lipid and aqueous phases were all shown to have significant impact on the particles prepared in terms of particles size and homogeneity. Stability studies were reported over two months in this thesis. However, these studies still ongoing as a future work to determine the shelf-life of the prepared formulations.

Different CN formulations were then prepared by microfluidic mixing and evaluated for their efficacy in siRNA delivery. Cationic charge was chosen to aid and facilitate siRNA condensation in the nanoparticles and also to enhance the stability of the particles through electrostatic repulsion. Moreover, it was anticipated that the cationic charge would facilitate the CN cellular uptake through the interaction with negative charge moieties in the cell membrane. This cationic charge was induced by the presence of the cationic lipid DDAB in the formulations. DDAB is an inexpensive commercially available cationic lipid that has been extensively used in the preparation of cationic liposomes for nucleic acids delivery [295-297].

For this reason, DDAB was used to prepare CN by microfluidics in order to facilitate the siRNA transfection using this type of nanoparticle. This means the CN prepared in this work have a low production cost, in contrast to liposomes, which is an important factor that needs to be considered in the development of nanoparticle-based medicines. The prepared CN by microfluidics were small and monodisperse with a spherical shape.

The experimental results in this thesis are very encouraging with respect to the capability of the CN to deliver siRNA. The CN formulations (which differed in terms of the type of non-ionic surfactant used) were evaluated first for their siRNA EE. All the formulations were shown to have high EE with minimal changes in size and surface charge. The CN formulations were then evaluated for their ability to deliver fluorescently labelled siRNA to assess the level of cellular uptake. Through fluorescent microscopy and FACS analysis, the CN formulations had high cellular uptake, which was significantly higher than the uptake of naked siRNA alone when evaluated on copGFP-A549 and B16-F10-LUC cells.

After proving the efficacy of these formulations in siRNA delivery, the inclusion of siRNA which targeted a specific cell protein was used to evaluate the ability of these formulations to deliver siRNA and suppress the target protein. Two expressed proteins were targeted in two different cell lines; GFP in copGFP-A549 cells and luciferase enzyme in B16-F10-LUC mouse melanoma cells. The level of protein expression after transfection was evaluated by several techniques such as fluorescence measurement, FACS, PCR, Western blot analysis, and bioluminescence measurement. The results showed that all three of the chosen formulations encapsulating siRNA were able to suppress both targets indicating high efficacy in siRNA delivery and protein suppression. Of these formulations, one CN formulation composed of T85:Chol:DDAB at a molar ratio of 40:40:20 was shown to induce superior protein knockdown compared to the other CN formulations. This formulation was able to induce more that 70% reduction of both target protein expression. The *in vitro* experiments in this thesis offer more

advancement and experience to enrich the current research and improve siRNA delivery using lipid-based nanoparticles such as NISV. These results will provide an encouraging and positive step forward towards the application of siRNA therapeutics in a clinical setting.

The most effective formulation of the ones examined was then chosen for *in vivo* experimentation to evaluate luciferase suppression by siRNA in an animal model. Intra-tumour injection of CN encapsulating siLUC were able to achieve significant luciferase suppression after 12h post-injection.

The work presented in this thesis opened up further opportunities of investigation for the use of NISV in the field of nucleic acid delivery. The results from this work can inform future research in which these optimised CN formulations can be used to deliver siRNA payloads, targeting and suppressing proteins and oncogenes that are vital for cancer cell growth and metastasis. Example of these proteins that can be suppressed by siRNA delivered by the CN are the c-Myc, CD47, MDM2, and VEGF [298, 299]. Moreover, future work can also explore the use of these CN for the delivery of siRNA in combination with, for example, a chemotherapeutic agent such as paclitaxel or doxorubicin. Combination therapy could be studied in terms of the synergistic effects of these agents in cancer treatment. In terms of formulations, another possible approach would be to explore the coating of these CN with PEG and to attach a targeting ligand that will increase the selectivity of these CN to cancer cells to avoid any off-target effects of the siRNA payload. Moreover, the use of higher lipid concentrations during the preparation through microfluidic mixing can be a valuable research area to explore the effects of the starting lipid concentration on the characteristics of the NISV and their stability. With regards to *in vivo* experiments, more work is needed to evaluate the treatment dose, the duration of treatment, particle distribution, elimination rate, and long term effects. Whilst limitations still remain, the delivery of siRNA through lipid nanoparticles offer a promising future for the development of more effective and safer medications.

Appendices

Appendix 1: The nucleotide and amino acid sequences of copGFP in copGFP-A549 cells (Cell Biolabs, Inc., UK).

>copGFP coding sequence
ATGGAGAGCGACGAGAGCGGCCTGCCCGCCATGGAGATCGAGTGCCGCATCACCGGCACCCT
GAACGGCGTGGAGTTCGAGCTGGTGGGCGGCGGAGAGGGCACCCCCAAGCAGGGCCGCATGA
CCAACAAGATGAAGAGCACCAAAGGCGCCCTGACCTTCAGCCCCTACCTGCTGAGCCACGTG
ATGGGCTACGGCTTCTACCACTTCGGCACCTACCCCAGCGGCTACGAGAACCCCTTCCTGCA
CGCCATCAACAACGGCGGCTACACCAACACCCGCATCGAGAAGTACGAGGACGGCGGCGTGC
TGCACGTGAGCTTCAGCTACCGCTACGAGGCCGGCCGCGTGATCGGCGACTTCAAGGTGGTG
GGCACCGGCTTCCCCGAGGACAGCGTGATCTTCACCGACAAGATCATCCGCAGCAACGCCAC
CGTGGAGCACCTGCACCCCATGGGCGATAACGTGCTGGTGGGCAGCTTCGCCCGCACCTTCA
GCCTGCGCGACGGCGGCTACTACAGCTTCGTGGTGGACAGCCACATGCACTTCAAGAGCGCC
ATCCACCCCAGCATCCTGCAGAACGGGGGCCCCATGTTCGCCTTCCGCCGCGTGGAGGAGCT
GCACAGCAACACCGAGCTGGGCATCGTGGAGTACCAGCACGCCTTCAAGACCCCCATCGCCT
TCGCCAGATCCCGCGCTCAGTCGTCCAATTCTGCCGTGGACGGCACCGCCGGACCCGGCTCC
ACCGGATCTCGCTAA

>copGFP amino acid sequence
MESDESGLPAMEIECRITGTLNGVEFELVGGGEGTPKQGRMTNKMKSTKGALTFSPYLLSHV
MGYGFYHFGTYPSGYENPFLHAINNGGYTNTRIEKYEDGGVLHVSFSYRYEAGRVIGDFKVV
GTGFPEDSVIFTDKIIRSNATVEHLHPMGDNVLVGSFARTFSLRDGGYYSFVVDSHMHFKSA
IHPSILQNGGPMFAFRRVEELHSNTELGIVEYQHAFKTPIAFARSRAQSSNSAVDGTAGPGS
TGSR

Appendix 2: Methods of preparations of buffers used in Western blot analysis

1. Preparation of lysis buffer

To prepare 100 ml of cell lysis buffers, the components in Table 1 were mixed together.

Table 1. Lysis buffer used in Western blot analysis.

Chemical	Weight/Volume
Tris base (62.5 mM final)	0.757 g
Sodium pyrophosphate ($Na_4P_2O_7$) (0.5 mM final)	13.25 mg
Ethylenediamine tetra-acetic acid (EDTA) (1.25 mM final)	46.5 mg
Sodium dodecyl sulphate (SDS) (1.25% final)	1.25 g
Bromophenol blue	50 mg
Glycerol (12.5% final)	12.5 ml
Distilled water	87.5 ml

2. Preparation of electrophoresis buffer

To prepare 10x concentration of electrophoresis buffer, the components in Table 2 were mixed together then the final solution were diluted 1/10 before electrophoresis running.

Table 2. 10x Electrophoresis Buffer (Running Buffer)

Chemical	Weight/Volume
Glycine	144 g
Sodium dodecyl sulphate (SDS)	10 g
Tris base	30 g
Distilled water	1000 ml

3. Preparation of blotting buffer

To prepare the blotting buffer, the components in Table 3 were mixed together in the same order mentioned in the table.

Table 3. Blotting Buffer (Transfer buffer)

Chemical	Weight/Volume
Glycine	14.4 g
Tris base	3.0 g
Distilled water	800 ml
Methanol	200 ml

4. Preparation of Tris-buffered saline with Tween 20 (TBST)

To prepare 10x solution of TBST, the components in Table 4 were mixed together. The final solution was diluted 1/10 before use.

Table 4. 10x Tris-buffered saline with Tween 20 (TBST)

Chemical	Weight/Volume
Sodium Chloride (NaCl)	58.5 g
Tris base	12.1 g
Tween 20	10 ml
Distilled water*	1000 ml

* pH adjusted to 7.5 before adding Tween 20

Appendix 3: The nucleotide and amino acid sequences of luciferase in B16-F10-LUC luciferase expressing cells (Caliper life Science, Inc., USA) cells.

>Luciferase coding sequence

ATGGAAGATGCCAAAAACATTAAGAAGGGCCCAGCGCCATTCTACCCACTCGAAGACGGGAC
CGCCGGCGAGCAGCTGCACAAAGCCATGAAGCGCTACGCCCTGGTGCCCGGCACCATCGCCT
TTACCGACGCACATATCGAGGTGGACATTACCTACGCCGAGTACTTCGAGATGAGCGTTCGG
CTGGCAGAAGCTATGAAGCGCTATGGGCTGAATACAAACCATCGGATCGTGGTGTGCAGCGA
GAATAGCTTGCAGTTCTTCATGCCCGTGTTGGGTGCCCTGTTCATCGGTGTGGCTGTGGCCC
CAGCTAACGACATCTACAACGAGCGCGAGCTGCTGAACAGCATGGGCATCAGCCAGCCCACC
GTCGTATTCGTGAGCAAGAAAGGGCTGCAAAAGATCCTCAACGTGCAAAAGAAGCTACCGAT
CATACAAAAGATCATCATCATGGATAGCAAGACCGACTACCAGGGCTTCCAAAGCATGTACA
CCTTCGTGACTTCCCATTTGCCACCCGGCTTCAACGAGTACGACTTCGTGCCCGAGAGCTTC
GACCGGGACAAAACCATCGCCCTGATCATGAACAGTAGTGGCAGTACCGGATTGCCCAAGGG
CGTAGCCCTACCGCACCGCACCGCTTGTGTCCGATTCAGTCATGCCCGCGACCCCATCTTCG
GCAACCAGATCATCCCCGACACCGCTATCCTCAGCGTGGTGCCATTTCACCACGGCTTCGGC
ATGTTCACCACGCTGGGCTACTTGATCTGCGGCTTTCGGGTCGTGCTCATGTACCGCTTCGA
GGAGGAGCTATTCTTGCGCAGCTTGCAAGACTATAAGATTCAATCTGCCCTGCTGGTGCCCA
CACTATTTAGCTTCTTCGCTAAGAGCACTCTCATCGACAAGTACGACCTAAGCAACTTGCAC
GAGATCGCCAGCGGCGGGGCGCCGCTCAGCAAGGAGGTAGGTGAGGCCGTGGCCAAACGCTT
CCACCTACCAGGCATCCGCCAGGGCTACGGCCTGACAGAAACAACCAGCGCCATTCTGATCA
CCCCCGAAGGGGACGACAAGCCTGGCGCAGTAGGCAAGGTGGTGCCCTTCTTCGAGGCTAAG
GTGGTGGACTTGGACACCGGTAAGACACTGGGTGTGAACCAGCGCGGCGAGCTGTGCGTCCG
TGGCCCCATGATCATGAGCGGCTACGTTAACAACCCCGAGGCTACAAACGCTCTCATCGACA
AGGACGGCTGGCTGCACAGCGGCGACATCGCCTACTGGGACGAGGACGAGCACTTCTTCATC
GTGGACCGGCTGAAGAGCCTGATCAAATACAAGGGCTACCAGGTAGCCCCAGCCGAACTGGA
GAGCATCCTGCTGCAACACCCCAACATCTTCGACGCCGGGGTCGCCGGCCTGCCCGACGACG
ATGCCGGCGAGCTGCCCGCCGCAGTCGTCGTGCTGGAACACGGTAAAACCATGACCGAGAAG
GAGATCGTGGACTATGTGGCCAGCCAGGTTACAACCGCCAAGAAGCTGCGCGGTGGTGTTGT
GTTCGTGGACGAGGTGCCTAAAGGACTGACCGGCAAGTTGGACGCCCGCAAGATCCGCGAGA
TTCTCATTAAGGCCAAGAAGGGCGGCAAGATCGCCGTG

>Luciferase amino acid sequence

MEDAKNIKKGPAPFYPLEDGTAGEQLHKAMKRYALVPGTIAFTDAHIEVDITYAEYFEMSVR
LAEAMKRYGLNTNHRIVVCSENSLQFFMPVLGALFIGVAVAPANDIYNERELLNSMGISQPT
VVFVSKKGLQKILNVQKKLPIIQKIIIMDSKTDYQGFQSMYTFVTSHLPPGFNEYDFVPESF
DRDKTIALIMNSSGSTGLPKGVALPHRTACVRFSHARDPIFGNQIIPDTAILSVVPFHHGFG
MFTTLGYLICGFRVVLMYRFEEELFLRSLQDYKIQSALLVPTLFSFFAKSTLIDKYDLSNLH
EIASGGAPLSKEVGEAVAKRFHLPGIRQGYGLTETTSAILITPEGDDKPGAVGKVVPFFEAK
VVDLDTGKTLGVNQRGELCVRGPMIMSGYVNNPEATNALIDKDGWLHSGDIAYWDEDEHFFI
VDRLKSLIKYKGYQVAPAELESILLQHPNIFDAGVAGLPDDDAGELPAAVVVLEHGKTMTEK
EIVDYVASQVTTAKKLRGGVVFVDEVPKGLTGKLDARKIREILIKAKKGGKIAV...

References

References

1. Underwood JC, Cross SS. *General and systematic pathology*. Elsevier Health Sciences, (2009).
2. Singhal S, Nie S, Wang MD. Nanotechnology applications in surgical oncology. *Annual review of medicine* 61 359 (2010).
3. Li S-D, Huang L. Stealth nanoparticles: high density but sheddable PEG is a key for tumor targeting. *Journal of controlled release: official journal of the Controlled Release Society* 145(3), 178 (2010).
4. Misra R, Acharya S, Sahoo SK. Cancer nanotechnology: application of nanotechnology in cancer therapy. *Drug Discovery Today* 15(19), 842-850 (2010).
5. Miele E, Spinelli GP, Miele E *et al*. Nanoparticle-based delivery of small interfering RNA: challenges for cancer therapy. *International journal of nanomedicine* 7 3637 (2012).
6. Parveen S, Misra R, Sahoo SK. Nanoparticles: a boon to drug delivery, therapeutics, diagnostics and imaging. *Nanomedicine: Nanotechnology, Biology and Medicine* 8(2), 147-166 (2012).
7. Wang M, Thanou M. Targeting nanoparticles to cancer. *Pharmacological Research* 62(2), 90-99 (2010).
8. Orive G, Hernandez RM, Gascón ARG, DomíNguez-Gil A, Pedraz JL. Drug delivery in biotechnology: present and future. *Current opinion in biotechnology* 14(6), 659-664 (2003).
9. Sahoo SK, Parveen S. Nanomedicine: Clinical Applications of Polyethylene Glycol Conjugated Proteins and Drugs. *Clinical pharmacokinetics* (10), 965-988 (2006).
10. Davis ME, Zuckerman JE, Choi CHJ *et al*. Evidence of RNAi in humans from systemically administered siRNA via targeted nanoparticles. *Nature* 464(7291), 1067-1070 (2010).
11. De Jong WH, Borm PJ. Drug delivery and nanoparticles: applications and hazards. *International journal of nanomedicine* 3(2), 133 (2008).
12. Ozpolat B, Sood AK, Lopez-Berestein G. Liposomal siRNA nanocarriers for cancer therapy. *Advanced drug delivery reviews* 66 110-116 (2014).
13. Díaz MR, Vivas-Mejia PE. Nanoparticles as drug delivery systems in cancer medicine: emphasis on RNAi-containing nanoliposomes. *Pharmaceuticals* 6(11), 1361-1380 (2013).
14. Allen TM, Cullis PR. Liposomal drug delivery systems: from concept to clinical applications. *Advanced drug delivery reviews* 65(1), 36-48 (2013).
15. Scheinberg DA, Villa CH, Escorcia FE, Mcdevitt MR. Conscripts of the infinite armada: systemic cancer therapy using nanomaterials. *Nature Reviews Clinical Oncology* 7(5), 266-276 (2010).
16. Bertrand N, Wu J, Xu X, Kamaly N, Farokhzad OC. Cancer nanotechnology: the impact of passive and active targeting in the era of modern cancer biology. *Advanced drug delivery reviews* 66 2-25 (2014).
17. Desai N, Trieu V, Yao Z *et al*. Increased antitumor activity, intratumor paclitaxel concentrations, and endothelial cell transport of cremophor-free, albumin-bound paclitaxel, ABI-007, compared with cremophor-based paclitaxel. *Clinical cancer research* 12(4), 1317-1324 (2006).
18. Rivera E. Liposomal anthracyclines in metastatic breast cancer: clinical update. *The oncologist* 8(Supplement 2), 3-9 (2003).
19. Glantz MJ, Jaeckle KA, Chamberlain MC *et al*. A randomized controlled trial comparing intrathecal sustained-release cytarabine (DepoCyt) to intrathecal methotrexate in patients with neoplastic meningitis from solid tumors. *Clinical Cancer Research* 5(11), 3394-3402 (1999).
20. Muggia FM, Hainsworth JD, Jeffers S *et al*. Phase II study of liposomal doxorubicin in refractory ovarian cancer: antitumor activity and toxicity modification by liposomal encapsulation. *Journal of Clinical Oncology* 15(3), 987-993 (1997).

21. Lee KS, Chung HC, Im SA *et al*. Multicenter phase II trial of Genexol-PM, a Cremophor-free, polymeric micelle formulation of paclitaxel, in patients with metastatic breast cancer. *Breast cancer research and treatment* 108(2), 241-250 (2008).
22. Rodriguez M, Pytlik R, Kozak T *et al*. Vincristine sulfate liposomes injection (Marqibo) in heavily pretreated patients with refractory aggressive non-Hodgkin lymphoma. *Cancer* 115(15), 3475-3482 (2009).
23. Venkatakrishnan K, Liu Y, Noe D *et al*. Pharmacokinetics and pharmacodynamics of liposomal mifamurtide in adult volunteers with mild or moderate hepatic impairment. *British journal of clinical pharmacology* 77(6), 998-1010 (2014).
24. Dinndorf PA, Gootenberg J, Cohen MH, Keegan P, Pazdur R. FDA drug approval summary: pegaspargase (Oncaspar®) for the first-line treatment of children with acute lymphoblastic leukemia (ALL). *The oncologist* 12(8), 991-998 (2007).
25. Lee J-M, Yoon T-J, Cho Y-S. Recent developments in nanoparticle-based siRNA delivery for cancer therapy. *BioMed research international* 2013 (2013).
26. Yingchoncharoen P, Kalinowski DS, Richardson DR. Lipid-Based Drug Delivery Systems in Cancer Therapy: What Is Available and What Is Yet to Come. *Pharmacological Reviews* 68(3), 701-787 (2016).
27. Gregoriadis G. The carrier potential of liposomes in biology and medicine. *New England Journal of Medicine* 295(14), 765-770 (1976).
28. Gregoriadis G. Engineering liposomes for drug delivery: progress and problems. *Trends in biotechnology* 13(12), 527-537 (1995).
29. Allen TM. Liposomal drug formulations. *Drugs* 56(5), 747-756 (1998).
30. Ellens H, Bentz J, Szoka FC. Destabilization of phosphatidylethanolamine liposomes at the hexagonal phase transition temperature. *Biochemistry* 25(2), 285-294 (1986).
31. Vemuri S, Rhodes C. Preparation and characterization of liposomes as therapeutic delivery systems: a review. *Pharmaceutica Acta Helvetiae* 70(2), 95-111 (1995).
32. Zhang J, Li X, Huang L. Non-viral nanocarriers for siRNA delivery in breast cancer. *Journal of Controlled Release* (2014).
33. Immordino ML, Dosio F, Cattel L. Stealth liposomes: review of the basic science, rationale, and clinical applications, existing and potential. *International journal of nanomedicine* 1(3), 297 (2006).
34. Yamauchi H, Yano T, Kato T *et al*. Effects of sialic acid derivative on long circulation time and tumor concentration of liposomes. *International journal of pharmaceutics* 113(2), 141-148 (1995).
35. Akbarzadeh A, Rezaei-Sadabady R, Davaran S *et al*. Liposome: classification, preparation, and applications. *Nanoscale research letters* 8(1), 1 (2013).
36. Nagayasu A, Uchiyama K, Kiwada H. The size of liposomes: a factor which affects their targeting efficiency to tumors and therapeutic activity of liposomal antitumor drugs. *Advanced drug delivery reviews* 40(1), 75-87 (1999).
37. Laouini A, Jaafar-Maalej C, Limayem-Blouza I, Sfar S, Charcosset C, Fessi H. Preparation, characterization and applications of liposomes: state of the art. *Journal of Colloid Science and Biotechnology* 1(2), 147-168 (2012).
38. Albanese A, Tang PS, Chan WC. The effect of nanoparticle size, shape, and surface chemistry on biological systems. *Annual review of biomedical engineering* 14 1-16 (2012).
39. Su G, Zhou H, Mu Q *et al*. Effective surface charge density determines the electrostatic attraction between nanoparticles and cells. *The Journal of Physical Chemistry C* 116(8), 4993-4998 (2012).
40. HüHn D, Kantner K, Geidel C *et al*. Polymer-coated nanoparticles interacting with proteins and cells: focusing on the sign of the net charge. *Acs Nano* 7(4), 3253-3263 (2013).
41. Alexis F, Pridgen E, Molnar LK, Farokhzad OC. Factors affecting the clearance and biodistribution of polymeric nanoparticles. *Molecular pharmaceutics* 5(4), 505-515 (2008).

42. Wang H-X, Zuo Z-Q, Du J-Z *et al*. Surface charge critically affects tumor penetration and therapeutic efficacy of cancer nanomedicines. *Nano Today* 11(2), 133-144 (2016).
43. Honeywell-Nguyen PL, Bouwstra JA. Vesicles as a tool for transdermal and dermal delivery. *Drug Discovery Today: Technologies* 2(1), 67-74 (2005).
44. Estanqueiro M, Amaral MH, Conceição J, Lobo JMS. Nanotechnological carriers for cancer chemotherapy: the state of the art. *Colloids and Surfaces B: Biointerfaces* 126 631-648 (2015).
45. Wan C, Allen T, Cullis P. Lipid nanoparticle delivery systems for siRNA-based therapeutics. *Drug Delivery and Translational Research* 4(1), 74-83 (2014).
46. Draz MS, Fang BA, Zhang P *et al*. Nanoparticle-mediated systemic delivery of siRNA for treatment of cancers and viral infections. *Theranostics* 4(9), 872 (2014).
47. Tam YYC, Chen S, Cullis PR. Advances in Lipid Nanoparticles for siRNA Delivery. *Pharmaceutics* 5(3), 498-507 (2013).
48. Chang H-I, Yeh M-K. Clinical development of liposome-based drugs: formulation, characterization, and therapeutic efficacy. *Int J Nanomedicine* 7(4), (2012).
49. Chae S-S, Paik J-H, Furneaux H, Hla T. Requirement for sphingosine 1–phosphate receptor-1 in tumor angiogenesis demonstrated by in vivo RNA interference. *The Journal of clinical investigation* 114(8), 1082-1089 (2004).
50. Yano J, Hirabayashi K, Nakagawa S-I *et al*. Antitumor activity of small interfering RNA/cationic liposome complex in mouse models of cancer. *Clinical Cancer Research* 10(22), 7721-7726 (2004).
51. Buyens K, De Smedt SC, Braeckmans K *et al*. Liposome based systems for systemic siRNA delivery: stability in blood sets the requirements for optimal carrier design. *Journal of Controlled Release* 158(3), 362-370 (2012).
52. Gomes-Da-Silva LGC, Fonseca NA, Moura V, Pedroso De Lima MC, SimõEs SR, Moreira JON. Lipid-based nanoparticles for siRNA delivery in cancer therapy: paradigms and challenges. *Accounts of chemical research* 45(7), 1163-1171 (2012).
53. Tagalakis AD, Do Hyang DL, Bienemann AS *et al*. Multifunctional, self-assembling anionic peptide-lipid nanocomplexes for targeted siRNA delivery. *Biomaterials* 35(29), 8406-8415 (2014).
54. Zhou Y, Zhang C, Liang W. Development of RNAi technology for targeted therapy—A track of siRNA based agents to RNAi therapeutics. *Journal of Controlled Release* (2014).
55. Morrissey DV, Lockridge JA, Shaw L *et al*. Potent and persistent in vivo anti-HBV activity of chemically modified siRNAs. *Nature biotechnology* 23(8), 1002-1007 (2005).
56. Judge AD, Robbins M, Tavakoli I *et al*. Confirming the RNAi-mediated mechanism of action of siRNA-based cancer therapeutics in mice. *The Journal of clinical investigation* 119(3), 661-673 (2009).
57. Kaur CD, Nahar M, Jain NK. Lymphatic targeting of zidovudine using surface-engineered liposomes. *Journal of drug targeting* 16(10), 798-805 (2008).
58. Forssen EA, Tökes ZA. Improved therapeutic benefits of doxorubicin by entrapment in anionic liposomes. *Cancer research* 43(2), 546-550 (1983).
59. Kapoor M, Burgess DJ. Efficient and safe delivery of siRNA using anionic lipids: formulation optimization studies. *International journal of pharmaceutics* 432(1), 80-90 (2012).
60. Mamot C, Drummond DC, Hong K, Kirpotin DB, Park JW. Liposome-based approaches to overcome anticancer drug resistance. *Drug Resistance Updates* 6(5), 271-279 (2003).
61. Merritt WM, Lin YG, Spannuth WA *et al*. Effect of interleukin-8 gene silencing with liposome-encapsulated small interfering RNA on ovarian cancer cell growth. *Journal of the National Cancer Institute* 100(5), 359-372 (2008).
62. Ozpolat B, Sood A, Lopez-Berestein G. Nanomedicine based approaches for the delivery of siRNA in cancer. *Journal of internal medicine* 267(1), 44-53 (2010).

63. Wong HL, Bendayan R, Rauth AM, Li Y, Wu XY. Chemotherapy with anticancer drugs encapsulated in solid lipid nanoparticles. *Advanced drug delivery reviews* 59(6), 491-504 (2007).
64. Feng L, Mumper RJ. A critical review of lipid-based nanoparticles for taxane delivery. *Cancer letters* 334(2), 157-175 (2013).
65. Lee M-K, Lim S-J, Kim C-K. Preparation, characterization and in vitro cytotoxicity of paclitaxel-loaded sterically stabilized solid lipid nanoparticles. *Biomaterials* 28(12), 2137-2146 (2007).
66. Chen D-B, Yang T-Z, Lu W-L, Zhang Q. In vitro and in vivo study of two types of long-circulating solid lipid nanoparticles containing paclitaxel. *Chemical and pharmaceutical bulletin* 49(11), 1444-1447 (2001).
67. Shahgaldian P, Da Silva E, Coleman AW, Rather B, Zaworotko MJ. Para-acyl-calix-arene based solid lipid nanoparticles (SLNs): a detailed study of preparation and stability parameters. *International journal of pharmaceutics* 253(1), 23-38 (2003).
68. Mehnert W, Mäder K. Solid lipid nanoparticles: production, characterization and applications. *Advanced drug delivery reviews* 47(2), 165-196 (2001).
69. Yang SC, Zhu JB. Preparation and characterization of camptothecin solid lipid nanoparticles. *Drug development and industrial pharmacy* 28(3), 265-274 (2002).
70. Wong HL, Rauth AM, Bendayan R *et al*. A new polymer–lipid hybrid nanoparticle system increases cytotoxicity of doxorubicin against multidrug-resistant human breast cancer cells. *Pharmaceutical research* 23(7), 1574-1585 (2006).
71. Tan SJ, Kiatwuthinon P, Roh YH, Kahn JS, Luo D. Engineering nanocarriers for siRNA delivery. *Small* 7(7), 841-856 (2011).
72. Akinc A, Zumbuehl A, Goldberg M *et al*. A combinatorial library of lipid-like materials for delivery of RNAi therapeutics. *Nature biotechnology* 26(5), 561-569 (2008).
73. Goldberg M. Lipidoids: a combinatorial approach to siRNA delivery. In: *RNA Interference from Biology to Therapeutics*, (Ed.^(Eds).Springer 143-160 (2013).
74. Brock A, Krause S, Li H *et al*. Silencing HoxA1 by intraductal injection of siRNA lipidoid nanoparticles prevents mammary tumor progression in mice. *Science translational medicine* 6(217), 217ra212-217ra212 (2014).
75. Arleth L, Ashok B, Onyuksel H, Thiyagarajan P, Jacob J, Hjelm RP. Detailed structure of hairy mixed micelles formed by phosphatidylcholine and PEGylated phospholipids in aqueous media. *Langmuir* 21(8), 3279-3290 (2005).
76. Mu L, Elbayoumi T, Torchilin V. Mixed micelles made of poly (ethylene glycol)–phosphatidylethanolamine conjugate and d-α-tocopheryl polyethylene glycol 1000 succinate as pharmaceutical nanocarriers for camptothecin. *International journal of pharmaceutics* 306(1), 142-149 (2005).
77. Kim T-Y, Kim D-W, Chung J-Y *et al*. Phase I and pharmacokinetic study of Genexol-PM, a cremophor-free, polymeric micelle-formulated paclitaxel, in patients with advanced malignancies. *Clinical cancer research* 10(11), 3708-3716 (2004).
78. Hamaguchi T, Matsumura Y, Suzuki M *et al*. NK105, a paclitaxel-incorporating micellar nanoparticle formulation, can extend in vivo antitumour activity and reduce the neurotoxicity of paclitaxel. *British journal of cancer* 92(7), 1240-1246 (2005).
79. Gill KK, Kaddoumi A, Nazzal S. Mixed micelles of PEG 2000-DSPE and vitamin-E TPGS for concurrent delivery of paclitaxel and parthenolide: Enhanced chemosenstization and antitumor efficacy against non-small cell lung cancer (NSCLC) cell lines. *European journal of pharmaceutical sciences* 46(1), 64-71 (2012).
80. Uchegbu IF, Vyas SP. Non-ionic surfactant based vesicles (niosomes) in drug delivery. *International Journal of Pharmaceutics* 172(1), 33-70 (1998).
81. Marianecci C, Di Marzio L, Rinaldi F *et al*. Niosomes from 80s to present: the state of the art. *Advances in colloid and interface science* 205 187-206 (2014).

82. Paecharoenchai O, Niyomtham N, Leksantikul L *et al*. Nonionic surfactant vesicles composed of novel spermine-derivative cationic lipids as an effective gene carrier in vitro. *AAPS PharmSciTech* 15(3), 722-730 (2014).
83. Moghassemi S, Hadjizadeh A. Nano-niosomes as nanoscale drug delivery systems: an illustrated review. *Journal of Controlled Release* 185 22-36 (2014).
84. Kumar GP, Rajeshwarrao P. Nonionic surfactant vesicular systems for effective drug delivery—an overview. *Acta Pharmaceutica Sinica B* 1(4), 208-219 (2011).
85. Tavano L, Vivacqua M, Carito V, Muzzalupo R, Caroleo MC, Nicoletta F. Doxorubicin loaded magneto-niosomes for targeted drug delivery. *Colloids and Surfaces B: Biointerfaces* 102 803-807 (2013).
86. Pawar S, Vavia P. Glucosamine anchored cancer targeted nano-vesicular drug delivery system of doxorubicin. *Journal of drug targeting* 24(1), 68-79 (2016).
87. Vyas S, Singh R, Jain S *et al*. Non-ionic surfactant based vesicles (niosomes) for non-invasive topical genetic immunization against hepatitis B. *International journal of pharmaceutics* 296(1), 80-86 (2005).
88. El-Ridy MS, Abdelbary A, Essam T, Abd El-Salam RM, Aly Kassem AA. Niosomes as a potential drug delivery system for increasing the efficacy and safety of nystatin. *Drug Development and Industrial Pharmacy* 37(12), 1491-1508 (2011).
89. Zidan AS, Rahman Z, Khan MA. Product and process understanding of a novel pediatric anti-HIV tenofovir niosomes with a high-pressure homogenizer. *European Journal of Pharmaceutical Sciences* 44(1), 93-102 (2011).
90. Pardakhty A, Varshosaz J, Rouholamini A. In vitro study of polyoxyethylene alkyl ether niosomes for delivery of insulin. *International journal of pharmaceutics* 328(2), 130-141 (2007).
91. Balakrishnan P, Shanmugam S, Lee WS *et al*. Formulation and in vitro assessment of minoxidil niosomes for enhanced skin delivery. *International journal of pharmaceutics* 377(1), 1-8 (2009).
92. Luciani A, Olivier J-C, Clement O *et al*. Glucose-Receptor MR Imaging of Tumors: Study in Mice with PEGylated Paramagnetic Niosomes 1. *Radiology* 231(1), 135-142 (2004).
93. Tavano L, Muzzalupo R, Mauro L, Pellegrino M, Andò S, Picci N. Transferrin-conjugated pluronic niosomes as a new drug delivery system for anticancer therapy. *Langmuir* 29(41), 12638-12646 (2013).
94. Hong M, Zhu S, Jiang Y, Tang G, Pei Y. Efficient tumor targeting of hydroxycamptothecin loaded PEGylated niosomes modified with transferrin. *Journal of Controlled Release* 133(2), 96-102 (2009).
95. Paolino D, Cosco D, Muzzalupo R, Trapasso E, Picci N, Fresta M. Innovative bola-surfactant niosomes as topical delivery systems of 5-fluorouracil for the treatment of skin cancer. *International journal of pharmaceutics* 353(1), 233-242 (2008).
96. Mozafari MR. Liposomes: an overview of manufacturing techniques. *Cellular and Molecular Biology Letters* 10(4), 711 (2005).
97. Bangham A, Standish MM, Watkins J. Diffusion of univalent ions across the lamellae of swollen phospholipids. *Journal of molecular biology* 13(1), 238-IN227 (1965).
98. Kohli AG, Kierstead PH, Venditto VJ, Walsh CL, Szoka FC. Designer lipids for drug delivery: From heads to tails. *Journal of Controlled Release* (2014).
99. Ranade VV, Cannon JB. *Drug delivery systems*. CRC press, (2011).
100. Szoka F, Papahadjopoulos D. Procedure for preparation of liposomes with large internal aqueous space and high capture by reverse-phase evaporation. *Proceedings of the National Academy of Sciences* 75(9), 4194-4198 (1978).
101. Lasic DD. Mechanisms of liposome formation. *Journal of Liposome Research* 5(3), 431-441 (1995).

102. Deamer D, Bangham A. Large volume liposomes by an ether vaporization method. *Biochimica et Biophysica Acta (BBA)-Nucleic Acids and Protein Synthesis* 443(3), 629-634 (1976).
103. Torchilin V, Weissig V. *Liposomes: a practical approach*. Oxford University Press, (2003).
104. Mozafari M, Reed C, Rostron C, Martin D. Transfection of human airway epithelial cells using a lipid-based vector prepared by the heating method. *J. Aerosol Med* 17 100 (2004).
105. Kikuchi H, Yamauchi H, Hirota S. A Spray-Drying Method for Mass Production of Liposomes. *Chemical and pharmaceutical bulletin* 39(6), 1522-1527 (1991).
106. Patil YP, Jadhav S. Novel methods for liposome preparation. *Chemistry and physics of lipids* 177 8-18 (2014).
107. Frederiksen L, Anton K, Hoogevest PV, Keller HR, Leuenberger H. Preparation of liposomes encapsulating water-soluble compounds using supercritical carbon dioxide. *Journal of pharmaceutical sciences* 86(8), 921-928 (1997).
108. Akbarzadeh A, Rezaei-Sadabady R, Davaran S *et al*. Liposome: classification, preparation, and applications. *Nanoscale Res Lett* 8(1), 102 (2013).
109. Kraft JC, Freeling JP, Wang Z, Ho RJ. Emerging research and clinical development trends of liposome and lipid nanoparticle drug delivery systems. *Journal of pharmaceutical sciences* 103(1), 29-52 (2014).
110. Wagner A, Vorauer-Uhl K, Kreismayr G, Katinger H. The crossflow injection technique: an improvement of the ethanol injection method. *Journal of Liposome Research* 12(3), 259-270 (2002).
111. Pradhan P, Guan J, Lu D, Wang PG, Lee LJ, Lee RJ. A facile microfluidic method for production of liposomes. *Anticancer research* 28(2A), 943-947 (2008).
112. Whitesides GM. The origins and the future of microfluidics. *Nature* 442(7101), 368-373 (2006).
113. Jahn A, Vreeland WN, Gaitan M, Locascio LE. Controlled vesicle self-assembly in microfluidic channels with hydrodynamic focusing. *Journal of the American Chemical Society* 126(9), 2674-2675 (2004).
114. Kurakazu T, Takeuchi S. Generation of lipid vesicles using microfluidic T-junctions with pneumatic valves. Presented at: *Micro Electro Mechanical Systems (MEMS), 2010 IEEE 23rd International Conference on*. 2010.
115. Teh S-Y, Lin R, Hung L-H, Lee AP. Droplet microfluidics. *Lab on a Chip* 8(2), 198-220 (2008).
116. Stroock AD, Dertinger SK, Ajdari A, Mezić I, Stone HA, Whitesides GM. Chaotic mixer for microchannels. *Science* 295(5555), 647-651 (2002).
117. Kastner E, Kaur R, Lowry D, Moghaddam B, Wilkinson A, Perrie Y. High-throughput manufacturing of size-tuned liposomes by a new microfluidics method using enhanced statistical tools for characterization. *International journal of pharmaceutics* 477(1), 361-368 (2014).
118. Obeid MA, Khadra I, Mullen AB, Tate RJ, Ferro VA. The effects of hydration media on the characteristics of non-ionic surfactant vesicles (NISV) prepared by microfluidics. *International Journal of Pharmaceutics* (2016).
119. Laouini A, Jaafar-Maalej C, Gandoura-Sfar S, Charcosset C, Fessi H. Spironolactone-loaded liposomes produced using a membrane contactor method: an improvement of the ethanol injection technique. In: *UK Colloids 2011*, (Ed.^(Eds).Springer 23-28 (2012).
120. Jaafar-Maalej C, Charcosset C, Fessi H. A new method for liposome preparation using a membrane contactor. *Journal of liposome research* 21(3), 213-220 (2011).
121. Letchford K, Burt H. A review of the formation and classification of amphiphilic block copolymer nanoparticulate structures: micelles, nanospheres, nanocapsules and polymersomes. *European journal of pharmaceutics and biopharmaceutics* 65(3), 259-269 (2007).

122. Lin P-C, Lin S, Wang PC, Sridhar R. Techniques for physicochemical characterization of nanomaterials. *Biotechnology advances* (2013).
123. Ferrari M. Nanogeometry: beyond drug delivery. *Nature Nanotechnology* 3(3), 131-132 (2008).
124. Brar SK, Verma M. Measurement of nanoparticles by light-scattering techniques. *TrAC Trends in Analytical Chemistry* 30(1), 4-17 (2011).
125. Lim J, Yeap SP, Che HX, Low SC. Characterization of magnetic nanoparticle by dynamic light scattering. *Nanoscale research letters* 8(1), 1-14 (2013).
126. Uskoković V. Dynamic light scattering based microelectrophoresis: main prospects and limitations. *Journal of dispersion science and technology* 33(12), 1762-1786 (2012).
127. Parot P, Dufrêne YF, Hinterdorfer P *et al*. Past, present and future of atomic force microscopy in life sciences and medicine. *Journal of Molecular Recognition* 20(6), 418-431 (2007).
128. Koçum C, Çimen EK, Pişkin E. Imaging of poly (NIPA-co-MAH)–HIgG conjugate with scanning tunneling microscopy. *Journal of Biomaterials Science, Polymer Edition* 15(12), 1513-1520 (2004).
129. Wang ZL. Transmission electron microscopy and spectroscopy of nanoparticles. 1 37-80 (2000).
130. Decuzzi P, Pasqualini R, Arap W, Ferrari M. Intravascular delivery of particulate systems: does geometry really matter? *Pharmaceutical research* 26(1), 235-243 (2009).
131. Mitragotri S. In drug delivery, shape does matter. *Pharmaceutical research* 26(1), 232-234 (2009).
132. Powers KW, Palazuelos M, Brown SC, Roberts SM. Characterization of nanomaterials for toxicological evaluation. *Nanotoxicology From In Vivo and In Vitro Models to Health Risks.(S. Sahu and D. Casciano, Eds.)* 1-27 (2009).
133. Andar AU, Hood RR, Vreeland WN, Devoe DL, Swaan PW. Microfluidic Preparation of Liposomes to Determine Particle Size Influence on Cellular Uptake Mechanisms. *Pharmaceutical research* 31(2), 401-413 (2014).
134. Luyts K, Napierska D, Nemery B, Hoet PH. How physico-chemical characteristics of nanoparticles cause their toxicity: complex and unresolved interrelations. *Environmental Science: Processes & Impacts* 15(1), 23-38 (2013).
135. Fröhlich M, Brecht V, Peschka-Süss R. Parameters influencing the determination of liposome lamellarity by 31 P-NMR. *Chemistry and physics of lipids* 109(1), 103-112 (2001).
136. Müller M, Mackeben S, Müller-Goymann CC. Physicochemical characterisation of liposomes with encapsulated local anaesthetics. *International journal of pharmaceutics* 274(1), 139-148 (2004).
137. Briscoe CJ, Hage DS. Factors affecting the stability of drugs and drug metabolites in biological matrices. (2009).
138. Celia C, Trapasso E, Cosco D, Paolino D, Fresta M. Turbiscan Lab® Expert analysis of the stability of ethosomes® and ultradeformable liposomes containing a bilayer fluidizing agent. *Colloids and Surfaces B: Biointerfaces* 72(1), 155-160 (2009).
139. Berger N, Sachse A, Bender J, Schubert R, Brandl M. Filter extrusion of liposomes using different devices: comparison of liposome size, encapsulation efficiency, and process characteristics. *International journal of pharmaceutics* 223(1), 55-68 (2001).
140. Laouini A, Jaafar-Maalej C, Sfar S, Charcosset C, Fessi H. Liposome preparation using a hollow fiber membrane contactor—Application to spironolactone encapsulation. *International journal of pharmaceutics* 415(1), 53-61 (2011).
141. Charrois GJ, Allen TM. Drug release rate influences the pharmacokinetics, biodistribution, therapeutic activity, and toxicity of pegylated liposomal doxorubicin formulations in murine breast cancer. *Biochimica et Biophysica Acta (BBA)-Biomembranes* 1663(1), 167-177 (2004).

142. Desai N. Challenges in development of nanoparticle-based therapeutics. *The AAPS journal* 14(2), 282-295 (2012).
143. Von Roemeling C, Jiang W, Chan CK, Weissman IL, Kim BY. Breaking Down the Barriers to Precision Cancer Nanomedicine. *Trends in Biotechnology* (2016).
144. Walkey CD, Olsen JB, Guo H, Emili A, Chan WC. Nanoparticle size and surface chemistry determine serum protein adsorption and macrophage uptake. *Journal of the American Chemical Society* 134(4), 2139-2147 (2012).
145. He C, Hu Y, Yin L, Tang C, Yin C. Effects of particle size and surface charge on cellular uptake and biodistribution of polymeric nanoparticles. *Biomaterials* 31(13), 3657-3666 (2010).
146. Hatakeyama H, Akita H, Harashima H. The polyethyleneglycol dilemma: advantage and disadvantage of PEGylation of liposomes for systemic genes and nucleic acids delivery to tumors. *Biological and Pharmaceutical Bulletin* 36(6), 892-899 (2013).
147. Dams ET, Laverman P, Oyen WJ *et al*. Accelerated blood clearance and altered biodistribution of repeated injections of sterically stabilized liposomes. *Journal of Pharmacology and Experimental Therapeutics* 292(3), 1071-1079 (2000).
148. Shiraishi K, Kawano K, Maitani Y *et al*. Exploring the relationship between anti-PEG IgM behaviors and PEGylated nanoparticles and its significance for accelerated blood clearance. *Journal of Controlled Release* 234 59-67 (2016).
149. Lila ASA, Kiwada H, Ishida T. The accelerated blood clearance (ABC) phenomenon: clinical challenge and approaches to manage. *Journal of Controlled Release* 172(1), 38-47 (2013).
150. Judge AD, Bola G, Lee AC, Maclachlan I. Design of noninflammatory synthetic siRNA mediating potent gene silencing in vivo. *Molecular Therapy* 13(3), 494-505 (2006).
151. Xu H, Wang KQ, Deng YH, Chen DW. Effects of cleavable PEG-cholesterol derivatives on the accelerated blood clearance of PEGylated liposomes. *Biomaterials* 31(17), 4757-4763 (2010).
152. Judge A, Mcclintock K, Phelps JR, Maclachlan I. Hypersensitivity and loss of disease site targeting caused by antibody responses to PEGylated liposomes. *Molecular Therapy* 13(2), 328-337 (2006).
153. Tagami T, Nakamura K, Shimizu T, Ishida T, Kiwada H. Effect of siRNA in PEG-coated siRNA-lipoplex on anti-PEG IgM production. *Journal of Controlled Release* 137(3), 234-240 (2009).
154. Tagami T, Nakamura K, Shimizu T, Yamazaki N, Ishida T, Kiwada H. CpG motifs in pDNA-sequences increase anti-PEG IgM production induced by PEG-coated pDNA-lipoplexes. *Journal of Controlled Release* 142(2), 160-166 (2010).
155. Owens DE, Peppas NA. Opsonization, biodistribution, and pharmacokinetics of polymeric nanoparticles. *International journal of pharmaceutics* 307(1), 93-102 (2006).
156. Kohli AG, Kierstead PH, Venditto VJ, Walsh CL, Szoka FC. Designer lipids for drug delivery: From heads to tails. *Journal of Controlled Release* 190 274-287 (2014).
157. Koide H, Asai T, Hatanaka K *et al*. Particle size-dependent triggering of accelerated blood clearance phenomenon. *International journal of pharmaceutics* 362(1), 197-200 (2008).
158. Fubini B, Ghiazza M, Fenoglio I. Physico-chemical features of engineered nanoparticles relevant to their toxicity. *Nanotoxicology* 4(4), 347-363 (2010).
159. Wicki A, Witzigmann D, Balasubramanian V, Huwyler J. Nanomedicine in cancer therapy: challenges, opportunities, and clinical applications. *Journal of Controlled Release* 200 138-157 (2015).
160. Lewinski N, Colvin V, Drezek R. Cytotoxicity of nanoparticles. *small* 4(1), 26-49 (2008).
161. Szebeni J, Muggia F, Gabizon A, Barenholz Y. Activation of complement by therapeutic liposomes and other lipid excipient-based therapeutic products: prediction and prevention. *Advanced drug delivery reviews* 63(12), 1020-1030 (2011).
162. Mayer A, Vadon M, Rinner B, Novak A, Wintersteiger R, Fröhlich E. The role of nanoparticle size in hemocompatibility. *Toxicology* 258(2), 139-147 (2009).
163. Zamboni WC, Torchilin V, Patri AK *et al*. Best practices in cancer nanotechnology: perspective from NCI nanotechnology alliance. *Clinical cancer research* 18(12), 3229-3241 (2012).

164. Fda. Considering Whether an FDA-Regulated Product Involves the Application of Nanotechnology. (2014).
165. Danhier F, Feron O, Préat V. To exploit the tumor microenvironment: passive and active tumor targeting of nanocarriers for anti-cancer drug delivery. *Journal of Controlled Release* 148(2), 135-146 (2010).
166. Kobayashi T, Ishida T, Okada Y, Ise S, Harashima H, Kiwada H. Effect of transferrin receptor-targeted liposomal doxorubicin in P-glycoprotein-mediated drug resistant tumor cells. *International journal of pharmaceutics* 329(1), 94-102 (2007).
167. Yang G, Yang T, Zhang W, Lu M, Ma X, Xiang G. In vitro and in vivo antitumor effects of folate-targeted ursolic acid stealth liposome. *Journal of agricultural and food chemistry* 62(10), 2207-2215 (2014).
168. Sato A, Takagi M, Shimamoto A, Kawakami S, Hashida M. Small interfering RNA delivery to the liver by intravenous administration of galactosylated cationic liposomes in mice. *Biomaterials* 28(7), 1434-1442 (2007).
169. Pirollo KF, Zon G, Rait A *et al*. Tumor-targeting nanoimmunoliposome complex for short interfering RNA delivery. *Human gene therapy* 17(1), 117-124 (2006).
170. Fire A, Xu S, Montgomery MK, Kostas SA, Driver SE, Mello CC. Potent and specific genetic interference by double-stranded RNA in Caenorhabditis elegans. *nature* 391(6669), 806-811 (1998).
171. Elbashir SM, Harborth J, Lendeckel W, Yalcin A, Weber K, Tuschl T. Duplexes of 21-nucleotide RNAs mediate RNA interference in cultured mammalian cells. *nature* 411(6836), 494-498 (2001).
172. Mccaffrey AP, Meuse L, Pham T-TT, Conklin DS, Hannon GJ, Kay MA. Gene expression: RNA interference in adult mice. *Nature* 418(6893), 38-39 (2002).
173. Miele E, Spinelli GP, Miele E *et al*. Nanoparticle-based delivery of small interfering RNA: challenges for cancer therapy. *Int J Nanomedicine* 7 3637-3657 (2012).
174. Hammond SM. Dicing and slicing. *FEBS letters* 579(26), 5822-5829 (2005).
175. Ameres SL, Martinez J, Schroeder R. Molecular basis for target RNA recognition and cleavage by human RISC. *Cell* 130(1), 101-112 (2007).
176. Matranga C, Tomari Y, Shin C, Bartel DP, Zamore PD. Passenger-strand cleavage facilitates assembly of siRNA into Ago2-containing RNAi enzyme complexes. *Cell* 123(4), 607-620 (2005).
177. Dykxhoorn DM, Lieberman J. Knocking down disease with siRNAs. *Cell* 126(2), 231-235 (2006).
178. David S, Pitard B, Benoît J-P, Passirani C. Non-viral nanosystems for systemic siRNA delivery. *Pharmacological research* 62(2), 100-114 (2010).
179. Resnier P, Montier T, Mathieu V, Benoit J-P, Passirani C. A review of the current status of siRNA nanomedicines in the treatment of cancer. *Biomaterials* 34(27), 6429-6443 (2013).
180. Kao S-C, Krichevsky AM, Kosik KS, Tsai L-H. BACE1 suppression by RNA interference in primary cortical neurons. *Journal of Biological Chemistry* 279(3), 1942-1949 (2004).
181. Kuphal S, Wallner S, Bosserhoff AK. Impact of LIF (leukemia inhibitory factor) expression in malignant melanoma. *Experimental and molecular pathology* 95(2), 156-165 (2013).
182. Taratula O, Kuzmov A, Shah M, Garbuzenko OB, Minko T. Nanostructured lipid carriers as multifunctional nanomedicine platform for pulmonary co-delivery of anticancer drugs and siRNA. *Journal of Controlled Release* 171(3), 349-357 (2013).
183. Lee S, Yoon CY, Byun S-S, Lee E, Lee SE. The role of c-FLIP in cisplatin resistance of human bladder cancer cells. *The Journal of urology* 189(6), 2327-2334 (2013).
184. Zheng Y, Wang Z, Bie W *et al*. PTK6 activation at the membrane regulates epithelial–mesenchymal transition in prostate cancer. *Cancer research* 73(17), 5426-5437 (2013).
185. Goldberg MS. siRNA Delivery for the treatment of ovarian cancer. *Methods* 63(2), 95-100 (2013).

186. Morrissey DV, Blanchard K, Shaw L *et al*. Activity of stabilized short interfering RNA in a mouse model of hepatitis B virus replication. *Hepatology* 41(6), 1349-1356 (2005).
187. Zimmermann TS, Lee AC, Akinc A *et al*. RNAi-mediated gene silencing in non-human primates. *Nature* 441(7089), 111-114 (2006).
188. Dykxhoorn D, Palliser D, Lieberman J. The silent treatment: siRNAs as small molecule drugs. *Gene therapy* 13(6), 541-552 (2006).
189. Soutschek J, Akinc A, Bramlage B *et al*. Therapeutic silencing of an endogenous gene by systemic administration of modified siRNAs. *Nature* 432(7014), 173-178 (2004).
190. Kim WJ, Kim SW. Efficient siRNA delivery with non-viral polymeric vehicles. *Pharmaceutical research* 26(3), 657-666 (2009).
191. Tagami T, Suzuki T, Matsunaga M *et al*. Anti-angiogenic therapy via cationic liposome-mediated systemic siRNA delivery. *International journal of pharmaceutics* 422(1), 280-289 (2012).
192. Gao J, Sun J, Li H *et al*. Lyophilized HER2-specific PEGylated immunoliposomes for active siRNA gene silencing. *Biomaterials* 31(9), 2655-2664 (2010).
193. Christensen J, Litherland K, Faller T *et al*. Biodistribution and Metabolism Studies of Lipid Nanoparticle–Formulated Internally [3H]-Labeled siRNA in Mice. *Drug Metabolism and Disposition* 42(3), 431-440 (2014).
194. Zuckerman JE, Davis ME. Clinical experiences with systemically administered siRNA-based therapeutics in cancer. *Nature Reviews Drug Discovery* 14(12), 843-856 (2015).
195. Bobbin ML, Rossi JJ. RNA interference (RNAi)-based therapeutics: delivering on the promise? *Annual review of pharmacology and toxicology* 56 103-122 (2016).
196. Http://Www.Apeiron-Biologics.Com/Index.Php/Projects/Apn401-Cbl-B.Html ABaC-B. 2014.
197. Http://Arbutusbio.Com/Portfolio/Tkm-Plk1.Php AT-P.
198. Https://Www.Genomeweb.Com/Rnai/Md-Anderson-Team-Preps-Phase-I-Testing-Rnai-Cancer-Dru MDMaTPFPITORCDGW.
199. Dicerna. 2015. Dicerna Pharmaceuticals Announces First Patient Dosed in Phase 1b/2 Clinical Trial of Dcr-Myc AIRTTTMO, In Patients with Advanced Hepatocellular Carcinoma. News Release, Febr. 2. Http://Investors.Dicerna.Com/Releasedetail.Cfm?Releaseid=893991.
200. Barata P, Sood AK, Hong DS. RNA-targeted therapeutics in cancer clinical trials: Current status and future directions. *Cancer Treatment Reviews* 50 35-47 (2016).
201. Handjani-Vila R, Ribier A, Rondot B, Vanlerberghie G. Dispersions of lamellar phases of non-ionic lipids in cosmetic products. *International journal of cosmetic Science* 1(5), 303-314 (1979).
202. Attia IA, El-Gizawy SA, Fouda MA, Donia AM. Influence of a niosomal formulation on the oral bioavailability of acyclovir in rabbits. *AAPS PharmSciTech* 8(4), 206-212 (2007).
203. Jadon PS, Gajbhiye V, Jadon RS, Gajbhiye KR, Ganesh N. Enhanced oral bioavailability of griseofulvin via niosomes. *AAPS PharmSciTech* 10(4), 1186-1192 (2009).
204. Arunothayanun P, Bernard M-S, Craig D, Uchegbu I, Florence A. The effect of processing variables on the physical characteristics of non-ionic surfactant vesicles (niosomes) formed from a hexadecyl diglycerol ether. *International journal of pharmaceutics* 201(1), 7-14 (2000).
205. Sahin NO. Niosomes as nanocarrier systems. In: *Nanomaterials and nanosystems for biomedical applications*, (Ed.^(Eds).Springer 67-81 (2007).
206. Mozafari M. Method and apparatus for producing carrier complexes. *UK Patent No. GB 0404993.8, Int. Appl. No. PCT/GB05/000825 (03/03/2005)* 14 (2005).
207. Mozafari MR, Reed CJ, Rostron C, Kocum C, Piskin E. Construction of stable anionic liposome-plasmid particles using the heating method: a preliminary investigation. *Cellular and Molecular Biology Letters* 7(3), 923-928 (2002).
208. Lo CT, Jahn A, Locascio LE, Vreeland WN. Controlled self-assembly of monodisperse niosomes by microfluidic hydrodynamic focusing. *Langmuir* 26(11), 8559-8566 (2010).

209. Belliveau NM, Huft J, Lin PJ *et al*. Microfluidic synthesis of highly potent limit-size lipid nanoparticles for in vivo delivery of siRNA. *Molecular Therapy—Nucleic Acids* 1(8), e37 (2012).
210. Carugo D, Bottaro E, Owen J, Stride E, Nastruzzi C. Liposome production by microfluidics: potential and limiting factors. *Scientific reports* 6 (2016).
211. Gebril AM, Lamprou DA, Alsaadi MM, Stimson WH, Mullen AB, Ferro VA. Assessment of the antigen-specific antibody response induced by mucosal administration of a GnRH conjugate entrapped in lipid nanoparticles. *Nanomedicine: Nanotechnology, Biology and Medicine* 10(5), 971-979 (2014).
212. Mann JF, Scales HE, Shakir E *et al*. Oral delivery of tetanus toxoid using vesicles containing bile salts (bilosomes) induces significant systemic and mucosal immunity. *Methods* 38(2), 90-95 (2006).
213. Abdelkader H, Alani AW, Alany RG. Recent advances in non-ionic surfactant vesicles (niosomes): self-assembly, fabrication, characterization, drug delivery applications and limitations. *Drug delivery* 21(2), 87-100 (2014).
214. Https://Www.Precisionnanosystems.Com/Systems/Scale-up/ P.
215. Heurtault B, Saulnier P, Pech B, Proust J-E, Benoit J-P. Physico-chemical stability of colloidal lipid particles. *Biomaterials* 24(23), 4283-4300 (2003).
216. Freitas C, Müller RH. Effect of light and temperature on zeta potential and physical stability in solid lipid nanoparticle (SLN™) dispersions. *International journal of pharmaceutics* 168(2), 221-229 (1998).
217. Freitas C, Müller R. Correlation between long-term stability of solid lipid nanoparticles (SLN™) and crystallinity of the lipid phase. *European Journal of Pharmaceutics and Biopharmaceutics* 47(2), 125-132 (1999).
218. Hood RR, Devoe DL. High-Throughput Continuous Flow Production of Nanoscale Liposomes by Microfluidic Vertical Flow Focusing. *small* 11(43), 5790-5799 (2015).
219. Bottaro E, Nastruzzi C. "Off-the-shelf" microfluidic devices for the production of liposomes for drug delivery. *Materials Science and Engineering: C* 64 29-33 (2016).
220. Jahn A, Vreeland WN, Devoe DL, Locascio LE, Gaitan M. Microfluidic directed formation of liposomes of controlled size. *Langmuir* 23(11), 6289-6293 (2007).
221. Yu B, Lee RJ, Lee LJ. Microfluidic methods for production of liposomes. *Methods in enzymology* 465 129-141 (2009).
222. Morris MC, Depollier J, Mery J, Heitz F, Divita G. A peptide carrier for the delivery of biologically active proteins into mammalian cells. *Nature biotechnology* 19(12), 1173-1176 (2001).
223. Dulbecco R, Vogt M. Plaque formation and isolation of pure lines with poliomyelitis viruses. *The Journal of experimental medicine* 99(2), 167-182 (1954).
224. Mozafari M. Nanoliposomes: preparation and analysis. *Liposomes: Methods and Protocols, Volume 1: Pharmaceutical Nanocarriers* 29-50 (2010).
225. Dua J, Rana A, Bhandari A. Liposome: methods of preparation and applications. *Int J Pharm Stud Res* 3 14-20 (2012).
226. Mohan C. Buffers. (2003).
227. Stoll VS, Blanchard JS. Buffers: Principles and Practice1. (1990).
228. Oh H, Shin T, Chang E. Determination of cholesterol in milk and dairy products by high-performance liquid chromatography. *Asian-Australasian Journal of Animal Sciences* 14(10), 1465-1469 (2001).
229. Zhang Y, Anchordoquy TJ. The role of lipid charge density in the serum stability of cationic lipid/DNA complexes. *Biochimica et Biophysica Acta (BBA)-Biomembranes* 1663(1), 143-157 (2004).
230. Claessens M, Van Oort B, Leermakers F, Hoekstra F, Stuart MC. Charged lipid vesicles: effects of salts on bending rigidity, stability, and size. *Biophysical journal* 87(6), 3882-3893 (2004).

231. Buyens K, De Smedt SC, Braeckmans K *et al*. Liposome based systems for systemic siRNA delivery: stability in blood sets the requirements for optimal carrier design. *Journal of controlled release* 158(3), 362-370 (2012).
232. Wang H, Zhao P, Liang X *et al*. Folate-PEG coated cationic modified chitosan–cholesterol liposomes for tumor-targeted drug delivery. *Biomaterials* 31(14), 4129-4138 (2010).
233. Lu Q, Lu P-M, Piao J-H *et al*. Preparation and physicochemical characteristics of an allicin nanoliposome and its release behavior. *LWT-Food Science and Technology* 57(2), 686-695 (2014).
234. Sou K. Electrostatics of carboxylated anionic vesicles for improving entrapment capacity. *Chemistry and physics of lipids* 164(3), 211-215 (2011).
235. Wu L, Zhang J, Watanabe W. Physical and chemical stability of drug nanoparticles. *Advanced drug delivery reviews* 63(6), 456-469 (2011).
236. Collado-Fernandez M, Gonzalez-Sanjosé M, Pino-Navarro R. Evaluation of turbidity: correlation between Kerstez turbidimeter and nephelometric turbidimeter. *Food chemistry* 71(4), 563-566 (2000).
237. Cui H, Zhao C, Lin L. The specific antibacterial activity of liposome-encapsulated Clove oil and its application in tofu. *Food Control* 56 128-134 (2015).
238. Gratton SE, Ropp PA, Pohlhaus PD *et al*. The effect of particle design on cellular internalization pathways. *Proceedings of the National Academy of Sciences* 105(33), 11613-11618 (2008).
239. Nel AE, Mädler L, Velegol D *et al*. Understanding biophysicochemical interactions at the nano–bio interface. *Nature materials* 8(7), 543-557 (2009).
240. Li S-D, Huang L-Y. Nonviral gene therapy: promises and challenges. *Gene therapy* 7(1), 31 (2000).
241. Manosroi A, Thathang K, Werner R, Schubert R, Manosroi J. Stability of luciferase plasmid entrapped in cationic bilayer vesicles. *International journal of pharmaceutics* 356(1), 291-299 (2008).
242. Perrie Y, Barralet J, Mcneil S, Vangala A. Surfactant vesicle-mediated delivery of DNA vaccines via the subcutaneous route. *International journal of pharmaceutics* 284(1), 31-41 (2004).
243. Paecharoenchai O, Teng L, Yung BC, Teng L, Opanasopit P, Lee RJ. Nonionic surfactant vesicles for delivery of RNAi therapeutics. *Nanomedicine* 8(11), 1865-1873 (2013).
244. Zhou C, Mao Y, Sugimoto Y *et al*. SPANosomes as delivery vehicles for small interfering RNA (siRNA). *Molecular pharmaceutics* 9(2), 201-210 (2011).
245. Bustin SA, Benes V, Garson JA *et al*. The MIQE guidelines: minimum information for publication of quantitative real-time PCR experiments. *Clinical chemistry* 55(4), 611-622 (2009).
246. Bustin SA, Beaulieu J-F, Huggett J *et al*. MIQE precis: Practical implementation of minimum standard guidelines for fluorescence-based quantitative real-time PCR experiments. *BMC molecular biology* 11(1), 74 (2010).
247. Huggett J, Dheda K, Bustin S, Zumla A. Real-time RT-PCR normalisation; strategies and considerations. *Genes and immunity* 6(4), 279-284 (2005).
248. Lee PD, Sladek R, Greenwood CM, Hudson TJ. Control genes and variability: absence of ubiquitous reference transcripts in diverse mammalian expression studies. *Genome Research* 12(2), 292-297 (2002).
249. Thellin O, Zorzi W, Lakaye B *et al*. Housekeeping genes as internal standards: use and limits. *Journal of biotechnology* 75(2), 291-295 (1999).
250. Ye J, Coulouris G, Zaretskaya I, Cutcutache I, Rozen S, Madden TL. Primer-BLAST: a tool to design target-specific primers for polymerase chain reaction. *BMC bioinformatics* 13(1), 1 (2012).

251. Deprez RHL, Fijnvandraat AC, Ruijter JM, Moorman AF. Sensitivity and accuracy of quantitative real-time polymerase chain reaction using SYBR green I depends on cDNA synthesis conditions. *Analytical biochemistry* 307(1), 63-69 (2002).
252. Wittwer CT, Herrmann MG, Moss AA, Rasmussen RP. Continuous fluorescence monitoring of rapid cycle DNA amplification. *Biotechniques* 22(1), 130-139 (1997).
253. Ririe KM, Rasmussen RP, Wittwer CT. Product differentiation by analysis of DNA melting curves during the polymerase chain reaction. *Analytical biochemistry* 245(2), 154-160 (1997).
254. Livak KJ, Schmittgen TD. Analysis of relative gene expression data using real-time quantitative PCR and the 2− ΔΔCT method. *methods* 25(4), 402-408 (2001).
255. Haimes J, Kelley M. Demonstration of a ΔΔ C q Calculation Method to Compute Relative Gene Expression from qPCR Data. *Thermo Scientific Tech Note* 1-4 (2010).
256. Gref R, Lück M, Quellec P *et al*. 'Stealth'corona-core nanoparticles surface modified by polyethylene glycol (PEG): influences of the corona (PEG chain length and surface density) and of the core composition on phagocytic uptake and plasma protein adsorption. *Colloids and Surfaces B: Biointerfaces* 18(3), 301-313 (2000).
257. Huang Y-Z, Gao J-Q, Chen J-L, Liang W-Q. Cationic liposomes modified with non-ionic surfactants as effective non-viral carrier for gene transfer. *Colloids and Surfaces B: Biointerfaces* 49(2), 158-164 (2006).
258. Obeid MA, Gebril AM, Tate RJ, Mullen AB, Ferroa VA. Comparison of the physical characteristics of monodisperse non-ionic surfactant vesicles (NISV) prepared using different manufacturing methods. *International Journal of Pharmaceutics* (2017).
259. Wu SY, Mcmillan NA. Lipidic systems for in vivo siRNA delivery. *The AAPS journal* 11(4), 639-652 (2009).
260. Rejman J, Oberle V, Zuhorn IS, Hoekstra D. Size-dependent internalization of particles via the pathways of clathrin-and caveolae-mediated endocytosis. *Biochemical Journal* 377(1), 159-169 (2004).
261. Xiang S, Tong H, Shi Q *et al*. Uptake mechanisms of non-viral gene delivery. *Journal of controlled release* 158(3), 371-378 (2012).
262. Caracciolo G, Amenitsch H. Cationic liposome/DNA complexes: from structure to interactions with cellular membranes. *European Biophysics Journal* 41(10), 815-829 (2012).
263. Amin ZR, Rahimizadeh M, Eshghi H, Dehshahri A, Ramezani M. The effect of cationic charge density change on transfection efficiency of polyethylenimine. *Iranian journal of basic medical sciences* 16(2), 150 (2013).
264. Fröhlich E. The role of surface charge in cellular uptake and cytotoxicity of medical nanoparticles. *Int J Nanomedicine* 7(1), 5577-5591 (2012).
265. Chithrani BD, Chan WC. Elucidating the mechanism of cellular uptake and removal of protein-coated gold nanoparticles of different sizes and shapes. *Nano letters* 7(6), 1542-1550 (2007).
266. Lu F, Wu SH, Hung Y, Mou CY. Size effect on cell uptake in well-suspended, uniform mesoporous silica nanoparticles. *Small* 5(12), 1408-1413 (2009).
267. Ge Y, Zhang Y, Xia J *et al*. Effect of surface charge and agglomerate degree of magnetic iron oxide nanoparticles on KB cellular uptake in vitro. *Colloids and Surfaces B: Biointerfaces* 73(2), 294-301 (2009).
268. Varkouhi AK, Scholte M, Storm G, Haisma HJ. Endosomal escape pathways for delivery of biologicals. *Journal of Controlled Release* 151(3), 220-228 (2011).
269. Tsien RY. The green fluorescent protein. *Annual review of biochemistry* 67(1), 509-544 (1998).
270. Davies D. Cell sorting by flow cytometry. In: *Flow Cytometry*, (Ed.^(Eds).Springer 257-276 (2007).

271. Zhu L, Perche F, Wang T, Torchilin VP. Matrix metalloproteinase 2-sensitive multifunctional polymeric micelles for tumor-specific co-delivery of siRNA and hydrophobic drugs. *Biomaterials* 35(13), 4213-4222 (2014).
272. Conti DS, Brewer D, Grashik J, Avasarala S, Da Rocha SR. Poly (amidoamine) dendrimer nanocarriers and their aerosol formulations for siRNA delivery to the lung epithelium. *Molecular pharmaceutics* 11(6), 1808-1822 (2014).
273. Chung H, Kim TW, Kwon M, Kwon IC, Jeong SY. Oil components modulate physical characteristics and function of the natural oil emulsions as drug or gene delivery system. *Journal of Controlled Release* 71(3), 339-350 (2001).
274. Ojeda E, Puras G, Agirre M *et al*. The role of helper lipids in the intracellular disposition and transfection efficiency of niosome formulations for gene delivery to retinal pigment epithelial cells. *International journal of pharmaceutics* 503(1), 115-126 (2016).
275. Pozzi D, Marchini C, Cardarelli F *et al*. Mechanistic evaluation of the transfection barriers involved in lipid-mediated gene delivery: interplay between nanostructure and composition. *Biochimica et Biophysica Acta (BBA)-Biomembranes* 1838(3), 957-967 (2014).
276. Huang Y, Rao Y, Chen J, Yang VC, Liang W. Polysorbate cationic synthetic vesicle for gene delivery. *Journal of Biomedical Materials Research Part A* 96(3), 513-519 (2011).
277. Liu F, Yang J, Huang L, Liu D. New cationic lipid formulations for gene transfer. *Pharmaceutical research* 13(12), 1856-1860 (1996).
278. Koltover I, Salditt T, Rädler JO, Safinya CR. An inverted hexagonal phase of cationic liposome-DNA complexes related to DNA release and delivery. *Science* 281(5373), 78-81 (1998).
279. Ghildiyal M, Zamore PD. Small silencing RNAs: an expanding universe. *Nature Reviews Genetics* 10(2), 94-108 (2009).
280. Siomi MC. Short interfering RNA-mediated gene silencing; towards successful application in human patients. *Advanced drug delivery reviews* 61(9), 668-671 (2009).
281. Whitehead KA, Langer R, Anderson DG. Knocking down barriers: advances in siRNA delivery. *Nature reviews Drug discovery* 8(2), 129-138 (2009).
282. Schroeder A, Levins CG, Cortez C, Langer R, Anderson DG. Lipid-based nanotherapeutics for siRNA delivery. *Journal of internal medicine* 267(1), 9-21 (2010).
283. Contag CH, Spilman SD, Contag PR *et al*. Visualizing gene expression in living mammals using a bioluminescent reporter. *Photochemistry and photobiology* 66(4), 523-531 (1997).
284. Fan F, Wood KV. Bioluminescent assays for high-throughput screening. *Assay and drug development technologies* 5(1), 127-136 (2007).
285. Reynolds A, Leake D, Boese Q, Scaringe S, Marshall WS, Khvorova A. Rational siRNA design for RNA interference. *Nature biotechnology* 22(3), 326 (2004).
286. Jackson AL, Linsley PS. Recognizing and avoiding siRNA off-target effects for target identification and therapeutic application. *Nature reviews Drug discovery* 9(1), 57-67 (2010).
287. Takemoto H, Ishii A, Miyata K *et al*. Polyion complex stability and gene silencing efficiency with a siRNA-grafted polymer delivery system. *Biomaterials* 31(31), 8097-8105 (2010).
288. Ragelle H, Riva R, Vandermeulen G *et al*. Chitosan nanoparticles for siRNA delivery: optimizing formulation to increase stability and efficiency. *Journal of Controlled Release* 176 54-63 (2014).
289. Li S-D, Chono S, Huang L. Efficient gene silencing in metastatic tumor by siRNA formulated in surface-modified nanoparticles. *Journal of Controlled Release* 126(1), 77-84 (2008).
290. Suma T, Miyata K, Ishii T *et al*. Enhanced stability and gene silencing ability of siRNA-loaded polyion complexes formulated from polyaspartamide derivatives with a repetitive array of amino groups in the side chain. *Biomaterials* 33(9), 2770-2779 (2012).
291. Dickins RA, Mcjunkin K, Hernando E *et al*. Tissue-specific and reversible RNA interference in transgenic mice. *Nature genetics* 39(7), 914-921 (2007).
292. Kanasty R, Dorkin JR, Vegas A, Anderson D. Delivery materials for siRNA therapeutics. *Nature materials* 12(11), 967-977 (2013).

293. Minakuchi Y, Takeshita F, Kosaka N *et al*. Atelocollagen-mediated synthetic small interfering RNA delivery for effective gene silencing in vitro and in vivo. *Nucleic acids research* 32(13), e109-e109 (2004).
294. Filleur S, Courtin A, Ait-Si-Ali S *et al*. SiRNA-mediated inhibition of vascular endothelial growth factor severely limits tumor resistance to antiangiogenic thrombospondin-1 and slows tumor vascularization and growth. *Cancer research* 63(14), 3919-3922 (2003).
295. Qu M-H, Zeng R-F, Fang S, Dai Q-S, Li H-P, Long J-T. Liposome-based co-delivery of siRNA and docetaxel for the synergistic treatment of lung cancer. *International journal of pharmaceutics* 474(1), 112-122 (2014).
296. Dass CR, Walker TL, Burton MA. Liposomes containing cationic dimethyl dioctadecyl ammonium bromide: formulation, quality control, and lipofection efficiency. *Drug delivery* 9(1), 11-18 (2002).
297. Li P, Li D, Zhang L, Li G, Wang E. Cationic lipid bilayer coated gold nanoparticles-mediated transfection of mammalian cells. *Biomaterials* 29(26), 3617-3624 (2008).
298. Song E, Zhu P, Lee S-K *et al*. Antibody mediated in vivo delivery of small interfering RNAs via cell-surface receptors. *Nature biotechnology* 23(6), 709-717 (2005).
299. Ruan R, Chen M, Sun S *et al*. Topical and Targeted Delivery of siRNAs to Melanoma Cells Using a Fusion Peptide Carrier. *Scientific Reports* 6 (2016).